FINAL REPORT
ON
STUDY ON THE EFFECT OF PARTIAL DE-SILTING OF SMALL TANKS

Submitted to

INDIAN NATIONAL COMMITTEE ON IRRIGATION AND DRAINAGE (INCID)
MINISTRY OF WATER RESOURCES
GOVERNMENT OF INDIA

Dr. MADHAVI GANESAN
Associate Professor
CENTRE FOR WATER RESOURCES
ANNA UNIVERSITY, CHENNAI – 600 025

DECEMBER 2012

Project Title	:	Study on the Effect of Partial De-silting of Small Tanks
Total cost of the Project	:	Rs.27.94 Lakhs
Date of Sanction of the project	:	6.02.2006
Research Station	:	Centre for Water Resources College of Engineering Anna University Chennai - 600 025 Phone: 044-22351075

Principal Investigator

Name	:	Dr. Madhavi Ganesan
Designation	:	Associate Professor
Address	:	CWR, AU, Ch - 25
Phone	:	94445 11425
Email	:	madhaviganesan@yahoo.com

Co - Investigators

Name	:	Mr. R. Balamurugan
Designation	:	Assistant Professor (Sr. Gr.) CWR, AU, Chennai - 25
Phone	:	9444971387
E-mail	:	mrbals@annauniversity.edu
Name	:	Dr. R. Saravanan
Designation	:	Assistant Professor (Sr. Gr.)
Address	:	CWR, AU, Chennai - 25
Phone	:	9176655520
E-Mail	:	rsaran@annauniv.edu

ABSTRACT

Tanks are prime surface water body, to support irrigation in Tamil Nadu. These tanks are system and non-system tanks which are totally 39000 exist in Tamil Nadu. Most of these tanks are now deposited with silt in turn lost its storage and also recharge capacity. In order to improve the storage and recharge capacity of the tanks, this project was undertaken. Two tanks were selected based on the objectives and methodology of the project with specific criteria such as non system tanks with command area of around 40 ha with open/bore wells. It is also expected that the farmers should take part in all the activities of the tank. Many tanks were visited in and around Chennai and also in Madurai. Finally one tank was chosen in the first order stream which is located near the hills and second tank was selected in the third order stream. First one is Ponpadi tank, near Tiruttani and the other one is Sengulam tank in Virudhunagar District. Two water years of 2007-2008 and 2008-2009 were considered for the study. Behaviour of the tank and its ground water aquifer system were studied with six stages.

i. Hydrologic and Hydraulic characteristic analysis;
ii. Tank bed characteristics and its recharge capacity evaluation study.
iii. Ground water aquifer parameter evaluation study through well dilution technique;
iv. Tank and Ground water inter connection study through resistivity survey;
v. Estimation of Tank's seepage rate through tracer application in the field;
vi. Tank and aquifer interaction evaluated through numerical simulation.

In four stages such as permeable zone delineation, infiltration test, soil texture analysis and permeability test at various depth were framed and the Sengulam tank bed was de-silted to an area of 1200 sq.m to a depth of 0.61m. Tracer study was conducted to evaluate the impact of partial de-silting. This project found that partial de-silting will definitely improve the seepage rate from 25 percent to 43 percent. In turn de-silted soil may be used for strengthening tank bund, to improve soil fertility and also be used for brick manufacturing. Tracer study and geophysical survey explicitly proved the nexus between tank and ground water aquifer system. Any tank which is to be de-silted can follow the procedure given in this report.

TABLE OF CONTENTS

CHAPTER NO.	TITLE	PAGE NO.
	ABSTRACT	iii
	TABLLE OF CONTENTS	v
	LIST OF FIGURES	xv
	LIST OF TABLES	xxvii
	LIST OF PHOTOGRAPHS	xxxii
	LIST OF ABBREVIATIONS	xxxiii
1	INTRODUCTION	
	1.1 GENERAL	1
	1.2 OBJECTIVES	2
	1.3 CONTRIBUTION TO WATER RESOURCES DEVELOPMENT	2
	1.4 APPLYING THE RESEARCH TO USE	2
	1.5 CURRENT STATUS OF THE TANK	3
	1.6 IAMWARM PROJECT	4
	1.7 IMPORTANCE OF DESILTING	5
	1.8 OVERVIEW OF THE PROJECT	6
2	LITERATURE REVIEW	7
	2.1 INTRODUCTION	7
	2.2 GROUNDWATER EXPLORATION METHODS	8
	2.3 DELINEATING PERMEABLE ZONE BY ELECTROMAGNETIC SURVEY	9
	2.4 GROUNDWATER EXPLORATION BY ELECTRICAL RESISTIVITY SURVEY	10
	2.4.1 Methods of Investigation	11
	2.4.2 Theoretical Foundations	11

CHAPTER NO.	TITLE	PAGE NO.

	2.4.4 Inverse Slope Method	15
	2.4.5 Relationship between Geo- electric and Aquifer Parameters	15
	2.4.6 Estimation of Aquifer Parameters from Geo-Electric Parameters	16
2.5	ESTIMATION OF INFILTRATION RATE	20
	2.5.1 Infiltration Rate at Various Slopes	20
	2.5.2 Infiltration in Complex Lateritic Soil Profile	20
	2.5.3 Artificial Recharge	21
	2.5.4 Infiltration Rate in Saturated Soil	22
	2.5.5 Infiltration Capacity during Summer and Winter	23
	2.5.6 Infiltration Rate Before and After Tillage	23
2.6	ESTIMATION OF AQUIFER PARAMETERS	24
	2.6.1 Hydraulic Conductivity in Unsaturated Soil	24
	2.6.2 Hydraulic Conductivity in Saturated Soil	25
	2.6.3 Estimation of Permeability through Well Dilution Techniques	26
	2.6.4 Estimation of Permeability and Specific Yield in an Unconfined Aquifer	27
	2.6.5 Tank water Balance components	28
	2.6.6 Simulation of Daily Tank Water Balance	29
2.7	LITERATURE ON FLUORESCENT DYES	33
	2.7.1 Effect of Positively and Negatively Charged Soil on Fluorescent Dyes	35
	2.7.2 Determination of Retardation Factor (R_f)	37
	2.7.3 Dye Study in streams / rivers	39
	2.7.4 Dye Study in Groundwater	43

CHAPTER NO.	TITLE	PAGE NO.
	2.8 LITERATURE ON GROUNDWATER MODELING	68
	2.8.1 Model Parameters	69
	2.8.2 Water Balance Equation	69
	2.8.3 Mass Balance Equation	69
	2.9 FLOW EQUATION	70
	2.10 GROUNDWATER MODELS	70
	2.10.1 Visual MODFLOW	71
	2.10.2 Visual PEST	72
	2.10.3 Genetic Algorithm	72
	2.11 GROUNDWATER FLOW MODEL APPLICATIONS	74
	2.12 PARAMETER ESTIMATION THROUGH GENETIC ALGORITHM	76
3	**METHODOLOGY**	
	3.1 GENERAL	79
	3.2 DETAILS OF METHODOLOGY	79
	3.2.1 Delineation of Feasible Zone for Partial De-silting	81
	3.2.2 Estimation of Aquifer Parameters	82
	3.2.3 Tank and Aquifer Interaction	83
	3.2.4 Estimation of Seepage Velocity	84
	3.2.5 Numerical Modeling of Surface and Groundwater Interaction	85

CHAPTER NO.	TITLE	PAGE NO.
4	**HYDROLOGICAL CHARACTERISTICS OF THE TANK SYSTEM**	
4.1	CRITERIA KEPT FOR THE SELECTION OF TANKS	87
4.2	PONPADI TANK – TIRUTTANI	90
4.2.1	Hydro meteorological Characteristics	92
4.2.2	Delineation of Catchment Area and Estimation of Tank Capacity - Ponpadi	94
4.2.3	Runoff Estimation – Ponpadi	102
4.2.4	Groundwater Potential	107
4.2.5	Groundwater Scenario at Ponpadi Tank	108
4.2.6	Well History	109
4.2.7	Groundwater levels in the Ponpadi Pumping Wells	119
4.2.8	Net Draft at Ponpadi Tank Command Area	122
4.2.9	Seepage Rate at Ponpadi Tank	123
4.2.10	Relationship between Tank Water Level and the Well Water Level at Ponpadi tank	124
4.3	SENGULAM TANK – VIRUDHUNAGAR	127
4.3.1	Rainfall and Climate	128
4.3.2	Delineation of Catchment and Estimation of Tank Capacity -Sengulam	133
4.3.3	Runoff Estimation – Sengulam	142
4.3.4	Groundwater Scenario at Sengulam Tank	145
4.3.5	Groundwater Level in the Command Area of Sengulam Tank	147
4.3.6	Net Draft in Sengulam Command Area	152
4.3.7	Seepage Rate at Sengulam Tank	154

CHAPTER NO. TITLE PAGE NO.

4.3.8 Groundwater Potential 155

4.3.9 Relationship between Tank Water Level and Well Water level at Sengulam tank 156

4.4 TANK VOLUME DAYS 162

4.5 SEEPAGE VELOCITY 167

4.6 SUMMARY 171

5 TANK BED CHARACTERISTICS AND ITS RECHARGE CAPACITY

5.1 GEOPHYSICAL SURVEY 176

5.1.1 Surface Profiling and Subsurface Depth Sounding 176

5.1.2 Terra Very Low Frequency (T-VLF) System 177

5.1.3 Principle of Operation 178

5.1.4 Limitation of VLF 179

5.1.5 Delineation of Permeable Zone 180

5.1.6 Iso-Resistivity Mapping 181

5.2 INFILTRATION RECHARGE SYSTEM 182

5.2.1 Infiltration Rate Analysis 184

5.3 SOIL TEXTURE TRIANGLE 188

5.3.1 Soil Texture Analysis 189

5.4 HYDRAULIC CONDUCTIVITY 192

5.4.1 Estimation of Coefficient of Permeability 192

5.4.2 Observed Hydraulic Conductivity 193

5.5 COMPUTED HYDRAULIC CONDUCTIVITY 195

5.5.1 Analytical Method 196

5.5.2 Modified Saxton Equation 197

CHAPTER NO.	TITLE	PAGE NO.
5.6	ESTABLISHMENT OF RELATIONSHIP BETWEEN SOIL TEXTURE, PERMEABILITY AND INFILTRATION RATE	200
5.7	STRATEGY FOR DE-SILTING	202
5.8	PARTIAL DE-SILTING OF SENGULAM TANK	203
5.9	SUMMARY	204
6	**ESTIMATION OF AQUIFER PARAMETERS THROUGH WELL DILUTION TECHNIQUE**	**207**
6.1	GENERAL	207
6.2	REQUIREMENT OF GROUNDWATER TRACER	207
6.3	WELL DILUTION TECHNIQUE	209
	6.3.1 Single well Dilution Technique	209
	6.3.2 Two well Dilution Technique	212
6.4	INSTALLATION OF BOREHOLE IN THE FIELD	214
	6.4.1 Single Well Dilution	215
	6.4.2 Two Well Dilution	222
	6.4.3 Permeability Estimation at Lab Scale	226
	6.4.4 Permeability	227
	6.4.5 Specific Capacity	228
	6.4.6 Specific Yield	228
	6.4.7 Aquifer Parameters Estimation	229
	6.4.8 Specific Capacity	229
	6.4.9 Specific Yield	230
	6.4.10 Permeability	230

CHAPTER NO.	TITLE	PAGE NO.
	6.5 SUMMARY	232
7	**ESTIMATION OF TANK AND AQUIFER INTERACTION THROUGH GEO-ELECTRICAL STUDIES**	233
	7.1 GENERAL	233
	7.2 RESISTIVITY MEASUREMENTS	235
	7.2.1 Apparent Resistivity	235
	7.2.2 True Resistivity	235
	7.2.3 Longitudinal Unit Conductance	235
	7.2.4 Transverse Resistance	236
	7.2.5 Formation Factor	236
	7.3 GEO-ELECTRIC PARAMETERS ESTIMATIONS	236
	7.3.1 Electrical Resistivity Survey	237
	7.3.2 Inverse Slope Method	237
	7.3.3 Model Calculation For Calculating True Resistivity For Well 1	243
	7.3.4 Geo Electrical sections along AA' , BB' and CC'	245
	7.3.5 Geo-electrical Parameters Estimation	247
	7.4 ESTABLISHMENT OF EMPIRICAL RELATIONSHIP BETWEEN RESISTIVITY PARAMETERS AND AQUIFER HYDRAULIC PARAMETERS	251
	7.4.1 Relationship between Geo-electric Parameters and Aquifer Parameters	252
	7.4.2 Relationship between Apparent Resistivity and Hydraulic Conductivity	253

CHAPTER NO.	TITLE	PAGE NO.
	7.5 GEOCHEMICAL ANALYSIS	253
	7.6 TANK AND AQUIFER INTERACTION	254
	7.7 SUMMARY	255
8	**EVALUATION OF SEEPAGE RATE THROUGH TRACER STUDY**	**256**
	8.1 TYPES OF ARTIFICIAL TRACERS	257
	8.1.1 Temperature	259
	8.1.2 Isotopes	259
	8.1.3 Inorganic Anions	259
	8.1.4 Fluorocarbon	260
	8.1.5 Sulfur Hexafluoride	260
	8.1.6 Ethanol, Benzoate, and Fluorobenzoates	261
	8.1.7 Spores and Particles	261
	8.1.8 Microorganisms	262
	8.1.9 Dyes	262
	8.2 CLASSIFICATION OF DYES	263
	8.2.1 Factors Affecting Dye Fluorescence	266
	8.3 FLUORESECENCE SPECTROSCOPY	273
	8.4 SELECTING DYE FOR INJECTION	278
	8.5 SELECTING QUANTITY OF DYE FOR INJECTION	280
	8.5.1 Dye Handling Procedures	282
	8.6 DYE RECOVERY EQUIPMENT AND PROCEDURE	283
	8.6.1 Calibration Procedure	283
	8.7 QUANTITATIVE DYE TRACING	286
	8.8 APPLICATION OF RHODAMINE B IN FIELD	288

CHAPTER NO.	TITLE	PAGE NO.
	8.8.1 Rhodamine B application in Sengulam Tank - Year 2008	289
	8.8.2 Rhodamine B application in Sengulam Tank - Year 2009	298
	8.8.3 Rhodamine B application in Ponpadi Tank - Year 2009	316
	8.8.4 Findings from Dye Study	329
	8.9 ADSORPTION CHARACTERISTICS OF THE ORGANIC TRACER DYES	332
	8.9.1 Calibration Curve for Rhodamine B, Sulpho-Rhodamine B and Fluorescein	333
	8.9.2 Batch Study Results	341
	8.9.3 Soil Column Experiment	342
	8.9.4 Adsorption Isotherm	348
	8.9.5 Characteristics of Soil Properties Before and After the Column Study	355
	8.9.6 Summary	356
9	**EVALUATION OF IMPACT OF PARTIAL DE-SILTING THROUGH NUMERICAL MODEL**	**359**
	9.1 GENERAL	359
	9.2 GROUNDWATER MODELING	359
	9.3 APPLICATION OF GROUNDWATER MODELING	360
	9.4 TYPES OF MODELING APPROACH	361
	9.4.1 Inverse Modeling	361
	9.5 STEPS BY STEP PROCEDURE OF MODELING	362
	9.5.1 Model Conceptualization	364

CHAPTER NO.	TITLE	PAGE NO.
	9.5.2 Primary and Secondary Data Collection	365
	9.5.3 Input Data to the Model	365
	9.5.4 Flow Model Calibration	367
	9.5.5 Parameter Estimation	376
	9.5.6 Comparison of Result between the Different Trials	382
	9.5.7 Validation Process	385
	9.5.8 Comparison of Mass Balance	389
	9.6 SIMULATING THE IMPACT OF PARTIAL DESILTING	391
	9.7 SUMMARY	394
10	**SUMMARY AND CONCLUSSION**	**396**
	REFERENCES	**403**
	ANNEXURE I	**411**
	ANNEXURE II	**413**

LIST OF FIGURES

FIGURE NO.	TITLE	PAGE NO
2.1	A Conventional Four Electrode Array to Measure the Subsurface Resistivity	10
2.2a)	Wenner electrode arrangement	14
2.2b)	Schlumberger electrode arrangement	14
2.3	Breakthrough Curve (D. A. Sabatini 'Ground Water', September – October 2000)	66
4.1	Location of Ponpadi and Sengulam Tanks	89
4.2	Base Map of Chennai Basin	91
4.3	Comparison of 2007 and 2008 Monthly Rainfall	94
4.4	Catchment Area of Ponpadi Tank	99
4.5	Contour Map of Ponpadi tank	99
4.6	Elevation vs Waterspread Area at Ponpadi Tank	100
4.7	Elevation vs Storage at Ponpadi Tank	100
4.8	Monthly Tank Storage for Two Water Years	103
4.9	Daily Tank Storage during Two Water Years at Ponpadi Tank	104
4.10	Pumping wells Location at Ponpadi Tank Command Area	108
4.11a)	Groundwater Levels in the Pumping Wells of R1, R3 to R5 at Ponpadi Tank	120
4.11b)	Groundwater Levels in the Pumping Wells of L1& L2 at Ponpadi Tank	120
4.11c)	Groundwater Levels in the Pumping Wells of L4, L6& L7 at Ponpadi Tank	121

FIGURE NO.	TITLE	PAGE NO

4.12	Net Draft at Ponpadi Tank Command Area	122
4.13	Comparison of Rainfall during 2007 and 2008 at Kavalur Raingauge Station	129
4.14	Catchment of Sengulam Tank	135
4.15	Location of Pumping Wells at Sengulam Tank	140
4.16	Elevation Vs Waterspread at Sengulam Tank	140
4.17	Elevation Vs Storage at Sengulam Tank	140
4.18a)	Monthly Storage of the Sengulam Tank for Two Water Years	145
4.18b)	Comparison of Tank Storage before and after de-silting	145
4.19a)	Groundwater Level in the Pumping Wells of W1 to W6 at Sengulam Tank	150
4.19b)	Groundwater Level in the Pumping Wells of W7 to W10 at Sengulam Tank	150
4.19c)	Groundwater Level in the Pumping Wells of W11 to W14 at Sengulam Tank	150
4.20a)	Groundwater Level in the Pumping Wells of W16 & W17 at Sengulam Tank	151
4.20b)	Groundwater Level in the Pumping Wells of W18 & W22 at Sengulam Tank	151
4.20c)	Groundwater Level in the Pumping Wells of W19, W20 & W21 at Sengulam Tank	151
4.21	Groundwater Level in the Pumping Wells of W23 & W24 at Sengulam Tank	152
4.22	Theissen Polygon Areas at Sengulam Command Area	153
4.23	Monthly Net Draft for Two Water Years at Sengulam Tank	153
4.24	Variation of Tank water level and Well water level	161

FIGURE NO.	TITLE	PAGE NO
4.25	Variation of Tank water level and Well water level Comparison of 23 wells water level and tank water level	162
4.26	Comparison of slope of a line before and after de-silting	166
4.27	Comparison of seepage velocity before and after de-silting	171
5.1	Steps followed to Delineate the Feasible zone for Partial De-silting	175
5.2	T-VLF System	177
5.3	Behaviour of Electric and Magnetic Field from a VLF Radio Antenna	178
5.4	Longitudinal Variation of Resistivity at Ponpadi Tank Bed	180
5.5	Longitudinal Variation of Resistivity at Sengulam Tank Bed	180
5.6	Iso-Resistivity Map of Ponpadi Tank	182
5.7	Iso-Resistivity Map of Sengulam Tank	182
5.8	Infiltration Recharge System	183
5.9	Double Ring Infiltrometer	183
5.10	Infiltration Test at Surface	185
5.11	Infiltration Test at 50 cm Depth below Ground Level	185
5.12	Location Map of Infiltration Test of Ponpadi Tank	186
5.13	Location Map of Infiltration Test of Sengulam Tank	186
5.14	Infiltration Rate at Various Location and Depth of Ponpadi Tank	187
5.15	Infiltration Rate at Various Location and Depth of Sengulam Tank	188
5.16	Soil Texture Triangle	189
5.17	Soil Texture Analysis	189

FIGURE NO.	TITLE	PAGE NO
5.18	Collection of Soil Sample at Various Location and Depth	190
5.19	Relationship between Flux and Hydraulic Gradient	192
5.20	Falling Head Permeameter	193
5.21	Experimental Setup - Falling Head Permeameter	195
5.22	Hydraulic Properties Software	196
5.23	Hydraulic Conductivity Curves Classified by Soil Texture	197
5.24	Validation of Modified Saxton Equation for all the Samples Collected	199
5.25	Validation of Modified Saxton Equation for all the Samples Collected except Sandy Clay and Sandy Clay Loam	200
5.26	Relationship between Infiltration Rate and Hydraulic Conductivity	200
5.27	Comparison of Observed and Computed Infiltration Rate of Clay, Silty Clay and Clay Loam	201
5.28	Partial De-silting Portion of Sengulam Tank	203
6.1	Diagrammatic Representation of Single Well Dilution	212
6.2	Diagrammatic Representation of Two Well Dilution	214
6.3	Block Diagram of Borehole Location at the Depth of 2 m	214
6.4	Single Well Dilution in L4 by SRB	216
6.5	Single Well Dilution in B1 by SRB	218
6.6	Single Well Dilution in L1 by NaCl	220
6.7	Single Well Dilution in L6 by NaCl	221
6.8	Two Well Dilution Technique by Natural Gradient	224
6.9	Two Well Dilution Technique by Forced Gradient	225
7.1	VES Resistivity at Well Location 1	238
7.2	VES Resistivity at well location 2	238

FIGURE NO.	TITLE	PAGE NO
7.3	VES Resistivity at Well Location 5	238
7.4	VES Resistivity at Well Location 6	239
7.5	VES Resistivity at Well Location 8	239
7.6	VES Resistivity at Well Location 9	239
7.7	VES Resistivity at Well Location 10	240
7.8	VES Resistivity at Well Location 12	240
7.9	VES Resistivity at Well Location 13	240
7.10	VES Resistivity at Well Location 14	241
7.11	VES Resistivity at Well Location 17	241
7.12	VES Resistivity at Well Location Near tank bund 1	241
7.13	VES Resistivity at Well Location Near Tank Bund 2	242
7.14	VES Resistivity at well Location Near Tank Bund 3	242
7.15	VES Resistivity at Location Inside The Tank 1	242
7.16	VES Resistivity at Location Inside the Tank 2	243
7.17	Wells lies along the straight line	245
7.18	Cross Sectional View Along The Line AA'	245
7.19	Cross Sectional View Along The Line BB'	246
7.20	Cross Sectional View Along The Line CC'	246
7.21	Relationship Between Formation Factor and Hydraulic conductivity	252
7.22	Relationship Between Resistivity and Hydraulic conductivity	253
8.1	Excitation Spectra of Amino G acid, Lissamine FF, and Rhodamine WT	265
8.2	Emission Spectra of Amino G acid, Lissamine FF and Rhodamine WT	265

FIGURE NO.	TITLE	PAGE NO
8.3	Schematic of a fluorometer with 90" geometry utilizing a Xenon light source (form Fluorescence Spectroscopy, 2009)	275
8.4	Raman Spectrum Affected by Impurities (from Instruction Manual for Model F - 2000 Fluorescence Spectrophotometer)	277
8.5	Optical System Configurations (from Instruction Manual for Model F - 2000 Fluorescence Spectrophotometer)	277
8.6	Calibration Curve for 1 – 100 ppb	285
8.7	Calibration Curve for 1 – 1000 ppb	285
8.8	Typical Dye Recovery Curve	287
8.9	Excitation and Emissions spectra of Rhodamine B dye	288
8.10	Rhodamine B fluorescence in the Sengulam Tank during 2008	293
8.11	Natural fluorescence in the Sengulam tank during 2008 after rainfall	293
8.12	Comparison of Natural fluorescence in Sengulam wells during 2008	294
8.13	Rhodamine B fluorescence in the Sengulam Tank in the year 2009	300
8.14	Natural fluorescence in the Sengulam Tank in the year 2009	301
8.15	Comparison of Natural fluorescence in Sengulam wells during 2009	303
8.16a	Comparison of Rhodamine B fluorescence between 2008 & 2009 in Well 1	305

FIGURE NO.	TITLE	PAGE NO

8.16b	Comparison of Rhodamine B fluorescence between 2008 & 2009 in Well 2	306
8.16c	Comparison of Rhodamine B fluorescence between 2008 & 2009 in Well 3	306
8.16d	Comparison of Rhodamine B fluorescence between 2008 & 2009 in Well 4	306
8.16e	Comparison of Rhodamine B fluorescence between 2008 & 2009 in Well 5	307
8.16f	Comparison of Rhodamine B fluorescence between 2008 & 2009 in Well 6	307
8.16g	Comparison of Rhodamine B fluorescence between 2008 & 2009 in Well 7	307
8.16h	Comparison of Rhodamine B fluorescence between 2008 & 2009 in Well 8	308
8.16i	Comparison of Rhodamine B fluorescence between 2008 & 2009 in Well 9	308
8.16j	Comparison of Rhodamine B fluorescence between 2008 & 2009 in Well 10	308
8.16k	Comparison of Rhodamine B fluorescence between 2008 & 2009 in Well 11	309
8.16l	Comparison of Rhodamine B fluorescence between 2008 & 2009 in Well 12	309
8.16m	Comparison of Rhodamine B fluorescence between 2008 & 2009 in Well 13	309
8.16n	Comparison of Rhodamine B fluorescence between 2008 & 2009 in Well 14	310
8.16o	Comparison of Rhodamine B fluorescence between 2008 & 2009 in Well 16	310

FIGURE NO.	TITLE	PAGE NO

8.16p	Comparison of Rhodamine B fluorescence between 2008 & 2009 in Well 17	310
8.16q	Comparison of Rhodamine B fluorescence between 2008 & 2009 in Well 18	311
8.16r	Comparison of Rhodamine B fluorescence between 2008 & 2009 in Well 19	311
8.16s	Comparison of Rhodamine B fluorescence between 2008 & 2009 in Well 20	311
8.16t	Comparison of Rhodamine B fluorescence between 2008 & 2009 in Well 21	312
8.16u	Comparison of Rhodamine B fluorescence between 2008 & 2009 in Well 22	312
8.16v	Comparison of Rhodamine B fluorescence between 2008 & 2009 in Well 23	312
8.16w	Comparison of Rhodamine B fluorescence between 2008 & 2009 in Well 24	313
8.17	Rhodamine B fluorescence in the Ponpadi Tank during 2009	320
8.18	Natural fluorescence in the Ponpadi Tank during 2009	320
8.19	Rhodamine B Detection in the Open wells of Ponpadi tank command area in the year 2009	322
8.20	Rhodamine B Detection in the shallow bore wells L1 & L7 of Ponpadi tank command area in the year 2009	322
8.21	Rhodamine B Detection in the shallow bore wells L4 & L6 of Ponpadi tank command area in the year 2009	322
8.22	Rhodamine B Detection in the shallow bore wells L2, L12, L15, and L16 of Ponpadi tank command area in the year 2009	323

FIGURE NO.	TITLE	PAGE NO
8.23	Rhodamine B Detection in the shallow bore wells L8 & L9 of Ponpadi tank command area in the year 2009	323
8.24	Rhodamine B Detection in the shallow bore wells L17 & L21 of Ponpadi tank command area in the year 2009	323
8.25	Standard Graph for Rhodamine B	334
8.26	Standard Graph for Sulforhodamine B	334
8.27	Standard Graph for Fluorescein	334
8.28	Photochemical Decay for Sulphorhodamine B and Fluorescein	336
8.29	Photochemical Decay for Rhodamine B	336
8.30	Chemical Decay for Sulphorhodamine B and Fluorescein	337
8.31	Chemical Decay for Rhodamine B	337
8.32	Batch Study with Waste Water for Sulphorhodamine B	338
8.33	Batch study with Tap Water for Sulphorhodamine B and Fluorescein	339
8.34	Batch study with Waste Water for Rhodamine B	339
8.35	Batch study with Tap Water for Rhodamine B	339
8.36	Batch study by varying the Sand Weight in gram	340
8.37	Batch study by varying the Clay Weight in gram	341
8.38	Soil Column Design	342
8.39	Recovery of Dye Concentration for 200 ppb	343
8.40	Recovery of Dye Concentration for 20 ppb	344
8.41	Percentage of Adsorbed Dye Concnetration for Sulphorhodamine B in sandy soil for 1000ppb	344
8.42	Percentage of Adsorbed Dye Concnetration for Sulphorhodamine B in sandy soil for 100 ppb	345
8.43	Percentage of Adsorbed Dye Concnetration for sulphorhodamine B in sandy soil for 20 ppb	345

FIGURE NO.	TITLE	PAGE NO

8.44	Percentage of Adsorbed Dye Concnetration for Sulphorhodamine B in Clay soil for 1000 ppb	346
8.45	Percentage of Adsorbed Dye Concnetration for Sulphorhodamine B in Clay soil for 100 ppb	346
8.46	Percentage of Adsorbed Dye Concnetration for Sulphorhodamine B in Clay soil for 20 ppb	346
8.47	Recovery of Dye Concentration of Fluorescein for 100 ppb	347
8.48	Recovery of Dye Concentration of Fluorescein for 20 ppb	347
8.49	Percentage of dye concnetration recovery for Fluorescein	348
8.50 a	Plot of Log C_e Vs Log x/m for Rhodamine B dye sediment vary from 10 to 80g	352
8.50 b	Plot of Log C_e Vs Log x/m for Sulphorhodamine B dye Sediment vary from 10 to 80g	352
8.50 c	Plot of Log C_e Vs Log x/m for Fluorescein sediment vary from 10 to 80g	353
8.51 a	Plot of Log C_e Vs Log x/m for Rhodamine B of different Concentration	353
8.51 b	Plot of Log C_e Vs Log x/m for three dyes of different Concentration	353
8.51 c	Plot of Log C_e Vs Log x/m for three dyes of different Concentration	354
9.1	Forward flow and transport model	361
9.2	Inverse flow and transport model	361
9.3	Methodology to Estimate the Impact of Partial De-silting	363
9.4	Model Domain	365

FIGURE NO.	TITLE	PAGE NO
9.5	Schematic Diagram for Recharge Boundary	366
9.6	Schematic Diagram of Hydraulic Conductivity	367
9.7	Calibration Graph for Steady State Condition	368
9.8	Calibrated Zone Wise Hydraulic Conductivity	369
9.9	Calibration Graph for Transient Condition	369
9.10	Calibration Graph for Varied Hydraulic Conductivity	370
9.11	Time Series Graph for Changes in Hydraulic Conductivity	371
9.12	Calibration Graph for Changes in Recharge Values	372
9.13	Time Series Graph for Changes in Recharge Values	372
9.14	Calibration Graph for Recharge Boundary Condition	373
9.15	Calibration Graph for Changes in Boundary Condition	373
9.16	Time Series Graph for Changes in Boundary Condition	374
9.17	Calibration Graph for Changes in Pumping Rates	374
9.18	Time Series Figure for Change in Pumping Rates	375
9.19	Schematic Representation of Layer with Dry Cells	377
9.20	Schematic Representation of Layer with Minimum Dry Cells	378
9.21	Variation of Objective Function for Trial – 1	380
9.22	Variation of Marquart Lambda for Trial – 1	380
9.23	Variation of Objective Function for Trial – 7	380
9.24	Variation of Marquart Lambda for Trial – 7	381
9.25	Calibration Graph for Optimum Hydraulic Conductivity at 30 days	383
9.26	Calibration Graph for Optimum Hydraulic Conductivity at 120 days	383
9.27	Calibration Graph for Optimum Hydraulic Conductivity at 360 days	384

FIGURE NO.	TITLE	PAGE NO
9.28	Time Series Graph for Optimum Hydraulic Conductivity for Well - 8	384
9.29	Time Series Graph for Optimum Hydraulic Conductivity for Well - 11	385
9.30	Time Series Graph for Optimum Hydraulic Conductivity for Well -20	385
9.31	Calibration Graph for Optimum Hydraulic conductivity at 480 days	386
9.32	Calibration Graph for Optimum Hydraulic Conductivity at 600 days	386
9.33	Calibration Graph for Optimum Hydraulic Conductivity at 720 days	387
9.34	Time Series Graph for Optimum Hydraulic Conductivity for Well - 8	387
9.35	Time Series Graph for Optimum Hydraulic Conductivity for Well - 12	388
9.36	Time Series Graph for Optimum Hydraulic Conductivity for Well – 20	388
9.37	Comparison of Seepage Rate	389
9.38	Comparison of Rainfall Recharge Rate	389
9.39	Comparison of Pumping Rate	390
9.40	Comparison of Monthly Groundwater Storage	390
9.41	Comparison of Seepage Rate Before and After De-silting	392
9.42	Comparison of Groundwater Storage Before and After De-silting	393

LIST OF TABLES

TABLE NO	TITLE	PAGE NO
4.1	Study Area Details and Hydraulic Particulars	90
4.2	Monthly Climatological Details of Tiruttani during the year 2006	96
4.3	Monthly Rainfall (mm) at Tiruttani Raingauge Station	97
4.4	Ponpadi Tank Capacity Estimation	101
4.5	Ponpadi Tank Storage Estimation	104
4.6	Cropping Pattern during November 2008 at Ponpadi Command area	111
4.7	Cropping Pattern during January 2009 at Ponpadi Command area	113
4.8	Cropping Pattern during February 2009 at Ponpadi Command area	115
4.9	Pumping Details at Ponpadi Command area	122
4.10	Monthly Rainfall (mm) for the Period 1974 - 2008 at Kavalur Raingauge Station	130
4.11	Seasonal Rainfall for the Period 1974 -2008 at Kavalur Raingauge Station	132
4.12	Water Spread Area and Storage Capacity of Sengulam Tank	141
4.13	Rainfall, Runoff and Storage of Sengulam Tank	143
4.14	Comparison of Tank Storage during Northeast Monsoon between the Year 2007 and 2008	143
4.15	Monthly Tank Water Level of the Sengulam with respect to msl and its Storage for the Period June 2007 to May 2009	144

TABLE NO	TITLE	PAGE NO
4.16	Pumping Wells Details at Sengulam Tank	149
4.17	Comparison of seepage rate between the year 2007-2008 and 2008-2009	154
4.18	Tank storage and tank volume days	163
5.1	Infiltration Rate of Ponpadi Tank Bed	186
5.2	Infiltration Rate of Sengulam Tank Bed	187
5.3	Soil Texture of Ponpadi Tank	190
5.4	Soil Texture of Sengulam Tank	191
5.5	Permeability of Ponpadi Tank	194
5.6	Permeability of Sengulam Tank	194
6.1	Details of Single Well Dilution in L4 by SRB	216
6.2	Details of Single Well Dilution in B1 by SRB	217
6.3	Details of Single Well Dilution in L1 by NaCl	219
6.4	Details of Single Well Dilution in L6 by NaCl	221
6.5	Estimated Filtration Velocity, Dispersivity and Dispersion Coefficient by Single Well Dilution Technique	222
6.6	Details of Two Well Dilution Technique by Natural Gradient	223
6.7	Details of Two Well Dilution Technique by Forced Gradient	225
6.8	Estimation of Dispersivity and Dispersion Coefficient by Two Well Dilution Technique	226
6.9	Aquifer Parameters Calculated Through Pumping Test	231
6.10	Hydraulic Conductivity Estimated by Conventional Methods	232
7.1	Corresponding Potential and Current Electrode Spacing	237

TABLE NO	TITLE	PAGE NO
7.2	Summary Of True Resistivity Values And Layer Thickness	244
7.3	Summary of Longitudinal Conductance	249
7.4	Summary of Transverse Resistance	250
7.5	Summary of Formation Factor for Wells	251
7.6	Geochemical Analysis of Water Samples	254
8.1	Artificial Water Tracer Analytic Techniques, Advantages, Disadvantages, and Pertinent References (from Boron Isotopes as an Artificial Tracer, 2006)	257
8.2	Generic Name, Excitation Emission Maximum, Minimum detectable Concentrations of the Tracer Dyes (from P.L. Smart and Laid law 1977)	264
8.3	Schedule for Dye Study in the year 2008	290
8.4	Rhodamine B and Natural fluorescence at Sengulam Tank water during 2008	292
8.5	Analysis of Rhodamine B fluorescence detection in the Sengulam Tank during 2008	295
8.6	Wells in the proximity of 150m from the bund	296
8.7	Wells in the proximity of 300m from the bund	297
8.8	Wells in the proximity of 450m from the bund	297
8.9	Natural fluorescence & TDS in Sengulam Tank during 2009	298
8.10	Schedule for dye study in the year 2009	300
8.11	Rhodamine B and Natural fluorescence in the Sengulam tank during 2009	301
8.12	First Detection Day of Rhodamine B	302
8.13	Analysis of Rhodamine B fluorescence detection in the Sengulam Tank during 2009	303

TABLE NO	TITLE	PAGE NO
8.14	Comparison of Ground water Velocity between the year 2008 and 2009	314
8.15	Rhodamine B Fluorescence in the Ponpadi Tank in the First Trial	318
8.16	Schedule of rhodamine B study at Ponpadi tank during 2009	319
8.17	Rhodamine B Detection in the Deep Bore wells	324
8.18	Analysis of Rhodamine B fluorescence Detection in the Ponpadi Tank during 2009	325
8.19	Pumping rate at Ponpadi bore wells during February – April 2009	327
8.20	Pumping Rate at Ponpadi Open wells during February – April 2009	328
8.21	Percent Recovery of Rhodamine B from the Ponpadi Wells	328
8.22	Intensity value for Sulphorhodamine B, Rhodamine B and Fluorescein	333
8.23	Reduction of dye loss due to Salinity	341
8.24	n and k Values for Three Types Dyes at Different Sediment Weight	354
8.25	n and k Values for Three Types of Dyes at Different Concentration	354
8.26	Soil Properties of Clay Soil Before and After the Column Test	356
9.1	Variation of RMS with Increase in Recharge	371
9.2	Comparison of Results between all Calibration Changes	375

TABLE NO	TITLE	PAGE NO
9.3	Comparison between PEST Estimated Optimum Hydraulic Conductivity and Simulated Hydraulic Conductivity	381
9.4	Estimated Hydraulic Conductivity from Four Trials	382
9.5	Comparison of Major Inflows and Out flows	391

LIST OF PHOTOGRAPHS

PHOTOGRAPH NO	TITLE	PAGE NO
4.1	View of Ponpadi Tank during December 2008	105
4.2	View of Surplus at Ponpadi Tank during December 2008	105
4.3	Sand Bag Packing to Arrest the Breach Ponpadi Tank during December 2008	106
4.4	Cultivation at Ponpadi Tank Command Area during December 2008	106
4.5	Farmers Meet at Ponpadi Tank	109
4.6	Farmers Participation at Ponpadi Tank	110
4.7	Cultivation at Ponpadi Command Area during February 2009	110
4.8	Supply Channel to the Sengulam Tank	135
4.9	Full Tank view of Sengulam during December 2007	136
4.10	Sengulam Tank during December 2008	136
4.11	Sengulam Tank Sluice No – 1	137
4.12	Sengulam Tank Sluice No – 2	137
4.13	Sengulam Tank Sluice No – 3	138
4.14	Surplus Weir at Sengulam Tank	138
4.15	Sengulam Tank Command Area during June 2007	139
4.16	Pumping Open Well at Sengulam Tank Command Area	139
5.1	Partial De-silting at Sengulam Tank	204

LIST OF ABBREVIATIONS

A	-	Cross Sectional Area of Soil Sample
a	-	Cross Sectional Area of Stand Pipe
C	-	Specific capacity (m^2/min)
Cl	-	Chloride in mg/l
CL	-	Percents by Weight of Clay in the Soil
cm	-	Centimeter
cm/hr	-	Centimeter per Hour
d	-	Depth of Ring Insertion into the Soil
DC	-	Direct Current
EC	-	Electrical Conductivity
EM	-	Electromagnetic
EPA	-	Environmental Protection Agency
E-W	-	East West
EX	-	Electric Field Component in X Direction
exp	-	Exponential
EZ	-	Electric Field Components in Y Direction
f	-	Infiltration Rate
FTL	-	Full Tank Level
h	-	Height of the Water in the Infiltrometer
H	-	Steady Depth of Ponded Water in the Ring
h	-	Thickness of the aquifer
h_0	-	Initial Head
h_1	-	Final Head
HY	-	Magnetic Field Component
K	-	Permeability
KHz	-	Kilo hertz
K_S	-	Saturated Hydraulic Conductivity
K_T	-	Transverse Hydraulic Conductivity

L	-	Length of the Soil Sample
L_c	-	Longitudinal Conductance
m	-	Meter
m/day	-	Meter per Day
m^2	-	Square meter
msl	-	Mean Sea Level
MWL	-	Maximum Water Level
NaCl	-	Sodium Chloride
N-S	-	North South
Ohm-m	-	Ohm meter
PPB	-	Parts Per Billion
q_s	-	Steady State Infiltration Rate
R	-	Resistance
S1	-	Drawdown at time pumping stops (m).
S2	-	Residual drawdown at time stops(m).
SA	-	Percents by Weight of Sand in the Soil
SI	-	Percents by Weight of Silt in the Soil
SRB	-	Sulphorhodamine B
t	-	Time Taken to Head Falls from h_0 to h_t
T	-	Transmissivity
t'	-	Time after pumping stops (min).
TDS	-	Total Dissolved Solids in mg/l
T_r	-	Transverse resistance
T-VLF	-	Terra Very Low Frequency
VES	-	Vertical Electrical Sounding
VLF	-	Very Low Frequency
Z	-	Depth of the Transmission Zone below the Infiltrometer
α	-	Inverse Soil Macroscopic Capillary Length Parameter

αr	-	Radius of the Inner Ring
ρa	-	Aquifer Resisivity
ρw	-	Water Resistivity
Ω m	-	Ohm meter
ϕ	-	Suction at the Bottom of the Transmission Zone

CHAPTER 1

INTRODUCTION

1.1 GENERAL

Irrigation in Tamil Nadu dates back to several centuries. Earliest irrigation works relate to small storages called tanks. Forming a low bund across a shallow valley to hold the runoff from its catchment forms a tank. The stored water will be utilized to irrigate the command area below the tank. Tamil Nadu lies on the rain shadow area of Western Ghats. The southwest monsoon has little effect over Tamil Nadu. But the northeast monsoon, which is unpredictable, often accompanied by cyclones, pours heavily in short spells. Under these geographical and climatic conditions, the importance of rainwater and its conservations led to the evolution of tank irrigation in large scale all over Tamil Nadu. In Tamil Nadu, there are about 39,202 tanks spread all over the State. Nearly 30,000 of these tanks have been formed centuries ago. These tanks receive water either from its own catchment or from rivers/streams through diversion channels.

Generally, a tank will have a specified command area as well as a specified water spread area. Both of them, by and large, may be equal to each other. For example, tanks with 100 ha command area may have around 80 to 100 ha water spread area. This means that an area as much as the command area is required to store the required water. One of the major implications of the large water spread area is that of the heavy evaporation losses.

Tanks are extremely an important source of water supply for agriculture. The purpose of the tank is to store the water required for the

irrigating the land hence the conservation of a specified quantum of water is the main objective. But these tanks have been lost their purpose mainly because of silting up of the tanks over years. In many situations, tank remains the main source of groundwater recharge to its command area wells. Therefore it is essential to remove the silt by deepening bed and to reduce the water spread area. Deepening the bed makes the tank to function as a percolation pond in which case the groundwater may be recharged, which adds to an effective way of conservation.

1.2 OBJECTIVES

The following are the objectives of the study

i To study the hydrological characteristics of a tank system;

ii To assess the capability of the tank in conserving the maximum yield from rainfall over its catchments;

iii To assess the recharge capability of the tank and develop a relationship between tankwater depth and groundwater level;

iv To find the impact of partial de-silting by deepening the tank bed on the above factors;

1.3 CONTRIBUTION TO WATER RESOURCES DEVELOPMENT

The results from the study will help in evolving a strategy for the de-silting of tanks in future. The results also would facilitate in deciding on the need and quantum of earth to be removed from tank bed.

1.4 APPLYING THE RESEARCH TO USE

The idea is to deepen the tank bed and to reduce the water spread area in order to avoid losses. De-silting the bed may also make the tank to function as a percolation pond in which case the groundwater may be

recharged which would conserve more quantum of water. The removed soil can be dumped in a conveniently in the suitable place so that the level can be brought up to the tank bund. The space created can be utilized for other purposes as public activity place such as play grounds. De-silted soil can be utilized for strengthening the bund as well as for manufacturing bricks. Based on its nutrient content, it can be definitely utilized for agricultural lands.

1.5 CURRENT STATUS OF TANK IRRIGATION

After the independence, the canal irrigation was developed in a massive way including in the tank irrigated areas. The government, even under the Five years planning had not given due attention to keep the tanks in the state in good repair. Most of the public investment in irrigation has gone to major and medium canal irrigation. Accordingly, the public works Department conducted a pilot study in Puliampakkam tank and the CWR conducted a pilot study in Padiyanallur tank. The findings of these studies evoked interest of the European Economic Community (EEC), now it is called European Union. The EEC came forward in 1984 to assist the Govt. of Tamil Nadu to rehabilitate 205 tanks in Phase I with a grant of 25 Million Euros. With the lessons learnt from Phase I, European Union provided another 25 Million Euros in Phase II programme. Under this Phase II, 216 PWD tanks were rehabilitated. Due to the appreciation of the currency value, additional funds became available. Hence another 148 tanks including three chains of tanks were modernized under this phase II Extension.

Modernisation Components

Under the tank modernisation project, major thrust was on the improvement of the physical system aiming at

- effective acquisition of water resource;

- safe storage and surplus disposal;
- efficient distribution of the acquired water resources for crop production;

The components of tank modernisation were

(i) Catchment treatment

(ii) Improvement to tank feeder channel

(iii) Tank bund, sluice and surplus improvement

(iv) Lining field channels

(v) On farm development works

(vi) Community well construction

(vii) Farmers association building

In addition to that, adoption of improved agricultural practices, promoting water management with conjunctive use of surface and groundwater, establishment of farmers organisation were also contemplated.

1.6 IAMWARM PROJECT

This project was launched during 2007 which will be over a period of 6 years with a project out lay of Rs.2567 Crore. Main objectives of the IAMWARM project are

(i) Improving irrigation service delivery including adoption of modern water - saving irrigation technologies;

(ii) Forming water users associations and involving farmers in water resources management;

(iii) Agriculture intensification and diversification;

(iv) Strengthening institutions and instrument dealing with water resources management;

(v) Stabilise and increase the area (hectares) served by irrigation systems in 63 sub-basins;

(vi) Increase in agricultural productivity and stake holder income (net benefits per unit of water delivered in Rs/m^3);

(vii) Enhanced farm income adopting allied sectors through increase in fish production and livestock out put;

(viii) Increase in marketable surplus and commodity arrivals to markets;

(ix) Improved knowledge base and analytical capacity development for water resources management;

1.7 IMPORTANCE OF DE-SILTING

This project concentrated on the main system of rehabilitation and institutional reformations. It has increased the irrigated area to extent of 215830 ha and intensified the agriculture of 17 percent. It was able to increase the production of agriculture products of Rs.7.1 Billion per year.

The de-silting of the tanks had not been considered as a part of Tank Modernisation project as well as in the IAMWARM project as it involved a huge transportation of removed silt. The number of tanks modernized is very negligible, compared with the total number of tanks in Tamil Nadu. The modernized tanks are the large sized tanks under the control of WRO/PWD. But there are nearly 30000 small tanks with less than 40 ha ayacut are in the state. With the limited water resource and vagrant monsoon rainfall, we have to conserve every drop of rainwater. This research project aimed to de-silt the tank to improve its recharge potential as well as storage capacity. To de-silt the tank bed, one should decide where to de-silt? What

depth it is to be de-silted? Hence this project has been proposed a step by step procedure to de-silt the tank for the future need. Based on the above objectives following chapters were written.

1.8 OVERVIEW OF THE PROJECT

Chapter 2 provides the extensive literature review on geophysical study, infiltration rate, soil texture analysis, pumping test, well dilution techniques, tracer study in groundwater and numerical modeling of tank and aquifer nexus.

Chapter 3 concentrated on methodology and step by step procedure to attain the goal.

Chapter 4 extensively analysed the hydrologic and hydraulics of surfacewater and groundwater system and their interaction.

Chapter 5 concentrated on delineating the permeable zone through geophysical study and paved a way for de-silting the tank bed.

Chapter 6 described on evaluating the aquifer parameters through pumping test and well dilution techniques.

Chapter 7 aimed to evaluate the tank and aquifer connectivity through electrical resistivity method.

Chapter 8 estimated the seepage velocity and increase in groundwater potential before and after de-silting.

Chapter 9 integrated all the above said work and simulated the tank and aquifer system and evaluated the improvement in the groundwater potential and groundwater dynamics numerically.

Chapter 10 is the summary and conclusion of the project outcome and limitations.

CHAPTER – 2

LITERATURE REVIEW

2.1 INTRODUCTION

A literature review is a summary of previous research on a topic in which project has been carried. Literature reviews can either be a part of a larger report of a research project, a thesis or a bibliographic essay that is published separately in a scholarly journal.

The purpose of a literature review is to convey to the reader what knowledge and ideas have been established on a topic and what are the strengths and weaknesses. The literature review allows the reader to be brought up to date regarding the state of research in the field and familiarizes the reader with any contrasting perspectives and viewpoints on the topic. There are good reasons for beginning a literature review before starting a research project. These reasons include:

- To see what has and has not been investigated;
- To identify potential relationships between concepts and to identify researchable hypotheses;
- To learn how others have defined and measured key concepts;
- To identify data sources that other researches have used;
- To develop alternative research projects;

Several research works have been carried out on sediment deposition, infiltration test, permeability estimation, bore dilution techniques, geophysical survey and tracer study. Some of them are reviewed below under respective headings.

2.2 GROUNDWATER EXPLORATION METHODS

Groundwater exploration can be divided into two major groups, one is geo-hydrological methods. This method involves the actual drilling of a bore well in the area. From the well log data, the presence of an aquifer and variation in its thickness can be determined. Further the Geo-hydrological methods are more time consuming and also expensive due to drilling costs. On the other hand, geophysical methods of aquifer exploration is faster and practiced successfully all over the world now a days. The following information can be derived from the exploration using geophysical methods:

i. Depth of occurrence and thickness of the aquifers;

ii. Delineation of aquifer boundaries of a very large groundwater basin;

iii. Determination of distinctly different water bearing layers;

iv. Quality of groundwater and the spread of the pollution zone;

Electrical Resistivity and Seismic refraction are geophysical methods that have been applied in real field exploration. In addition, electromagnetic methods are also in practice to indicate the presence of conductive zone.

2.3 DELINEATING PERMEABLE ZONE BY ELECTROMAGNETIC SURVEY

Riberiro and Nunes (1999), have carried out a study to determine Permeable zone by geophysical survey. This approach may be a very useful tool for an aquifer parameterization when the available information is scarce. The VLF-R profiles were made at 183 kHz. The Profiles were made in the E-W direction, therefore it favouring the detection of structures with an N-S alignment. Electrode spacing was constant and equal to 5 m. The field data collected was out of phase Φ and apparent electrical resistivity ρ_a in each of the frequencies. The following heuristic relations between resistivity and permeability were assumed.

ρ_a<55 Ωm - high conductive fractures (very high potential permeability)

55<ρ_a<110 Ωm - less conductive fractures (high permeability)

110<ρ_a<220 Ωm - small fractures (low permeability)

ρ_a> 220 Ωm - unaltered rock (very low permeability).

Sharma *et al* (2005) carried out a study for delineation of groundwater-bearing fracture zone. Integrated electrical and electromagnetic surveys were carried out in hard rock areas of Purulia district (West Bengal). The entire area was surveyed in a relatively short time by the combined use of resistivity and electromagnetic surveys. The efficacy of the combination of VLF electromagnetic, DC resistivity soundings, and Wenner Profiling is to map the fractures in a hard rock area. The anomaly obtained in VLF measurements is an indication of the presence of conductive zone.

Metwaly *et al* (2006) have carried out a study to estimate the amount of fresh water recharge from Lake Nasser. There it has been no

information about seepage values, particularly in the northwestern part of the lake, due to the complete absence of boreholes. The average porosity of the Nubian sandstone aquifer is calculated using bulk resistivities by applying the Archie formula. The void ratio is estimated from the calculated porosity. The calculated void ratio is used to estimate hydraulic conductivity. Then Darcy's law is applied to calculate the seepage value of the lake water in the adjacent Nubian sandstone aquifer. The main result of the study shows that the anticipated water seepage value is 2.6×10^6 m^3 per year. This value seems reasonable in comparison with the total seepage value inferred from isotope studies around Lake Nasser.

2.4 GROUNDWATER EXPLORATION BY ELECTRICAL RESISTIVITY SURVEY

The resistivity measurements are normally made by passing current into the ground through two current electrodes (C1 and C2), and measuring the resulting voltage difference at two potential electrodes (P1 and P2), as shown in figure 2.1.

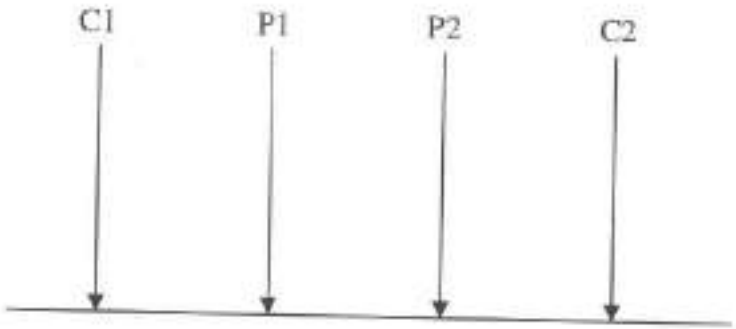

Figure 2.1 A Conventional Four Electrode Array to Measure the Subsurface Resistivity

From the current (I) and voltage (V) values, an apparent resistivity (ρ) value is calculated.

$$\rho_a = k\,V / I$$

where k is the geometric factor which depends on the arrangement of the four electrodes. Resistivity meters normally give a resistance value, R = V/I.

The calculated resistivity value is not the true resistivity of the subsurface, but an "apparent" value which is the resistivity of a homogeneous ground which will give the same resistance value for the same electrode arrangement. The relationship between the "apparent" resistivity and the "true" resistivity is a complex relationship. To determine the true subsurface resistivity, an inverse slope method is used.

2.4.1 Methods of investigation

(i) Resistivity depth probing or sounding is to detect vertical changes. Here the centre of the electrode spread remains fixed and the spacing between the electrodes is progressively increased until the maximum required depth is reached.

(ii) Electrodes separation in the traversing or profiling method is kept constant for two or three values and the centre of electrode is moved from one station to another to have the same constant electrode separations. Traversing or profiling is used to detect subsurface changes in horizontal direction or the lateral spread. Profiling can be carried out along a series of parallel lines and a resistivity contour map of the area showing iso resistivity lines can be prepared. This will indicate areas of high resistivity and will be useful in identifying aquifer formations.

2.4.2 Theoritical Foundations

For exploration of groundwater by geo electric methods the theory and mathematical expressions are well established. Mathematically, electrical

current flow (J) in a conducting medium is governed by Ohm's law. Similarly groundwater flow in a porous medium by Darcy's law.

Both having similar forms of equations:

$$J = -\sigma \frac{dv}{dr} \tag{2.1}$$

$$q = -k \frac{dh}{dr} \tag{2.2}$$

Where, J, σ, V, r, q, K, h are denoted respectively as current density (amps per unit area), electrical conductivity (Siemens/m = reciprocal resistivity, ρ ohm.m or Ω.m), electrical potential (volts), distance (metres), specific discharge (discharge per unit area), hydraulic conductivity (or permeability; m/s) and hydraulic head (m). The analogy between these two macroscopic phenomenon is widely accepted. Thus, the electrical method provides a powerful analogue and tool for groundwater exploration.

For homogeneous and isotropic medium, electric current and groundwater flow both satisfy the Laplace equation.

For electrical flow,

$$\frac{d^2v}{dr^2} + \frac{2}{r}\frac{dv}{dr} = 0 \tag{2.3}$$

and for groundwater flow,

$$\frac{d^2h}{dr^2} + \frac{1}{r}\frac{dh}{dr} = 0 \tag{2.4}$$

For a point current source, the solution of Eq. (2.3) in a semi-infinite, homogeneous medium for (hemispherical earth) electrical flow can be written as:

$$V = \frac{\rho I}{2\pi} \frac{1}{r} \tag{2.5}$$

and for hydraulic flow a similar equation can be written as:

$$h = \frac{Q}{2\pi T} \ln r \tag{2.6}$$

Transmissivity of an aquifer of saturated thickness b is expressed by

$$T = Kb \tag{2.7}$$

The solution to equation 2.4 is,

$$h = \frac{Q}{2\pi T} \ln r \tag{2.8}$$

There are no direct relations between resistivity and hydraulic parameters. Therefore, in this study, nonlinear relations between resistivity, transmissivity and permeability were established.

2.4.3 Types of electrode arrangement

There are mainly two common systems of electrode arrangement.

i) Wenner electrode arrangement
ii) Schlumberger electrode arrangement

Wenner Electrode Arrangement

In the Wenner system, the electrodes are spaced at equal distances and the apparent resistivity ρ_a for a measured resistance R(=V/I) is given by

$$\rho_a = 2\pi aR$$

and the field curve is plotted on a semi log paper 'ρ_a versus **a** ', ρ_a being in ohm-metres in logarithmic scale and metres in arithmetic scale.

Schlumberger Electode Arrangement

In Schlumberger system, the distance between the two inner potential electrodes 'b' is kept constant for some time and the distance between the current electrodes(L) is varied. The apparent resistivity ρ_a for a measured resistance R(=V/I) is given by

$$\rho a = \pi \frac{(L/2)^2-(b/2)^2}{b} R, \qquad L >> b \qquad (2.9)$$

$$\rho a = \frac{\pi L^2}{4b} R, \qquad \text{if} \quad L > 5b \qquad (2.10)$$

and the field curves are plotted on a log-log paper ρ_a versus L/2, ρ_a being in ohm-metres and L/2 in metres. The Wenner electrode arrangement and Schlumberger electrode arrangement are as shown in figure 2.2 (a and b).

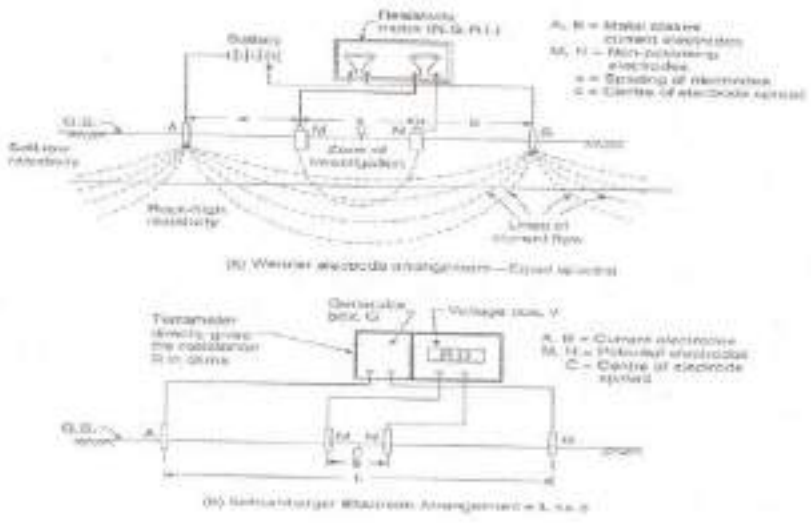

Figure 2.2 **a) Wenner electrode arrangement, b) Schlumberger electrode arrangement**

2.4.4 Inverse slope method

Sankara Narayan and Ramanuja Chary (1967) showed that it is possible to solve the field equations directly to get the resistivities and thickness of the sub-surface layers from the field data. Inverse slope method is used for the Schlumberger sounding to determine the true resistivity of the sub-surface layer. The inverse slope method identifies the thin layers, which is not possible with the curve matching/ inversion technique.

2.4.5 Relationship between geoelectric and Aquifer Parameters

Kelly (1977) correlated aquifer resistivities and hydraulic conductivity obtained from pumping test results in Rhode Island, USA. Heigold et al., (1979) found an inverse relationship between aquifer resistivity and hydraulic conductivity in Central Illinois, USA. Niwas Sri and Singhal (1981) in their analysis of the data concluded, that the relations between transverse resistance and transmissivity are more meaningful in alluvial aquifers than relations between longitudinal conductance and transmissivity. They gave case studies for alluvial aquifers in varying geological environments of northern India by establishing relations to these parameters. Frohlich and Kelly (1985) confirmed the applicability of relations between apparent formation factor and hydraulic conductivity for granular aquifers and transverse resistance and hydraulic conductivity in glacial aquifers in different parts of the USA. Shakeel et al (1988) used the method of co-kriging to estimate the transmissivity from measurements of specific capacity and electrical transverse resistance. In recent years, De Lima and Niwas Sri (2000) have estimated these parameters for sandstone aquifers by using IP-resistivity measurements and they concluded that the field and calculated values are in agreement.

2.4.6 Estimation of Aquifer Parameters from Geo-electric Parameters.

Singh et al (2005) correlated non-linearly, the observed permeability data of fractured rock aquifers with electrical resistivity of the aquifers estimated from resistivity sounding data. The empirical relations between aquifer parameters and resistivity are established for transforming resistivity distribution into permeability and transmissivity of the aquifer. In this study area, Schlumberger resistivity soundings have been assessed in both alluvial and fractured hard rock aquifers for possible relationships with the hydraulic parameters. Permeability is calculated from the published pumping test data for the study area. Then the resistivity values are exponentially fitted with the permeability data. From the permeability values, for the homogenous aquifer, transmissivity is determined.

Ratnakar and Singh et al (2005) carried out an integral approach of subsurface exploration. They expressed the application of geophysical methods in combination with pumping test at few sites, provides a cost effective and efficient alternative to estimate aquifer parameters. A correlation is established between apparent resistivity obtained through resistivity survey and aquifer parameters through pumping test. They conducted this study in Sukhinda valley, Jaipur District, Orissa. To determine the aquifer geometry and groundwater quality, 27 VES with maximum of half current electrode separation of 100 m have been carried out using Schlumberger electrode configuration system. Pumping test was performed in the five wells and finally correlated the geophysical and aquifer parameters. The Dar-Zarrouk parameters Longitudinal Unit conductance(s) and Transverse Resistance (T_R) were calculated for interpreted sounding layer parameters after taking into account only aquifer resistivities and its thickness. The value of formation factor (FF) is calculated using the aquifer resistivity (ρ) estimated from VES

and water resistivity of the formation (ρ_w) measured during the field investigation using the well known Archie's law. The hydraulic conductivity was estimated using the well-known equation T = K h. Using the calculated hydraulic conductivity (K) and formation factor (FF), a relationship was established between these parameters. Using this relationship the K values for remaining points were calculated and plotted against FF. Then the relationship between modified aquifer resistivity and hydraulic conductivity were obtained. The transmissivity of the study area was calculated using the equation hydraulic conductivity, transverse resistance and longitudinal conductance. The relation between transmissivity and transverse resistance was obtained by plotting the respective values. In this study the calculated aquifer parameters were well within the range of observed aquifer parameters.

Israil et al (2004) carried out a new method for groundwater recharge estimation using a surface resistivity method and isotope technique. The data used for the study are 32 vertical electrical resistivity sounding measurements at a station interval of 2 km. For the geological interpretation of resistivity values, the interpreted resistivity values were correlated with the known available borehole data in the study area. Tritium tagging studies were carried out at six sites selected on the basis of the resistivity values and the unsaturated soil layer of the study area. Ground water recharge was estimated by monitoring the vertical movement of the injected tritium and the position of the tracer is indicated by a peak in tritium activity versus depth plot. The soil samples were collected at the time of injecting the tritium and after three months and volumetric moisture content of each soil sample was estimated. The amount of recharge during the time interval of tritium injection and sampling was estimated by multiplying the peak shift and effective average volumetric content in the tritium peak shift region. Mathematically the equation for the estimation of percentage of recharge to groundwater is determined. The depth of water table was also monitored from these sites and

the linear relationship between water table fluctuation and recharge percentage was plotted. It shows that the vertical infiltration which constitutes the net recharge in the study area.

Balasubramanian et al (1985) used the resistivity method along the coastal aquifers of Tamiraparni Basin, Tirunelveli district, Tamil Nadu had analysed by preparing the combined maps of iso-resistivity and iso-pach. The results of an integrated approach using geophysical and geochemical investigations to delineate the fresh-water salt-water interface and also to demarcate the ground water potential zones. Since the individual interpretations are site specific an iso resistivity map of the area had been prepared. The depth of bed rock, conductivity map below the present exposed formations of the basin has been determined. Isochlor and Isolines map of Na+K provides the information about the quality of Groundwater.

Kenneth R Bradbury and Robert W Taylor (1984) combined Geophysical, Hydro-geologic data to evaluate the Lake-Aquifer relationships. Water depth and sediment thickness are measured on high resolution acoustic profiles at all sites. Sediment type inferred from offshore samples and acoustic profiles. Plot of log leakance values versus log longitudinal conductance values provide the relationship between these two variables. The limited offshore geophysical and hydrogeologic data show that a statistically inverse relationship exists between the leakance and longitudinal electrical conductance. Leakance is a measure of the potential for hydraulic connection , thus the longitudinal conductance values may be used to spatially map the relative hydraulic connection between lakes and aquifers.

Sharma et al (1985) conducted Geoelectrical investigations were in a close grid pattern in 70 sq.kms.area around Siwana, Western Rajasthan. Thirteen Vertical Electrical Soundings of Schlumberger configuration were conducted. Field data were interpreted using standard master curves. The

lithology of a piezometer was also compared with the resistivity data. Based on the results of the resistivity data and prevailing Hydro-geological features, a general picture of groundwater conditions around Siwana was obtained. Values of longitudinal conductance and transverse resistance help us to identify potential aquifer in the investigated area. This gives an idea of future exploitation of groundwater in the investigated area.

Reinhard Frolich et al (1989) related the electrical resistivity of the unsaturated zone to pore-water resistivity, porosity, saturation, electrical matrix conductivity and lithologic constants. The bulk electrical resistivity depends on water quality and quantity due to its dependence on pore-water resistivity and porosity. There is a decrease in the saturation of the vadose zone during the transition from late springs to the dry summer season. This decrease was correlated with the trasverse resistance of the unsaturated zone derived from an interpretation of geoelectrical depth soundings near the test wells in the fine to medium sand of the glacial outwash material, the surface conduction of the grains was found to negligibly small.

Sankar Kumar Nath et al (2000) carried out long duration pump tests at six locations, selected after detailed soundings to estimate transmissivity and hydraulic conductivity. Transverse resistance is obtained from resistivity values and plotted against transmissivity of the aquifer which is found to be functionally analogous. The formation factor is obtained through resistivity of the formation completely saturated with water, resistivity of the formation water obtained through the analysis of water samples and plotted against hydraulic conductivity. It is concluded that transmissivity is obtained from transverse resistance and can also be computed from resistivity formation factor.

2.5 ESTIMATION OF INFILTRATION RATE

2.5.1 Infiltration Rate at Various Slopes

Sharma and Singh (1983) had established relations between rainfall, basin characteristics and infiltration. Field experiments were conducted on a representative loamy sand soil for a period of six years (1975 - 1980). Basin width was kept constant to 2 m. Plots with three slopes - 0.5, 5 and 10 percent, and five slope lengths - 5.12, 7.0, 8.5, 10.75 and 14.5 m were used. With dry antecedent soil conditions, infiltration is governed by rainfall depth, whereas with wet antecedent soil conditions, raindrop impact (intensity) which forms a crust over the soil surface is the deciding factor. Also rainwater infiltration significantly decreases with increasing basin slope and reducing the slope length.

2.5.2 Infiltration in Complex Lateritic Soil Profile

Bruprecht and Schofield (1993) had carried out a study on infiltration characteristics of a complex lateritic soil profile. Large infiltration ponds (10-15m^2) were used, in conjunction with a double ring infiltrometer and a well permeameter, to determine the infiltration characteristics of a complex lateritic soil profiles. The infiltration ponds effectively measured the conductivity of a subsurface lateritic duricrust which was found to have a relatively high saturated hydraulic conductivity (Ks) of 2.7 meter per day. Removal of the topsoil identified large (about 1 m^2) unfilled holes penetrating the duricrust over about 6% by area. Measurements indicated that these large 'holes' had a high Ks value (about 10 m/d), whereas the remaining duricrust had a lower Ks value which is about 2 meters per day.

2.5.3 Artificial Recharge

Central Groundwater Board (1997), South Western Region, Bengaluru carried out a study on artificial recharge and stated that infiltration tests results at percolation tank beds prior and after de-silting showed an improvement in tank bed percolation. The infiltration rate ranged from 0.17 to 2.4 cm/hr prior to de-silting whereas the rate has increased in the range of 1.8 to 8.8 cm/hr after de-silting at Errapothenahalli. At Manchiganahalli, it ranged from 1.2 to 5.8 cm/hr prior to de-silting whereas the same was observed to be in the range of 10 to 16.8 cm/hr after de-silting. The ground water level data during post de-silting periods reveals a built-up in storage in the order of 2 to 4.5 m on the downstream of the tanks.

Muralidharan et al (2005), explained a procedure to evaluate the economically viable depth of de-siltation in old tanks to achieve a substantial increase in percolation and storage. An old minor irrigation tank and a newly constructed percolation tank were selected in a granitic terrain and infiltration studies were carried out with different thickness of silt removal. Tritium tracer studies were coupled with the infiltration studies to follow the infiltrated water and evaluated the effectiveness of silt removal in percolation. The study indicated that in the case of irrigation tank, a steady state infiltration rate of 67 mm/h has increased to 350 mm/h with the removal of 65 cm silt showing a six fold increase in infiltration rate. Infiltration rate was found to be reducing at the depth of 25 cm and 50 cm respectively. The reason for such was due to presence of clay at these depths. The study at percolation tank indicated that the infiltration rate of 10 - 20 mm/h has increased to a maximum of 310 mm/h with removal of 40 cm silt. The tritium tracer migration study supported a faster movement of percolated water at de-silted sites by showing a greater dilution of tracer concentration and deeper penetration. The research study strongly supports a necessity of carrying out infiltration studies at different

places within the tank bed area with removal of varying thickness of silt to decide the optimal level of de-siltation especially in the older tanks before commencing the revival of tank system.

The study by David Rugh (2006) aimed to assess the role of geologic structure on groundwater recharge at the Fractured Rock Research Site in the Blue Ridge province. Evaluating suspected recharge pathways for this study required applying large volumes of saline tracers at the surface and monitoring plume migration through regolith and fractured rock. Multi-level samplers and a deep well were installed for chemical sampling along the study transect. Physical monitoring of the unsaturated zone was performed using time domain reflectometry logging and tensiometers to evaluate recharge mechanisms at the site. The results of this study suggest that the shallow saprolite aquifer and the deep fault plane aquifer exhibit distinct and different recharge processes that reflect the underlying geology.

2.5.4 Infiltration Rate in Saturated Soil

Telis (2001) had carried out a study to estimate the infiltration rate of saturated soils. Soil infiltration measurements were made at 23 sites in the Caloosahatchee River Basin in southwestern Florida. In accordance with this designation by the South Florida Water Management District, 11 sites are classified in the rock landscape group, 7 in the flat woods landscape group, 4 in the slough landscape group, and 1 in the depression landscape group. Data from 16 sites were fitted to Horton's equation by using a regression analysis to estimate the infiltration rates of saturated soils. Seven of the sites did not fit the Horton's equation. The infiltration rate of saturated soils for these sites was estimated by averaging the data collected after the first 20 minutes of the test. For all sites, the estimated infiltration rates of saturated soils ranged from 9.8 to 115 centimeters per hour in flat woods, 3.4 to 66 centimeters per hour in rock, and 2.5 to 55 centimeters per hour in slough.

2.5.5 Infiltration Capacity during Summer and Winter

Diamond and Shanley (2003) had estimated the infiltration capacity of the dominant component of major soil associations and evaluated the reliability of infiltration tests. The objective of this study is to assess the infiltration capacity of some extensive soils in Ireland and also its spatial and temporal variability. Infiltration capacity was measured using double-ring Infiltrometer at one poorly drained, another imperfectly drained and other eight freely drained sites. The first series of measurements was performed for one day in summer. Eight years later a second series was performed for two days in winter and two days in summer at the same sites. There was a significant relationship between infiltration capacity and the antecedent soil water content, which contributed to the seasonal effect. Capacities in summer were 3.5 times of the winter values.

2.5.6 Infiltration Rate Before and After Tillage

Lipiec *et al.* (2005) had conducted an experiment on soil porosity and water infiltration as influenced by tillage method. The experiment was carried out on brown alluvial soil with particles < 0.02 mm, water content 48%, and organic matter content 2.3%. Four treatments, with four replicates arranged in a randomized block design, were as follows:

- Loosening to a depth of 20 cm which is named as CT.
- Loosening to a depth of 20 cm every 6 years and 5 cm every year which is named as S/CT.
- Shallow loosening to a depth of 5 cm each year which is named as S.
- Sowing to the uncultivated soil (No-till) in micro plot experiment.

A measurement of infiltration of water into the soil was determined by the double ring infiltrometer. To analyse the water-conducting pores methylene blue solution was infiltrated from the soil surface on delimited areas. The tillage treatments significantly affected pore size distribution. CT had greater percentage of pore volume for larger pore diameter (>100 μm) and lower pore volume of smaller pores (< 6 μm) compared to all other tillage treatments. The results indicate that pore system of conventionally tilled had large pores compared to no-till.

2.6 ESTIMATION OF AQUIFER PARAMETERS

2.6.1 Hydraulic Conductivity in Unsaturated Soil

Hoorn (1992) had carried out a study to determine hydraulic conductivity with the use of double ring infiltrometer. To determine the hydraulic conductivity of the various layers of a soil profile, one often encounters a situation where the groundwater table is 2 to 3 m below surface. In such cases the infiltrometer method can provide a solution. The infiltrometer can be used at successive depths in a soil pit to estimate the hydraulic conductivity of the various layers. According to the law of Darcy, the infiltration rate of water in unsaturated soil under a cylinder infiltrometer can be written as:

For unsaturated soil

$$v = K_T \frac{\phi + z + h}{z} \qquad (2.11)$$

Where,

v = infiltration rate

K_T = hydraulic conductivity of the transmission zone

ϕ = suction at the bottom of the transmission zone

Z = depth of the transmission zone below the infiltrometer

h = height of the water in the infiltrometer

2.6.2 Hydraulic Conductivity in Saturated Soil

Bodhinayake and Noborio (2004) had conducted a study for estimation of Field-Saturated Hydraulic Conductivity from Double-Ring Infiltrometer Measurements. The objective of this study is to examine if double-ring infiltrometer is suitable for determination of soil hydraulic properties on sloping soil surfaces. Experimental and numerical results of this study suggest that double-ring infiltrometer is suitable for characterization of surface soil hydraulic properties in landscapes with slopes up to 20 percent.

Field-saturated hydraulic conductivity, K_{fs} was estimated for each experimental unit from the one dimensional steady state infiltration rates obtained from the double ring infiltrometer following the procedure outlined by Reynolds et al (2002). The K_{fs} is given by

$$K_{fs} = \frac{q_s}{\left[\frac{H}{(C_1 d + C_2 \alpha_r)}\right] + \left[\frac{1}{[\alpha(C_1 d + C_2 \alpha_r)]}\right] + 1} \qquad (2.12)$$

Where,

q_s - Steady state infiltration rate

H - Steady depth of ponded water in the ring

d - depth of ring insertion into the soil

α_r - radius of the inner ring

α - inverse soil macroscopic capillary length parameter

C_1 - 0.316π and C_2 -0.184π are dimensionless quasi empirical constants

2.6.3 Estimation of Permeability through Well Dilution Techniques

Leap and Kaplan (1988) had derived an equation for determining the advection velocity from the single well drift and pump back tracer test from the laboratory experiments. Jui et al (1999) had evaluated transverse dispersion coefficient for tracer test conducted in a radially convergent flow field by two well methods.

Atkinson et al (2000) had conducted a laboratory study and concluded that Fluorscein had little sorption on chalk and it was assumed that the field results were unaffected by retardation. Three models were compared and he has concluded the estimation of transport parameter depends strongly on the model employed, with six fold variation in dispersivity.

Kumar and Nachiappan (2000) explained the single well dilution technique by using NaCl and Tritium. When compared, the K values estimated by the NaCl tracer are lower than those estimated by the tritium tracer. Since tritium is part of the water molecule itself and acts as a perfect tracer of groundwater movement, the results of the tritium dilution can be considered as the standard ones. The relationship between the K values estimated by the two methods is linear and is expressed by a simple equation. The linear relationship can be used to obtain comparatively accurate values of K for unconfined alluvial aquifers, when the NaCl tracer is used. In the single well dilution technique only Darcy Velocity can be estimated.

Tonder et al (2002) had done pumping test and estimated the aquifer parameter by using generalized Theis equation for fractured aquifer written by Barker (1988). He developed a generalized equation for fractured flow regime and recorded the video of borehole and they have identified the number of fracture and their size. The flow dimension and the extent of the

flow region are applied to the generalized equation. The cross area for dimensional flow given by half the borehole circumference. They had used NaCl, NaBr and Uranium for their tracer study. Tracer study was conducted by using single well injection, withdrawal and two well techniques. They had used the generalized equation for fractured flow regime and estimated filtration velocity, seepage velocity, forced velocity and dispersion coefficient and concluded that the values merge estimated by using the generalized equation for fractured flow regime is two times higher than the standard equation. Because the flow behavior of a fractured aquifer can be described with a generalized model like the Generalized Radial Flow Model, which accounts for the uncertainty in geometry, it is also correct to implement the fractional-flow dimension for the estimation of transport parameters. Transport and transport parameters depend more on the geometry of the flow system than the hydraulic properties of the aquifer.

Fank and Rock (2004) had estimated longitudinal dispersivity and analytically calibrating Peclet type curves on measured breakthrough curves. He compared the results with the two dimensional transport models for the test field based on a transient groundwater flow model.

2.6.4 Estimation of Permeabilty and Specific Yield in an Unconfined Aquifer

In areas of crystalline and basaltic rocks in India dug wells of large diameter may offer the opportunity to test the hydrologic characteristics of the shallow unconfined aquifer. Jacobs or Theis method is used only for estimating aquifer parameters in small diameter bore holes. But large diameter dug wells are seen in the study area . Hence this method cannot be adopted. For large diameter wells Slichter method is used to determine the specific yield and specific capacity of the well.

Slichter (1906) developed an equation to determine the specific capacity for the large diameter wells. It is based on the assumption that flow is from the bottom. It is based on the drawdown as well as the recovery performance. Specific capacity determine through Slichter's method depends on the area of the well. The Specific yield is determined through the Slichter's method which is independent of the area of the well. M.Kumaraswamy method is used to determine the permeability of the large diameter well in the unconfined aquifer.

2.6.5 Tank water Balance Components

Effective water balance components of the tank cascade system simulated by the cascade model, in start tanks, which are normally located in the upstream end of the cascade, the runoff from the catchment and rainfall on the tank water surface form the inflow components. The outflow components include evaporation of tank water, seepage through the tank embankment and percolation through the tank bed which referred as tank seepage, water issue for irrigation and spillway discharge

In normal and confluence tanks, in addition to the runoff generated in their own catchment and the rainfall on tank water surface, a fraction of the outflow from the immediately upstream tank(s) can flow in, increasing the total available water in the tanks. This additional inflow is treated as two different components of return flow, due to seepage and water issue, and return flow due to spillway discharge. In normal tanks, these flow components occur from the immediately upstream tank, whereas, in confluence tanks, inflow from the immediately upstream tanks (more than one) that are linked to the confluence tank which need to be incorporated. But outflow components of normal tanks and confluence tanks are similar to those of start tanks. In all three types of tanks, the fraction of outflow can only reach the immediately downstream tank as return flow.

The relevant information on the node-link system configuration needs to be specified as part of the input to the model that describes the physical system. Based on the survey data at each tank, mathematical expressions representing (1) tank area (2) tank water volume as functions of the tank water height and (3) tank water height as a function of tank water volume need to be formulated.

2.6.6 Simulation of Daily Tank Water Balance

The components of the tank water balance represent complex hydrological processes associated with the tank cascade system. For example, generating runoff from rainfall on a catchment is a complex process that involves interaction of effective climatic, geologic and topographic factors; vegetation characteristics; and antecedent conditions; of which the catchment accurate simulation of these complex processes can impose a substantial input data requirement and a detailed mathematical representation of the physical system and the relevant process on the model. The cascade model approximates the physical system and the effective water balance components with the use of several expressions and assumptions. Starting from the most upstream end of the tank cascade, the model performs water balance computations for each tank on a daily basis, based on the processing procedure illustrated in the flow chart. The model input consists of meteorological data and water release for irrigation on a daily basis and information on the physical system. In the process of calibration of the model, water released for irrigation measured in the field is used as the model input. In using the model for predictions, the required water release needs to be estimated considering the water requirements for land preparations and the crop water requirements for land preparation during the growing stage, based on cultivation events of different types of crops in the command area. In

either case, through the daily water balance computations, the model allows release of the required irrigation water when the storage is adequate.

If the storage is insufficient, the model calculates the allowable water release and it will be less than the measured water release for the day. In addition to the allowable water issue, the model provides output at the end of each day including the tank water height, tank storage and information on the tank water balance components.

Runoff generation is a complex process influenced by several factors such as antecedent precipitation index, soil type, topographic slope and vegetation. Slope and vegetation are the two parameters used in the model that need calibration. The model calculates the tank seepage based on the functions derived from an analysis of the observed tank water loss during the time period of without rainfall.

Ponrajah (1984) expressed the tank seepage is estimated as 50 percent of the tank volume per month. Tasumi et al. 1999 expressed the tank seepage is 2.4 percent of the water volume per day.

Dekker et al used seepage barrels to measure seepage losses through the bottom of small reservoirs. Seepage barrels is used to measure seepage velocity. It is installed in such a way to get a good representative of the spatial variability of seepage. Experiments were carried out at six locations in the reservoir. Average seepage rate is 1.12 mm/hr which is half of the average evaporation in the region and is 1.26 times greater than the reservoir storage capacity. Seepage in small reservoirs can reach values as high as 24 mm/day representing a significant components of the water balance.

Kevin Kahmark and Van Matt reviewed intensive literature to estimate seepage rate. Techniques identified in the literature include seepage meter, infiltrometer or piezometer installations, water balance methods, tracer studies and numerical simulations. There are two methods that emerged with potential application to the paper industry are seepage meter and infiltrometer. Seepage meters would provide the best approach to measure the seepage of an unlined canal. Field trails confirmed that modified seepage materials could be a useful tool in measuring the seepage.

Grismer and Mccullough-Saden studied the effects of salinity at the time of ponding on estimated seepage from evaporation ponds using infiltrometers. Seepage rates calculated through infiltrometers proved to be similar to seepage estimated by mass balance calculations. Gradual increases in salinity had only a minor effect on seepage rates. Seepage rates irreversibly decreased over time may be the impact of biological activity and deposition of suspended matter.

Wallace et al. studied the seepage rate using Darcy's law

$$Q = kiA, \qquad (2.13)$$

Where,

Q = discharge quantity L^3/T

K = hydraulic conductivity L/T

I = hydraulic gradient L/L

A = area of interest (L^2)

The cross sectional area of interest was the length of the basin parallel to the river multiplied by the depth of the basin. Seepage rates was

reduced over time due to deposition of fine organic material that fills up available pore space.

Chescheir (1988) estimated seepage rates of stormwater infiltration bonds through mass balance approach. He used to develop an approximate analytic solution for calculating 3-D pond seepage rates and compared the results with numerical models.

Literature review on seepage rates, identified numerous techniques including pre-construction methods, mathematical models, field methods or laboratory studies. Laboratory studies under estimates the actual hydraulic conductivity. Mathematical equations give a general understanding of the possible mechanics involved in a system but are typically a simplification of real world system. Pre-construction methods are completed prior to lagoon flooding and therefore not accurate. In-situ field methods such as permeability tests and infiltration tests can be more accurate than laboratory tests or models. In general these methods almost completely replicate the actual field condition.

From the literature review, it is understood that once the relationship between aquifer parameters and geo-electric parameters are established for a particular area, then aquifer parameters of concern area can be estimated through empirical relationship without carrying out further field study.

The following inferences can be obtained from the above studies:

- Electromagnetic method is fast and suitable method for studying the geology of an area;
- The suitable method for delineating a permeable zone is geophysical method;

- Double ring infiltrometer is the most suitable method for determining infiltration rate;
- Infiltration test results of the percolation tanks after de-silting, the value of infiltration rate increases considerably;

2.7 LITERATURE ON FLUORESCENT DYES

Fluorescent dye tracing techniques are now widely used in hydrology. In surface water they are commonly used for dye dilution - gauging [Cobb and Balley, 1965] in particularly for the calibration of structures [Kilpatrick, 1968] where current meter is difficult, for instance, under an ice cover [Kilpatrick, 1967] or in steep rocky channels [Church and Kellerhals, 1970]. Dyes are used for time of travel studies [Buchanan, 1964] for dispersion experiments in rivers [Yotsukura et al 1970] and in marine estuarine environments [Pritchard and Carpenter, 1960]. The tracing of karst ground water has been frequently carried out by using fluorescent dyes [Drew, 1968; Brown et al 1969]; though application in other aquifers have been largely limited to oil fields [Sturm and Johnson, 1950]. Dyes have also been employed for point dilution studies in wells [Lewis et al 1966]. Reynolds [1966] reported the use of fluorescent dye for tracing soil water, while Robinson and Donaldson [1967] had studied water uptake in plants, using these tracer. There are also significant application of dye tracing technique in engineering , for instant circulation studies in chlorine contact chambers [Deaner, 1970] and infiltration measurements in foul water sewers [Smith and Kepple, 1972].

Of the commonly used fluorescent dyes, fluorescein (Colour Index (CI) 45350) had been used since in the end of the nineteenth century [Dole, 1960]. It is visibly detected in low concentration but has very poor stability under sunlight. Thus in the early 1960's when workers in the United States

and Japan were assessing fluorescent dye for quantitative tracing work in surface water, they adopted the equally fluorescent dye rhodamine B (CI 45170 [Pritchard and Carpenter, 1960]). However it became apparent that rhodamine B was readily adsorbed onto sediments and subsequently sulphorhodamine B (CI 45100) was introduced. Although these dyes were resistant to adsorption, it was comparatively expensive and was later replaced by the cheaper dye rhodamine WT which was developed specifically for tracing work. Reynolds [1966] used the green dye pyranine (CI 59040) for tracing percolation water because it was very resistant to adsorption. Recently a group of blue fluorescent dyes, known as optical brighteners have been applied to water tracing [Glover, 1972].

Feuerstein and Selleck (1963) investigated the behavior of three fluorescent dyes, including fluorescein, for use in surface water tracing (flow rate) studies. The following parameters were found to affect the analysis of the dyes: (1) temperature, (2) salinity, (3) pH, (4) background fluorescence of dye free sample, and (5) turbidity and suspended solids. Fluorescein exhibited high photochemical decay, and high levels of background fluorescence were encountered when analyzing for fluorescein. The fluorescence of fluorescein was seen to decrease at pH values below 5. The fluorescein was the least adsorbed of the three dyes, investigated on suspended solids and algae.

Smart and Laidlaw (1977) discussed the use of eight fluorescent dyes, including Rhodamine WT (RWT) and fluorescein, in surface water tracing (flow rate) studies. The fluorescence of both RWT and fluorescein was shown to be a function of temperature. The fluorescence of the dyes was seen to decrease at low pH and was observed to be a function of the ions causing the pH change and the buffering system. The presence of organic matter in the water samples produced greater background fluorescence for fluorescein than for rhodamine WT. Photochemical decay was observed to be

significant for fluorescein (greater for sunlight than artificial light) but relatively insignificant for rhodamine WT. It was observed that rhodamine WT strongly adsorbed to organic and inorganic solid phases than fluorescein. The organic phases (sawdust, humus, heather) were observed that more adsorption than inorganic phases (clays, limestone, orthoquartzite) for both rhodamine WT and fluorescein.

2.7.1 Effect of positively and negatively charged soil on fluorescent dyes

Kasnavia et al (1999) discusses the importance of fluorescent dye adsorption when selecting dye for tracer studies. The effect of dye and media properties on dye adsorption was evaluated using four fluorescent dyes namely fluorescein, rhodamine B, rhodamine WT and sulphorhodamine B with two different soil component such as alumina and silica (net negative & positive charges as neutral pH respectively). Fluorescent dyes are large organic molecules that would not only increase the water solubility with its ionic functional group, but also decrease the dye sorption due to hydrophobic force.

Batch and column studies were conducted with four fluorescent dyes for the experiment studies. The dyes were analyzed using spectro fluoro meter. In column study 1 cm diameter 15 cm in length column was used and it saturated slowly at a constant flow rate of 0.5 ml/min and here methanol was used as conservative tracer for column study with alumina and bromide was used with silica. The isotherm data were interpreted using the Freundlich isotherm (KFR) and experiment conducted on two pH of 7 and 9 on alumina; Fluorescein which has only negative functional groups adsorbed least on the negatively charged silica but most onto positiviely charged alumina. The Rhodamine dyes, with a permanent positively charged and negatively charged functional group adsorbed on both alumina and silica. Sulforhodamine B,

with two strongly electronegative group adsorbed less on to negatively charged silica than Rhodamine WT which has two carboxyl groups. They concluded that the fluorescent dyes were subjected to sorption depends on the dye selection which is based on their chemical properties, media characteristics.

Francisco et al (2000) explored the chemical characteristics and sorption behavior of tracer grade Rhodamine WT and EPA approved fluorescent tracer that is structurally similar to several polar/inorganic, organic agrochemicals to develop a interrelationships between the environment behavior of rhodamine WT. This research provides a systematic analysis of the composition and structure of tracer grade Rhodamine WT constituent, a comparison affinity with the various subsurface materials such as (i) fine grain sand (ii) iron oxide (iii) aluminium oxide (iv) iron oxide coated fine sand (v) coarse sand treated with water by removing organic contents.

Batch experiments were conducted to examine the sorption behavior as a function of dissolved RWT concentration, pH and time. The Rhodamine WT isomers are differing in structure with respect to the position of the carboxylic acid group on the aromatic ring. The sand possesses variable charges and the sorption isotherm could vary and depends upon the sand based material. The sorption in aluminium oxide is greater when compared to iron oxide, and sorption was grater on to fine sand than coarse grain material, this was due to small particle size and high surface area. The greater extent of sorption on the coarse grain sand, containing organic matter suggest RWT isomers, interact with minerals and organic surface and was less in treated coarse sand and concluded that RWT does not partition to organic matter alone and also subject to hydrophobic compounds.

Sabatini (2000) evaluated the sorption of two fluorescent dyes namely fluorescein and sulforhodamine B with two oppositely charged consolidated aquifer materials such as sandstone and limestone. Fluorescein which had an anionic carboxylic group experienced negligible sorption onto negatively charged sandstone and sorbed much less than sulforhodamine B, with its two sulfonic groups, on to positively charged limestone. The cationic charge on sulforhodamine B caused to adsorb onto negatively charged sandstone. Sorption kinetic rates decreased with increasing particle size, which is consistent with diffusion limited intraparticle adsorption. Tortuosity factor were determined by fitting a diffusion limited intraparticle sorption model to kinetic data for one particle size. Close agreement between experimental data and model prediction gives intraparticle diffusion limited sorption as an important process. Diffusion limited adsorbtion can impact dye transport in unconsolidated grains having internal porosity or consolidated or fractured media having dual porosity. The results demonstrated the importance of understanding both equilibrium and kinetics of dye sorption for tracer studies.

2.7.2 Determination of Retardation Factor (R_f)

Thomas et al (2003) reported that locating and characterizing dense non aqueous phase liquids (DNAPL) is one of the most important challenges in groundwater remediation. Partitioning tracers is one way to meet this task. In this study, five fluorescent dyes were evaluated as partitioning traces for detection and quantification of tetra chloro ethylene (PCE): fluorescein, rhodamine WT (RWT), sulforhodamine B (SRB), eosine, and pyranine. The objective of the study is to evaluate best suitable tracer in water saturated porous media with tetra chloro ethlene (PCE) using column study. Five fluorescent dyes were tested and conducted at room temperature. Column test experiment was conducted in Chromatography column by using Ottawa sand

and the soil is allowed to saturate for 48 hours. Its Weight was measured and parameter properties such as column length, diameter, pore volume, porosity, bulk density and water content were considered. The flow was pumped through the column vertically using peristaltic pump.

Effect of sulfonic group sorption

Mon et al (2006) compared the adsorption characteristic of four triarylmathane dyes and investigated the suitability of column experiment for measuring the sorption isotherms. Sorption isotherm determined with column experiment using sandy soil. Batch experiment was conducted with nine different concentration maximum up to 2000 mg/l, and dye adsorbed was calculated by mass balance equation by considering adsorbed concentration and final solution concentration. Porosity, flow rate and bulk density. The column breakthrough data were used to determine the sorption isotherm of a chemical. The sorption isotherm can be derived from the desorption of breakthrough curve as shown in Burgisser et al (1993).

The results of both column and batch studies show that C.I. Food Blue 2 and C.I. Food Green 3 were sorbed less than C.I Acid Blue 7 and C.I. Acid Green 9. The main difference among these four dyes is the number of sulfonic acid groups in their structures: C.I. Food blue 2 and C.I. Food Green 3 contain three sulfonic acid groups, while C.I. Acid Blue 7 and C.I. Acid Green 9 contain only two sulfonic acid groups. It had been reported that dyes consisting of more sulfonic acid groups tend to sorb less and have a better mobility in soils than dyes with fewer sulfonic acid groups (Corey, 1968; Reife and Freeman, 1996).

2.7.3 Dye Study in streams / rivers

Bauwens et al (1982) carried out travel time measurement in a river with alluvial sediment and organic material to study the influence of adsorption of fluorescent tracer on the travel time determination. Three types of dyes, rhodamine B, rhodamine WT, sulphorhodamine B were used in the laboratory and also in the field.

Laboratory Tests

Bottom samples were taken from the bed of the river soil contained 4.25 % clay and 0.7 % organic material. A solution of 500 ml with dye concentration of 30 ppb was brought into contact with 150 gm of soil without shaking and stirring. The change of concentration with time was measured. The exposed soil area was about 100 cm^2 and the pH of the solution was in the range of 6.5% to 7.0% for all the tests. The loss in concentration after 40 min was about 72 % for rhodamine B and 11 % for rhodamine WT. A similar experiment with a soil that contained only 0.5 % organic material and no clay, showed values of 55 and 12 % respectively.

Rhodamine B is for more liable to adsorption than rhodamine WT. The amount of clay and organic material present in the water, influence the adsorption. Rhodamine B is a cationic dye and will be more prone to adsorption than the anionic one.

Field Experiment

Comparative travel time measurements were carried out on the river over a length of 3.5 km. For the first test, 5.5 g of rhodamine B and rhodamine WT were injected with a time interval of 2 hours. The time of the concentration are delayed for the rhodamine B concentration curve with

respect to the rhodamine WT curve. The curve of the rhodamine B concentration is much more asymmetric than the rhodamine WT curve. A possible explanation for this phenomenon is the adsorption of rhodamine B on sediment that moves slower than the water. Approximately 47 and 38 % of rhodamine B and rhodamine WT were lost respectively during this experiment.

Similarly rhodamine WT and sulpho rhodamine B was injected and both curves of rhodamine WT and sulpho rhodamine B have the same form and same lead front, peak and centroid velocity. About 25 and 34 % of the rhodamine WT and sulpho rhodamine B were lost, respectively.

Travel time Measurement in the River

The length between the injection and the measurement point is about 8300 m and the overall slope 0.78 parts per thousand. Sulpho rhodamine B was used as a tracer.

Four measurements were carried out at discharge of about 5, 7, 18, and 26 m^3/s during the period of 15 January to 15 April, 1981. According to Leopold et al., (1964)and Pilgrim (1976 and 1977) the relationship between the velocity and discharge can be estimated by

$V = aQ^b$

For small river

b= 0.39 to 0.51

Experiment found b= 0.24

An empirical relationship between V and Q was

$V = aQ/1 + bQ$

a = 0.285 and b = 0.299

Experimental values of D_t were compared with different values found in the literature. The coefficient given by Elder (1959) is too low since he did not take into account the lateral velocity gradient. Satisfactory predictions are given by the equation of Fischer (1975) and Liw (1977).

Experimental travel time measurement in a river with a alluvial sediment and polluted organic material showed that rhodamine B is not reliable tracer, especially when the time of the centroid of the concentration curve is used as the travel time. Other tracers rhodamine WT and sulpho rhodamine B can be used for travel time measurement. It showed that the velocity tends to a limit with increasing discharge.

Suijlen et al (1994) measured the dispersal of 0.13 kg of water tracer rhodamine WT in the Loosdrecht lakes surveyed during 19 months. Solid phase extraction and liquid chromatography were used to measure the very low concentration of rhodamine WT. The detection limit was approximately 2×10^{-11} kg/m^3. This dispersal was assessed with a numerical model that mimics the photolysis and dilution of photolytic water tracer on relatively long time scales, for which the model was developed. Model results matched well with observation showing that rhodamine WT is well suited for tracer experiments on large time and space scales, provided that photolysis is taken into account. Three model simulations were made. First simulation shows the photolysis. Second takes account only of the flushing of lakes. Both are accounted for in the third simulation. The measurements and the calculated concentration were matched well.

Winfield Wright and Bravan Moore (2003) described a tracer-injection studies that were done in the river watershed to determine whether the stream from the river infiltrates into the mine or nearby area. This study was designed to determine it stream infiltration into the mine. Four separate tracer-injection tests were done, by using lithium bromide (LiBr), optical

brightener dye, and sodium chloride (NaCl) as tracer solution. Two of the tracers were injected continuously for 24 hours, and one of the NaCl tracer was injected continuously for 12 hours, and one of NaCl tracer was injected over a period of 1 hour. More than 200 water samples were collected from the mine. Increase in tracer constituents were detected in water discharging from the mine, concluding a surface water and groundwater connection between the stream and the mine. Different timing and magnitude of tracer breakthroughs indicated multiple flow paths with different residence times from the stream to the mine. Discharge measurements indicated that about 0.5 ft^3/s may be flowing into the mine.

Bala´zs Fekete et al (2006), widely used isotope tracers to study hydrological processes in small catchments, but their use in continental-scale hydrological modeling has been limited. This paper describes the development of an isotope-enabled global water balance and transport model capable of simulating key hydrological processes and associated isotopic responses at the large scale. Simulations and comparisons of isotopic signals in precipitation and river discharge from available datasets, particularly the IAEA GNIP global precipitation climatology and the USGS river isotope dataset spanning the contiguous United States, as well as selected predictions of isotopic response in yet unmonitored areas illustrate the potential for isotopes to be applied as a diagnostic tool in water cycle model development. Various realistic and synthetic forcing of the global hydrologic and isotopic signals are discussed. The test runs demonstrate that the primary control on isotope composition of river discharge is the isotope composition of precipitation, with land surface characteristics and precipitation amount having less impact. Despite limited availability of river isotope data at present, the application of realistic climatic and isotopic inputs in the model also provides a better understanding of the global distribution of isotopic variations in evapo transpiration and runoff, and reveals a plausible approach

for constraining the partitioning of surface and subsurface runoff and the size and variability of the effective groundwater pool at the macro-scale.

2.7.4 Dye Study in Ground Water

Field Study

James F. Wilson used rhodamine family to measure the time of travel, dispersion and stream flow. The primary purpose of this paper is to describe the methodology and also to illustrate the versatility of dye tracing such as estuarine dispersion studies, herbicide tracing, stream flow measurements and ground water studies.

Time of travel can be estimated by the volume displacement method. In a given reach of stream, the mean velocity of water is equal to the ratio of average discharge in the reach to the average cross sectional area and mean travel time is the ratio of length of reach to the mean velocity. The dye tracers are used to estimate mean travel time of solution, and also dispersion pattern of the solute material.

Rhodamine B was used for the measurement of time travel. The USGS measured on nearly 100 streams in approximately 30 states, the amount of dye used is up to 1800 kg which depends on discharge, velocity and reach length. Empirically determined in many studies that 5×10^{-6} g of 40 % of rhodamine B solution for every kilogram of water in reach yield maximum concentration of 5, 10 ppb at lower end. From the result of the various field, it shows that there is no limit to the size and length of river, which may be studied by dye tracing. Cumulative mean travel time for 8 sub reaches were 182 and 254 hours at index discharge of 1.54 and 10.6 m^3/s respectively, indicating that time of travel varies with discharge, so this objective is made to study at different discharge .

The other applications, that are given in the paper are dyes such as rhodamine WT similar to rhodamine B was used that have significantly less tendency to be absorbed on solid which are preferred for dye dilution discharge measurement. Dyes undoubtedly are less suitable for ground water studies than for surface water studies, but nevertheless have been used successfully in a variety of experiment.

The authors Steppuhn and Meiman (1971), determined the water discharge rates at chosen instant of time and also measured the time of travel. He used field component of the film system for detecting water borne fluorescent tracer. Fluorescence was measured directly through a field sited fluorometer or by bringing the samples to a laboratory. Two basic methods are used in tracer dilution gauging; total recovery and constant rate methods. Both methods involve the release of a tracer solution of known concentration into a water course and the samplings were done at a down stream. In the total recovery method, a sudden release of the tracer into the water, while a continuous, steady release is employed in other method. From the total recovery method the discharge rates are

$$Q = \frac{VC_1}{\int_0^t C2\, dt} \qquad (2.14)$$

$$Q = q\, C_1/C_2 \qquad (2.15)$$

Q is the instantaneous rate of discharge under the steady rate flow condition.

V is the volume of tracer solution.

C_1 is the initial concentration released suddenly into the water.

C_2 is concentration of the tracer in the water after complete mixing.

dt is infinitesimal segment of total time.

q is constant rate of tracer injection into the water of a tracer concentration C_i.

t is the time required to pass the sampling point.

Time of the travel of a stream refers to the average speed with which a volume of its water flows through a given reach. Time of travel was determined by timing the travel of fluorescent tracer through a known distance stream reach.

The film system proved applicable to the production of water discharge hydrograph. It was tested with a 12 ppb rhodamine WT dye solution containing 2600 parts per million (ppm) of suspended bentonite composed of 76 % clay, 19 % silt, and 5 % fine sand. From this study it was found that the quality of dye taken up was 2.5 % less than from a comparable solution free sediment, using a dye strength of 10 ppb, suspended sediment concentration of 1000 ppm, and measuring the fluorescence of discrete liquid samples, they found 6% of dye loss by sorption.

The use of fluorescent tracer to detect ground water movement has not been universally successful. It is suggested that these tracer would be used more in ground water and surface studies.

Stephen Hall et al estimated ground water velocity and effective porosity. Estimation of ground water velocity based either on Darcy's law or on the single well drift and the pump back tracer method require prior knowledge of effective porosity. This paper is based on the data gathered during aquifer characterization project, conducted for the purpose of designing an efficient well field for an aquifer thermal energy storage system. Leap and Kaplan (1988) described a single well drift and pump back tracer test and useful for estimating ground water velocity.

Unlike Darcy's law, test results were independent of gradient and hydraulic conductivity. The test was performed by injecting a tracer solution into the test wells, by allowing the tracer to travel. Under the influence of the natural gradient for a period of time and by pumping the test well, the tracer was recovered. No monitoring well is required. The ground water velocity is calculated as a function of time, the time required to reach the center of mass of the tracer, the pumping rate, the aquifer thickness and the effective porosity.

In this paper, the Darcy's equation and the equation for the drift and pump back test were treated as two simultaneous nonlinear equation having two unknowns (i) velocity and (ii) effective porosity. By solving the equation either graphically or algebraically, a unique solution for these parameters were obtained. This approach has been tested in the field and corroborated using a dual well tracer test conducted under natural gradient.

Darcy's law including an effective porosity can be written as:

$$V=KI/n \tag{2.15}$$

Where,

V is average linear groundwater velocity

K is horizontal hydraulic conductivity

I is hydraulic gradient

n is effective porosity

Drift and pump back test equation described by Leap and Kaplan (1988) is

$$V= (Qt / \pi bn)^{1/2} / d \tag{2.16}$$

Q is pumping rate during recovery of the tracer

t is the time elapsed from the start of pumping until the center of the mass of the tracer is recovered

b is aquifer thickness

d is time elapsed from the injection of the tracer until the center of the mass of the tracer is recovered by pumping (i.e. drift time plus t)

Equation (2.16) was derived for homogeneous confined aquifers dominated by steady state horizontal advective transport and having a locally constant hydraulic gradient. Equation (2.15) and (2.16) were rearranged to yield algebraic expression for velocity and porosity,

Where

$V = Qt / \pi bd^2 kI$

$n = \pi bk^2 I^2 d^2 / Qt$

Thus velocity and porosity can be directly calculated from experimental results. This drift and pump back method was applied at alabama in the unconfined aquifer. Bromide was injected under natural gradient for 3760 min from the midpoint of tracer injection. The bromide concentration was approximately 1.4 mg/l just after pumping began and then to zero after 5 minutes. There were two spike observed. The dual peaks may have been caused by the use of the fresh water chaser to force the bromide solution out or the well bore and into the sediments. Dual well tracer test was at a distance of 80 ft directly down gradient from the test well, therefore serve as a monitoring well for a dual well tracer test conducted under natural gradient.

If the transmissivity of a well and the local horizontal hydraulic gradient are known, ground water velocity can be estimated using a drift and pump back tracer test. Tracer solution must be concentrated than dual well test because of dilution during pump back. The peak bromide concentration observed during pump back was less than 2 % of the concentration of the

injected tracer solution. In contrast, the peak bromide concentration observed during dual well test was 24 % of the injected concentration despite dispersion along the 80 ft drift path. The error may be due to sampling the concentration through the bore of the monitoring well.

Roy F. Weston, reported the dye trace study used water-soluble dyes that could be detected both visually and by measuring the fluorescent emissions resulting from ultraviolet light excitation. Roy F. Weston, (1991) explains both qualitative and quantitative information about dye tracer study. The author explains the basic design for the dye trace study was a two-dye approach consisting of injecting one dye into the outlet of the UVB system (diverging test) and injecting a second dye in well PW2 (converging test), the intermediate depth well from the well cluster nearest the UVB system. A two-dye approach was selected to reduce the time required to demonstrate circulation in the zone between the UVB system and wells PW1 and PW2. This information provides data that are used to demonstrate the hydraulic interconnection between the UVB system and wells PW1, PW2, and PW3, calculate aquifer characteristics and indicating a high degree of groundwater circulation within the system. Analytical methodology included both field and laboratory methods. Field analysis consisted of visual examination of water samples using both ambient and ultraviolet lighting to examine for dye presence. At low concentrations (approximately 10 µg/L), both dyes were readily visible with these simple methods. Additionally, a scanning spectro fluoro meter was used in the on-site laboratory for the analysis of fluorescent emissions.

The author explained the following activities associated with the dye trace study included, (1) collecting background samples and evaluating background fluorescence, (2) injecting the dye, (3) collecting carbon bugs and groundwater grab samples, (4) qualitatively analyzing carbon bug samples to

determine the presence or absence of dye, (5) quantitatively analyzing groundwater samples to measure dye concentrations, and (6) field and laboratory quality assurance, quality control (QA/QC) samples, calibration checks to measure accuracy, precision, and instrument performance.

Kelvin De Fosset, (2004) explained Econfina Creek flows from its headwaters in southwest Jackson County to Bay County; ultimately discharging to Deer Point Lake, the primary water supply for Bay County. Along the middle portion of Econfina Creek in Washington and Bay counties, thirty-nine known Floridan Aquifer springs exist, represented as both individual springs and spring groups. A fluorescent dye tracer study was completed as an initial attempt to demonstrate the existence of individual spring sheds within the more general zone of contribution, established by the earlier work. To accomplish this, ground water flow connections that exist between areas of recharge to the Floridan Aquifer and springs located along Econfina Creek was understood. Fluorescent tracer studies have proven effective in determining such connections in karst aquifer systems. Two tracer studies were completed during the course of the study. Knowledge gained of existing ground water flow connections and flow patterns allowed a preliminary understanding of individual springsheds that exist in the basin. This information should aid similar future efforts in the basin. The ground water flow connections established by the two dye tracers provide an initial understanding of the ground water flow pattern in the area. The results reveal that in this portion of the basin, a dispersive ground water flow pattern exists between areas of aquifer recharge and springs located along Econfina Creek. This pattern is demonstrated in the first trace by the recovery of dye at seven different monitoring sites representing approximately 20 springs located along one mile of Econfina Creek. Dye introduced during the second trace was recovered at three different monitoring sites representing 11 known springs located along one and half mile of Econfina Creek.

Reide Corbett et al (2000) monitored ground water flow on an island down field from waste water systems using artificial tracer technique sulphur hexafluoride and fluorescein dye were used to determine ground water velocity, hydraulic conductivity and dispersivity at selected sites on the island. Monthly hydraulic head fluctuation is due to rainfall recharge and tidal influences. The direction and magnitude of ground water flow has been influenced by the tides with in 30m of the water heads. The results from this study helps to develop a better management plans to protect ecosystems.

The water level fluctuation in a well in response to changes in sea level may be used to determine certain aquifer characteristics. The transmissivity of the aquifer was estimated using the time delay that occurs between the high tide and low tide.

Aquifer's transmissivity as

$$T = \frac{X^2 S t_0}{4\pi t^2} \qquad (2.17)$$

where

T is transmissivity (m^2 day^{-1})

x is distance from tidal source (m)

S is Storage Coefficient

t_0 is period of tidal (Day)

t is time delay to successive, maximum or minimum between surface water body and well (Day)

Hydraulic conductivity was estimated by

T=kb

k is hydraulic conductivity (m day^{-1})

b is saturated aquifer thickness

Aquifer thickness changes with respect to tidal action

Hydraulic conductivity varies from 20 - 180 m/day. The largest 180 m/day and smallest 20 m/day were observed in the wells furthest inland and shoreward respectively. Tracer studies also provided information about the hydrologic characteristics dispersivity and hydraulic conductivity

Two tracer experiments were conducted at the site. In each case the tracer was dissolved in 190 liters tap water from the site and the fluorescein was then injected directly through a 5 cm PVC into monitoring well and sulphur hexafluoride (SF_6) into the drain field by pass in the waste water tank. The tracer was then followed by 100 L of tap water action and chaser wells were monitored at least monthly down field from the injection sites over 8 - 18 months.

Fluorescein tracer appeared above detection limits only in two wells. The dye was never detected in five wells on either side of the injection point. The horizontal transport range was 0.12 – 0.13 m/day at one site. Similarly SF_6 was only detected in two wells. The ground water velocity were 0.16 m/day to 0.42 m/day.

The results obtained from one site were similar to those observed during the experiment site. There was very little dilution of the injected tracer on the order of 3-5 times less than the injected values.

Aquifer characteristics were

Porosity was measured gravimetrically from the sample collected. The average (v) ground water velocity was calculated using the tracer results. The hydraulic gradient changes dramatically. Estimated hydraulic conductivity is 4.5 to 75 m/day at SP site and 2.7 to 7.1 m/day at JA site.

Longitudinal and transverse dispersivity was estimated using Parr (1994) equation with the help of break through curves. Dispersivity was 67 m at SP site and 7 m at JA site.

Velocity is 66m/year at SP site and 26 m/year at JA site. The two independent approaches agreed very well with an estimated ground water flux from that are in the range of 1 - 9×10^{6} m^{3} $year^{-1}$.

Sebastien Lamontagne et al., (2002) had developed a simple method, i.e., point dilution test to estimate the velocity of ground water in the riparian zones of stream, lakes and estuaries. It involves the loss by ground water advection of a tracer added to a single well. Here a simple apparatus was used in a shallow alluvial aquifers is described together with a graphical method to estimate ground water velocities from the dilution curves. The shape of the water table must be determined independently to know the direction of ground water flow. During field trials the velocity varied from 0.5 to 3 cm per hour. It was 40 cm/hr during ebbing tides in the inter tidal zone of estuary. Though, the test is done in the semi arid and sub tropical sand bed rivers, the method should be applicable in similar riparian environments adjacent to lakes and estuaries. The main technical difficulty associated with the test design was the potential for the well mixing mechanism to increase the rate at which tracer moves out of the well.

Smart and Karunaratne evaluated the environmental fluorescence spectrum and the back ground fluorescence in a dye tracer depends largely on the organic chemical hydrology of a region. These are evident by the arising peaks in the analytical equipments mimicing the peaks of a tracer, suggesting the acute contamination by dye mimic [the orange area is resilient]. There may be fluorescence peaks, associated with runoff events, but in no consistent manner. Powerful software and highly sensitive equipments

may capture imperceptible peaks but never to say the apt source (extraneous) and accidental events.

Hence retaining the raw series of data will ensure due impaction and consideration. The traditional solution (use of abundant qualities of the tracer dyes) also would not be favoring the environment. Pre monitoring and analog sites both have their own disadvantages and misleading. Using two tracers or a series of injection would make the interpretation less analogous and may be followed in a simple general way. Perhaps, evaluation of a dye tracer to exceed background concentration is largely based on the judgment of the operator and more sophisticated injection encoding, rather than any objective protocol.

Marisa, Cox et al (2003) evaluated the interaction of surface and hyporheic water along the Santa Clara River, Los Angeles and Ventura counties, California by conducting tracer tests and analyzing water-quality data under different flow conditions in October 1999 and May 2000. The first type of tracer test was a slug injection of rhodamine WT dye, to determine the travel times and to indicate when lagrangian water-quality sampling could be performed at each site. The second was a constant rate injection of sodium bromide at the water reclamation plants to evaluate the surface water and shallow ground water interactions in the hyporheic zone. Flow measurements were taken at the sampling locations during the tracer tests to quantify gains and losses in flow.

The differences between the rhodamine WT dye and sodium bromide travel times in the river for all reaches both the injections were less than 1 hour. Within both reaches, there was a trend of increasing nitrate concentrations and decreasing ammonia concentrations, indicating probable nitrification.

It is important to emphasize that the exchange of river and hyporheic water can occur at different scales from the interaction between the river and the regional ground water system, river water may move into the hyporheic zone within gaining reaches and hyporheic water may move into the river within losing reaches.

Fank and Rock (2003) carried out a tracing experiment in September 2001 at the ground water field of 400 x 300 m in the Mur valley aquifer system. He used 75 kg of sodium bromide as a tracer and injected during 20 min at the ground water table as a pulse injection. Due to the density of the solute the tracer has been distributed over the whole aquifer depth in a very short time.

For estimating the longitudinal dispersivity from tracing experiments the calculation of Peclet type curves was used. For one dimensional tracer transport from injection point in ground water flow direction normalized time–concentration curve was calculated and fitted to measure tracer break through curves ,varying the Peclet number, longitudinal dispersion coefficient was calculated by using the equation,

$$D_L = (V_a * D)/P_e \qquad (2.18)$$

D_L is longitudinal dispersion coefficient

V_a is flow velocity

D is flow distance

P_e is Peclet number

Longitudinal dispersivity (α_L) was estimated from D_L/V_a. Transversal (α_T) dispersivity was estimated by using 2D analytical model calibration. In this experiment, α_L was in the range between 5 to 20 m and α_L: α_T were from 17:1 to 30:1

The results of analytical modeling to determine, α_L and α_T were used as initial condition for the calibration of a 2D horizontal numerical tracer transport model. Measured break through was used for calibration of the model. The calibration of the model was well done on the flow line of tracer transport with few modification of longitudinal dispersivity. The spatial distribution of α_L shows values between 2 m near injection point and 20 m at the end of test field in a flow distance of 300 m.

Although the result of analytical modeling α_T was modified in some regions to values higher than 3 m it was not possible to fit measured tracer break through and numerical modeling results. The tracer concentration values are much higher than the measured ones.

Chand et al (2004) estimated natural groundwater recharge using tracer injection technique in the watershed. Environmental and injected tracer techniques (tritium) have been deployed for estimating the recharge on the basis of piston flow model. This study involved geoelectric soundings at 47 locations, estimating recharge at 36 locations using the injected tracer technique besides water level monitoring at 110 observation wells. Tracer profiles have been collected after one hydrological cycle and recharge has been estimated. The soil samples of 10 cm sections were collected up to a depth of 2.5 m. Recharge estimated using tracer technique was found varying from nil to 200 mm.

Olsen and Frederick (2004) designed and conducted in a tidal freshwater wetland at west branch canal creek, Aberdeen proving grand, Maryland. The objective to characterize solute transport and determine the ground water velocity in the upper wetland sediment, and to compose a conservative, ionic tracer (Bromide) to a volatile tracer (sulphur hexafluoride) and to ascertain whether volatization could be an important process in attenuation of volatile organic compounds in the ground water.

The inferred movement of bromide tracer coupled with the apparent loss of tracer maximum through out the test, shows qualitatively that in addition to vertical flow, there is a north ward horizontal component to ground water flow in the area of the tracer array. As was the case with the bromide tracer, sulfur hexafluoride also indicated that a northward horizontal component of ground water flow was present along with the vertical component. Because the sulfur hexafluoride tracer did not move as a discrete pulse, it is difficult to accurately calculate the magnitude and direction of the velocity vector from these data.

As a result of comparison of tracers, the fluorescein showed much less spreading than the bromide and sulfur hexafluoride after injection and its centre of mass remained near the injection point. This is because, fluorescein participated in sorption with mineral surfaces and organic matter analysis of break through data showed difference between the two tracer in almost every sampling level of the tracer array and 80 concentration contour plots for bromide and sulfur hexafluoride also showed that the bromide pulse generally moved away from the injection point more rapidly than the sulfur hexafluoride pulse. However, at few specific sampling points in the middle upper levels of the tracer array in which a portion of the sulphur hexafluoride appeared to have outpaced the bromide.

On concluding,g fluorescein dye proved to be a good tracer for evaluating the hydrologic integrity of the array of piezometers that were used in the tracer test. It was also useful as a non conservative tracer to illustrate the effects of sorption on retarding the movement of solutes.

On the basis of the predominantly upward movement of the conservative tracer and the outward movement in all direction from the injection point, diffusion and advection are the major process responsible for the tracer movement. Dilution, possibly enhanced by intermittent interaction

with the overlying tidal surface water, likely decreased the concentration of the tracer as they were transported upwards. Potential losses of sulfur hexafluoride due to volatization from the surface of the water table could not be measured in the tracer array because the wetland sediments had remained saturated to land surface through out the tracer test.

A portion of sulfur hexafluoride could have volatilized into ambient bubbles of biogenic marsh gases at depth. This could explain the early presence of sulfur hexafluoride in a few sampling point in the upper levels of the tracer array (because of gas bubble rise) and the retardation of the bulk of the sulfur hexafluoride (because of gas bubble trapping) in the lower levels of the array. Methane was detected at depths of 6 - 42 inches below the land surface, with the largest concentration in the shallowest levels.

Physical and chemical processes responsible for difference in the transport of fluorescein and sulphur hexafluoride compared to bromide are likely to similarly affect the transport of volatile organic compounds in the upper wetland sediments in the area around.

Jeffrey Turner and Lloyd Townley (2005), explained to understand the groundwater interaction with the coastal lakes and wetlands of the coastal plain. The wet lands in the coastal plains are being impacted by groundwater withdrawal. The tracer information is collected in the field in order to estimate the geometry of groundwater surface water interaction. Data collected in this project are depth of water in the lake, rate of inflow per unit area, rate of outflow per unit area, rainfall per unit area, rate of evaporation, solute concentration in the lake water, chloride concentration inflow into the lake. Finally the authors concluded that there is the interaction between the wet land along coastal plain and lake by analyzing the sodium chloride concentration variation.

Charles and Greene planned and executed dye tracer test. If a dye is injected and not detected, the investigation is faced with difficult and often costly decision that may include whether or not to repeat the test, to change the type or amount of dye injected to use additional monitoring sites to conduct monitoring for a longer period of time, to evaluate the sensitivity of the analytical method being used to detect the presence (or) concentration of the injected dye. Usually, the temporal changes in the hydraulic gradient are rapid, due to the flow velocities, and flow direction of typical many conduit dominated karst aquifers. The result obtained during the specific dye-tracer test is strictly speaking, only one of the flow condition existing at the time of the test. However, injected tracer dyes themselves may become too diluted and resurge in springs at concentration below detection limits, the increased turbidity may interfere, physical access to dye monitoring sites may be induced, and in site dye monitoring equipment may be damaged by flooding. Hydraulic damming of conduits due to flooded stream may temporarily halt or delay the resurgence of tracer dyes.

These are ensured by the proper determination of the amount of dye to be injected that the dye resurges at detectable but not unacceptable high concentration. The concentration limits, may not always be achieved due to unpredictable subsurface flow routes, field variable affecting transportation rates, dispersion and dye concentration discharged through conduits. Efficient Hydrologic Tracer Test Design [EHTD] method by field (2003) includes a computer program calculating the amount of dye needed for injection by various forms of advection dispersion equation. The methods proposed by Worthington and Smart (2003)

$$M = 19(LQC)^{0.95} \quad (2.19)$$

$$M = 0.73(TQC)^{0.97} \quad (2.20)$$

where

M- Mass of tracer dye injected (g/m^3)

L - Anticipated distance between the injection site and the anticipated primary resurgence site (m)

Q - Discharge at the anticipated resurgence (m^3/sec)

C - Peak tracer concentration at the anticipated resurgence (g/m^3)

T- Travel time determined from prior tracing test results(seconds)

In practice, dye injection is best accomplished at location that provided rapid, direct transport of the tracer into conduits, thus minimizing loss of dye through photochemical decay, sorption and other field conditions. Open throated swallets in sink holes and the swallow holes of sinking streams are ideal sites.

Error in dye detection in determining dye concentration in water is dominated by issues of ambient (background) fluorescence, the single largest source of systematic error in dye tracing, loss of tracer and improper sampling frequency. Potential source of interference with tracer dyes include humic and fulvic acids, certain species of algae, petroleum hydrocarbons, optical brighteners discharged in septic or treated waste-water effluent, automotive antifreeze chemicals and hundreds of other dyes and organic chemicals. The duration and intensity of fluorescence can vary considerably depending on its sources, during this period over which ambient fluorescence is being monitored.

It is learnt from the literature, that many researchers apply an arbitrary 10:1 signal to noise ratio for fluorescent intensity or dye concentration measured at the expected emission peak of the tracer dye as a minimal threshold for repeating the positive detection of dye in a sample. Evidence of dye breakthrough and detection is more conclusive if repeated positive detection is obtained

Interpretation of complex or multi peaked dye breakthrough curve may be difficult due to tracer dispersion which may include bifurcated conduit flow paths, flow reversal in eddies and variability in conduit cross-sectional areas, intermittent storage and flushing of hydraulically stagnant zones and interconnected zones of higher and lower fracture permeability.

Mean tracer dye residence time is estimated by the equation

$$t_m = \int_0^{\infty} tC(t)\,Q(t)\,dt \qquad (2.21)$$

where

t - Time of sample collection

C (t) - Measured dye concentration of the sample.

Q (t) - Discharge measured at the sampling location

It is the length of time required for the centroid (gravity mass) of the tracer dye to transverse the entire length of the karst basin, thus representing the average time of the flow through the basin.

Mean dye velocity represents the average rate of travel of dye through the karst basin and estimated by

$$V_m = \int (1.5\ x/t)\ C(t)\ Q(t)\ dt \qquad (2.22)$$

where

x – straight line distance between the dye injection and resurgence site.

1.5 – constant representing the conduit sinuosity factor.

Laboratory study

Finkner and Gilley (1986) conducted a laboratory study to identify the effects of sediments and dye concentration on absorption for selected soils. Sediment and dye concentration were both significantly affect adsorptive dye loss of rhodamine WT, sulphorhodamine B and lissamine FF.

Three bench mark soils from different location were used. Particle size analysis and organic matter concentration were carried out. It was found that the clay particles ranged from 11.9 to 45.8 % and organic matter 1.61 to 2.55 % for the Caribou and Houston Black soils respectively. Third type soil was black loam. The soils were air dried and sieved through a 2 mm screen prior to testing. For a given dye concentration soil was added to a 400 ml solution at the rates of 2.5, 10, 40, 70 and 100 g/l. The samples were stirred and allowed to stand for one hour. Sediment was removed from the solution by filtering. A fluorometer was used to determine remaining fluorescence of the solution which was carried out at a temperature of 25 °c.

From this experiment the author developed the multiple linear regression analysis to determine the effect of sediment and dye concentration on adsorption for each of the soils.

In the statistical analysis, the following equation was evaluated.

$$Y_{ij} = \mu + \beta_1(X_{1j} - X_1) + \beta_2(X_{2j} - X_2) + \beta_{11}(X_{1j} - X_1) + \beta_{21}(X_{2j} - X_2) + T_i + e_{ij} \quad (2.23)$$

where

Y_{ij} is percentage of initial fluorescence for j^{th} soil and j^{th} level of sediment

μ is sample mean

β_1 is regression coefficient for sediment concentration

X_{1j} is sediment concentration

X_1 is mean sediment concentration

β_2 is regression coefficient for dye concentration

X_{2j} is dye concentration

X_2 is mean dye concentration

T_i is additive error term for unexplained variation

Multiple linear regression analysis was used to determine the F ratios in which the percentage of initial dye was concentrated. By using the equation correction for adsorptive dye loss can be made for each soil. Adsorptive dye loss was less for lissamine FF than for the other fluorescent materials. However the minimum delectability was much higher and linear range much less for lissamine FF than the other two.

The minimum delectability for sulpho rhodamine B was five times greater than the rhodamine WT. Sulphorhodamine B and rhodamine WT displayed similar dye adsorptive characteristics. Finally the author concluded that the regression equation for sulphorhodamine B provided the best statistical fit. Hence sulphorhodamine B was recommended as the dye of choice for the given experimental condition.

David Sabatini and Austin conducted rhodamine WT and fluorescein limited the appearance of the atrazine and alachlor (the selected two herbicides) in alluvial aquifer sand. The order was fluorescein, atrazine, alachlor and rhodamine WT. The adsorption characteristics of fluorescent dyes different from the pesticides showing adsorption levels in higher magnitude (divalent cations) than expected from the empirical relationship based on K_{ow} and f_{oc}. It was evident from the break through curves of

rhodamine WT, which was not of the conventional sigmoidal shape. These variation raise concerns to transfer the result to other sub surface media.

Omoti and Wild (1979), investigated the need of fluorescein as a groundwater tracer utilizing loamy sand soil (85 % sand, 10 % clay, and 2 % organic matter– foc = 0.012) and a pore water velocity of 2.44 cm/h, the K_p value was determined to be 1.3 cm^3/g. The corresponding value of K_{oc} is 108 cm^2/g.

Bencala et al (1983) used rhodamine WT as a water tracer in a mountain stream environment resulted in a Kp value of 5.6 cm^3/g for the batch studies between rhodamine WT and stream bed sediments. Trudgill (1987) conducted batch experiments with rhodamine WT and a silty loam soil (f_{oc} of 0.034 to 0.053) resulted in a K_p value of 54 cm^3/g. This corresponds to a K_{oc} value of 1000 to 1600 cm^3/g for rhodamine WT.

Kasnavia et al (1999) evaluated the dye sorption on media properties by column studies. He tested with four dyes such as fluorescein, rhodamine B, rhodamine WT, sulphorhodamine B on two appositively charged mineral surfaces alumina and silica.

Negative functional group fluorescein sorbed least onto silica but most onto positively charged alumina. The rhodamine dyes with a permanent positively charged and negatively charged functional groups sorbed onto both alumina and silica. Sulphorhodamine B electro functional groups sorbed less onto negatively charged silica than rhodamine B which has two carboxyl groups.

Equilibrium sorption, studies were conducted and the isotherm data were plotted. Since these isotherms were conducted at a pH of T, which is atleast two pH units above the dye pK_a values, the dyes predominantly

exhibited their ionic nature. At pH 7 the alumina has a net positive charge and the silica has a net negative charge. On alumina, fluorescein exhibited the highest sorption while the rhodamine dyes exhibited lower sorption. On silica, the opposite trend was observed. Fluorescein does not have a positively charged group as rhodamine dyes, which reduced the repulsion on the positively charged alumina surface and then increased the sorption. Hence fluorescein appears to be good tracer for negatively charged media. For the rhodamine dyes, rhodamine WT has the highest sorption on alumina followed by sulphorhodamine B and rhodamine B has only one ionized carboxylic group and hence the attraction towards the positively charged alumina was low. Sulpho rhodamine B has two highly electronegative sulfonic acid groups, was expected to have higher sorption than rhodamine WT. It is due to the presence of two rhodamine WT isomer in rhodamine WT, It showed more sorption than many other rhodamine dyes.

For sorption dyes in silica, the order was rhodamine B > rhodamine WT > sulpho rhodamine B. Sulpho rhodamine B sorption was lowest due to the repulsion between the highly electronegative sulfonic groups and the negatively charged silica. The results were consistent with the expectation, based on electrostatic repulsion. Hence the dual cationic and anionic nature of the rhodamine dyes will get sorbed onto any mineral surfaces making it less attractive as a conservative tracer.

On increasing the pH 9.0, alumina approaches a net neutral charge. Fluorescein sorption decreased dramatically, while rhodamine dyes decreased to a lesser extent. The lesser sorption may be due to the dissolution / attraction of the mineral surfaces at higher pH values.

Dharani Vasudevan et al conducted batch experiments to measure the sorption of rhodamine WT onto (i) fine grain sand, (ii) iron oxide, (iii) aluminum oxide, (iv) iron oxide coated fine grain sand, (v) coarse grain sand,

and (vi) H_2O_2 treated sand. H_2O_2 treatment is intended to remove organic matter from the mineral surfaces. Rhodamine WT sorbed to a greater extent onto aluminum oxide compared to iron oxide. This is due to higher surface area of aluminum oxide (90.1 m^2/gm) compared to iron oxide (10.1m^2/gm) sorption was maximum on the fine grain sand, that is because of its small particle size and high surface area untreated coarse grain sand sorption was comparatively less. Sorption on treated coarse grain sand was minimum since organic matter was removed. These findings provide evidence that rhodamine WT does not sorb onto organic matter alone which is sorbed by the hydrophobic organic compounds.

David Sabatini evaluated dye sorption equilibria and kinetics with natural aquifer media, specifically limestone and sandstone materials. Oberermuschel Limestone and the Rhaet Sandstone were the two consolidated aquifer media. Fluorescein and sulphorhodamine B were two fluorescent dyes.

The data were evaluated using the Freundlich isotherm based on the non-linear data resulted from the equilibrium sorption isotherm,

$$q = K_f C^N \qquad (2.24)$$

where

q- dye mass absorbed per mass of soil

C- Equilibrium aqueous concentration

K_f – Freundlich sorption co efficient

N- Freundlich exponent

Diffusion limited intra particle sorption was assessed using Fick's second law of solute diffusion from an aqueous phase into spherical porous grains.

Observing equilibrium sorption studies, SRB is highly anionic sulfonic group adsorb strongly onto the positively charged surface, while the weaker fluorescein carboxylic groups sorbs less strongly onto the same media. Fluorescein with one anionic charge, sorbs negligibly onto the negatively charged medium. The permanent cationic charge on SRB causes it to sorb with the negatively charged RhS, although to a charged OML.

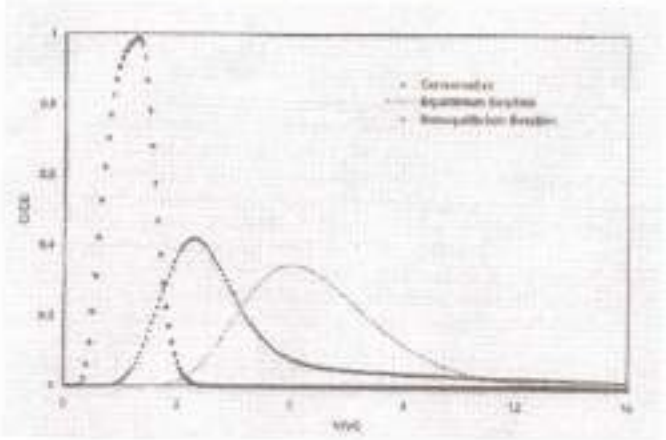

Figure 2.1 Breakthrough Curve (D. A. Sabatini 'Ground Water', September – October 2000)

The earliest breakthrough curve illustrates conservative breakthrough. The latest curve demonstrates the impact of equilibrium sorption on dye transport. The intermediate curve illustrates non-equilibrium sorption and its impact on dye transport with increasing non-equilibrium, the dye appears earlier but taken longer to approach complete elution (the tail is longer). The earlier dye appearance due to non-equilibrium transport will reduce the error in the ground water velocity estimate if sorption is not considered. The increased spreading caused by non-equilibrium transport can be mistakenly attributed to hydrodynamic dispersion, resulting in artificially high dispersion co-efficient. Non-equilibrium effect, which increases with increasing diffusion distance, will be amplified for consolidated and fractured media, with longer diffusion distance. These results thus demonstrate the

importance of understanding both the equilibrium and kinetics of dye sorption when designing and interpreting tracer studies.

From the above literature reviews following information are gathered and they are listed below,

- The fluorescence of dye was seen to decrease at low pH and was observed to be a function of the ion exchange causing the pH change. The presence of organic matter in the water samples produced greater background fluorescence.
- pH effect on RWT showed that sorption decreased with increasing pH, adsorption of RWT was much more significant at low value pH and decrease at a value of pH 11.3
- Fluorescein which has only negative functional groups sorbed least on the negatively charged silica but most onto positively charged alumina. The Rhodamine dyes, with a permanent positive charge and negatively charged functional group adsorbed on to both alumina and silica.
- Adsorption is one of the main important factors that have to be considered. Sorption was greater onto fine sand than coarse grain material; It was due to small particle size and high surface area.
- Sorption kinetic rates decreased with increasing particle size, which is consistent with diffusion limited intraparticle adsorption.
- Hydrocarbon tracer was proved to be suitable tracer used for field studies. Perfluorokerosene that eliminate problem with sorption, breakdown, volatility and toxic and also low water solubility.

- The dyes consisting of more sulfonic acid groups tend to sorb less and have a better mobility in soils than dyes with fewer sulfonic acid groups.
- The fluorescent dyes were subjected to sorption that depends on the dye selection which is based on their chemical properties, media characteristics.

2.8 LITERATURE ON GROUNDWATER MODELING

Groundwater modeling is generally used to simulate the flow and contaminant transport process in the aquifer system based on certain mathematical equations. The equations that describe the groundwater flow and transport processes can be solved using different types of models. Analytical models give exact solutions to equations that describe very simple flow or transport conditions, whereas numerical models give approximation results but solving complex field conditions. For the groundwater modeling, the primary data would be the observed field data. Modeling result depends mainly on the availability and accuracy of the field data.

2.8.1 Model Parameters

Model parameters include hydraulic parameters and solute transport parameters. Hydraulic parameters include hydraulic conductivity and specific elastic storage. Solute transport parameters include dispersivity and porosity. The most important model parameters are hydraulic conductivity and dispersivity.

2.8.2 Water Balance Equation

Water balance equation for the groundwater system is based upon inflows such as precipitation, return flow from the irrigation areas, return flow

from the canals and the outflows such as evaporation, abstraction due to pumping. Generally water balance equation can be stated as

INFLOW – OUTFLOW = CHANGE IN STORAGE

2.8.3 Mass Balance Equation

The equation governing the movement of dissolved constituents in the groundwater by advection and dispersion process based on the conservation of mass approach is stated as

$$\sum I + \sum P - \sum O - \sum L = \sum A$$

I = Input

P = Production

O = Output

L = Loss

A = Accumulation

2.9 FLOW EQUATION

Modeling is translating the physical system into mathematical terms. The governing flow equation for three dimensional saturated flows in saturated porous media is

$$\frac{\partial}{\partial x}\left(K_x \frac{\partial h}{\partial x}\right) + \frac{\partial}{\partial y}\left(K_y \frac{\partial h}{\partial y}\right) + \frac{\partial}{\partial z}\left(K_z \frac{\partial h}{\partial z}\right) \pm Q = S_s \frac{\partial h}{\partial t}$$

Kx, Ky, Kz = Hydraulic conductivity along x, y, z axis, m/sec

h = Piezometric head, m

Q = Volumetric flux per unit volume representing source

Ss = Specific storage coefficient

t = Time, sec

2.10 GROUNDWATER MODELS

Models are the conceptual descriptions or approximations that describe the physical system using the mathematical equations. Models are not the exact descriptions of the system or the processes. Groundwater models describe the groundwater flow and transport process using mathematical equations based on certain simplifying assumptions. These assumptions typically involve the direction of flow, geometry of the aquifer, the heterogeneity or anisotropy of sediments or bedrocks within the aquifer, the contaminant transport mechanisms and chemical reactions. By mathematically representing the hydro - geological system, reasonable alternative scenarios can be predicted, tested and compared. The applicability of a model depends on how closely the mathematical equations approximate the physical system being modeled. In order to evaluate the applicability of the model, it is necessary to have a thorough understanding of the physical system and the assumptions used in the derivation of the mathematical equations. There are several types of groundwater models such as 3D – FEMFAT, AQUA3D, CHEMFLO, CHEMFLUX, FEFLOW, FLOWPATH, MODFLOW, PEST, Visual MODFLOW, Visual PEST being used for the groundwater studies. The mostly used groundwater flow model is MODFLOW. PEST which is inbuilt in the MODFLOW is used to optimize the parameters using various optimization techniques like Genetic algorithm etc.

2.10.1 Visual MODFLOW

VISUAL MODFLOW is the Integrated Modeling Environment for MODFLOW, MODPATH, and MT3D. Visual MODFLOW provides

professional 3D groundwater flow and contaminant transport modeling using MODFLOW-2000, MODPATH, MT3DMS and RT3D. Visual MODFLOW combines the standard Visual MODFLOW package with Win PEST. It also combines with Visual MODFLOW 3D-Explorer to give the most complete and powerful modeling environment. This fully-integrated groundwater modeling environment allows to:

i. Design the model grid, properties and boundary conditions;
ii. Visualize the model input parameters in two or three dimensions;
iii. Run the groundwater flow, path line and contaminant transport simulations;
iv. Display and groundwater flow, path line and contaminant transport simulations;

2.10.2 Visual PEST

Visual PEST is the Figureical Model – Independent Parameter Estimation and Optimization. Visual PEST combines the parameter estimation capabilities of PEST 2000 with the Figureical processing and display features of Win PEST. PEST2000 is the latest version of PEST. PEST has undergone continued development with the addition of many new features that have improved its performance and utility to a level which makes it to uniquely applicable to any existing model. PEST is now widely used for automated model calibration and data interpretation in groundwater and surface hydrology, geophysics, geotechnical , mechanical and mining engineering.

2.10.3 Genetic Algorithm

Genetic algorithm is one of the optimization technique used for the inverse modeling adopted by the PEST to estimate the parameters like hydraulic conductivity and dispersivity. Genetic algorithms are a particular class of evolutionary algorithms that use techniques inspired by evolutionary biology such as inheritance, mutation, selection, and crossover. General steps involved in the Genetic algorithm to find out the best appropriate solution are given below,

(i) Initially GA creates a random population of parent individuals;

(ii) The quality of these individuals is then analyzed using a specified numerical objective function normally called as fitness function;

(iii) In this study the objective function is to minimize the discrepancies between the observed and calculated head or concentration values;

Generation of initial population

In this step, initial population of the parameters is generated by the random generator. In this study the main aim is to estimate the hydraulic conductivity and dispersivity. Hence one has to generate the initial population for these two parameters by random generation.

Encoding the values

Binary coding method is used to transform the parameters to a binary string of specific length. All the parameters will encode in terms of 0 and 1. Each variable has its own length corresponding to the allowed maximum and minimum values of that parameter.

Simulation runs

After the encoding process, simulation process will be performed by the model for all the sets of parameter variables.

Computation of the fitness function

Once the simulation run finishes, then the fitness function of all the variables with respect to the objective function should be analyzed. The objective function is to minimize the error between the observed values from the field measurements and calculated values from the model.

Selection of the best string

In this step, the best string which has the least weighted square error between the observed and calculated values has to be selected. There are several types of method for the selection of the best string which includes Roulette wheel selection, Fitness- Proportionate selection, and Rank selection.

Computation with genetic operators

After the selection of the best string, operations such as cross over and mutation has to be performed. In the cross over scheme, two members from the population will be selected and the modification is performed by swapping the two members at a selected position. In the mutation process, the modification is performed at the particular position in the selected member to facilitate the early convergence towards the optimal solution.

Repeat Evaluation

After performing all the operations, again fitness function is evaluated for the variable with respect to the objective function. If there is

least error between the observed and calculated head or concentration values then the search process is said to terminate.

2.11 GROUNDWATER FLOW MODEL APPLICATIONS

Husam Baalousha (2002) developed the groundwater flow model for the Ruataniwha basin. The results of the model were used to build the transient model. The main purpose of the model is to simulate the groundwater conditions in the study area under steady state. With the transient model, groundwater responds to the different abstraction scenarios were studied. In this study, input data like rainfall data, river data were obtained from previous records. PEST (Parameter Estimation) was used for the calibration of the hydraulic conductivity and recharge. Observations from nearby 47 wells were used for the calibration and another set of data were used for the validation. From the model results they concluded that major amount of recharge was coming from rainfall. The contribution of the river to the groundwater recharge is less compared to rainfall. Sensitivity analyses showed that hydraulic conductivity is the most important factor that greatly affects the model results.

RajaManickam et al (2010) developed the groundwater quality modeling for the Amaravathi river basin which is at the downstream of Karur Town is severely polluted due to the discharge of partially treated effluent from the textile bleaching and dyeing units. Due to this, groundwater in that region was affected to the greater extent that affected nearby agricultural areas. Because of that impact they have conducted the study using Visual MODFLOW and MT3D models. Both the models were calibrated and validated. For the calibration process PEST was used. The validated model was then used for the simulation of the ground water quality for next 15 years under five different scenarios : (i) if the present system with 10,000mg / l TDS discharge into river (ii) if the CETPs meet the TDS discharge standards

of 2100 mg / l (iii) if the quantum of the discharge is doubled with TDS level of 2100mg / l (iv) if the dyeing units undergoes reverse osmosis plant for recycling the entire effluent and achieve zero discharge (v) if the recharge rates increase by 1.5 times . From the analyses they found out that there was no improvement in the groundwater quality even if the effluents meet the discharge standards for next ten years. They concluded that, there will be improvement in the quality of the groundwater only if the units go for zero discharge.

Fank et al (2001) carried out the tracing experiment in the groundwater test field in the Mur valley aquifer system in the September 2001. In this study sodium bromide was used as the tracer and pulse injection method was adopted. Hydraulic and transport parameters of the aquifer were estimated. For estimating the longitudinal dispersivity they used the Peclet type curves. Transversal dispersivity was assumed as $1/10^{th}$ of the longitudinal dispersivity. The results of the analytical modeling were used as the initial conditions for the calibration of the numerical transport models. Once the model was calibrated, they compared the model results with the field results and they found there is good match between the model values and field values.

Kyle Thomas et al (2005) simulated the behavior of the oxidant (sodium persulfate) under various injection scenarios. Model simulations were performed to support the full scale application of the ISCO at the site area. In-Situ Chemical Oxidation (ISCO) is the soil and groundwater remediation technology that has been employed at the site in the Northern New York site contaminated with petroleum hydrocarbons. In this technology sodium persulfate was used as the base catalyst. A three dimensional, finite difference groundwater flow model Visual MODFLOW was used to simulate the groundwater conditions in the study area. MT3D a solute transport model

incorporated in the Visual MODFLOW was used to simulate the behavior of the chemical oxidant in the groundwater. It was found from the results that the model did not provide the accurate results due to the insufficient information regarding the concentration of the mass injected. The author suggested that reevaluation of the validation and calibration of the model by better knowing the amount of mass injected, the model can provide the reliable results.

2.12 PARAMETER ESTIMATION THROUGH GENETIC ALGORITHM

Mingguang Wang et al (1996) used Genetic Algorithm for the estimation of aquifer parameters under transient and steady state conditions. In this study they used Visual Modflow for the flow simulation. They calculated the heads in 50 days and 100days and under steady state condition. Nine different tests were conducted with the changes in quantity and quality of the data. The impacts of data quantity and quality in the estimation error were also studied. It showed that there was no change in the estimation error with the decrease of observation points. There was also no improvement in the estimated error even with a second time step of 100 days. In the steady state condition, estimated error was increased by five times than that of estimated error calculated under transient state. From the result, they understood that transient head data were much more sensitive to hydraulic conductivity than the steady state head data. Then genetic algorithm solutions were compared with the Gauss - Newton solutions and results showed that genetic algorithm has the smaller estimation error than the Gauss – Newton method.

Giacobbo et al (1996) studied feasibility of using Genetic Algorithm for estimating the parameters of a groundwater contaminant transport model was investigated. In this study transport of contaminants was numerically simulated by an advection – dispersion model. The dispersivity

and velocity was estimated using genetic algorithm. Genetic algorithm search procedure was used to estimate the values of parameters. The goal of the study was to find six parameters (Velocity Vi and Dispersivity Di) in three layers which minimize the objective function. The results showed that the first four unknown parameters were estimated with good accuracy. From the results they understood that model output was influenced more by the three velocity parameters and one dispersivity and little influenced by the next two dispersivities. They have concluded that genetic algorithm, besides estimating efficiently the values of the parameters, this method also allowed us to provide a qualitative ranking of their importance in contributing to model output.

Evans et al (1996) dealt with the uncertainty associated with hydraulic parameters estimated during the calibration of a groundwater flow model. In the aquifer system where the hydraulic conductivity is anisotropic, the calibration process becomes more complex. Preliminary attempts of model calibration using low anisotropy ratios resulted in satisfactory match between simulated and observed water levels. In this study, two dimensional flow and transport model was analyzed. For the two simulations, anisotropy factors of 3:1 and 30:1 were assigned in the model. For the flow simulation, it was noted that RMS error increases as the anisotropy ratio (Kx : Ky) increases. In the transport model, even the hydraulic conductivity ratio of 1:1 provided the lowest RMS error, the velocities calculated using this ratio did not satisfactorily simulate the flow directions observed in the field. But an anisotropy ratio of 10:1 provided the best matching between the observed water levels and calculated water levels and also provided the velocities that reasonably match the observed flow direction in the field. The results of this analysis strongly indicate that use of water level data alone would not adequately represent the site condition. Addition of plume data to the water level data will improve the calibration process and resulted in more reliable model.

Lakshmi Prasad et al (2001) demonstrated the effectiveness of the Genetic algorithm optimization model and suggested its preference for inverse modeling. In this case study they, used Genetic algorithm to estimate the hydraulic conductivity and zonal recharge of an aquifer. For the estimation of hydraulic conductivity, net recharge was estimated from water balance approach. Then the aquifer properties and recharge were assigned in the model. Range for hydraulic conductivity was taken between (20 to 200m/day). Estimated hydraulic conductivity from GA found good agreement with water balance approach. For the estimation of net average annual recharge, it was computed using empirical formulae. Range for the aquifer recharge was taken between (0.00005 – 0.005). From the results they found out that estimated annual recharge using GA were well compared with water balance approach.

The above literatures describe the basic concepts of the Numerical groundwater modeling, MODFLOW software for modeling and the concepts about the Genetic algorithm.

Extensive literature review on such a infiltration percolation , seepage, Geophysical methods, tracer techniques and numerical methods lead to proceed the project work in a positive direction.

CHAPTER 3

METHODOLOGY

3.1 GENERAL

Based up on the objectives and literatures, the methodology for the research project was framed. It involved primary and secondary data collection, Runoff estimation from the catchment, estimation of aquifer parameter, hydro-geological investigation, tracer study and numerical modelling of tank and its command area.

3.2 DETAILS OF METHODOLOGY

- Selection of Tanks
- Hydrological characteristics of a Tank system
  - Hydro-meteorological characteristics
  - Hydraulic particulars of Tanks
- Delineation of Catchment Area and Tank capacity Estimation
- Run off Estimation
- Tank Storage Estimation during Monsoon
- Hydrogeology of the Tank and its command area.
- Groundwater fluctuation and change in storage
- Pumping Rate Estimation
- Tank bed characteristics and its Recharge capacity
- Groundwater prospects
- Aquifer parameter Estimation
- Water Balance study
- Tracer study
- Estimating the impact of partial de-silting of tank bed through field study and numerical study

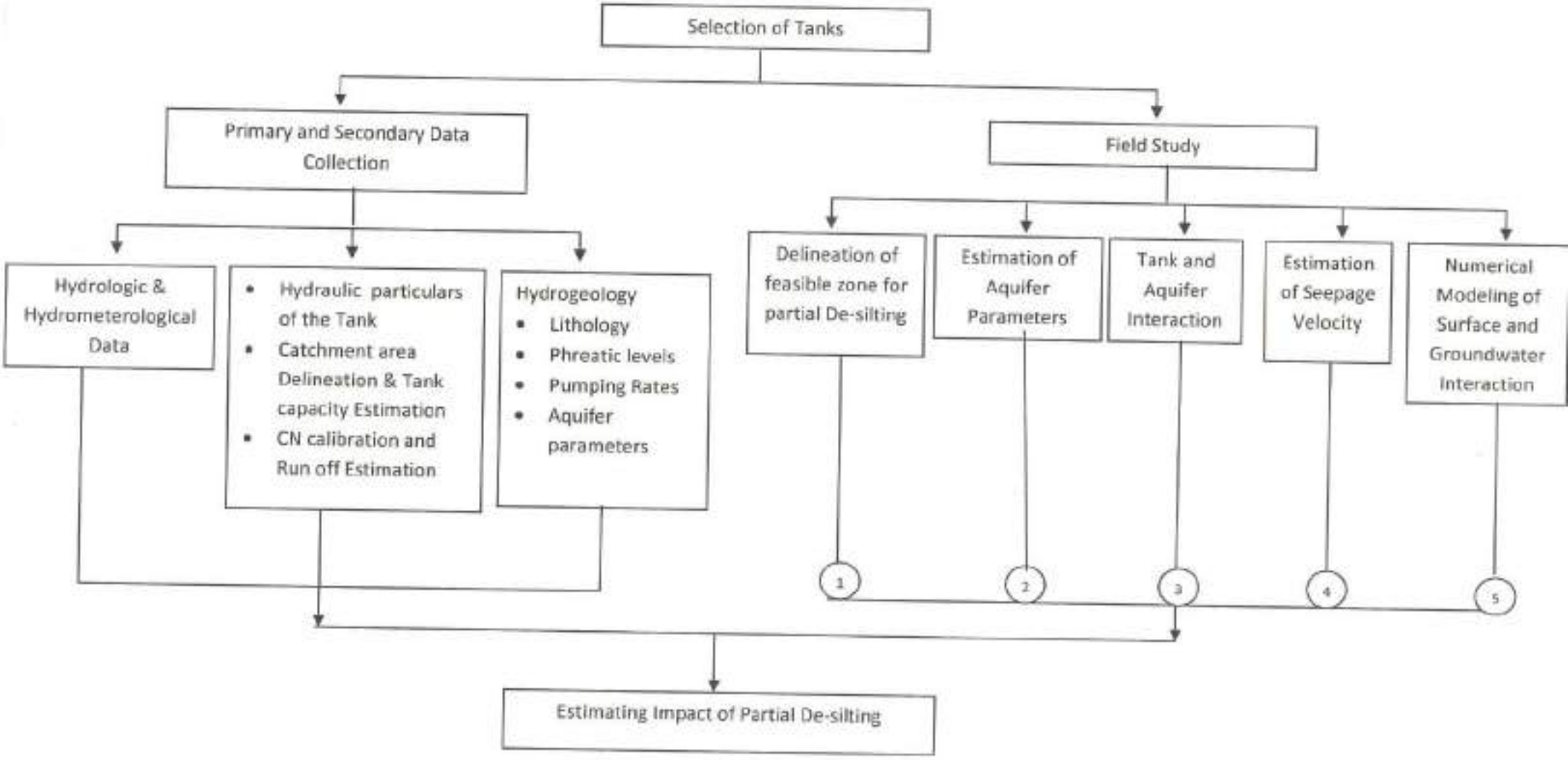

Figure 3.1 Detail Methodology

3.2.1 Delineation of Feasible Zone for Partial De-silting

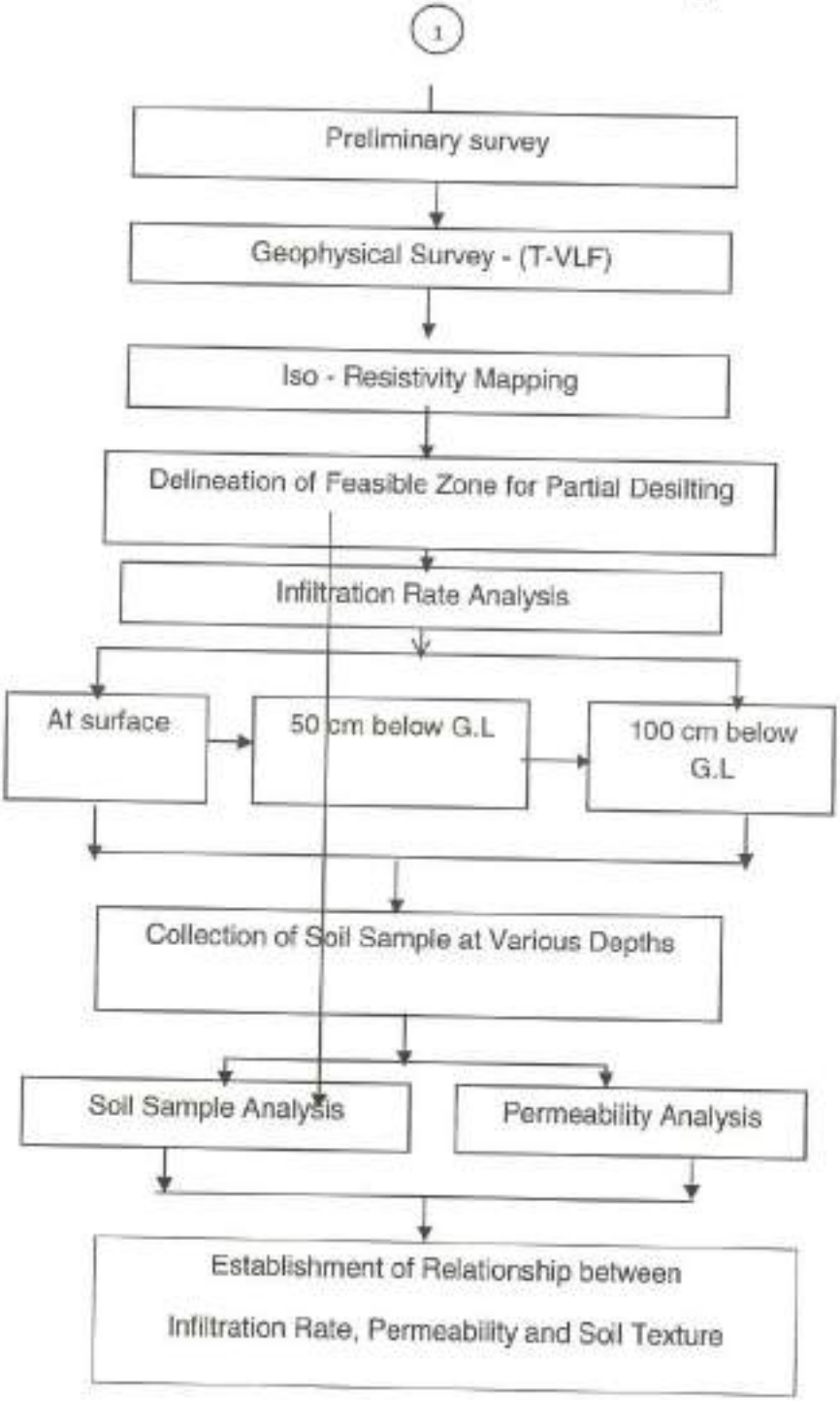

3.2.2 Estimation of Aquifer Parameters

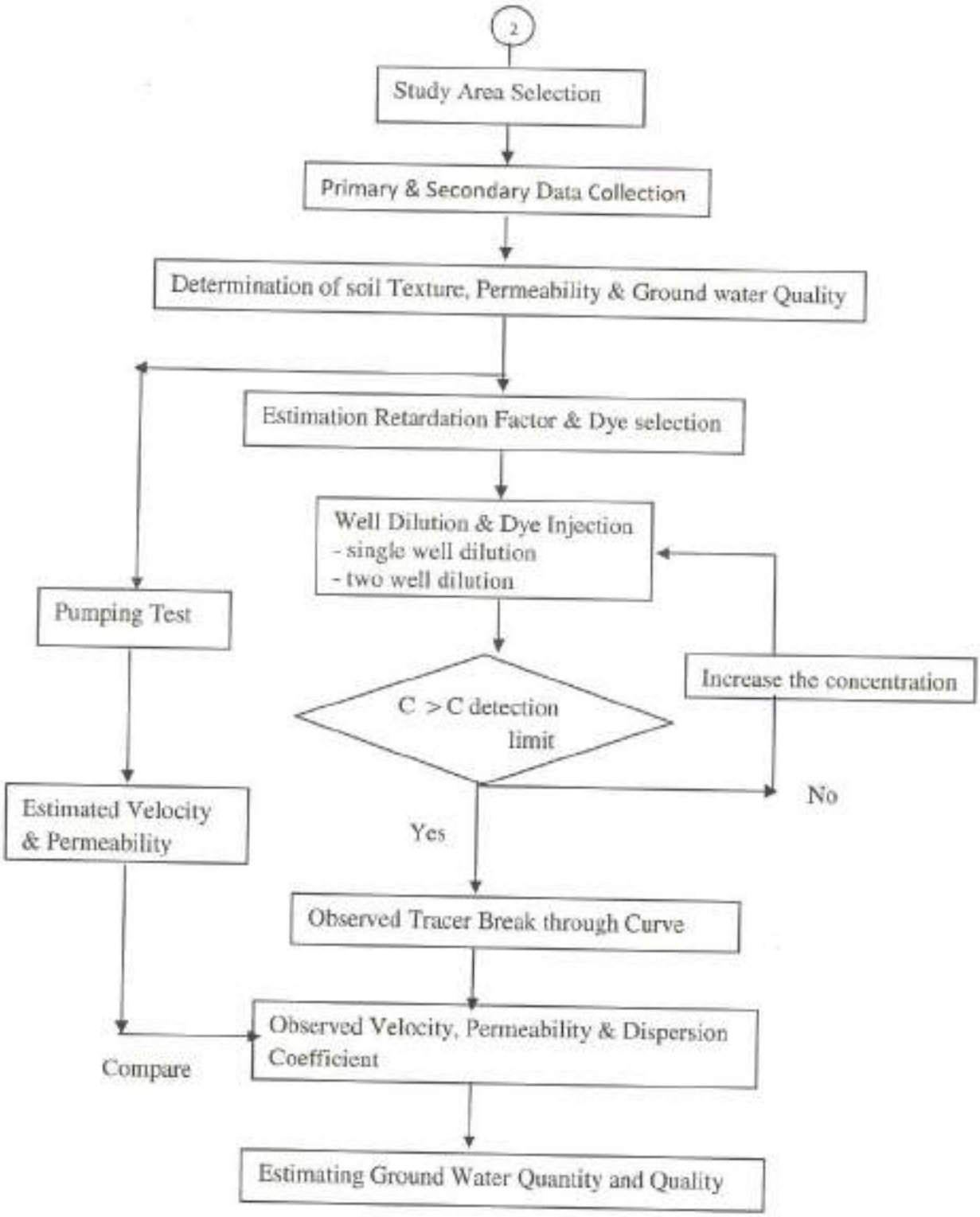

3.2.3 Tank and Aquifer Interaction

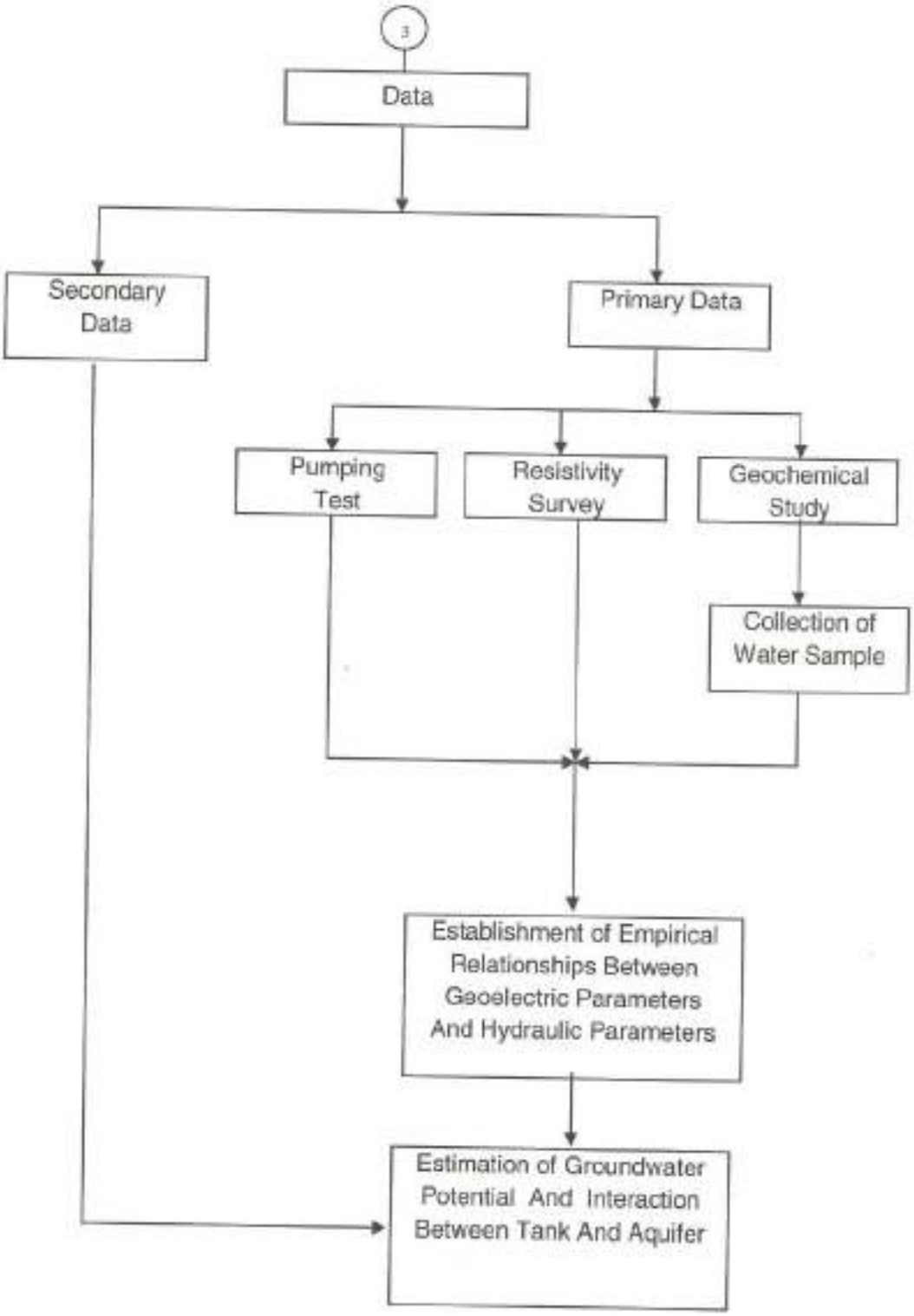

3.2.4 Estimation of Seepage Velocity

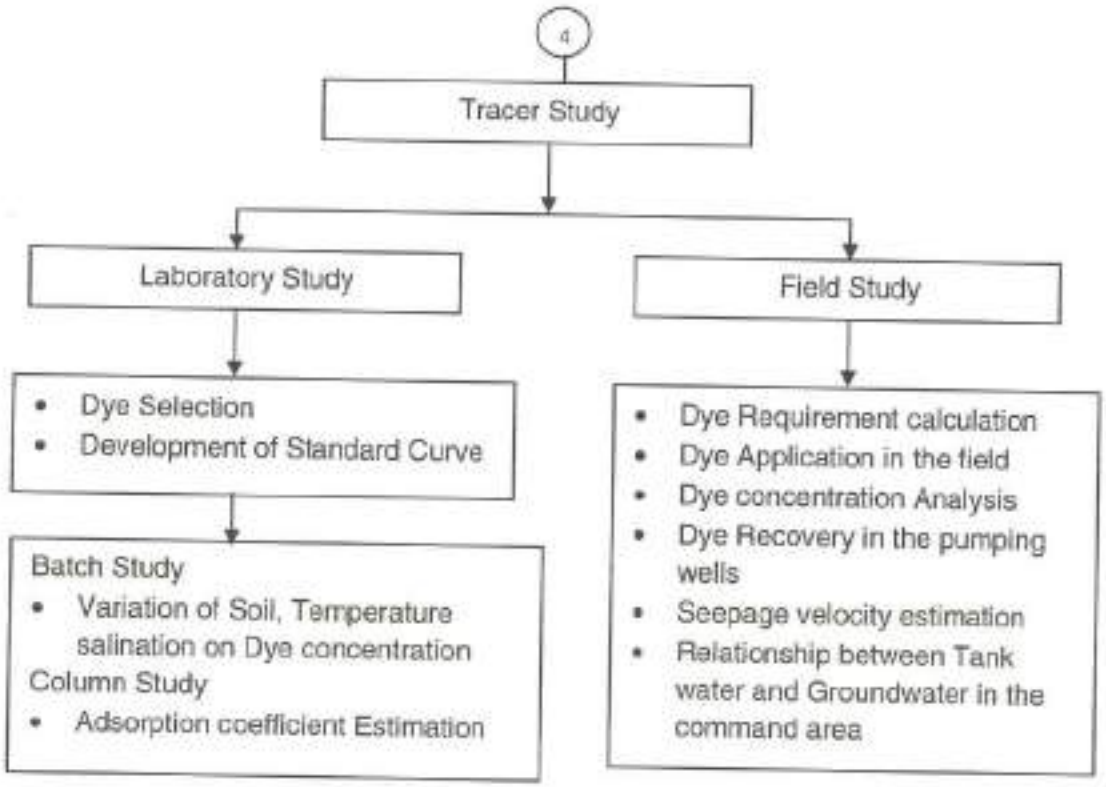

3.2.5 Numerical Modeling of Surface water and Ground water Interaction

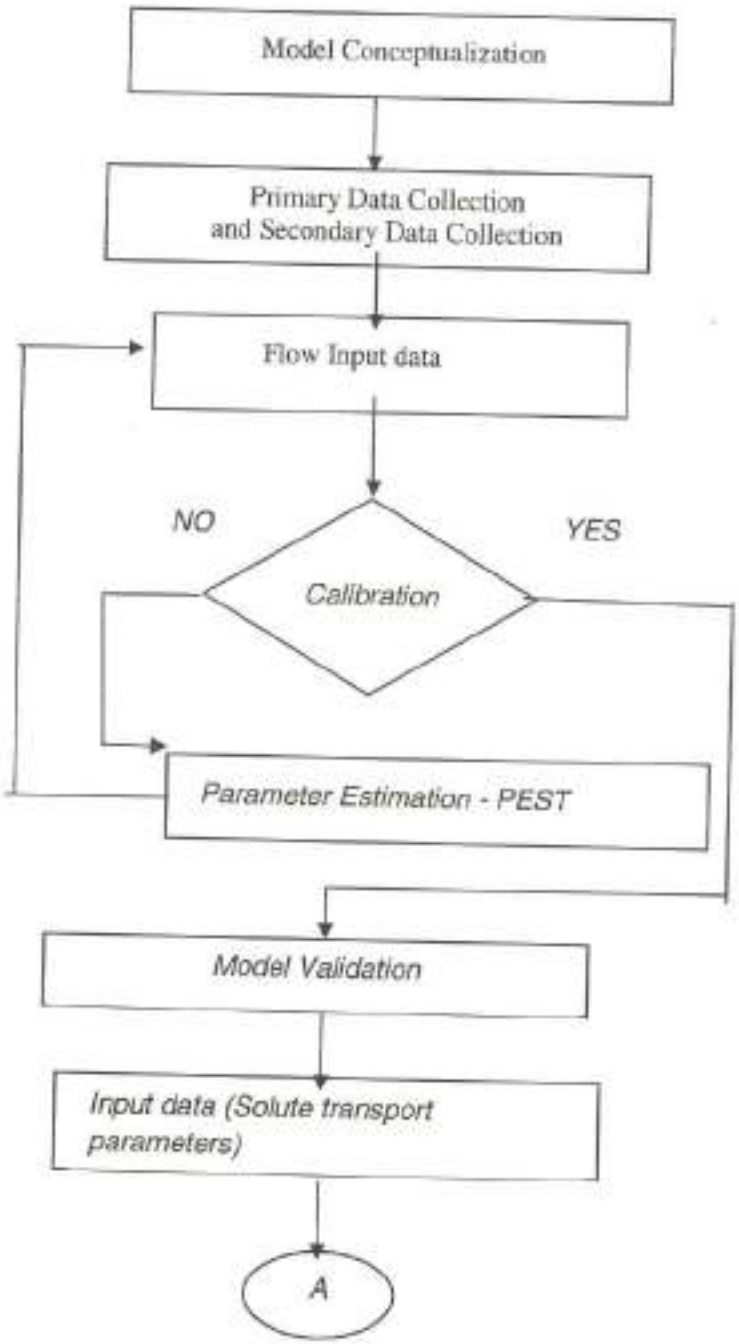

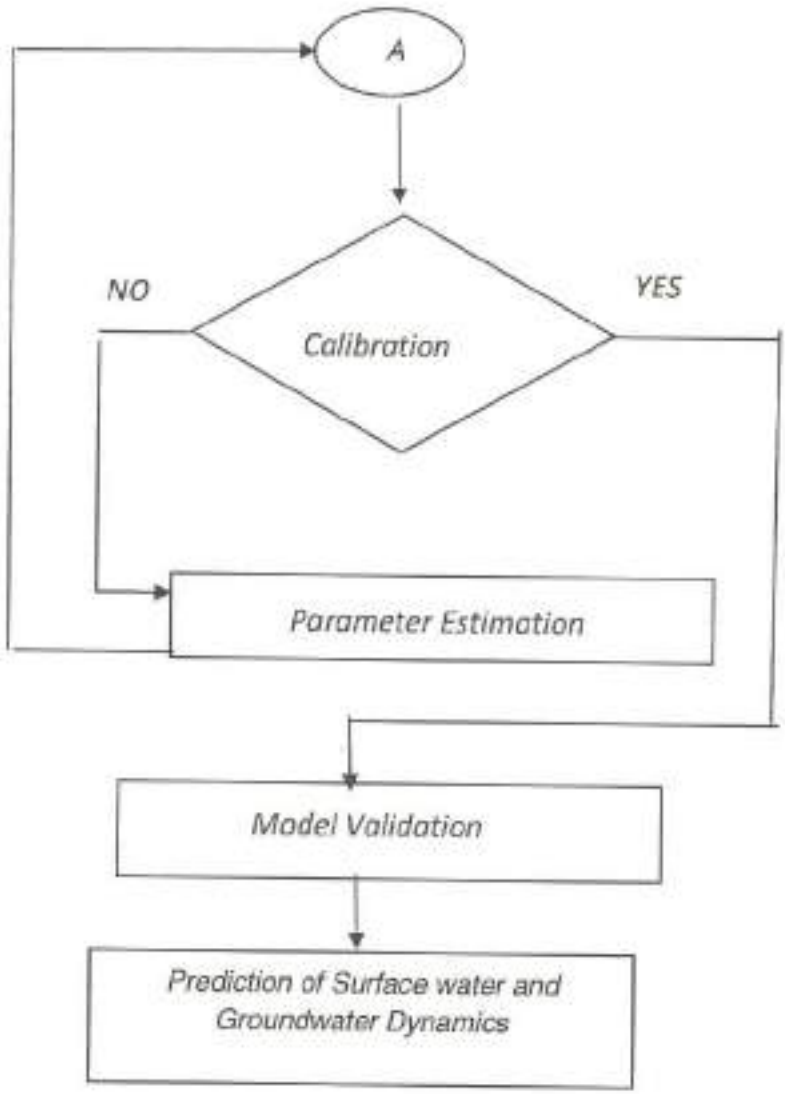

In the forthcoming chapters various stages of methodology has been carried out in the lab and field to evaluate the impact of partial de-silting in the tank. It includes analysis of primary and secondary information, geophysical study, soil and water sample analysis, tracer study and numerical modeling of tank and aquifer system.

CHAPTER – 4

HYDROLOGICAL CHARACTERISTICS OF THE TANK SYSTEM

The Study tanks were selected based on the objectives and methodology of the project. One tank was taken in the first and second order stream which is located near the hills. Runoff depends on length, width and slope of the catchment. Second tank was selected in the third and fourth order stream which is located at middle reach. Irrigation tanks located in the first order stream might deposit sediments frequently and erode the bund of the tank. Tanks located at third order stream are uniform and reliable.

4.1 CRITERIA KEPT FOR THE SELECTION OF TANKS

- System / Non system tanks with specific problem
- Sluice command area of around 40 ha
- Well irrigation (open / bore wells) should be practiced in the command area catchment
- Command area with paddy / commercial crop
- The tanks should be controlled by Public Works Department (PWD)
- Active Farmers Organization / Self Help Group to improve tank efficiency
- De-Silting (to be commenced / commenced)

- Active participation between farmers and Public Work Department
- Site accessibility
- Within a radius of 60 Km from Chennai

Many tanks were visited in Madurai, Virudhunagar, Kancheepuram, Thiruvallur and near to Chennai. After visiting many tanks and discussing with Water Resources Organization/Public Works Department, two tanks one located near to Chennai and the second is far away from Chennai were selected. The tank near to Chennai is Ponpadi tank, near Tiruttani while the other is Sengulam tank, in Virudhunagar District.

OBJECTIVES OF THIS CHAPTER

- To study the hydrological characteristics of a tank system;
- To assess the capability of the tank in conserving the maximum yield from rainfall over its catchment;
- To assess the recharge capability of the tanks and develop a relationship between tank water depth and ground water level;

The Ponpadi village is situated 7 km from Tiruttani town. Ponpadi tank which was taken for the research study is situated is about 0.6 km from Ponpadi village in Thiruvallur District. The latitude and longitude of the tank are 13°13′58" N and 79°35′59" E respectively with an altitude of 99 m above M.S.L. The another one Sengulam tank is situated at the end of Sengulam village which is at a distance of 15 km from Virudhunagar town in Virudhunagar District. The latitude and longitude of the tank are 9° 38' 33" N and 77 ° 49' 47" E respectively with an altitude of 125.578 m above M.S.L. The location of the study tanks is shown in the Figure 4.1. The Study area

details and Hydraulic particulars of the Ponpadi and Sengulam Tanks are presented in Table 4.1.

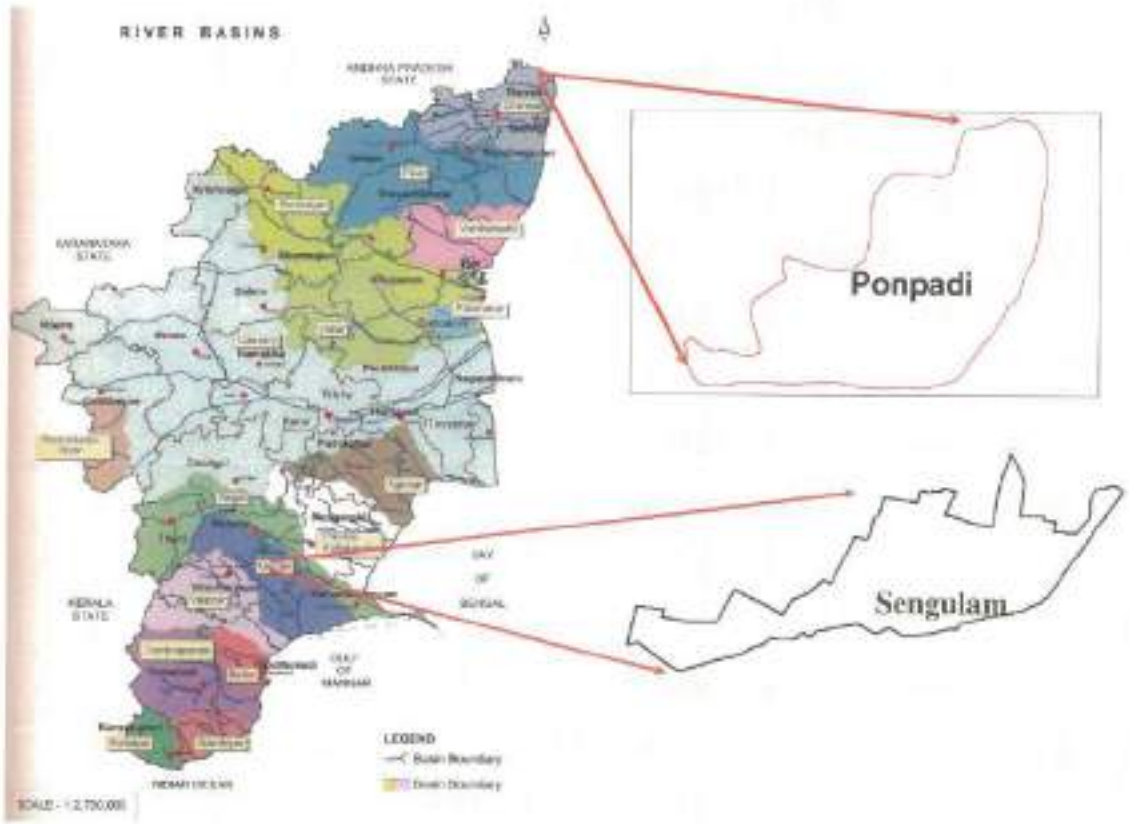

Figure 4.1 Location of Ponpadi and Sengulam Tanks

Table 4.1 Study Area Details and Hydraulic Particulars

Tank Particularly	Ponpadi	Sengulam
Type of Tank	Rainfed	Rainfed
District	Thiruvallur	Virudhunagar
Latitude	13° 09' 20" N	9° 38' 32.45" N
Longitude	79° 32' 20" E	77° 49' 47.24" E
FTL	95.2 m	121.110 m
MWL	95.6 m	121.710 m
No. of Sluices	1	3
Ayacut	145.35 Ha	50 Ha
Original Capacity	1.61 M m^3	0.295 M m^3
Present Capacity	1.16 M m^3	0.270 M m^3
Catchment area	11.75 km^2	4.60 km^2
Average Rainfall	1008.4 mm	780.63 mm
Southwest	464.49 mm	165. 9 mm
Northeast	441.31 mm	410.2 mm
Winter	20.91 mm	40.6 mm
Summer	77.80 mm	164.2 mm
Dependable Rainfall	850 mm	604.1mm

4.2 PONPADI TANK – TIRUTTANI

Tiruttani lies in the Nanthiyar basin which is one of the sub basins of Chennai basin as shown in Figure 4.2. Nanthiyar sub basin covers an area of 718 sq.km that originates from Puttur hill at an altitude of 582 m near Singasamudrom in Andhra Pradesh. Then it enters Tamil Nadu and feeds Sholingur tank. Nanthiyar passes through Tiruttani and joins with Nagari River and which empties into the Sathiyamoorthy Sagar reservoir in Poondi.

Geology

Tiruttani is underlined by crystalline rocks of Archean age, comprising granite gneiss, charnockite and associated basic igneous and metamorphic rocks. The granite occurs as linear bodies in East and Southeast of Tiruttani and Southwest and Northeast of Sholinghur. It is pink to grey, coarse grained granodioritic composition.

Figure 4.2 Base Map of Chennai Basin

Hydrogeology

The occurrence and movement of groundwater in hard rock is heterogeneous in nature and flow is restricted to the weathered formation of the top zones followed by fissured and jointed zones. Top portion of the surface is a sandy soil which is a depth of 1.5 to 3 m followed by highly weathered formation of granite and granitic gneisses up to 7.5m followed by fractured formation at two depths of 30m and 70m underlined by the bed rock. Groundwater occurs under water table condition in a weathered zone

and acts as shallow aquifer which forms the water bearing zones. In general, the winter water level varies from 4.00 m to 8.20 m and the summer water level varies from 5.30 m to 9.40 m.

Aquifer Characteristics

The yield in hard rock ranges between 45 and 220 lpm. Transmissivity (T) ranges from 10 to 80 m^2/day. The Permeability (k) ranges from 0.5m / day to 2.5m / day. The storativity (S) ranges from $2.6 * 10^{-6}$ to $3.6 * 10^{-2}$. According to the depth of occurrence, the depth to bed rock is discussed under three general categories viz

1. At shallow depth 11 - 45m bgl
2. At intermediate depth 45 - 75m bgl
3. At deeper depth > 75m bgl

Shallow aquifer made up of weathered rock, moderate to deep aquifer made up of fractured rock. Shallow dug wells are used at depths up to 11 to 12m beyond which bore wells are in use.

4.2.1 Hydro-meteorological characteristics

Nearest rain gauge station is at Tiruttani meteorological station for Ponpadi tank. From the same station pan evaporation, relative humidity, minimum and maximum temperature, sunshine, wind velocity and evapotransportation were collected (table 4.2). The salient features of climatic data are:

- The monthly average maximum temperature of the station varies from 23.12°C to 42.91°C. The monthly average minimum temperature of the station varies from 16.15°C to 35.02°C;

- The monthly average relative humidity of the station from varies from 34% to 94% ;
- Wind velocity is an important meteorological parameter which has considerable influence on evapotranspiration phenomena. Wind has direct impact on climate and vegetation and is linked with circulation pattern of the monsoon. The average monthly wind velocity of the station from 0.44 Kmph to 17.45 Kmph;
- The monthly average sunshine hours of the station varies from 2 hrs to 11.17 hrs;
- More than thirty years of monthly rainfall data (1972 – 2008) were collected from the Thiruthani rain gauge station. Average annual rainfall is 1008.4 mm;
- Annual average of 1972 – 1989 was 948 mm and 1990 – 2008 was 1066 mm. Average rainfall from January to May is 102 mm and from June to December is 906 mm as shown in table 4.3. Fifty and seventy five percentage dependable rainfall is 960 and 850 mm per year respectively;
- Even though Tiruttani is getting good amount of rainfall during Southwest and Northeast monsoon, Ponpadi tank is not getting sufficient water as expressed by the farmers. It is found that last six years Tiruttani has got rainfall more than 1000 mm as shown in figure 4.3. However tank got filled to its fullest capacity during Northeast monsoon of 2005 and 2008. Rainfall in the 2007 (1275 mm) was more than in the year 2008 (1052 mm). However the tank filled to its fullest capacity only in the year 2008 and not in the year 2007. This is because tank filling is function of rainfall intensity rather than annual rainfall. That is why tank filled during

November 2008 due to continuous three days rainfall of 378 mm (26/11/2008 to 28/11/2008);

- Farmers expressed that one time filling is sufficient enough to meet two years demand of their agriculture. Since this tank is the first tank of the cascade system which is affected by the siltation problem both in the supply channel and also in the tank bed whose catchment is part of a hill lying far of from the tank as shown in figure 4.4. Slope from catchment to tank is relatively high. Hence enormous quantum of silt being deposited into the tank. From the enquiry and also by capacity survey it was found that the tank has lost its one fourth capacity i.e. reduced from 1.6 M m^3 to 1.2 M m^3;

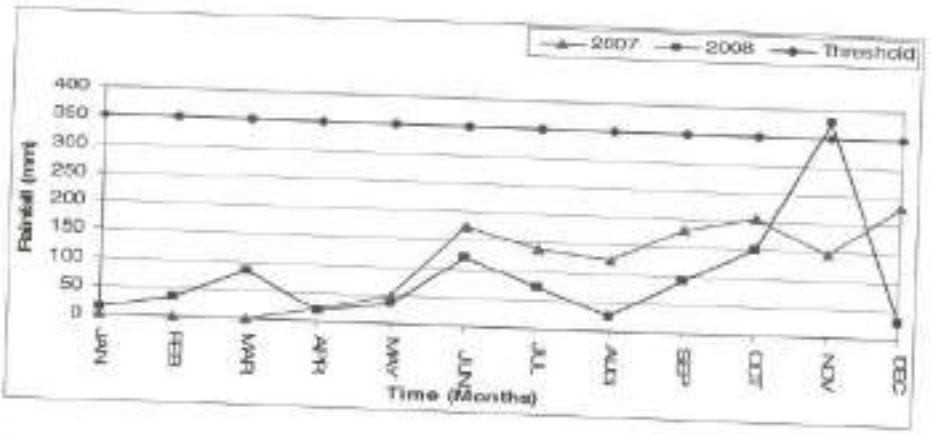

Figure 4.3 Comparison of 2007 and 2008 Monthly Rainfall

4.2.2 Delineation of Catchment area and Estimation of Tank Capacity - Ponpadi

Catchment area of the Ponpadi tank is 11.75 km^2 which was delineated using survey of India toposheet of scale 1:25000. The same map was scanned and digitized through Map Info GIS software package. Figure 4.4 shows the Ponpadi tank and its catchment. Engineering survey was conducted in Ponpadi tank to estimate the present capacity of the tank. The survey was carried out with the help of the Geophysical Positioning System

(GPS) and Dumpy level. The reduced levels noted by the GPS were verified by the Dumpy level survey. Both the data were used for the mapping and analysis. Based on these, contour maps were drawn which are shown in figure 4.5. The capacity of the tank was estimated as 1.16 M m^3 which was 1.61 Mm^3 thirty years before. Its dead storage is 0.0738 M m^3 at 92.8 m above mean sea level. Tank surpluses at 95.8 m at which tank capacity is 1.16 M m^3 which is shown below.

Components	R.L wrt m.s.l (m)	Remarks
Top of the Platform	97.55	
Bottom of the Sluice	92.8	0.0738 M m^3 Dead Storage
R.L. of the Surplus Weir	95.8	1.16 M m^3 Tank Surplused
Maximum Depth of the Tank	4.75 m	At Sluice

Table 4.2 Monthly Climatological Details of Tiruttani during the year 2006

Monthly Average	Jan.	Feb	Mar	Apr.	May	June	July	Aug.	Sep.	Oct.	Nov.	Dec.	Avg
Pan Evaporation (mm)	103.95	122.75	171.59	196.29	241.13	359.05	178.29	165.29	145.28	117.94	89.41	89.37	165.03
Relative Humidity (%)	72.74	69.30	61.60	60.87	54.26	57.42	63.84	66.32	70.43	75.96	78.57	75.97	67.27
Maximum Temp (°C)	28.86	30.86	34.30	36.28	38.95	36.04	35.59	32.66	32.88	30.80	29.02	28.33	32.88
Mean Temp (°C)	24.18	26.07	28.67	31.05	33.20	31.80	30.03	29.45	29.03	28.27	25.89	24.45	28.51
Minimum Temp (°C)	20.00	20.88	22.74	25.58	27.62	27.20	26.65	26.09	25.19	23.89	22.93	20.47	24.10
Sunshine (hrs / day)	7.95	8.87	9.26	9.41	8.68	6.53	5.37	5.82	6.33	6.02	5.81	6.98	7.25
Wind Velocity (km / hr)	3.53	3.93	4.74	5.28	6.16	7.47	6.53	5.89	4.58	2.91	3.19	3.88	4.84
Evapotranspiration (mm / day) (Penrnman Monteith Method)	3.4	4.2	5.1	5.8	6.2	5.7	4.9	4.7	4.4	3.8	3.3	3.2	4.5

Table 4.3 Monthly Rainfall (mm) at Tiruttani Raingauge Station

S. No	Year	Jan	Feb	Mar	Apr	May	Jun	Jul	Aug	Sep	Oct	Nov	Dec	Total
1	1972	20.2	0.0	0.0	0.0	62.8	88.4	40.0	63.2	87.2	162.0	122.2	280.0	**926.0**
2	1973	0.0	0.0	0.0	0.0	57.6	29.8	80.0	164.6	172.6	105.8	90.0	58.6	**759.0**
3	1974	0.0	0.0	0.0	0.0	82.2	112.0	139.9	54.0	121.8	100.2	40.6	0.0	**650.7**
4	1975	26.8	0.0	4.0	0.0	62.4	54.6	283.2	229.0	188.4	234.2	241.4	1.5	**1325.5**
5	1976	4.2	0.0	0.0	9.6	14.4	71.6	263.4	241.8	24.6	182.8	235.7	41.0	**1089.1**
6	1977	3.0	4.9	0.0	0.3	32.0	53.9	108.5	120.8	39.0	297.7	460.6	0.1	**1120.8**
7	1978	1.2	6.1	0.0	22.5	20.6	37.6	218.2	44.8	121.4	105.2	156.3	258.4	**992.3**
8	1979	7.0	18.8	0.0	10.8	27.3	42.0	110.8	47.5	273.5	126.0	432.0	27.0	**1122.7**
9	1980	0.0	0.0	0.0	0.0	66.0	0.0	109.0	311.0	76.5	78.5	224.5	75.0	**940.5**
10	1981	10.0	0.0	24.0	0.0	30.0	126.0	109.4	168.4	94.0	213.8	52.0	20.0	**847.6**
11	1982	0.5	0.0	0.0	21.0	10.0	24.0	166.7	14.0	164.5	191.5	273.0	0.0	**865.2**
12	1983	0.0	0.0	9.0	30.0	87.0	30.4	107.2	291.6	240.0	100.1	48.0	189.6	**1132.9**
13	1984	0.0	95.0	0.0	0.0	0.0	0.0	119.5	43.1	181.0	77.0	68.0	9.0	**592.6**
14	1985	35.0	0.0	0.0	42.5	0.0	50.8	205.4	78.0	173.2	140.2	386.8	67.9	**1179.8**
15	1986	137.2	42.4	0.0	7.0	36.0	0.0	23.1	67.5	122.0	149.5	184.3	0.4	**769.4**
16	1987	11.3	0.0	42.0	0.0	14.2	113.6	19.0	148.6	94.9	247.0	168.5	248.0	**1107.1**
17	1988	0.0	0.0	0.0	35.0	59.0	17.5	115.5	104.3	202.0	106.0	89.0	87.0	**815.3**
18	1989	0.0	0.0	6.5	0.0	22.0	72.0	217.0	58.0	143.0	24.0	219.0	64.0	**825.5**
19	1990	13.0	3.0	23.0	15.0	159.0	25.0	38.0	110.0	346.0	226.0	161.5	39.0	**1158.5**

20	**1991**	3.0	0.0	0.0	2.0	2.0	133.5	51.0	117.0	209.0	279.0	370.0	0.0	**1166.5**
21	**1992**	43.0	0.0	0.0	3.7	71.0	0.0	46.0	84.0	59.0	76.0	162.0	15.0	**559.7**
22	**1993**	0.0	23.0	0.0	0.0	0.0	12.0	180.0	110.0	177.0	128.0	361.0	101.0	**1092.0**
3	**1994**	0.0	0.0	0.0	0.0	54.5	22.0	126.0	150.0	125.0	187.0	234.0	19.0	**917.5**
24	**1995**	42.0	0.0	1.5	0.0	369.0	138.0	111.5	260.5	99.0	104.0	60.0	3.5	**1189.0**
25	**1996**	0.0	0.0	0.0	73.0	0.0	277.0	123.0	236.0	170.0	117.0	117.4	376.0	**1489.4**
26	**1997**	0.0	0.0	0.0	0.0	67.0	97.0	12.0	88.0	332.0	114.0	231.0	170.5	**1111.5**
27	**1998**	0.0	73.0	0.0	0.0	0.0	0.0	86.0	94.0	132.0	136.0	350.0	125.0	**996.0**
28	**1999**	0.0	0.0	0.0	0.0	0.0	11.0	113.0	240.0	30.0	71.0	125.0	120.0	**710.0**
29	**2000**	0.0	120.0	0.0	15.0	26.0	65.0	45.0	173.0	118.0	112.0	88.0	115.0	**877.0**
30	**2001**	7.0	0.0	5.0	175.5	55.0	22.0	89.0	86.0	176.5	363.0	85.0	95.5	**1159.5**
31	**2002**	2.0	0.0	0.0	0.0	80.0	16.0	106.0	22.0	149.0	209.0	65.0	44.0	**693.0**
32	**2003**	0.0	0.0	60.0	70.0	8.0	79.0	290.0	133.0	197.0	133.0	31.0	24.0	**1025.0**
33	**2004**	0.0	0.0	0.0	25.0	236.0	11.0	125.0	22.0	278.0	180.0	150.0	3.0	**1030.0**
34	**2005**	0.0	0.0	24.0	107.0	50.0	12.0	154.0	130.0	199.0	**418.0**	280.0	**305.0**	**1679.0**
35	**2006**	0.0	0.0	0.0	0.0	24.0	148.0	42.0	85.0	270.0	**308.5**	114.5	74.0	**1066.0**
36	**2007**	0.0	0.0	0.0	22.0	50.0	174.0	140.0	125.0	182.0	205.0	147.0	230.0	**1275.0**
37	**2008**	13.0	35.0	84.0	18.0	35.0	119.0	74.0	26.0	91.0	150.0	**378.0**	29.5	**1052.5**
38	**2009**	0.0	0.0	0.0	0.0	0.0	31.0	37.0	142.0					
	average	**10.3**	**11.4**	**7.6**	**19.1**	**53.2**	**61.8**	**118.6**	**122.7**	**158.4**	**166.4**	**189.3**	**89.6**	**1008.4**

Figure 4.6 and Figure 4.7 show the depth versus water spread area and depth versus storage graphs respectively. Table 4.4 shows the cumulative water spread area and storage of the tank against elevation of the tank. Maximum depth of the Ponpadi tank is 4.75 m at sluice.

- Water spread area at 3m above the sill level is approximately 280000 m^2 and the same is 300000 m^2 to a depth of 4.26m;
- Storage below the sill level is 0.0738 Mm^3 which is a dead storage. Up to a depth of 93.4m the incremental storage was 0.04 Mm^3 resulting in a cumulative volume of 0.15 Mm^3. Beyond this depth 93.4m, the incremental storage increases progressively from 0.05 to 0.15 Mm^3;
- Height of the surplus weir has been reduced in order to avoid the submergence of the railway track passing through Ponpadi tank. It is also one of the reasons for the reduction of the Ponpadi tank capacity;

Figure 4.4 Catchment Area of Ponpadi Tank

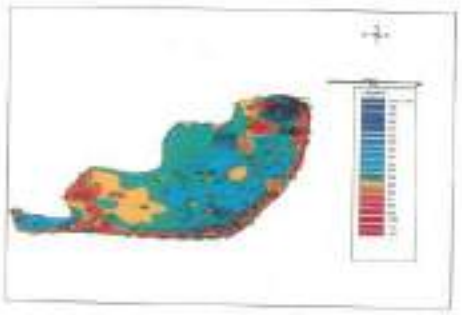

Figure 4.5 Contour Map of Ponpadi tank

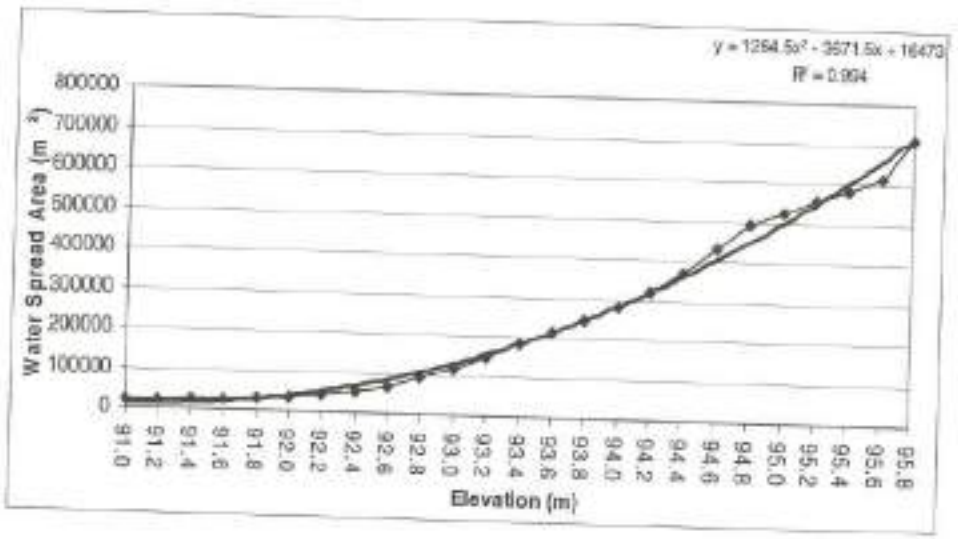

. Figure 4.6 Elevation vs Water spread Area at Ponpadi Tank

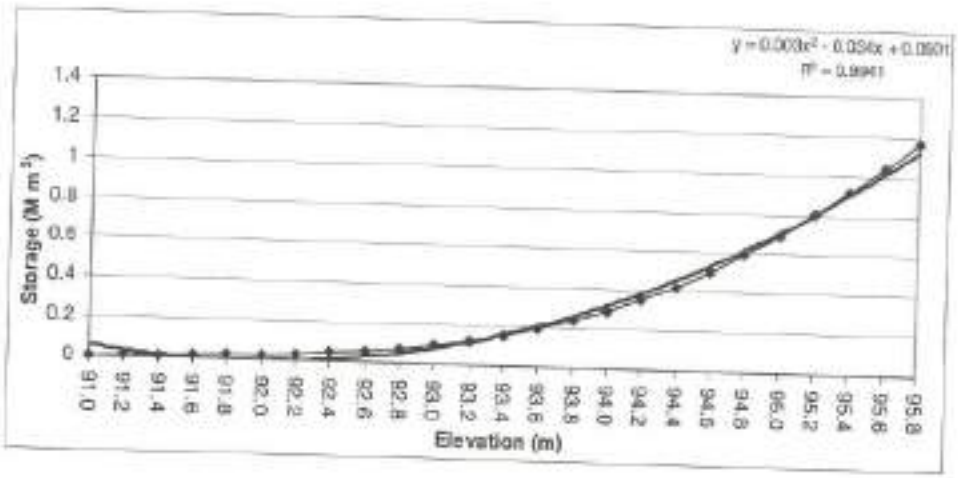

Figure 4.7 Elevation vs Storage at Ponpadi Tank

Table 4.4 Ponpadi Tank Capacity Estimation

Elevation (m)	Incremental Area (m^2)	Cumulative Area (m^2)	Volume (m^3)	Incremental Volume (M m^3)	Cumulative Volume (M m^3)	Remarks
91	21033.94	21033.943	0		0	
91.2	2105.902	23139.845	4417.4	0.004417379	0.004417379	
91.4	2183.022	25322.867	4846.3	0.004846271	0.00926365	
91.6	2436.178	27759.045	5308.2	0.005308191	0.014571841	
91.8	3695.865	31454.91	5921.4	0.005921395	0.020493237	
92	4977.703	36432.613	6788.8	0.006788752	0.027281989	
92.2	8291.778	44724.391	8115.7	0.0081157	0.035397689	
92.4	10687.340	55411.729	10014	0.010013612	0.045411301	
92.6	13382.380	68794.112	12421	0.012420584	0.057831885	
92.8	22550.890	91345.001	16014	0.016013911	0.073845797	Dead Storage
93	25851.250	117196.25	20854	0.020854125	0.094699922	
93.2	31114.470	148310.72	26551	0.026550697	0.12125062	
93.4	34609.620	182920.34	33123	0.033123106	0.154373725	
93.6	29441.780	212362.11	39528	0.039528245	0.19390197	
93.8	31553.760	243915.88	45628	0.045627799	0.23952977	
94	36219.810	280135.68	52405	0.052405156	0.291934926	
94.2	38382.030	318517.71	59865	0.059865339	0.351800265	
94.4	49279.580	367797.29	68631	0.0686315	0.420431765	
94.6	64308.890	432106.18	79990	0.079990346	0.500422111	
94.8	59211.860	491318.04	92342	0.092342421	0.592764532	
95	34902.090	526220.13	101754	0.101753817	0.694518349	
95.2	27579.950	553800.08	108002	0.108002021	0.80252037	
95.4	28797.000	582597.08	113640	0.113639716	0.916160086	
95.6	28558.950	611156.03	119375	0.119375311	1.035535397	
95.8	99822.600	710978.64	132213	0.132213467	1.167748864	Full Capacity 4.75 m depth

4.2.3 Runoff Estimation - Ponpadi

The rainfall during the year 2007 was 1275 mm which was measured at Tiruttani Raingauge Station. It was also observed that even if there is rain at Tiruttani, some times no rainfall took place at Ponpadi. Runoff takes place only during continuous rainy days that too at high intensity of rainfall. This situation was observed in the year 2007.

Year 2007 and 2008

From April to August 2007, Ponpadi had 511 mm rain which produced very very less runoff to the tank. Sufficient inflow to the tank was observed from 3rd September 2007 (51 mm rainfall on 03.09.2007) which was followed on 14th of September. It contributed about 0.1 M m^3. Rainfall during the month of October and November, contributed 0.28 M m^3 which was followed by the December 2007 rainfall that increased the storage capacity to 0.44 M m^3 against its full capacity of 1.16 M m^3 as shown in figure 4.8. Even after the rain stopped, the runoff was observed for next ten days that can be observed in the table 4.5. The total runoff from the catchment was 0.24 M m^3. Volume of water fed to the tank through direct rainfall was 0.13 M m^3. Maximum storage in the Ponpadi was 0.43 M m^3 which was observed on 30th December 2007. Since power supply to the farmers is free, no water from the tank was discharged. All the needs of the crop met out by pumping. Hence the tank storage was decreased by seepage, evaporation and by sluice leakage. It becomes completely dry during March 2008 which is very clear from the figure 4.8.

Total rainfall during the year 2008 was 1053 mm. Even though the rainfall during 2008 was less than 2007, the rainfall intensity was very high which was 378 mm in three days of November 2008. Actually rain was started

on 26/11/2008 which continued for three days, filled the tank. Tank was full till 9/12/2008 and started decreasing as shown in figure 4.8 and 4.9. Photograph 4.1 shows the tank with its full capacity during December 2008. It was surplused for many days as shown in photograph 4.2. Weaker portion of the tank breached as shown in photograph 4.3 which were arrested with the sand bag packing. The area of cultivation during December 2007 was only 50 acres since the tank has got one third of its capacity. But in the year 2008, the area of cultivation was initially 72 acres which increased to 205 acres as shown in table 4.6 to 4.8 which can also be seen in photograph 4.4.

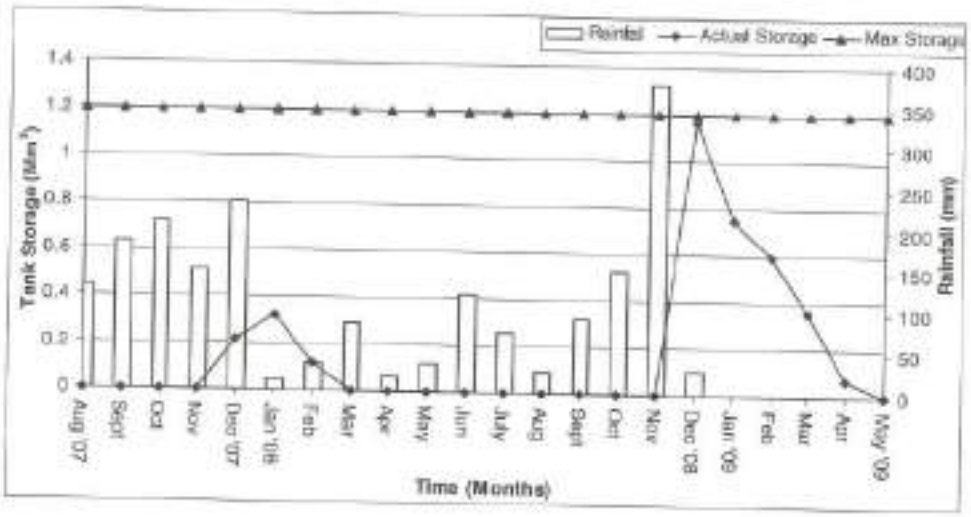

Figure 4.8 Monthly Tank Storage for Two Water Years

Table 4.5 Ponpadi Tank Storage Estimation

Date	Runoff from the delineated catchment (m^3)	Direct Rainfall over the tank (m^3)	Water spread Area (m^2)	Evaporation loss (m^3)	Actual Storage (m^3)	Change in storage, ΔS (m^3)
19-Dec-07					281500	
20-Dec-07	42703	59011	301246	2711	324900	43407
21-Dec-07	61712	70387	333302	3000	372400	47529
22-Dec-07	38034	3555	338230	3044	379300	6863
23-Dec-07	30159		340201	3062	382000	2745
24-Dec-07	22274		345621	3111	389500	7549
25-Dec-07	14327		357941	3221	406700	17158
26-Dec-07	9610		371013	3339	424400	17726
27-Dec-07	6346		372620	3354	426400	2000
28-Dec-07	6346		374228	3368	428400	2000
29-Dec-07	4211		374871	3374	429200	800
30-Dec-07	4539		377444	3397	432400	3200
Total	240261	132953		34980		

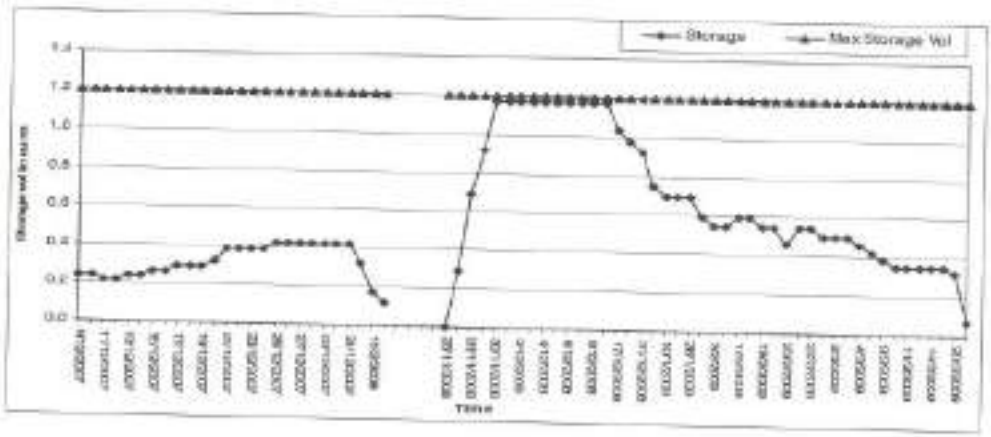

Figure 4.9 Daily Tank Storage during Two Water Years at Ponpadi Tank

Photograph 4.1 View of Ponpadi Tank during December 2008

Photograph 4.2 View of Surplus at Ponpadi Tank during December 2008

Photograph 4.3 **Sand Bag Packing to Arrest the Breach at Ponpadi Tank during December 2008**

Photograph 4.4 **Cultivation at Ponpadi Tank Command Area during December 2008**

4.2.4 Ground Water Potential

The water table represents the ground water reservoir level and changes in its level, represent the changes in the ground water in storage. The rise or fall of the water table in a specific time interval was prepared from water level data of wells. A decline in the water table represents ground water abstraction in excess of recharge, while a rise represents groundwater recharge in excess of abstraction. Water level fluctuation is due to rainfall recharge, hydrologic influences such as fluctuation of surface water bodies and man made disturbances like application of irrigation water, artificial recharge and with with drawls from wells etc.

In areas with well defined seasonal rainfall, the water table rises and falls follow annual cycles, the rise corresponding to the rainfall period and the low stage corresponding to the dry period. The water level rise does not commence immediately with the onset of the rainy season as the initial rains have to satisfy the soil moisture deficit which is at maximum level at the end of dry spell. The fluctuations are caused by evaporation and transpiration of groundwater by phreatophyte that dissipates considerable volumes of groundwater. The high losses after midday, usually with strong sunlight, cause a decline in the water table, followed by partial recovery during the nights when the losses are low. The recovery is attributable to the replenishment of storage losses from adjacent areas withdrawal of groundwater by pumping wells causing decline in water levels. It reflects the cumulative effect of natural recharge and discharge condition. During the period of operation of the pump, there is a draw down in the water levels followed by recovery when the pumps are shut off. As long as the pumpage does not exceed the recharge, water levels recovers to original levels during rest periods. Prolonged overdevelopment of ground water

in a heavily pumped areas results in a downward trend of the water table due to the draft exceeding the recharge.

4.2.5 Groundwater Scenario at Ponpadi Tank

The command area of Ponpadi tank is 1.45 square kilometer (145 Ha) which has more than thirty open dug wells and twenty dug cum bore wells. Before selecting wells, Ponpadi tank farmers were met and discussed about the tank's characteristics such as number of fillings, number of times the tank surpluses, tank's capacity, well depth, pumping rate, the land area each well supports etc. The photographs 4.5 and 4.6 show the Ponpadi tank's farmers. Initially five open wells at the right of the sluice and seven open wells at the left of the sluices with respect to flow direction which are named as R1 to R5 and L1 to L7, respectively were considered for the study to collect ground water levels. At later stages some more open wells and bore wells were chosen to study the ground water movement. Pumping wells are represented as P1, P2 etc as shown in figure 4.10

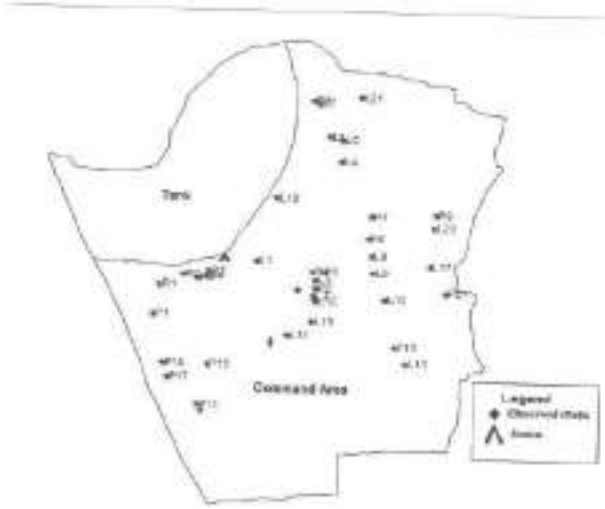

Figure 4.10 Pumping wells Location at Ponpadi Tank Command Area

Photograph 4.5 Farmers Meet at Ponpadi Tank

Photograph 4.6 Farmers Participation at Ponpadi Tank

4.2.6 Well History

Extensive information about pumping wells and cropping pattern were collected which are given in Table 4.6, Table 4.7 and Table 4.8. The land holding

by farmers ranges from 2 to 20 acres and some farmers are landless also. Most of the big farmers are living in Tiruttani Town. Small and landless farmers are living in a Ponpadi village. Farmers had concentrated on cultivation when the tank has sufficient water. Once the Ponpadi tank gets water with capacity to its full, or more than fifty percent of its capacity, the farmers are cultivating two times in that year. Mostly third crop will be a dry crop such as groundnut, corn, etc,. Even though the Ponpadi tank gets filled to its full capacity once in two years they are able to cultivate for two years continuously using groundwater. This was stated by farmers. The total command area is 145 hectares (360 acres). It was found that 72 acres were under cultivation during November 2008. Most of the wells are dug cum bore well or bore wells, from which pumping of 3 to 6 m^3 per hour was observed. During January 2009, about 147 acres of land were under cultivation. Most of the crops are paddy and sugarcane. One of the farmers Yasothamma cultivated 15 acres of casuarinas and eucalyptus during January 2009 which is given in Table 4.7. Extensive cultivation of 205 acres was found during February 2009. Entire Ponpadi command area was filled with paddy and sugarcane during February 2009 as shown in photograph 4.7

Photograph 4.7 Cultivation at Ponpadi Command Area during February 2009

Table 4.6 Cropping Pattern during November 2008 at Ponpadi Command area

Farmers Name	Well No	land Area (Acres)	Land Cultivated (Acres)	Season wise Crop (Nov '08)	No of Crops in a Year	Pump Capacity (HP)	Depth of the Well (m)
Krishna Moorthy Naidu	R1	4			Single	5	8.8
Ramaiya	R2	2			Single	5	
Narayanasamy Pillai	R3						9.4
Kurrappaa Naidu	R4	15	4	Paddy	Double	5	10.0
Narayanasamy	R5						
Yasothamma	L1	15	15	Casuarina and Eucalyptus		5	11.6
Padmanaba Naidu	L2	2					9.1
Puzzinka Naidu	L3	4				5	8.0
Baburao Naidu	L4	5	2	Paddy	Single	5	11.5
Ravi Naidu	L5	7	2	Paddy	Single	5	12.4
Kanniya Naidu	L6	5	4	Paddy	Triple	5	11.9
Loganadha Naidu	L7	8					12.7
Lakshmaya Naidu (Rajendra Naidu)	L8	6	2	Paddy	Double	5	13.4
G Rama Naidu G Ravi	L9	6	3	Paddy	Double	5	14.8
Dhanasekar	L10	3	1	Paddy	Single	5	14.5

Govindan	L11	6	4	Paddy and Groundnut	Double	5	12.6
Puzzinka Rao	L12	4					12.8
Nagathar	L13	4			Single	5	13.5
Raghupadhi	L14	2					14.9
Ramachandra Naidu	L15	4					11.9
Lakshumaya Naidu	L16	2					13.8
Nataraja Pandithar	L17	10	4	Paddy	Double	5	14.4
Krishna Moorthy	P1	10	2	Paddy	Double	5	75
Puzzinka Naidu	P2	4	1	Paddy	Double	5	105
Ramesh, Jeganathan, Bhaskar, and Babuji	P3	12	1	Paddy	Double	5	54
Yasothamma	P4	15	15			5	114
Rajendran	P5	5	2	Paddy	Double	5	105
Loganadha Naidu	P6	8	4	Paddy	Double	5	75
Subramani	P7	2	2	Paddy	Double	5	45
Krista Naidu	P8	4	4	Sugarcane	Single	5	60
Total		**174**	**72**				

Table 4.7 Cropping Pattern during January 2009 at Ponpadi Command Area

Farmers Name	Well No	land Area (Acres)	Land Cultivated (Acres)	Season wise Crop (Jan '09)	No of Crops in a Year	Pump Capacity (HP)	Depth of the Well (m)
Krishna Moorthy Naidu	R1	4		Paddy	Single	5	8.77
Ramaiya	R2	2		Paddy	Single	5	
Narayanasamy Pillai	R3						9.37
Kurrappaa Naidu	R4	15	14	Paddy	Double	5	10
Narayanasamy	R5		4				
Yasothamma	L1	15	16.5	Casuarina and Eucalyptus		5	11.6
Padmanaba Naidu	L2	2					9.07
Puzzinka Naidu	L3	4				5	8
Baburao Naidu	L4	5	5	Paddy and Ground nut	Single	5	11.48
Ravi Naidu	L5	7	6	Paddy	Single	5	12.4
Kanniya Naidu	L6	5	6.5	Paddy	Triple	5	11.9
Loganadha Naidu	L7	8					12.7
Lakshmaya Naidu (Rajendra Naidu)	L8	6	4.5	Paddy	Double	5	13.4
G Rama Naidu G Ravi	L9	6	12	Paddy	Double	5	14.8

Dhanasekar	L10	3	1	Paddy	Single	5	14.5
Govindan	L11	6	10	Paddy and Groundnut	Double	5	12.6
Puzzinka Rao	L12	4					12.8
Nagathar	L13	4	3.5	Paddy and Dhal	Single	5	13.5
Raghupadhi Naidu	L14	2					14.9
Ramachandra Naidu	L15	4	2	Paddy	Single		11.9
Lakshumaya Naidu	L16	2					13.8
Nataraja Pandithar	L17	10	8	Paddy	Double	5	14.4
Krishna Moorthy	P1	10	5	Paddy	Double	5	75
Puzzinka Naidu	P2	4	4	Paddy	Double	5	105
Ramesh, Jeganadhan, Bhaskar, and Babuji	P3	12	6	Paddy	Double	5	54
Yasothamma	P4	15	16.5			5	114
Rajendran	P5	5	4.5	Paddy	Double	5	105
Loganadha Naidu	P6	8	8	Paddy	Double	5	75
Subramani	P7	2	4	Paddy	Double	5	45
Krista Naidu	P8	4	6	Sugarcane	Single	5	60
Total		**174**	**147**				

Table 4.8 Cropping Pattern during February 2009 at Ponpadi Command Area

Farmers Name	Well No	Total land Area (Acres)	Land Cultivated	Season wise Crop (Feb '09)	No of Crops in a year	Pump Capacity (HP)	Depth of the well (m)
Krishna Moorthy Naidu	R1	9	3.5	Paddy	Single	5	8.77
Ramaiya (Sridhar)	R2	2		Paddy	Single		
Narayanasamy Pillai	R3						9.37
Kurrappaa Naidu	R4	20	6	Paddy	Double	5	10
Narayanasamy	R5	4	4				
Yasothamma	L1	5	5	Casuarina and Paddy		5	11.6
Padmanaba Naidu	L2	4	4	Paddy	Single		9.07
Puzzinka Naidu	L3	4	3	Paddy	Double	5	8
Baburao Naidu	L4	10	5	Paddy and Ground nut	Single	5	11.48
Ravi Naidu	L5	10	10	Paddy	Single	5	12.4
Kanniya Naidu	L6	10	6	Paddy	Triple	5	11.9
Loganadha Naidu	L7	5	4	Paddy			12.7
Lakshmaya Naidu (Rajendra Naidu)	L8	7	10	Paddy	Double	5	13.4
G Rama Naidu G Ravi	L9	12	15	Paddy	Double	5	14.8

Dhanasekar	L10	2	1	Paddy	Single	5	14.5
Govindan	L11	6	6	Paddy and Groundnut	Double	5	12.6
Puzzinka Rao (Lakshmipathy & Bandari)	L12	4	4	paddy			12.8
Nagathar (ragupathi)	L13	5	1	Paddy and Dhal	Single	5	13.5
Ragupadhi Naidu	L14	2	2				14.9
Ramachandra Naidu	L15	4		Paddy	Single		11.9
Lakshumaya Naidu	L16	2	1				13.8
Nataraja Pandithar	L17	10	6	Paddy	Double	5	14.4
Krishna Moorthy	L18	8	8	Paddy and Sugarcane	Single	5	14.0
Balaram Naidu	L19	12				5	13.8
Balaraman	L20	5	5	Paddy	Single	5	14.5
Gopal	L21	15	15	Paddy	Double	5	14.8
Yasothamma	P4	5	5	Eucalyptus		5	114
Subramani	P7	4	2	Paddy	Double	5	45
Krista Naidu	P8	4	4	Paddy and Sugarcane	Single	5	60
Rajendran	P9	1.5	1.5	Paddy	Double	5	54
Ranjanan	P12	4	3	Paddy	Double	5	75
Raja	P13	2	3	Paddy and Groundnut	Double	5	60
Logan	P14	6	6	Paddy	Double	5	45
Samuvel	P15	2	2	Paddy	Double	5	45

Lokaiya Naidu	P16	5	1	Paddy	Single	7.5	42
Veltech College	P17	13	13	Coconut	Single	5	75
Balan	P18	1.5	4	Paddy	Double	5	8.1
Balakrishnan	P	4	4	Paddy	Double	5	
Sadasivam	P	2	2	Sugarcane	Single	5	
Jaganathan & Nanthan	Tank	4	2	Paddy	Single		
Sridhar	Tank	2					
Nagathar	Tank	2					
Baburao	Tank	3					
Loganathan Naidu	Tank	6	1	Paddy	Single		
Gopal	Tank	2	2	Paddy	Single		
Subramani	Tank	2	2	Paddy	Single		
Vengatapathi	Tank	2					
Ramesh Govindan	Tank	2	2	Paddy	Single		
Padmanaba Naidu	Tank	2					
Arumugam	Tank	2	2	Paddy	Single		
Lakshmaya Naidu	Tank	6					
Arumugam	Tank	2	2	Paddy	Single		
Gangan	Tank	3	3	Paddy	Single		
Munusamy Naidu	Tank	4	4	Paddy	Single		

Arasan	Tank	1	1	Paddy	Single		
Mani	Tank	1.5	1.5	Paddy	Single		
Citibabu	Tank	1.5	1.5	Paddy	Single		
Jaganatha Naidu	Tank	10					
Periyasamy (Teacher)	Tank	33					
Sakarapani	Tank	2					
Thanigaivel	Tank	2	2	Paddy	Single		
Vajaravel	Tank	1.5					
Yesu	Tank	0.75					
Kirupa	Tank	0.75					
Gopal	Tank	1.5	1.5	Paddy	Single		
Subramani	Tank	1.5	1.5	Paddy	Single		
Sakarapani - Mallika	Tank	1	1	Paddy	Single		
Total		**333**	**205**				

4.2.7 Groundwater levels in the Ponpadi Pumping Wells

Groundwater levels were observed monthly from August 2007 to August 2009 in the pumping wells itself as shown in figure 4.11 a, b, c. Open well R2 was dry for the entire study period.

- The water levels in all the wells on either side of the sluice observed were far below the measuring point. Open wells R1, R2, R4, R5, L1 and L2 were completely dry during August to October 2007 even though there was a sufficient rainfall of 125 + 182 + 205 = 512 mm. The rain was continued during November and December 2007 that increased water level in the open wells.
- Water levels were suddenly increased in all the wells due to heavy rainfall from 26/11/2008. (This rainfall made the Ponpadi tank at maximum level which was surplused also). Water levels were almost closer to the ground surface which can be seen from the figure 4.11 a, b, c.

The observation of the two years indicated that continuous down pour of rain especially during northeast monsoon alone can fill the tank. Then only the wells are getting recharged, otherwise most of the rain gets lost in meeting soil moisture requirement.

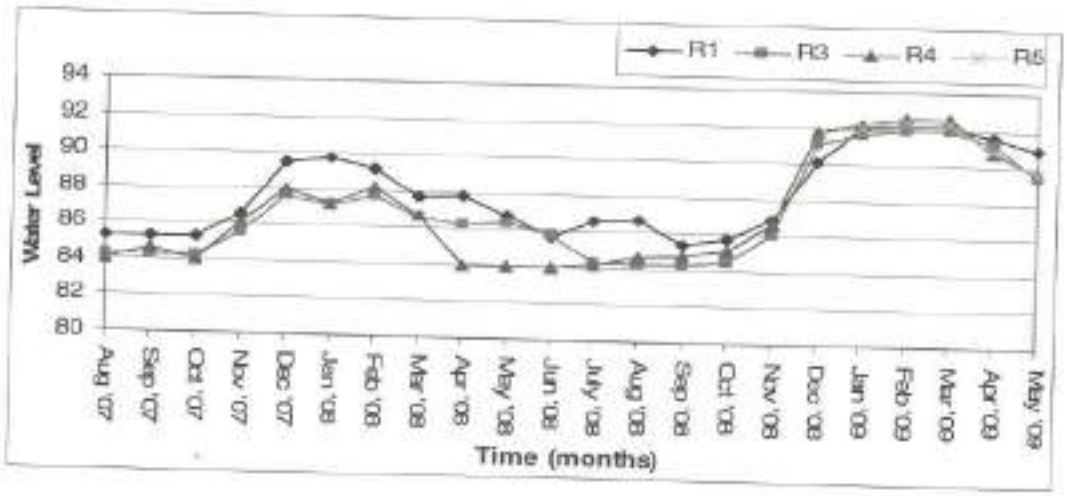

Figure 4.11a Ground Water Levels in the Pumping Wells of R1, R3 to R5 at Ponpadi Tank

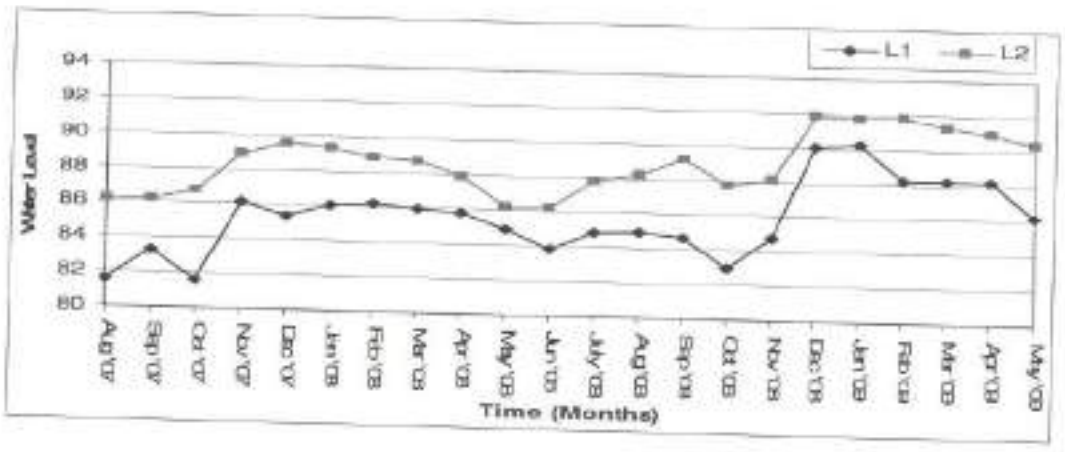

Figure 4.11b Groundwater Levels in the Pumping Wells of L1& L2 at Ponpadi Tank

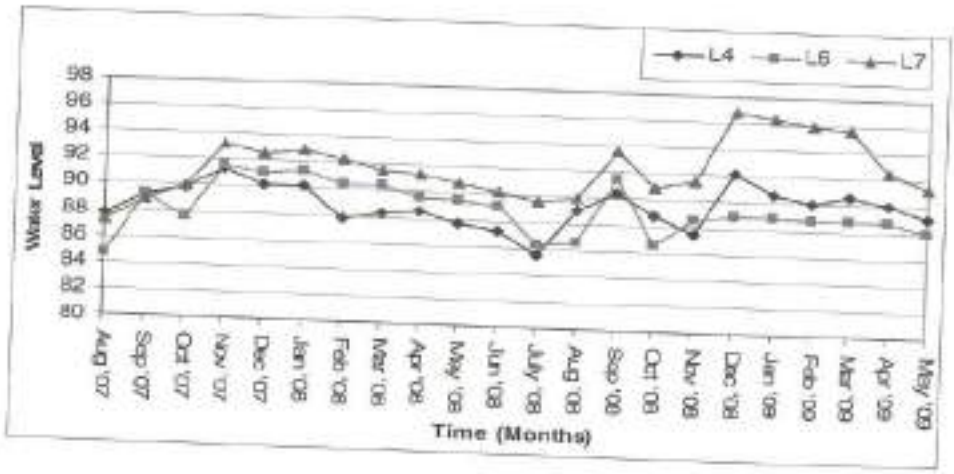

Figure 4.11c **Groundwater Levels in the Pumping Wells of L4, L6& L7 at Ponpadi Tank**

Pumping Details from December 2008 – May 2009

Pumping pattern at Ponpadi command area was observed from December 2008 to May 2009. Tank water was not released from the tank since electricity is free and farmers can use groundwater at free of cost. Farmers started intense cultivation of paddy and sugarcane after rain was started on 26/11/2008. This rain filled the tank to its fullest capacity. Farmers used 3 HP, 5 HP and rarely 7 HP motors to pump the groundwater. They operated the pump set four to ten hours depending upon the electricity availability. Most of the pumping was observed in the second deeper aquifer which ranges from 45 m to 75 m depth. Yield was observed as three to six cubic meter per hour. Pumping details from December 2008 to May 2009 are shown in Table 4.9.

Table 4.9 Pumping Details at Ponpadi Command Area

Observed Monsoon Months	Pumping (m^3)	Observed Non Monsoon Months	Pumping (m^3)
Dec-08	8105	Mar-09	9605
Jan-09	11444	Apr-09	9759
Feb-09	15820	May-09	5061
Total	**35369**		**24425**

4.2.8 Net Draft at Ponpadi Tank Command Area

From the monthly groundwater fluctuation data, net draft from the Ponpadi command area were estimated. Net draft is the algebraic sum of the recharge and discharge of the area which was 0.1 Mm^3 in the year 2007 – 2008 and 0.15 Mm^3 in the year 2008 - 2009. Monthly net drafts for two years are shown in figure 4.12.

- But total pumping may be 0.76 Mm^3 in the year 2007 – 2008 and 1.65 Mm^3 in the year 2008 – 2009;
- Monsoon pumping is 20% of the monsoon recharge and non monsoon pumping is more than 75% of the non monsoon recharge;
- Farmers at Ponpadi were waiting for a tank to get water then they started cultivation. It was observed that cultivated area during November 2008 was 72 acres, January 2009 was 177 acres and February 2009 was 205 acres;

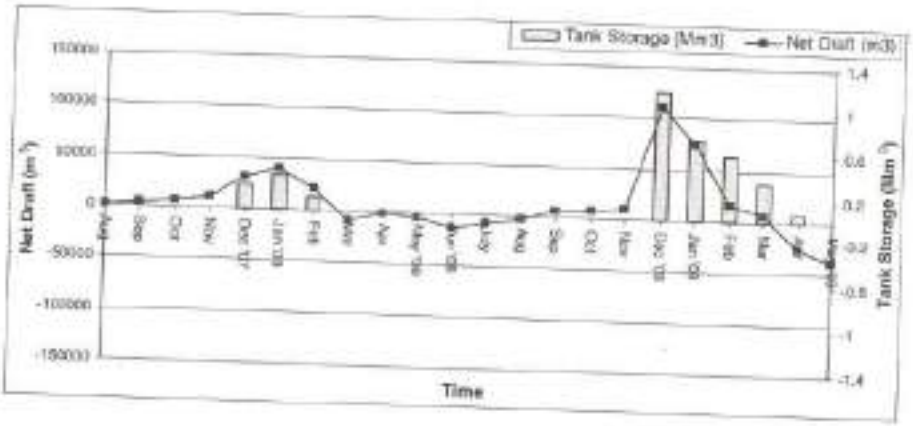

Figure 4.12 Net Draft at Ponpadi Tank Command Area

4.2.9 Seepage Rate at Ponpadi Tank

Seepage rate can be calculated as 50 percent of the tank storage of the corresponding months and also 2.4 percent per day of the tank storage. Tank storage is observed once in a month, it was considered as 50 percent per month that is given below.

Month	Tank Storage Mm^3	Seepage Rate Mm^3
Dec'07	0.22	0.11
Jan'08	0.32	0.16
Feb'08	0.12	0.06
Total	**0.66**	**0.33**
Dec'08	1.2	0.66
Jan'09	0.75	0.38
Feb'09	0.60	0.30
Mar'09	0.35	0.18
Apr'09	0.07	0.04
Total	**2.90**	**1.49**

Rainfall in the year 2007 – 2008 was more than 2008 - 2009. However tank got filled only during the second wet year due to very high rainfall of 400 mm in three days. This tank had one fourth of its capacity during January 2008 and 1.2 Mm^3 during December' 2008.

4.2.10 Relationship between Tank Water Level and the Well Water Level at Ponpadi Tank

It is observed that the tank influences the command area groundwater storage. Main source of the aquifer is the tank recharge. Graph between tank water level and well water levels were drawn. Hence it was planned to develop relationship between the tank water level and well water level. Using this relationship if tank water level is known the ground water level can be determined.

There is no specific trend was observed. Open wells are behaving different from deep bore well water level. Open wells are R1, R2, R4, L1, L2, L4, L6 and L7 in which tank water varies quadratically with groundwater levels as shown in figures below. Empirical relationship for the open wells were given below.

Well R1 – $1.393 x^2 + 257 x - 11747$

Well R2 – $1.218 x^2 + 225 x - 10316$

Well R4 – $1.336 x^2 + 247 x - 11335$

Well L1 – $0.234 x^2 + 44.6 x - 2032$

Well L2 – $0.456 x^2 + 84.87 x - 3851$

Well L4 – $0.075 x^2 - 12.86 x + 632.1$

Variation of tank water level, water table of open wells and piezometric surface of bore wells

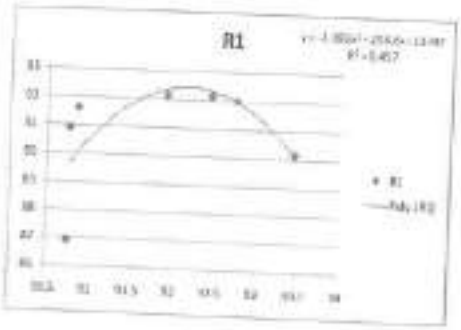

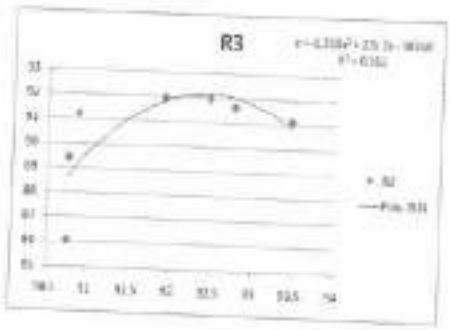

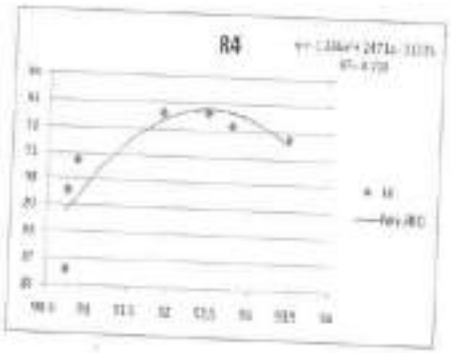

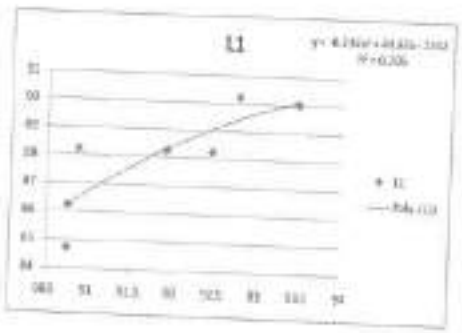

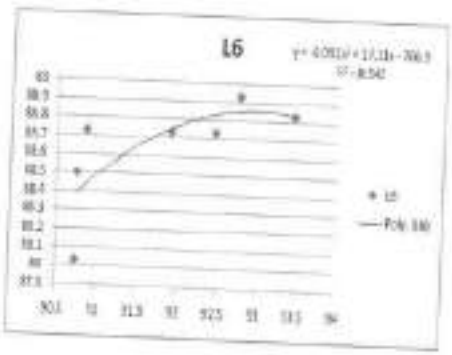

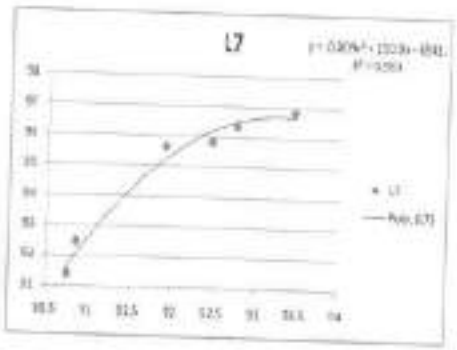
L7

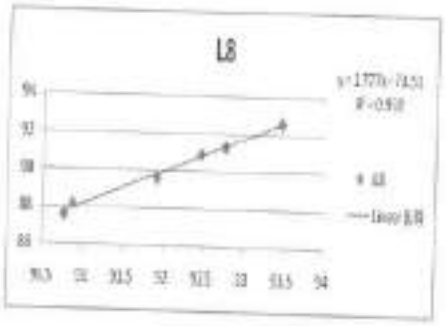
L8

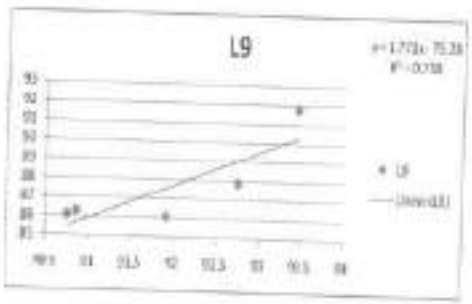
L9

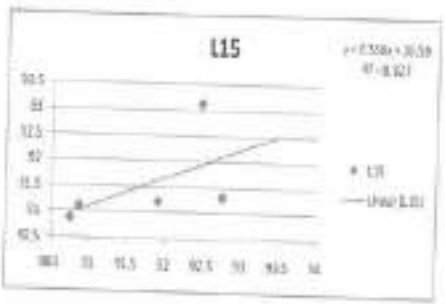
L15

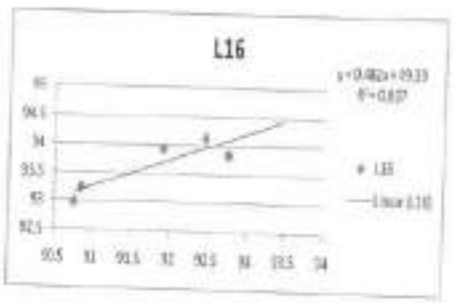
L16

Bore wells L8 and L9 and L15 and L16 varied similar. Their analytical relationship is given below.

L8 $Y = 1.777\ x - 73.51$

L9 $Y = 1.771\ x - 75.28$

L15 $Y = 0.566\ x + 39.59$

L16 $Y = 0.482\ x + 49.39$

4.3 SENGULAM TANK - VIRUDHUNAGAR

Virudhunagar district is divided into eight Taluks. It lies between Vaippar River and Gundar river basin. All the rivers are seasonal and carry substantial flow during monsoon period. The chief irrigation sources in the area are the tanks, dug wells and tube/ bore wells.

The Sengulam tank is situated at a distance of 15 km from Virudhunagar town in Virudhunagar District. The latitude and longitude of the tank are 9° 38' 33"N and 77° 49' 47"E respectively with an altitude of 125.578 m above m.s.l.

Geomorphology

A major part of the district constitutes a plain terrain with a gentle slope towards East and Southeast, except for the hilly terrain in the West. The prominent geomorphic units are flood plains, bazada pediment, shallow and deep buried pediment and structural hills.

Soil

Soil in the area have been classified into deep red loam, black soil and red sandy soil. The majority of the study area is covered by black soil. Black soils are very deep and generally occur in the depression adjacent to hilly areas.

Hydrogeology

The Virudhunagar district is underlain by both porous and fissured formation, unconsolidated formation and weathered. The important aquifer systems in the district are in fissured and fractured crystalline rocks. The thickness of the weathered zone in the district is 4 to 15 m. The depth of dug wells ranged from 10 to 15 m bgl. The yield of large diameter wells in the weathered mantle ranges from 40 to 110 lpm and are able to sustain for 2 to 6 hours per day. The specific capacity of large diameter wells in the crystalline rock ranges from 6.26 to 183.8 lpm/m of draw down. The yield of bore wells drilled down to a depth of 40 to 70 m for domestic purpose ranged from 10 to 250 lpm. The depth to water level in the district varied between 0.67 and 12.12 m bgl during pre monsoon and varied between 0.49 and 8.78 m bgl during post monsoon.

4.3.1 Rainfall and Climate

Virudhunagar receives, rain under the influence of both Southwest and Northeast monsoon. The Northeast monsoon chiefly contributes to the rainfall in the district. Most of the precipitation occurs in the form of cyclonic storm caused due to depression in the Bay of Bengal. The Southwest monsoon rainfall is more regular compare to Northeast monsoon.

Kavalur is the nearest rain gauge station for the Sengulam tank and is considered for the rainfall analysis. Annual and seasonal rainfall analysis was carried out from 1974 to 2009. Thirty five years average annual rainfall is 780 mm as shown in table 4.10. The average southwest monsoon and northeast monsoon 166 mm and 410 mm respectively as shown in table 4.11. Fifty percent dependable rainfall in 721.6 mm which occurred during the year 1992 and seventy five percent dependable rainfall in 604.1 mm which occurred during the year 1991. Rainfall in the year 2007 was 1011 mm and in the year 2008 was 1073 mm which are shown in figure 4.13.

Sengulam has a subtropical climate. The period from April to June is generally hot and dry and the weather is pleasant during the period from November to January. Usually mornings are more humid than afternoons. The relative humidity is on an average between 65 % and 85 % in the mornings and between 40 % and 70 % in the afternoons. The annual mean minimum and maximum temperature are 23.78°C and 33.95°C respectively. The day time heat is oppressive and the temperature is as high as 40.2°C. The lowest temperature recorded is 19.3°C.

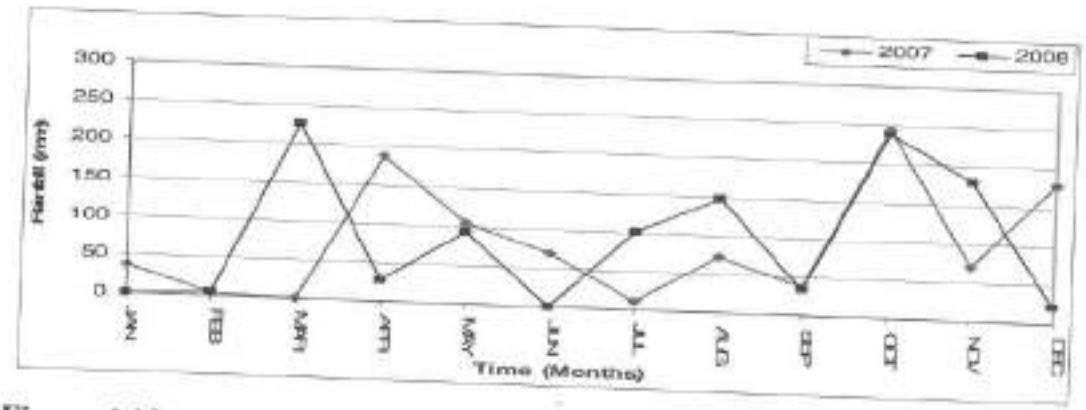

Figure 4.13 **Comparison of Rainfall during 2007 and 2008 at Kavalur Raingauge Station**

Table 4.10 Monthly Rainfall (mm) for the Period 1974 - 2008 at Kavalur Raingauge Station

S.NO	Rainfall Station - Kavalur Rainfall for the Year 1974 - 2008													
1	Year	Jan	Feb	Mar	Apr	May	Jun	Jul	Aug	Sep	Oct	Nov	Dec	Annual
2	1974	0.00	0.00	9.00	157.00	0.00	9.00	5.00	40.00	97.00	152.80	198.50	7.50	**675.80**
3	1975	9.50	8.00	17.50	12.00	64.20	0.00	118.80	15.50	97.20	104.60	87.00	3.50	**537.80**
4	1976	0.00	0.00	50.50	61.20	65.00	41.50	30.00	33.00	45.50	156.50	181.50	15.00	**679.70**
5	1977	0.00	37.50	38.00	43.50	138.10	0.00	54.00	33.00	138.00	317.00	270.90	9.00	**1079.00**
6	1978	0.00	22.00	6.00	39.10	21.50	0.00	5.80	0.00	37.00	53.80	99.70	124.00	**408.90**
7	1979	0.00	160.50	6.00	0.50	80.00	61.80	14.50	23.30	54.80	126.20	761.50	12.00	**1301.10**
8	1980	0.00	0.00	0.00	55.00	76.50	0.00	0.00	0.00	99.50	50.50	186.30	61.80	**529.60**
9	1981	0.00	21.50	11.00	14.00	58.40	9.20	63.70	24.70	68.50	258.50	82.50	74.00	**686.00**
10	1982	0.00	0.00	0.00	6.50	58.50	11.00	34.50	0.00	46.00	78.00	172.00	41.60	**448.10**
11	1983	0.00	0.00	0.00	21.50	39.00	36.50	23.00	0.00	55.50	238.20	169.40	59.50	**642.60**
12	1984	74.80	125.50	126.00	25.00	6.00	5.50	15.10	0.00	281.70	115.60	63.50	30.00	**868.70**
13	1985	94.40	0.00	66.20	0.00	45.80	0.00	14.50	17.50	72.60	95.00	97.70	58.50	**562.20**
14	1986	9.00	135.00	18.00	13.00	225.00	11.60	14.00	58.00	99.00	184.00	63.00	35.00	**864.60**
15	1987	0.00	0.00	21.00	4.00	115.00	10.00	0.00	62.10	116.50	377.70	171.70	132.00	**1010.00**
16	1988	0.00	6.00	40.20	228.50	18.50	2.00	24.00	170.00	100.00	159.00	73.00	22.00	**843.20**
17	1989	0.00	0.00	0.00	113.70	125.00	0.00	191.40	2.00	189.50	192.00	122.00	15.00	**950.60**
18	1990	173.00	19.00	80.00	11.00	3.00	0.00	9.00	16.00	111.50	259.00	91.20	12.00	**784.70**

19	1991	96.00	0.00	10.00	59.00	41.50	41.10	5.50	0.00	117.50	198.30	16.50	18.70	**604.10**
20	1992	0.00	0.00	0.00	107.50	19.30	41.00	37.00	22.50	120.30	91.50	248.50	34.00	**721.60**
21	1993	0.00	27.00	15.00	20.00	85.00	72.00	0.00	4.00	73.20	192.40	298.80	100.60	**888.00**
22	1994	12.30	9.00	8.00	61.80	0.00	0.00	2.20	6.00	52.50	124.50	90.70	0.00	**367.00**
23	1995	0.00	3.20	16.00	89.80	225.50	0.00	18.30	72.00	84.50	135.00	42.00	0.00	**686.30**
24	1996	0.00	12.00	8.00	187.30	16.10	0.00	0.00	144.00	39.00	174.00	24.00	139.00	**743.40**
25	1997	0.00	0.00	25.00	108.00	74.00	0.00	0.00	0.00	48.00	326.00	355.00	221.00	**1157.00**
26	1998	0.00	0.00	0.00	0.00	27.00	6.00	75.00	78.00	74.00	52.00	322.00	182.00	**816.00**
27	1999	0.00	24.00	0.00	122.00	69.40	0.00	0.00	27.00	127.50	381.20	204.20	30.40	**985.70**
28	2000	22.00	189.80	7.00	39.00	37.00	0.00	17.00	52.00	111.00	30.40	99.20	51.00	**655.40**
29	2001	11.00	2.00	25.00	120.00	78.00	6.00	35.00	14.00	139.40	117.90	274.90	27.10	**850.30**
30	2002	0.00	45.00	11.30	62.80	53.80	5.00	0.00	17.00	117.00	266.60	47.00	6.80	**632.30**
31	2003	0.00	4.00	64.20	76.00	56.60	24.00	14.20	75.80	38.20	244.40	100.00	0.00	**697.40**
32	2004	2.00	0.00	32.00	53.80	51.40	4.40	4.00	4.60	86.20	136.10	194.80	9.00	**578.30**
33	2005	2.00	0.00	24.60	220.60	57.80	0.00	20.00	11.00	29.00	333.00	116.00	111.00	**925.00**
34	2006	6.80	0.00	107.40	24.60	79.00	18.20	0.00	18.80	65.60	330.40	404.60	2.30	**1057.70**
35	2007	36.60	2.80	0.00	187.00	104.20	69.40	11.80	71.40	36.40	243.20	70.80	177.60	**1011.20**
36	2008	0.00	5.00	225.80	26.60	93.60	0.40	101.80	147.20	33.80	238.90	179.30	20.40	**1072.80**
37	2009	16.60	0.00	148.50	81.60	114.00	17.20	0.00	57.00					
	Average	**15.72**	**23.86**	**33.81**	**68.14**	**67.30**	**13.97**	**26.64**	**36.59**	**88.65**	**186.69**	**170.85**	**52.67**	**780.63**

Table 4.11 Seasonal Rainfall for the Period 1974 - 2008 at Kavalur Raingauge Station

Seasonal and Annual rainfall (mm) at Kavalur raingauge station						
S. No	Year	Southwest (Jun-Sept) mm	Northeast (Oct-Dec) mm	Winter (Jan-Feb) mm	Summer (Mar-May) mm	Total
1	1974	151.0	358.8	0.0	166.0	**675.8**
2	1975	231.5	195.1	17.5	93.7	**537.8**
3	1976	150.0	353.0	0.0	176.7	**679.7**
4	1977	225.0	596.9	37.5	219.6	**1079.0**
5	1978	42.8	277.5	22.0	66.6	**408.9**
6	1979	154.4	899.7	160.5	86.5	**1301.1**
7	1980	99.5	298.6	0.0	131.5	**529.6**
8	1981	166.1	415.0	21.5	83.4	**686.0**
9	1982	91.5	291.6	0.0	65.0	**448.1**
10	1983	115.0	467.1	0.0	60.5	**642.6**
11	1984	302.3	209.1	200.3	157.0	**868.7**
12	1985	104.6	251.2	94.4	112.0	**562.2**
13	1986	182.6	282.0	144.0	256.0	**864.6**
14	1987	188.6	681.4	0.0	140.0	**1010.0**
15	1988	296.0	254.0	6.0	287.2	**843.2**
16	1989	382.9	329.0	0.0	238.7	**950.6**
17	1990	136.5	362.2	192.0	94.0	**784.7**
18	1991	164.1	233.5	96.0	110.5	**604.1**
19	1992	220.8	374.0	0.0	126.8	**721.6**
20	1993	149.2	591.8	27.0	120.0	**888.0**
21	1994	60.7	215.2	21.3	69.8	**367.0**
22	1995	174.8	177.0	3.2	331.3	**686.3**
23	1996	183.0	337.0	12.0	211.4	**743.4**
24	1997	48.0	902.0	0.0	207.0	**1157.0**
25	1998	233.0	556.0	0.0	27.0	**816.0**
26	1999	154.5	615.8	24.0	191.4	**985.7**
27	2000	180.0	180.6	211.8	83.0	**655.4**

28	2001	194.4	419.9	13.0	223.0	**850.3**
29	2002	139.0	320.4	45.0	127.9	**632.3**
30	2003	152.2	344.4	4.0	196.8	**697.4**
31	2004	99.2	339.9	2.0	137.2	**578.3**
32	2005	60.0	560.0	2.0	303.0	**925.0**
33	2006	102.6	737.3	6.8	211.0	**1057.7**
34	2007	189.0	491.6	39.4	291.2	**1011.2**
35	2008	283.2	438.6	16.6	344.1	**1082.5**
Average		**165.9**	**410.2**	**40.6**	**164.2**	**780.9**

4.3.2 Delineation of Catchment and Tank Capacity Estimation of Sengulam

The catchment area of the Sengulam tank is 4.60 km^2. Figure 4.14 shows the catchment map of Sengulam tank. It has both intercepted and free catchment. Main supply channel is from free catchment and the other one is from intercepted catchment. This tank has got three sluices and one surplus weir as shown in Figure 4.14. The Photograph 4.8 shows supply channel from the free catchment to the Sengulam tank. Photograph 4.9 shows the Sengulam tank when it was full during December 2007. Photograph 4.10 shows the Sengulam tank during November 2008. Photograph 4.11, 4.12 and 4.13 show the structure of Sluice 1, Sluice 2, and Sluice 3 respectively. Photograph 4.14 shows the surplus weir at Sengulam tank. The surplus water from this tank is directed to the next eri (tank) called Muruganeri as shown in figure 4.14. The Photograph 4.15 shows the crop cultivation at Sengulam tank command area during December 2007. Photograph 4.16 shows one of the pumping activities from the open wells at Sengulam command area which was taken during June 2007.

Top soil was 3 m depth at Sluice 3, 7 m depth at Sluice 2 and 10 m depth at Sluice 1. This Top soil is underlained by weathered rock that is shown in Photograph 4.16. Totally Twenty four pumping wells were found in the Sengulam command area as shown in figure 4.15.

Figure 4.16 shows the depth versus water spread area of the Sengulam tank. Through GPS the reduced level data capacity of the Sengulam tank was estimated as 0.278 Mm^3 as shown in figure 4.17. Table 4.12 gives information on water spread area and storage at different depths. Sluices 2 sill level is at 119.5 m above the mean sea level at which the storage is 0.1 M m^3. Hence, only when tank storage is above 0.1 M m^3, water can be conveyed to the command area through Sluice 2. However water may be discharged through sluice 1 which is located at a depth of 119.98 m above the mean sea level at which storage is 0.143 M m^3. The reduced levels of Sluices and Surplus weir are given below.

Sluices	**Above Mean Sea Level (m)**	**Storage (Mm^3)**
Sluices 1	119.98	0.143
Sluices 2	119.50	0.1
Sluices 3	118.85	0.04
Surplus weir	121.18	full capacities

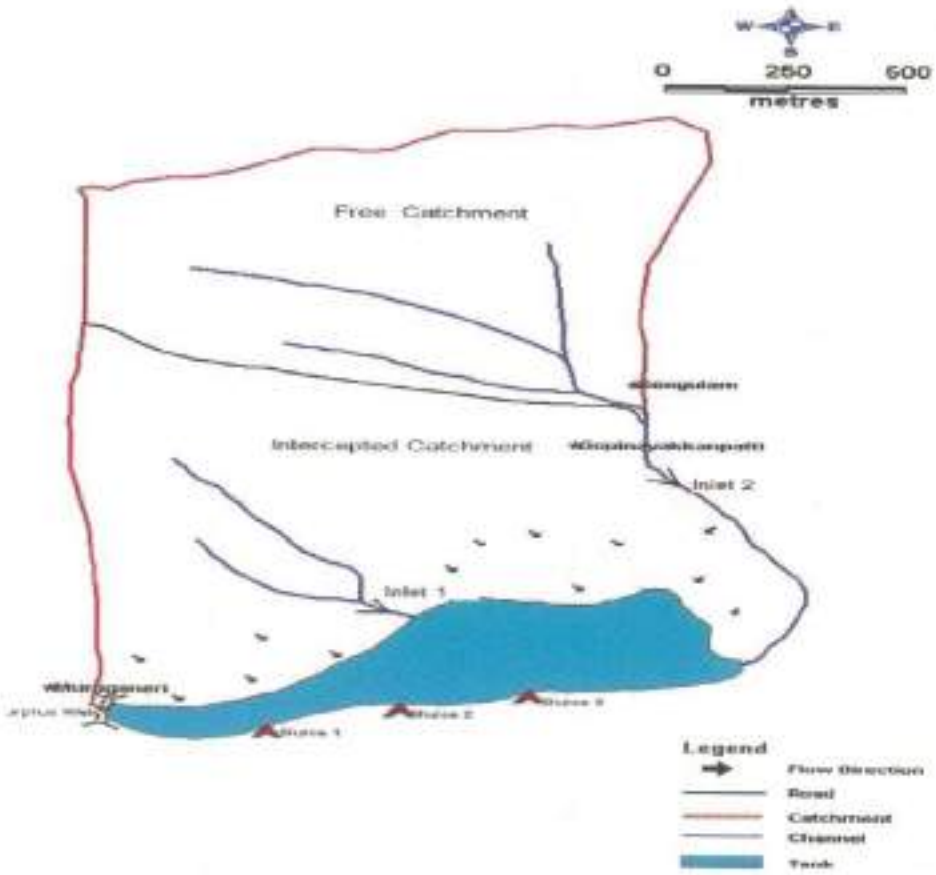

Figure 4.14 Catchment of Sengulam Tank

Photograph 4.8 Supply Channel to the Sengulam Tank

Photograph 4.9 Full Tank view of Sengulam during December 2007

Photograph 4.10 Sengulam Tank during December 2008

Photograph 4.11 Sengulam Tank Sluice No – 1

Photograph 4.12 Sengulam Tank Sluice No - 2

Photograph 4.13 Sengulam Tank Sluice No – 3

Photograph 4.14 Surplus Weir at Sengulam Tank

Photographs 4.15 Sengulam Tank Command Area during June 2007

Photographs 4.16 Pumping Open Well at Sengulam Tank Command Area

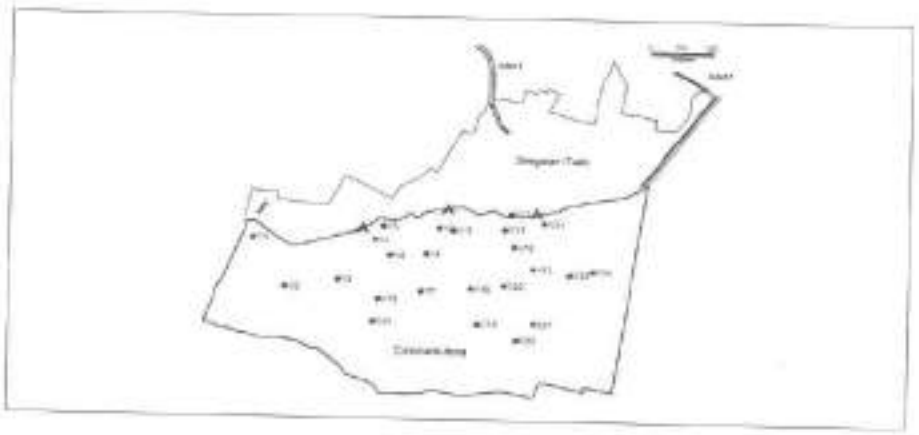

Figure 4.15 Location of Pumping Wells at Sengulam Tank

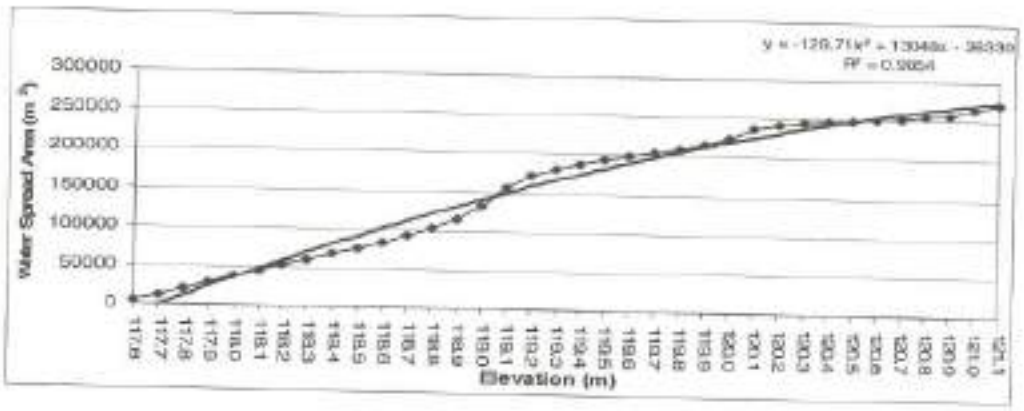

Figure 4.16 Elevation Vs Waterspread at Sengulam Tank

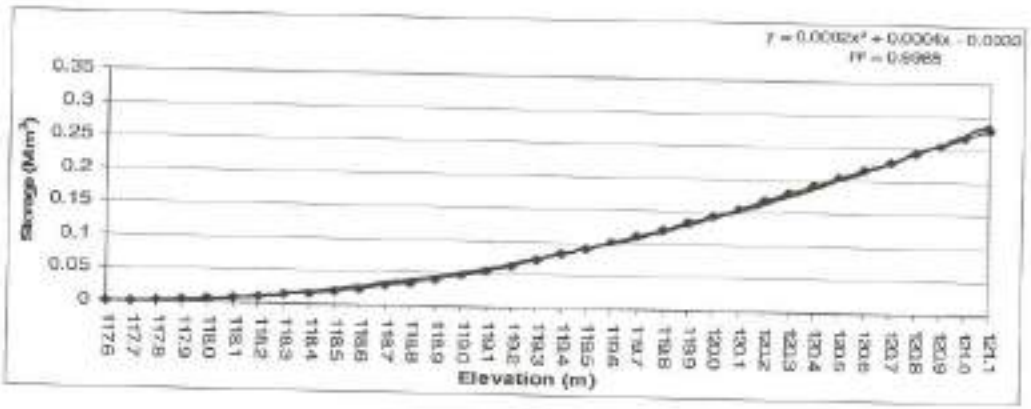

Figure 4.17 Elevation Vs Storage at Sengulam Tank

Table 4.12 Water Spread Area and Storage Capacity of Sengulam Tank

Elevation (m)	Area of contour (km^2)	Cumulative Area (km^2)	Volume ($M\ m^3$)	Cumulative Volume ($M\ m^3$)
117.584	0.006	0.0058	0.0002	0.0003
117.684	0.006	0.0119	0.0006	0.0008
117.784	0.008	0.0195	0.0009	0.0019
117.884	0.009	0.0284	0.0014	0.0033
117.984	0.009	0.0373	0.0019	0.0052
118.084	0.008	0.0451	0.0023	0.0074
118.184	0.008	0.0527	0.0026	0.0101
118.284	0.007	0.0599	0.0029	0.01303
118.384	0.007	0.0672	0.0033	0.0164
118.484	0.008	0.0753	0.0038	0.0202
118.584	0.008	0.0836	0.0042	0.0243
118.684	0.009	0.0922	0.0046	0.02895
118.784	0.011	0.1031	0.0052	0.03411
118.884	0.011	0.1146	0.0057	0.0398
118.984	0.017	0.1321	0.0066	0.0464
119.084	0.023	0.1551	0.0078	0.0542
119.184	0.017	0.1723	0.0086	0.0628
119.284	0.008	0.1807	0.0090	0.0718
119.384	0.007	0.1881	0.0094	0.0812
119.484	0.005	0.1934	0.0097	0.0909
119.584	0.005	0.1982	0.0099	0.1008

119.684	0.005	0.2031	0.0102	0.1109
119.784	0.006	0.2089	0.0104	0.1214
119.884	0.006	0.2149	0.0107	0.1322
119.984	0.01	0.2246	0.0112	0.1434
120.084	0.012	0.2365	0.0118	0.1552
120.184	0.006	0.2422	0.0121	0.1673
120.284	0.003	0.2449	0.0122	0.1796
120.384	0.002	0.2470	0.0124	0.1919
120.484	0.002	0.2489	0.0124	0.2044
120.584	0.002	0.2508	0.0125	0.2169
120.684	0.002	0.2526	0.0126	0.2296
120.784	0.002	0.2547	0.0127	0.2423
120.884	0.003	0.2573	0.0129	0.2552
120.984	0.008	0.2652	0.013	0.2684
121.072	0.007	0.2719	0.0103	0.2787

4.3.3 Runoff Estimation - Sengulam

Runoff estimation was carried out using Soil Conservation Service method.

Year 2007 and 2008

Initial storage in the Sengulam tank as on 30/9/2007 was 0.05 M m^3 which was far below the sill level of the sluice 2. Northeast monsoon was set during 13.10.2007 which was continued till 29.10.2007 which produced a rainfall of 243.2 mm. This rainfall produced a runoff of 0.412 Mm^3 which made the tank to surpluses for many days. Rainfall of 70.8 mm and 177.6 mm during the month

of November and December 2007 respectively, produced a runoff of 0.0136 M m^3 and 0.1245 M m^3 as shown in table 4.13. Inflows from the two supply channels were measured before estimating the runoff. Runoff coefficients were evaluated from the inflow rate.

Initial storage in the Sengulam tank as on 29.9.2008 was 0.0052 M m^3. Northeast monsoon was set during 12th October 2008 that increased the storage capacity up to 0.1552 M m^3. Subsequently Sengulam was blessed with 179.3 mm rainfall during November 2008 which increased the tank storage upto 0.2295 M m^3. But the tank storage was reduced to 0.1322 M m^3 because the rainfall during December month was only 20.4 mm as shown in figure 4.14

Table 4.13 Rainfall, Runoff and Storage of Sengulam Tank

Day / Month	Rainfall (mm)	Runoff Volume (M m^3)	Tank Water Level above MSL (m)	Tank storage (M m^3)
31st October, 2007	243.2	0.411886	121.072	0.2787
30th November, 2007	70.8	0.0136	120.235	0.1795
31st December, 2007	177.6	0.1245	120.655	0.2294

Table 4.14 Comparison of Tank Storage during Northeast Monsoon between the Year 2007 and 2008

Day / Month	2007		2008	
	Rainfall (mm)	Tank storage (M m^3)	Rainfall (mm)	Tank storage (M m^3)
October	243.2	0.2787	238.9	0.1552
November	70.8	0.1795	179.3	0.2295
December	177.6	0.2294	20.4	0.1322

Table 4.15 Monthly Water Level of the Sengulam tank with respect to msl and its Storage for the Period June 2007 to May 2009

Month	Tank Water Level (m)	Tank Storage (Mm^3)	Rainfall (mm)
Jun '07	119.30	0.072	69.4
July '07	118.90	0.040	11.8
Aug '07	120.20	0.167	71.4
Sept '07	119.10	0.054	36.4
Oct '07	121.10	0.279	243.2
Nov '07	120.24	0.180	70.8
Dec '07	120.70	0.229	177.6
Jan '08	120.50	0.204	-
Feb '08	120.50	0.204	5
Mar '08	120.70	0.230	225.8
Apr '08	120.20	0.167	26.6
May '08	119.80	0.121	93.6
Jun '08	117.80	0.002	0.4
July '08	119.00	0.052	101.8
Aug '08	118.90	0.040	147.2
Sept '08	118.80	0.034	33.8
Oct '08	120.07	0.155	238.9
Nov '08	120.66	0.230	179.3
Dec '08	119.93	0.132	20.4
Jan '09	119.14	0.054	16.6
Feb '09	118.34	0.013	-
Mar '09	119.30	0.072	148.5
Apr '09	119.00	0.046	81.6
May '09	118.00	0.005	114

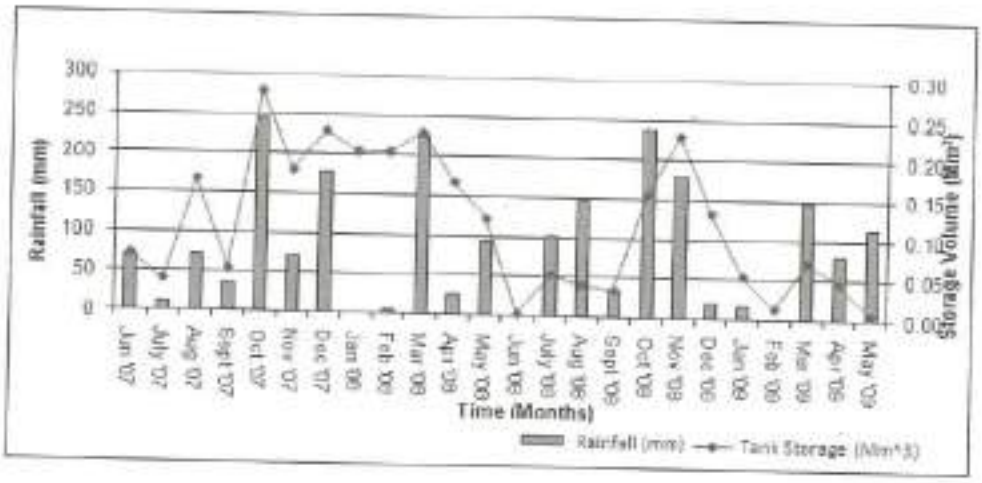

Figure 4.18a Monthly Storage of the Sengulam Tank for Two Water Years

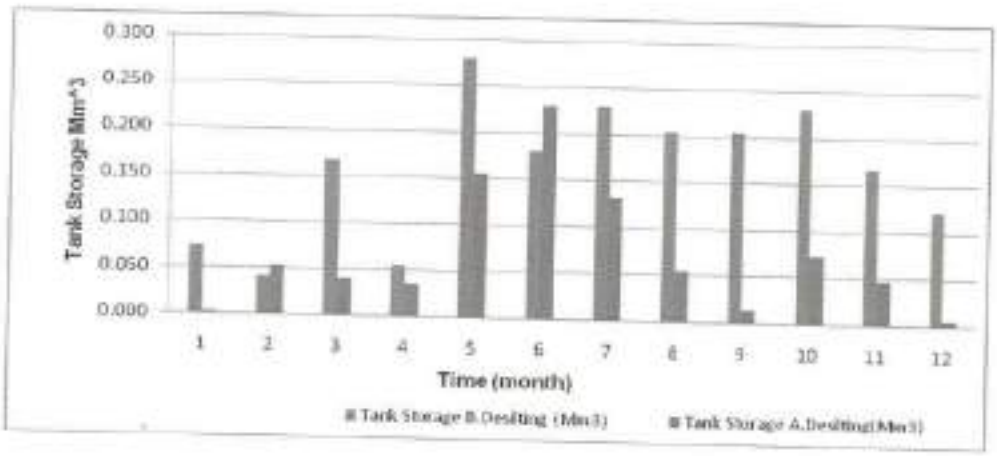

Figure 4.18b Comparison of Tank Storage before and after De-silting

4.3.4 Groundwater Scenario at Sengulam Tank

Groundwater occurs under phreatic condition in the weathered formation and is being developed by means of dugwells. The water bearing

properties of formation lack of primary porosity. It depends on the extent of development of secondary inter granular porosity. The occurrence and movement of groundwater in these rocks are generally confined to such spaces. These aquifers are highly heterogeneous in nature due to variation in lithology, texture and structural features even with in the short distances.

The thickness of weathered zone in the district is in the range of 4 to 15 m. The depth of dug wells ranged from 10 to 15 m bgl. The yield of large diameter wells in the district, tapping the weathered mantle of crystalline rocks ranges from 40 to 110 lpm that are able to sustain pumping for 2 to 6 hours per day. The specific capacity of large diameter wells ranges from 6 to 184 lpm / m of draw down.

Pumping Test

Pumping test was carried out in the well number 1 and 5 during December 2007. In an open well (W1), the top soil has a depth of 10.13m and weathered rock to a depth of 7.9 m have been encountered. Total depth of W1 is 18 m. This well is a pumping well which is being used extensively for pumping daily, that was used for pumping test analysis to estimate the aquifer parameters. The static water level during pretest was 6.75 min. below measuring point and water level during post test was 6.69 min. below measuring point for a discharge of 6 lpm. The discharge from the pumping well was maintained uniform by and the draw down was also the same. The test was carried out for 62 minutes until the draw down reaches steady state. Hence the observed well data was plotted in a semi log graph and the aquifer parameters are estimated. The estimated parameters are given in table below.

	Well 1	Well 5
Hydraulic conductivity	4.37 m / day	3.08 m / day
Specific yield	4 %	1%

4.3.5 Groundwater Level in the Command Area of Sengulam Tank

Most of the wells in the Sengulam tank command area are open wells. All the wells are used for irrigating the agricultural lands. Water levels were measured in the pumping well itself. All the existing pumping wells were chosen for the project as shown in Figure 4.15. Their distance from the bund, depth of the well and their reduced levels are given in Table 4.16. Water year is considered as June of the year to May of the next year. The water level is with respect to mean sea level which is considered for two consecutive water years (June 2007 - May 2008 and June 2008 - May 2009).

Monthly water levels were measured in the pumping wells that represent the pumping and recharge behaviors. Pumping, direct rainfall recharges, seepage from the tank, irrigation return flow are responsible for groundwater fluctuation.

- Water level in all wells showed an increasing trend from June 2007 to May 2008 as shown in figure 4.19 a, b, c. This increasing trend had started during October 2007 during that time there was a heavy rainfall of 243.2 mm that made the tank to get surplused. Tank had sufficient water (i.e. two third capacities) during February 2008. Due to heavy rainfall during March 2008 tank had 0.23 M m^3 of water as shown in Table 4.15. From the tank storage had started reducing and reached to

dead storage. The ground water level started falling down from June 2008 which continued till August 2008.

- There was a little rise in the groundwater level during October 2008 which had 238.9 mm rainfall. This rain brought 0.15 M m^3 of water to the tank. At the end of November 2008 there was a heavy rainfall of 179.3 mm brought 0.2295 M m^3 of runoff to the tank that rejunuvated the wells in the command area as shown in figure 4.20 a, b, c. This situation made the farmers to go for increased cultivation of Paddy and Sugarcane during January to April 2009.

- Due to increased cultivation and pumping, groundwater level started falling during January and February 2009. During this time the tank had only dead storage.

- Suddenly there was an ample amount of rainfall (148.50 mm) during March 2009. This brought a 0.072 M m^3 runoff to the tank which helped the groundwater level to rise in the following wells. W1, W2, W3, W4, W5, W6, W7, W8, W9, W10, W16, W17, W21 and W24 as shown in figure 4.19. At the same time this increment was not observed in the wells W11, W12, W13, W14 and W22 which can be seen from figure 4.19c and 4.20a.

- Most of the wells behaved more or less in a similar manner indicating very good response to tank water level. If there is water in the tank, ground water level rises and falls when there is limited water;

Table 4.16 Pumping Wells Details at Sengulam Tank

Well No	Distance from the Tank bund (m)	RL of the measuring point wrt msl (m)	Bottom of the I Layer wrt msl (m)	Thickness of the I Layer (m)	Bottom of the II layer wrt msl (m)	Thickness of the II Layer (m)
W1	49	121.55	111.411	10.13	103.479	7.932
W2	153	120.59	112.257	8.33	106.53	5.727
W3	164	119.92	113.38	6.54	107.397	5.983
W4	68	120.18	110.929	9.25	103.892	7.037
W5	30	119.43	109.492	9.94	103.85	5.642
W6	131	121.25	111.021	10.23	106.501	4.52
W7	281	121.11	112.081	9.02	106.283	5.798
W8	152	119.23	110.532	8.69	107.021	3.511
W9	66	119.90	111.821	8.08	107.553	4.268
W10	82	119.61	112.891	6.72	108.545	4.346
W11	50	119.55	113.108	6.44	110.147	2.961
W12	109	119.93	113.941	5.99	111.029	2.912
W13	198	119.54	113.973	5.57	109.141	4.832
W14	38	119.40	114.451	4.94	108.278	6.173
W16	298	119.43	110.667	8.76	105.024	5.643
W17	367	118.75	112.248	6.50	105.742	6.506
W18	288	118.81	110.826	7.98	106.479	4.347
W19	407	118.90	112.531	6.37	108.443	4.088
W20	459	118.75	112.923	5.83	105.364	7.559
W21	402	119.30	113.308	5.99	106.358	6.95
W22	257	119.41	112.461	6.95	108.147	4.314
W23	255	119.41	111.654	7.75	106.617	5.037
W24	261	121.73	116.273	5.46	106.413	9.86

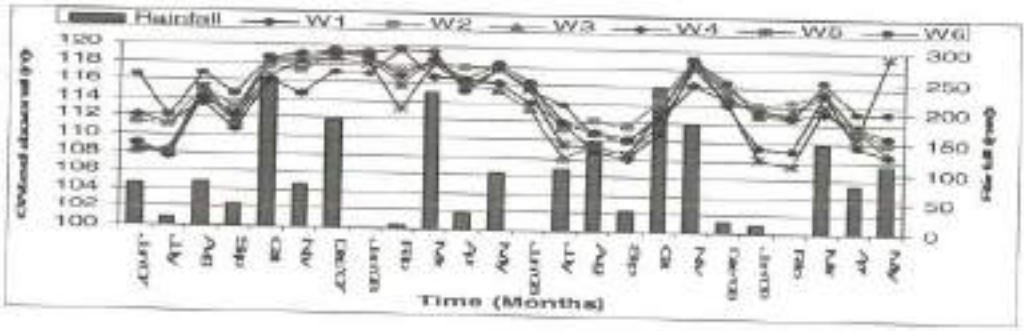

Figure 4.19a Groundwater Level in the Pumping Wells of W1 to W6 at Sengulam Tank

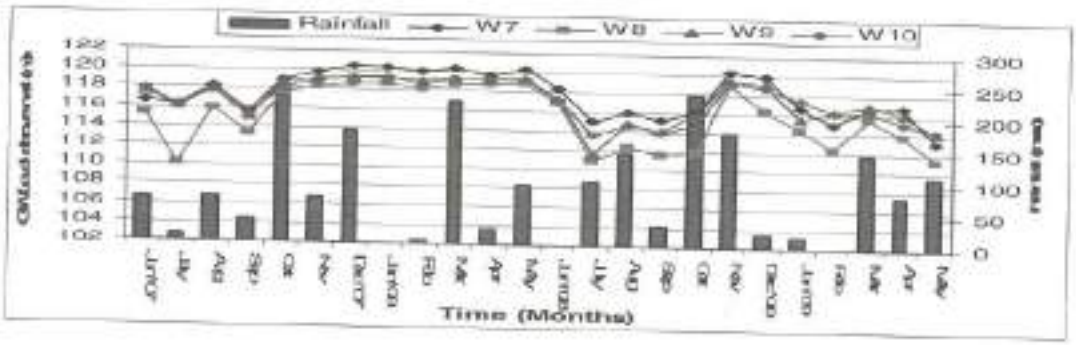

Figure 4.19b Ground Water Level in the Pumping Wells of W7 to W10 at Sengulam Tank

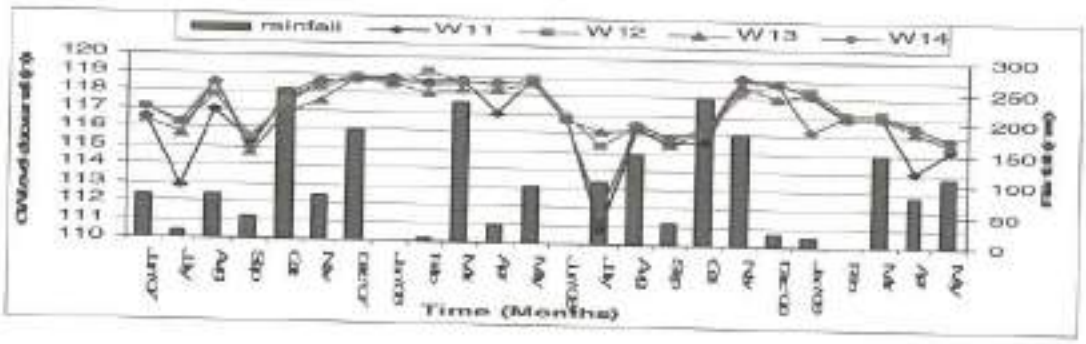

Figure 4.19c Ground Water Level in the Pumping Wells of W11 to W14 at Sengulam Tank

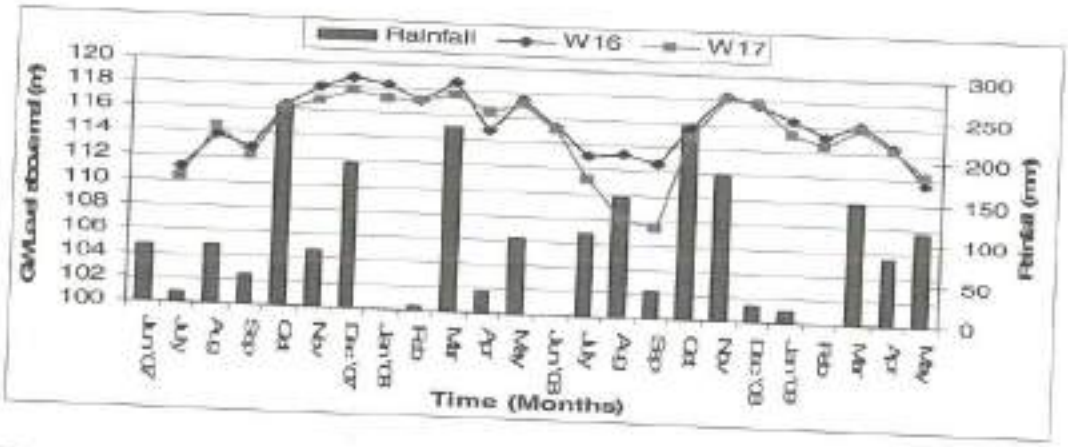

Figure 4.20a Ground Water Level in the Pumping Wells of W16 & W17 at Sengulam Tank

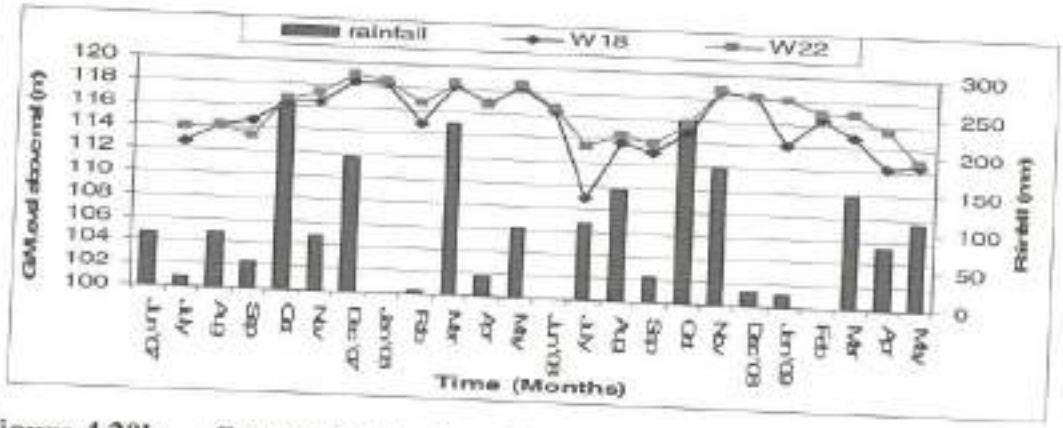

Figure 4.20b Ground Water Level in the Pumping Wells of W18 & W22 at Sengulam Tank

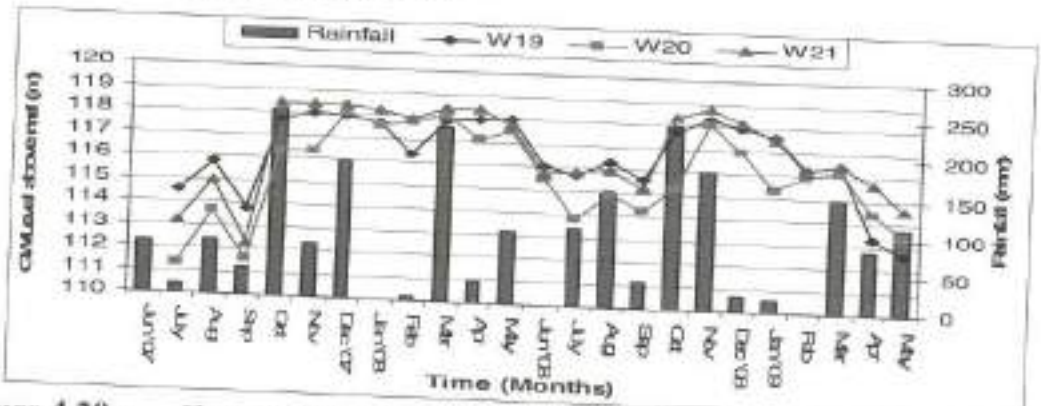

Figure 4.20c Ground Water Level in the Pumping Wells of W19, W20 & W21 at Sengulam Tank

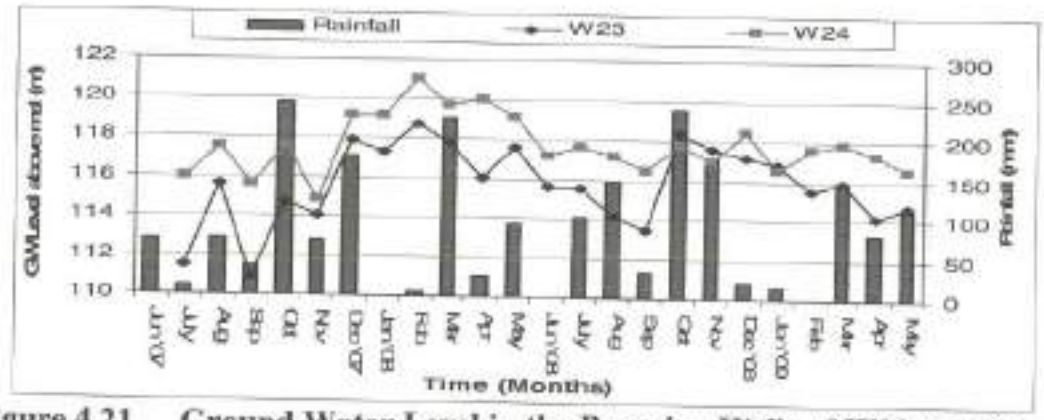

Figure 4.21 Ground Water Level in the Pumping Wells of W23 & W24 at Sengulam Tank

4.3.6 Net Draft in Sengulam Command Area

Net draft in Sengulam command area was calculated as follows.

- The difference in the water levels for two successive months for each well was taken as change in head (Δh)
- The contributing area for each well was calculated by Theissen polygon method as shown in figure 4.22
- Specific yield ranges between 0.02 and 0.16.

Change in Groundwater

Storage = (Area * Specific yield) * (Monthly Change in head)

(or)

Net Draft = $S_y * A * \Delta h$

- Using above formulae, change in groundwater storage or net draft was calculated for each well for every month.

- This net draft added algebraically, which provided monthly change in groundwater storage at Sengulam for the two water years 2007 - 2008 and 2008 – 2009 which are shown in figure 4.23.

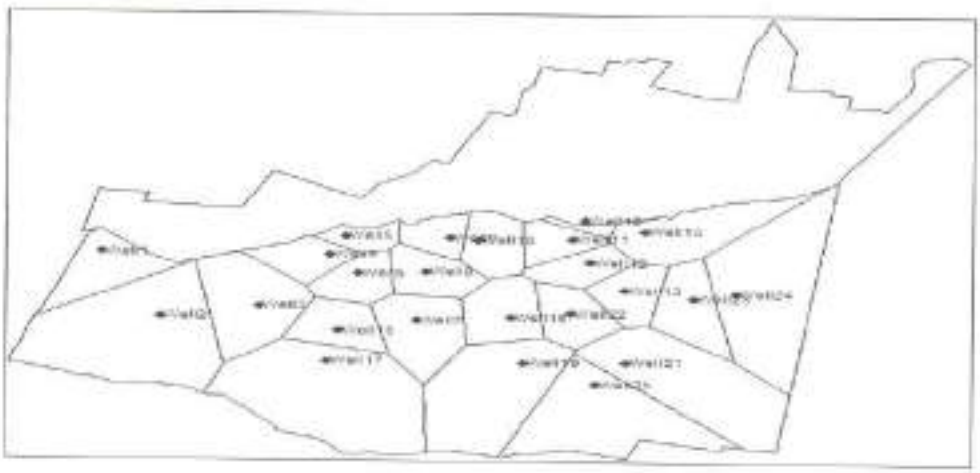

Figure 4.22 Theissen Polygon Areas at Sengulam Command Area

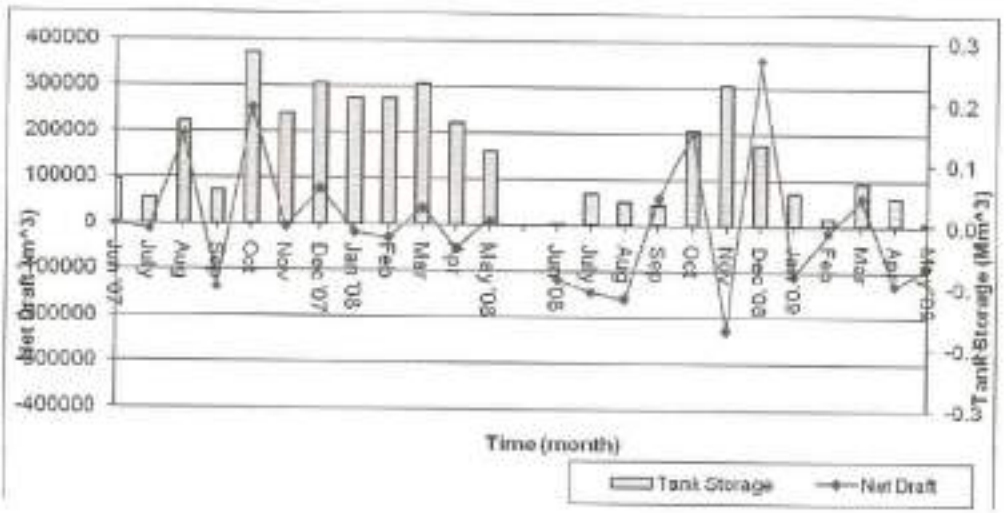

Figure 4.23 Monthly Net Draft for Two Water Years at Sengulam Tank

4.3.7 Seepage Rate at Sengulam Tank

Monthly Seepage rate at Sengulam tank was calculated as 50 percent of corresponding month tank storage and also estimated through a mathematical expression Darcy's law as given in table 4.17.

Table 4.17 Comparison of Seepage Rate between the year 2007 – 2008 and 2008 – 2009

Month	Tank Storage (Mm^3)	Seepage Rate 50 percent of Tank Storage (Mm^3)	Seepage Rate Darcy's law Mm^3
Jun '07	0.072	0.036	0.039
July '07	0.040	0.020	0.054
Aug '07	0.167	0.084	0.083
Sept '07	0.054	0.027	0.045
Oct '07	0.279	0.139	0.124
Nov '07	0.180	0.090	0.089
Dec '07	0.229	0.115	0.155
Jan '08	0.204	0.102	0.124
Feb '08	0.204	0.102	0.106
Mar '08	0.230	0.084	0.077
Apr '08	0.167	0.084	0.094
May '08	0.121	0.065	0.074
Total		**0.983**	**1.064**
June'08	0.002	0.001	0.0136
July '08	0.052	0.026	0.0511
Aug '08	0.040	0.020	0.0332
Sept '08	0.034	0.017	0.0396
Oct '08	0.155	0.078	0.0640

Nov '08	0.230	0.115	0.1060
Dec '08	0.132	0.067	0.0323
Jan '09	0.054	0.027	0.0403
Feb '09	0.013	0.007	-0.0015
Mar '09	0.072	0.036	0.0279
Apr '09	0.046	0.023	0.0602
May '09	0.005	0.003	0.0476
Total		**0.43**	**0.51**

4.3.8 Groundwater Potential

The commonly used method for estimating groundwater storage available annually is based on

Q = (Area) x (Depth of fluctuation in Groundwater Table) x (Porosity)

The area in the equation is the area of influence of the well in the command area. This is obtained by Thiessen polygon method. By this method, the command area is subdivided into polygonal sub areas using the wells as nodes. The Thiessen polygon around each well permits the assignment of weights on the basis of the relative areas of the respective polygons. The sub areas were used as weights in estimating the average depth of fluctuation for each well.

The dynamic reserve has been computed by measuring the net change in storage of the phreatic aquifer. The storage of the groundwater in the aquifer is dependent upon the input components such as precipitation, seepage and return flow of irrigated water during various seasons. The fluctuation of groundwater depth over the study period was analysed to understand the behaviour of the

aquifer. High variations in annual recharges to groundwater body were observed between monsoons. Annual groundwater recharge was estimated using water level fluctuation method. The fluctuation of groundwater level is taken as the difference between highest groundwater level of the second season and the lowest groundwater level of first season was used for estimating the recharge values for two years 2007 – 2008 and 2008 – 2009.

The groundwater fluctuation over two years were analysed. It showed a depletion and subsequent recharge of groundwater every year. Year 2008-2009 had high recharge due to the high storage space available as a result of the lowering of water table due to delay in the rainfall. Groundwater storage during 2007-2008 and 2008-2009 were 0.77 Mm^3 and 0.895 Mm^3 respectively. Further it was found that the groundwater storage received bulk of the recharge from monsoon precipitation and seepage from the tank.

4.3.9 Relationship between Tank water level and ground water level at Sengulam tank

Relationship between the tank water level and groundwater level were drawn for individual wells which are grouped later based on their behavior. Wells below the sluice and farther away behaved differently. In the graph, x axis represents tank water level and y represents groundwater level.

Group I : W1, W2, W6, W8

I group wells variations are shown in figure 4.24

W1 $Y = 0.302\ x^2 - 69.99\ x + 4162$

W2 $Y = 0.505\ x^2 - 117.8\ x + 6973$

W6 $Y = 0.229\ x^2 - 52.37\ x + 3096$

W8 $Y = 0.343\ x^2 - 79.57\ x + 4721$

II group W3, W4, W5 below sluice 1

W3 $Y = 0.693\ x^2 - 161.6\ x + 9529$

W4 $Y = 0.612\ x^2 - 142.5\ x + 8393$

W5 $Y = 0.57\ x^2 - 133.1\ x + 7841$

III group

W17 $Y = 0.55\ x^2 - 11.03\ x + 6432$

IV group below sluice 2

W7 $Y = 0.369\ x^2 - 85.8\ x + 5102$

W9 $Y = 0.167\ x^2 - 38.28\ x + 2308$

W10 $Y = 0.158\ x^2 - 36.16\ x + 2178$

W16 $Y = 0.350\ x^2 - 81.43\ x + 4841$

V group Immediately below sluice 3

W12 $Y = 0.175\ x^2 - 40.71\ x + 2470$

W13 $Y = 0.138\ x^2 - 31.85\ x + 1949$

W14 $Y = 0.068\ x^2 - 15.39\ x + 982.5$

W11 $Y = 0.560\ x^2 - 131.2\ x + 7794$

W18 $Y = 0.505\ x^2 - 118.1\ x + 7014$

VI group away from sluice 3

W19 $Y = 0.011\ x^2 - 1.96\ x + 194.51$

W20 $Y = 0.33\ x^2 - 77.93\ x + 4661$

W21 $Y = 0.144\ x^2 - 33.43\ x + 2048$

W22 $Y = 0.292\ x^2 - 68.19\ x + 4082$

W23 $Y = 0.006\ x^2 - 0.617\ x + 96.26$

W24 $Y = 0.409\ x^2 - 95.55\ x + 5692$

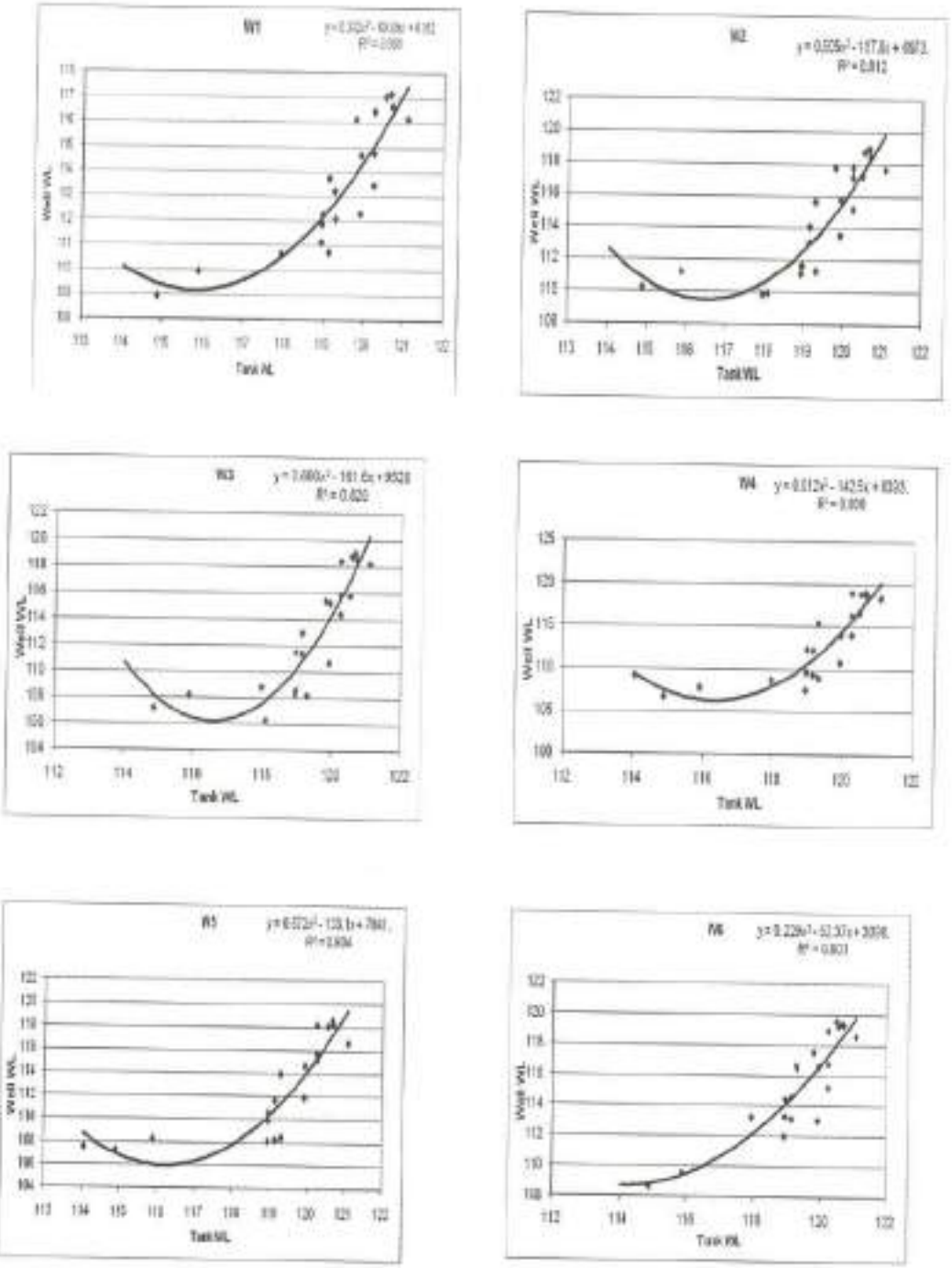

Figure 4.24 Variation of Tank Water level and well water level (continued)

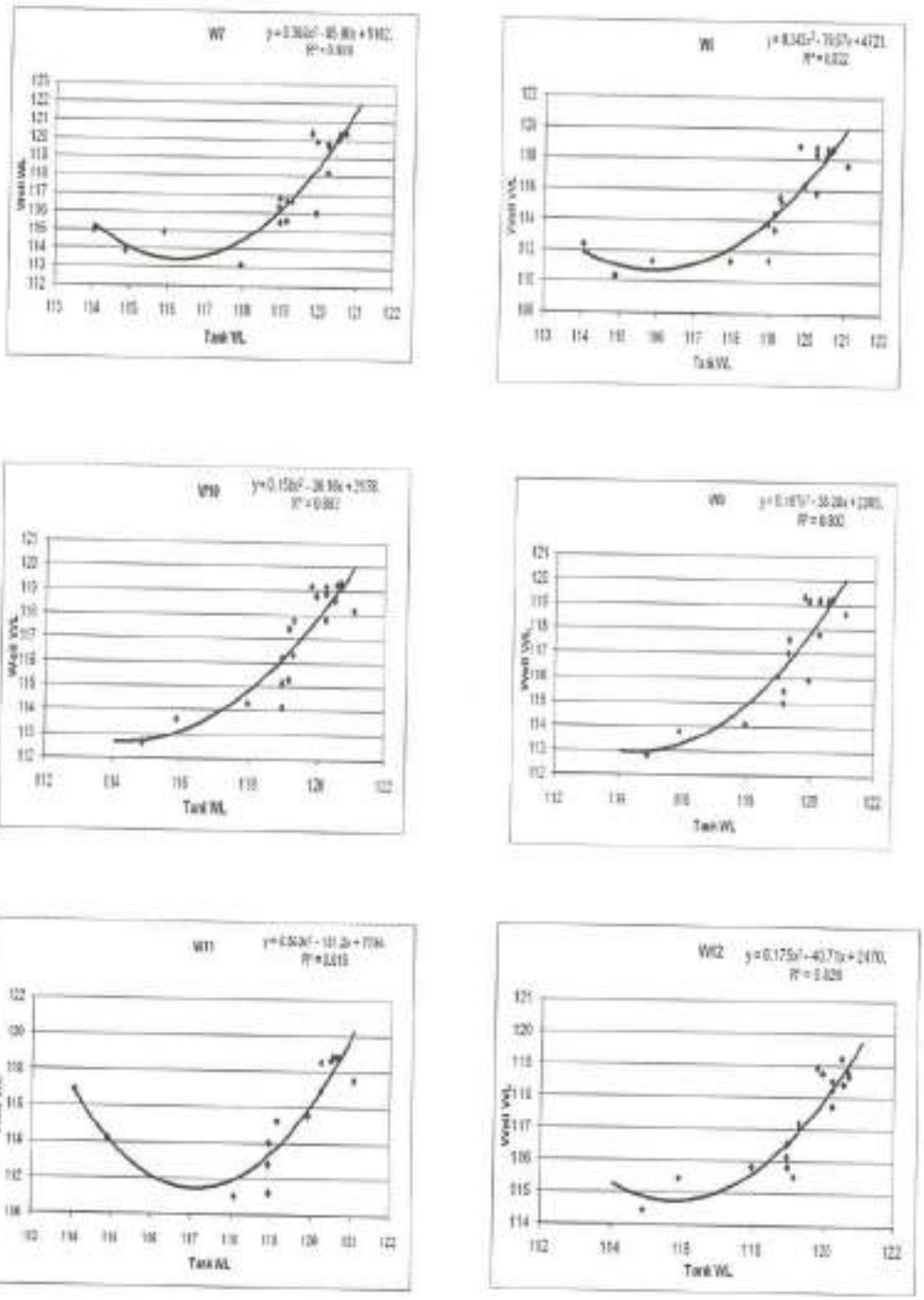

Figure 4.24 Variation of Tank Water level and well water level (continued)

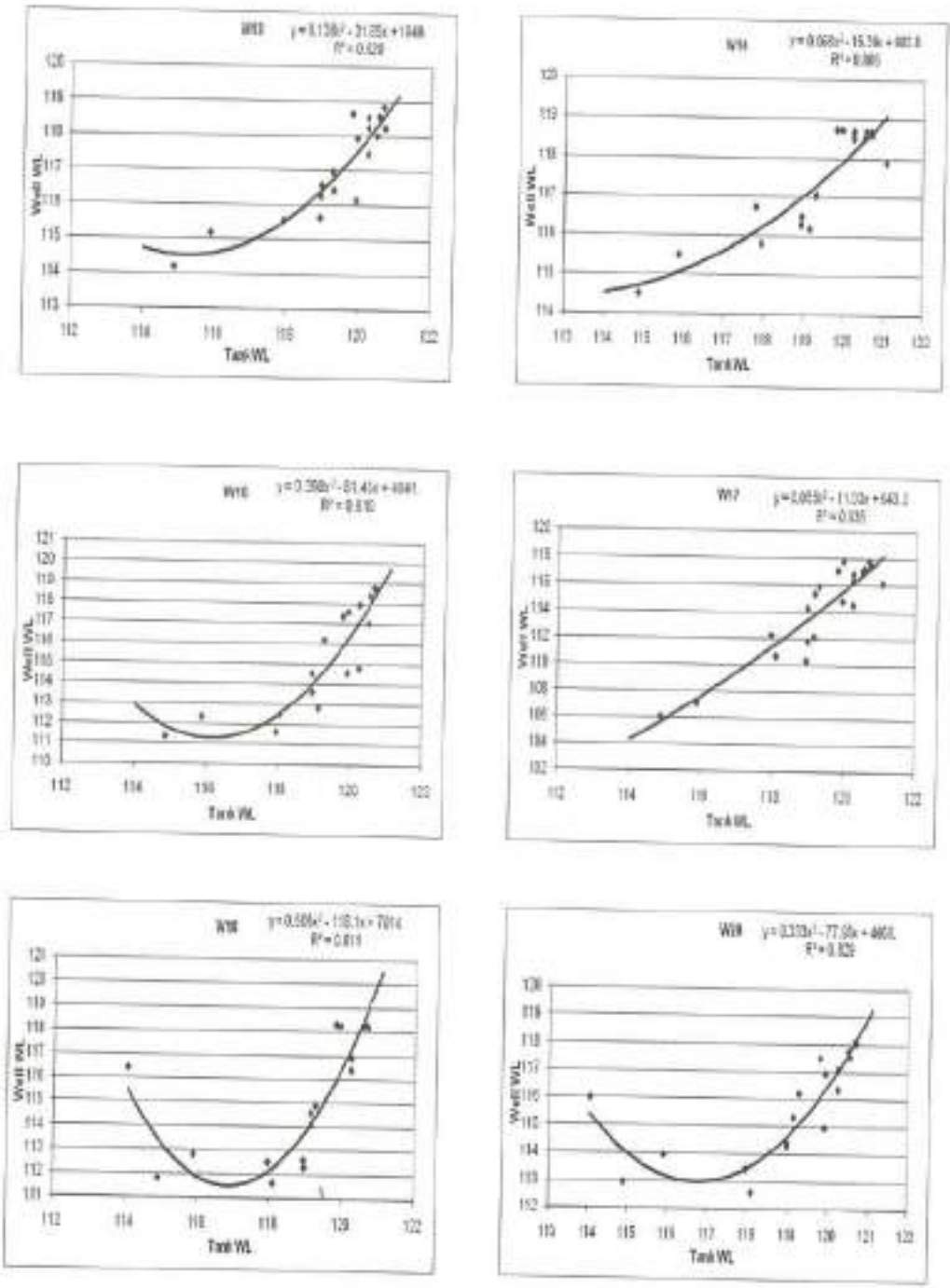

Figure 4.24 Variation of Tank Water level and well water level (continued)

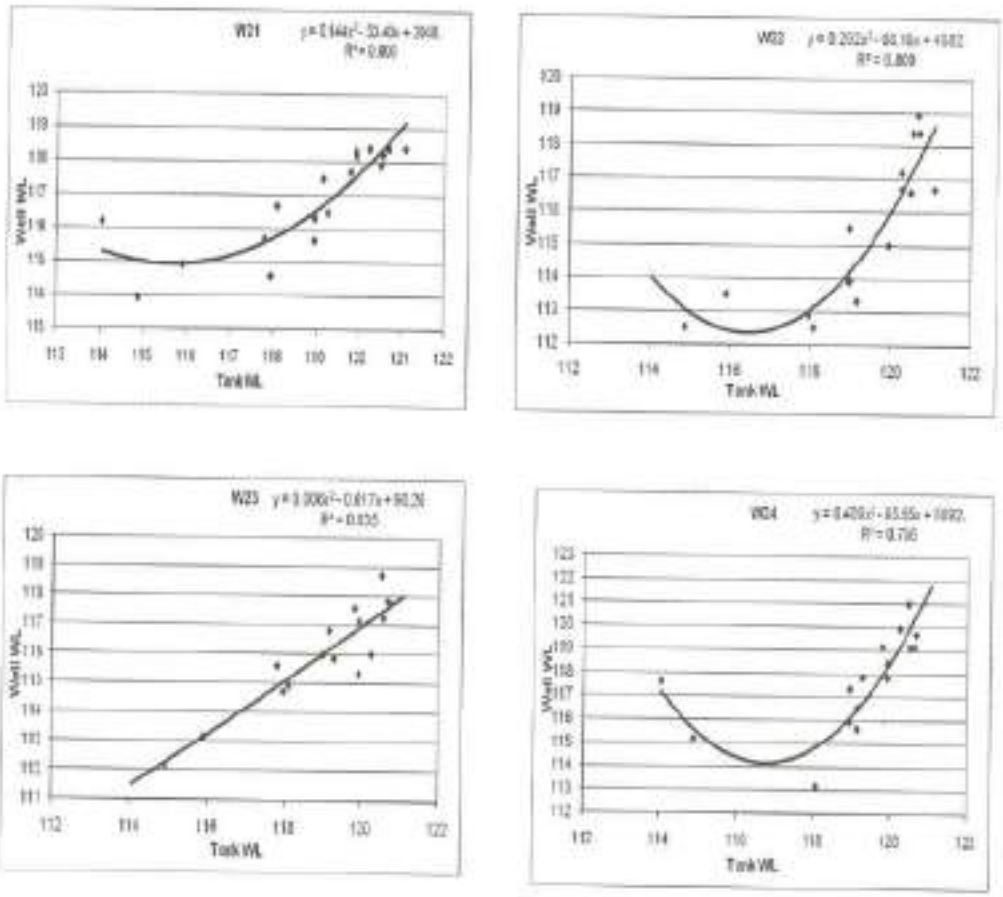

Figure 4.24 Variation of Tank water level and Well water level

In general almost all the wells behaved similar except some wells. However some wells like W3, W4 and W5 and W17 were not responding to tank water level. Even if the tank water level rises, above said wells water level was not increased.

- Off all wells, wells below sluice 2 W12, W13 and W14 and W19, W20, W21, W22, W23 and W24 are highly responding to tank water levels which are very effectively used for pumping;
- Even though W11 and W18 are below sluice 2, their response is poor;

- Well W17 is not at all responding to tank storage. It is surviving with direct rainfall recharge and groundwater storage. It seems as if separated from the tank shows different zone of influence;
- Figure 4.25 shows the graph between tank water level and 23 wells groundwater levels;
- The response during non moon soon is different from monsoon period. During non monsoon period even for higher tank water level, groundwater level is lower than monsoon period.
- It is observed that the wells in the Sengulam command area were getting recharged at threshold tank water level of 119 m. Below that level response is relatively less.

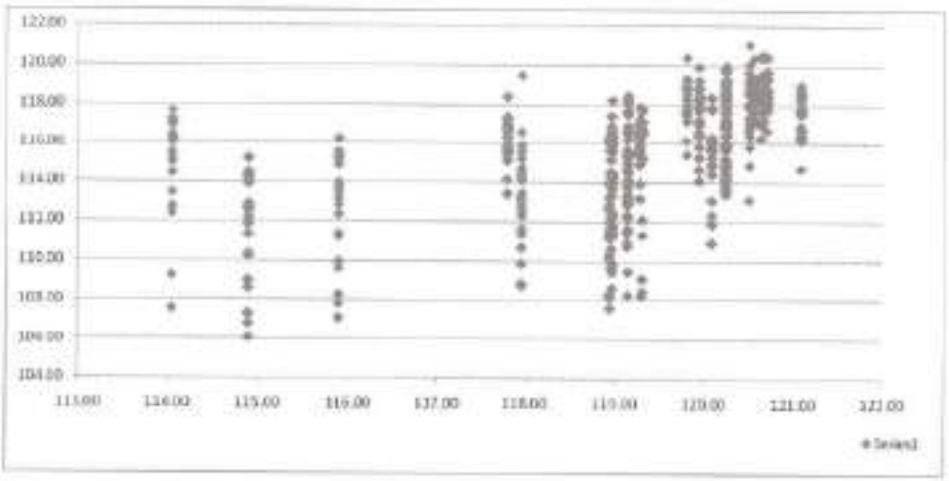

Figure 4.25 Comparison of 23 wells water level and Tank water level

4.4 TANK VOLUME DAYS

Equivalent tank volume days means as number of days water exist in the tank per year that is given in the table 4.18.

Table 4.18 Tank Storage and Tank Volume Days

Month	Tank Storage (Mm^3)	Tank Volume – Days (Mm^3 days)
Jun '07	0.072	2.16
July '07	0.040	2.4
Aug '07	0.167	7.41
Sept '07	0.054	5.22
Oct '07	0.279	13.17
Nov '07	0.180	11.01
Dec '07	0.229	14.10
Jan '08	0.204	14.52
Feb '08	0.204	15.72
Mar '08	0.230	17.70
Apr '08	0.167	17.01
May '08	0.121	16.83
Total		123.54
Jun '08	0.002	0.06
July '08	0.052	1.62
Aug '08	0.040	1.32
Sept '08	0.034	1.2
Oct '08	0.155	4.89
Nov '08	0.230	7.2
Dec '08	0.132	4.32
Jan '09	0.054	2.04
Feb '09	0.013	0.87
Mar '09	0.072	2.7
Apr '09	0.046	1.98
May '09	0.005	0.81

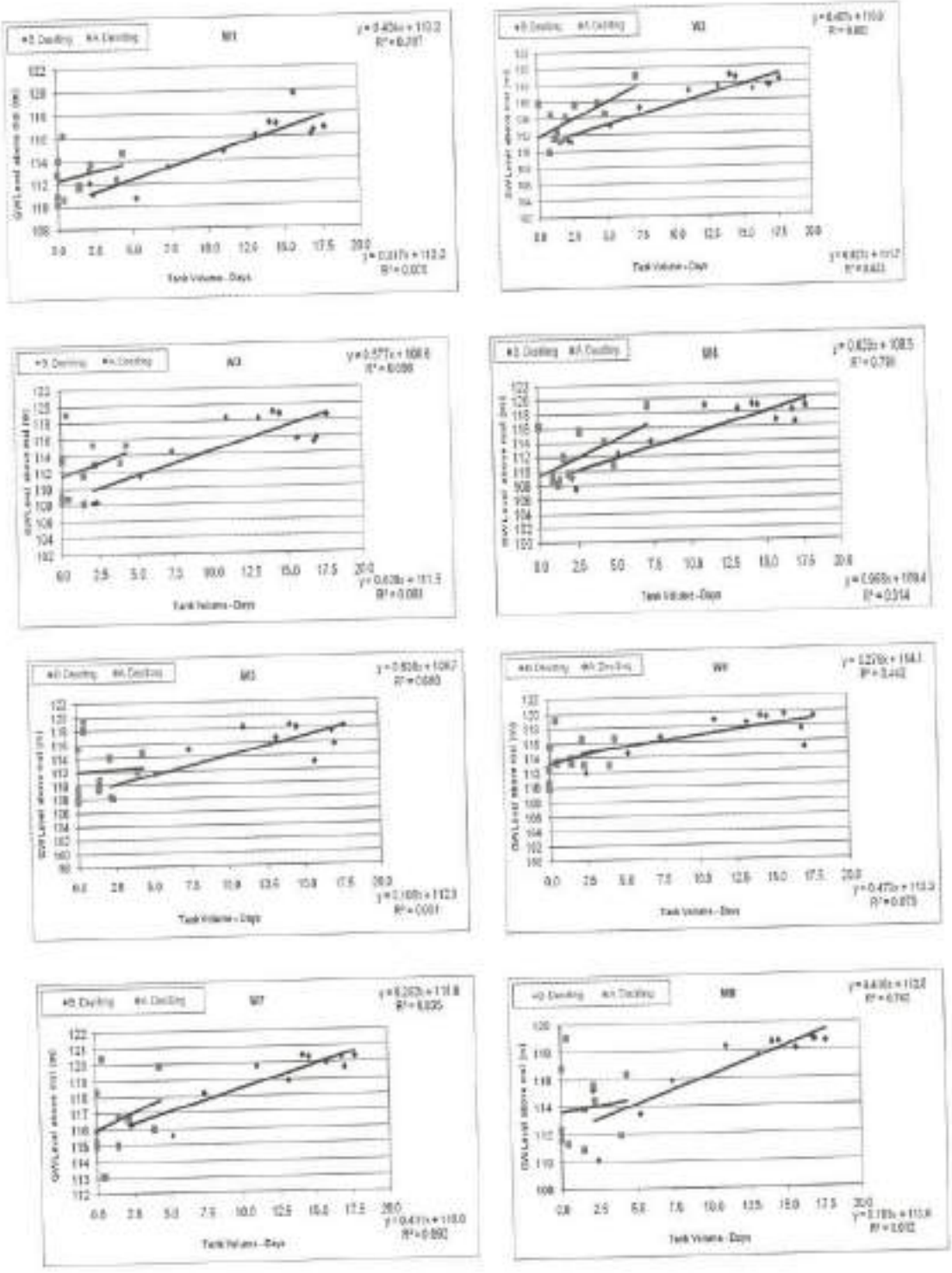

Figure 4.26 **Comparison of slope of a line before and after de-silting (Continued)**

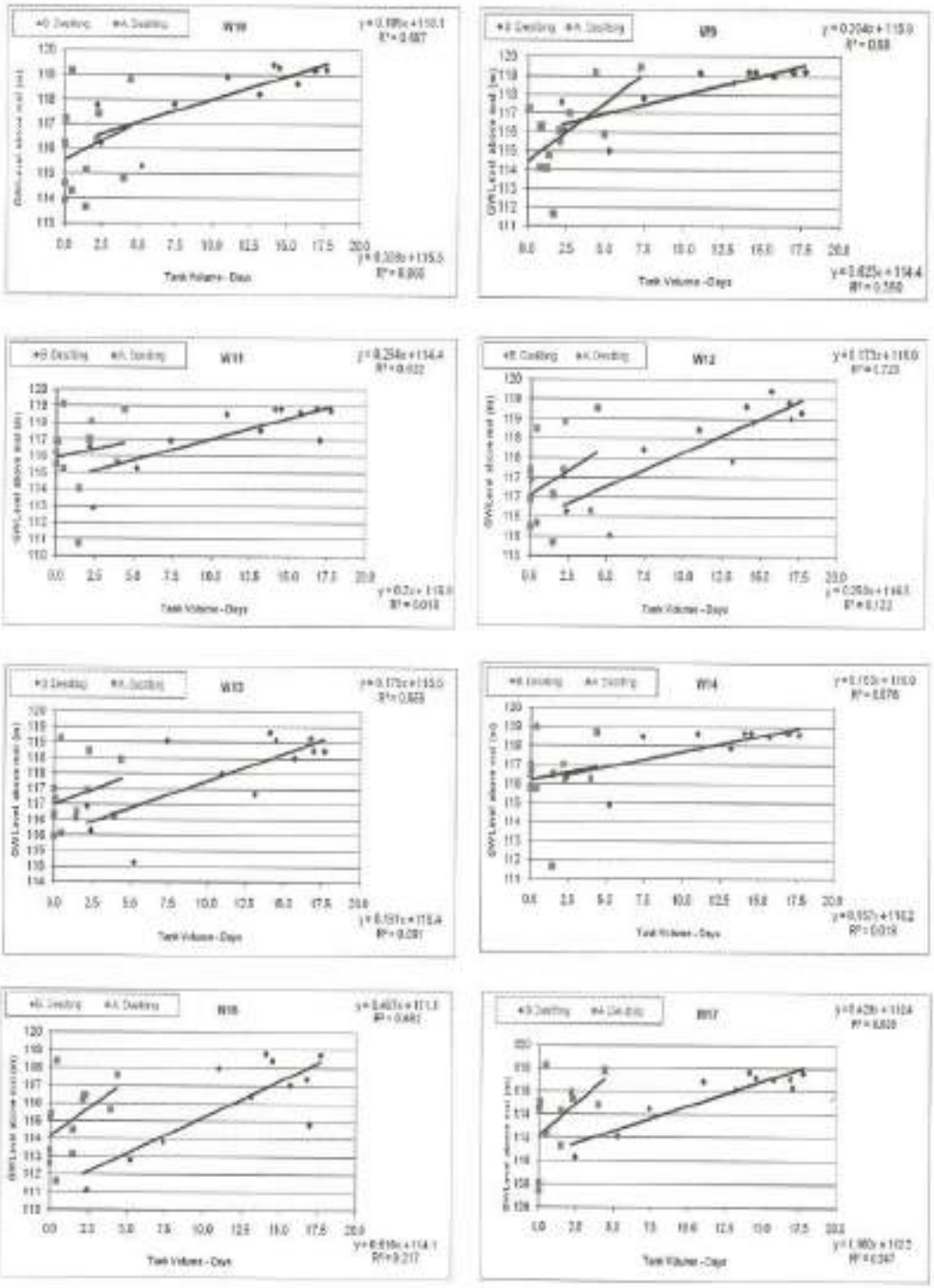

Figure 4.26 Comparison of slope of a line before and after de-silting (Continued)

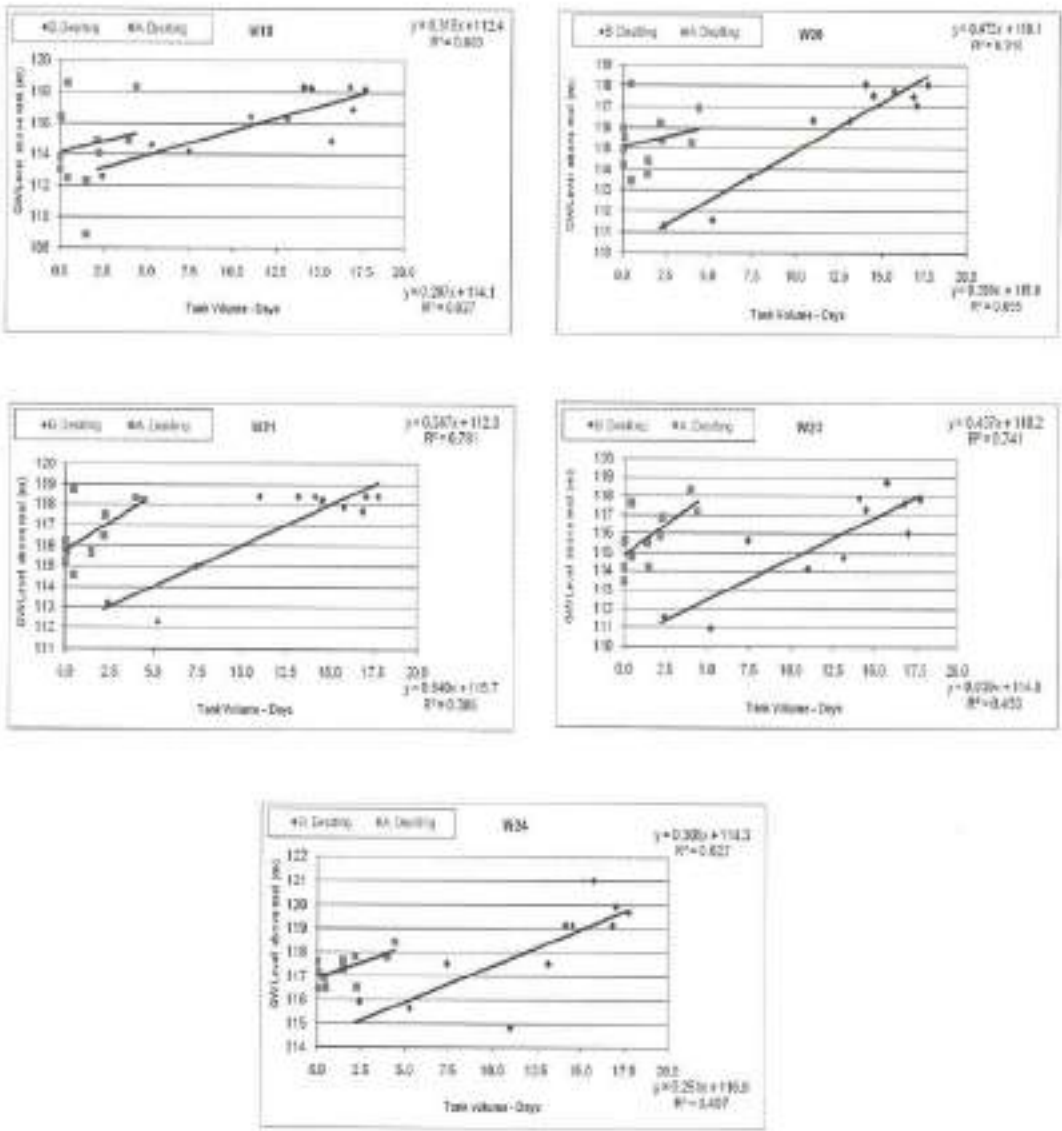

Figure 4.26 Comparison of slope of a line before and after de-silting

Graphs (figure 4.26) were drawn between Tank volume days and individual well water level for the year 2007-2008 and 2008-2009. Slope of the line before de-silting is less than slope of the line after de-silting as shown in table 4.18

- On studying the graph, almost all the wells have higher water level with very less volume days than the volume - days before de-silting;

- W2, W3, W4, W6, W7, W8, W9, W10, W14, W16, W17, W18, W19, W24 had High steep slope;

- W5, W8, W11, W12, W13, W21, W22, W23 had Medium steep slope;

- W20 had Flat steep slope;

➢ Most of the wells showed steep increasing trend after de-silting. This steepness is attributed to the partial de-silting of the tank. Higher water levels with lower volume days after de-silting was attributed to increased recharge from the tank.

4.5 SEEPAGE VELOCITY

Seepage velocity was calculated using Darcy's law

$V = ki$

$= k_{avg}\, h_T - h_A / D$

$k_{avg} = k_T + k_A / 2$

Where

k_T =Tank hydraulic conductivity L/T (m/day)

k_A = Aquifer hydraulic conductivity L/T (m/day)

h_T = Tank water head

h_A = Aquifer water level

D = Distance between tank at sluice 2 and individual well

Graphs were drawn between Time in months in x axis and seepage velocity m/day in y axis as shown in figure 4.27.

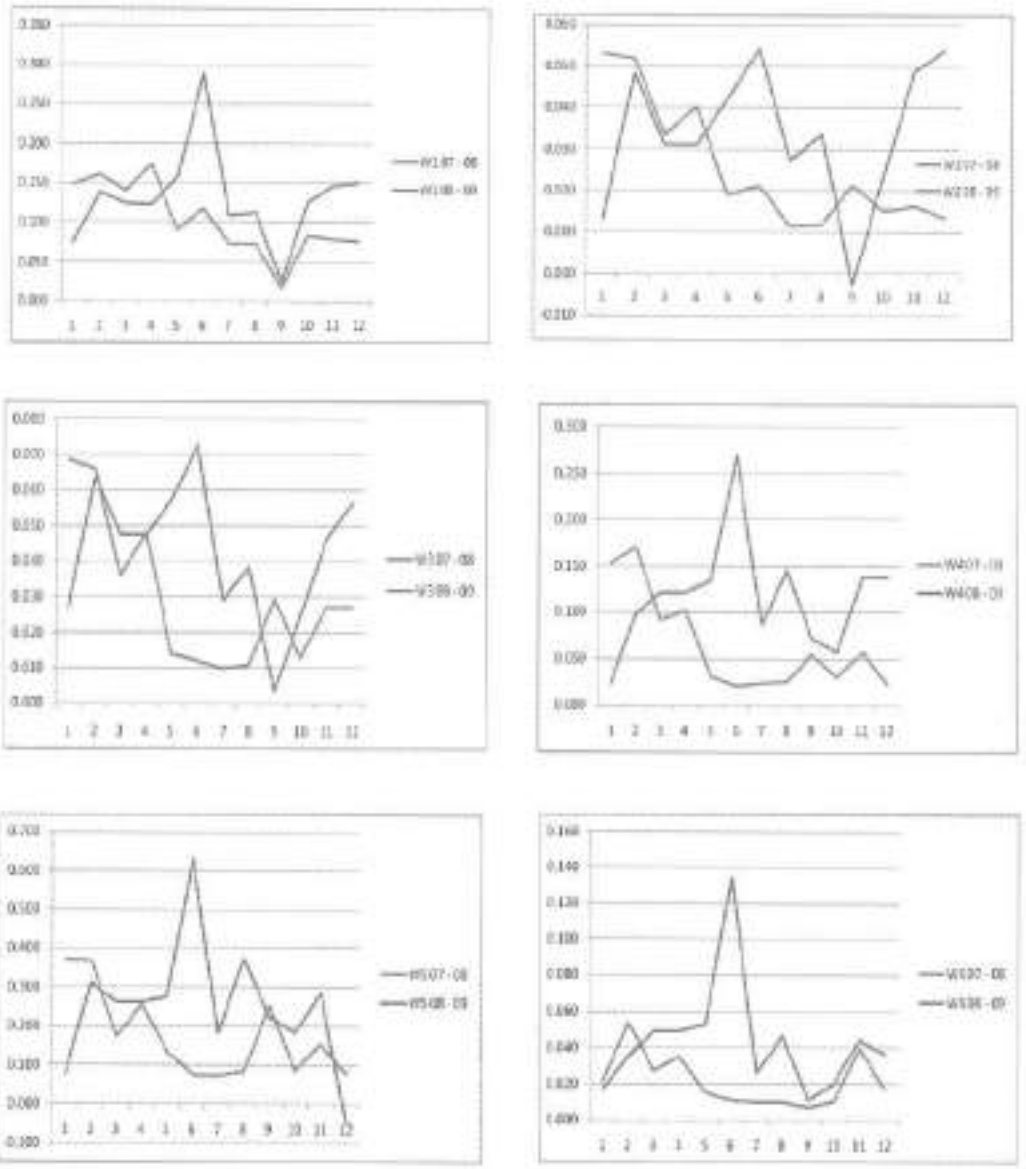

Figure 4.27 Comparison of seepage velocity before and after de-silting (Continued)

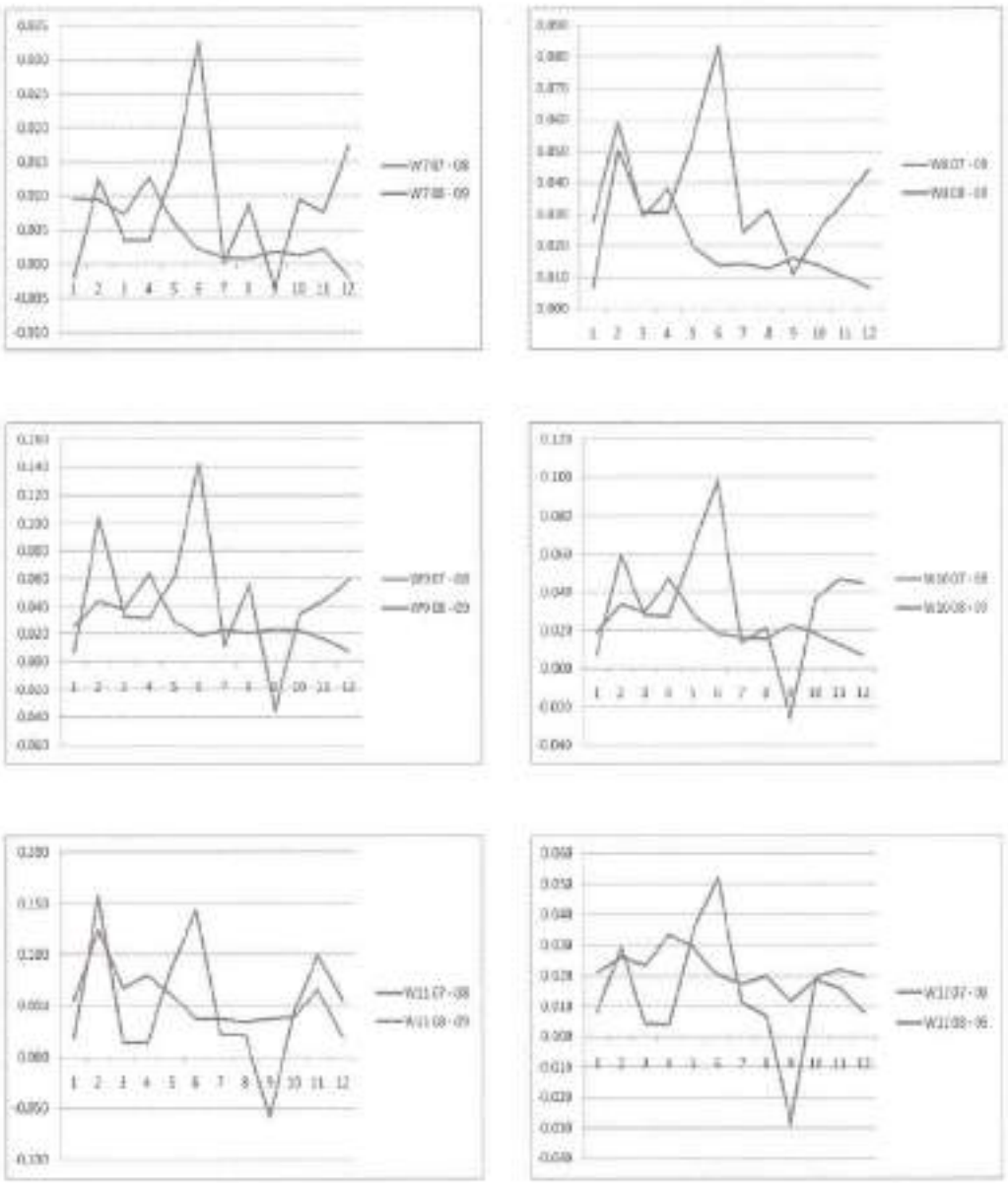

Figure 4.27 Comparison of seepage velocity before and after de-silting (Continued)

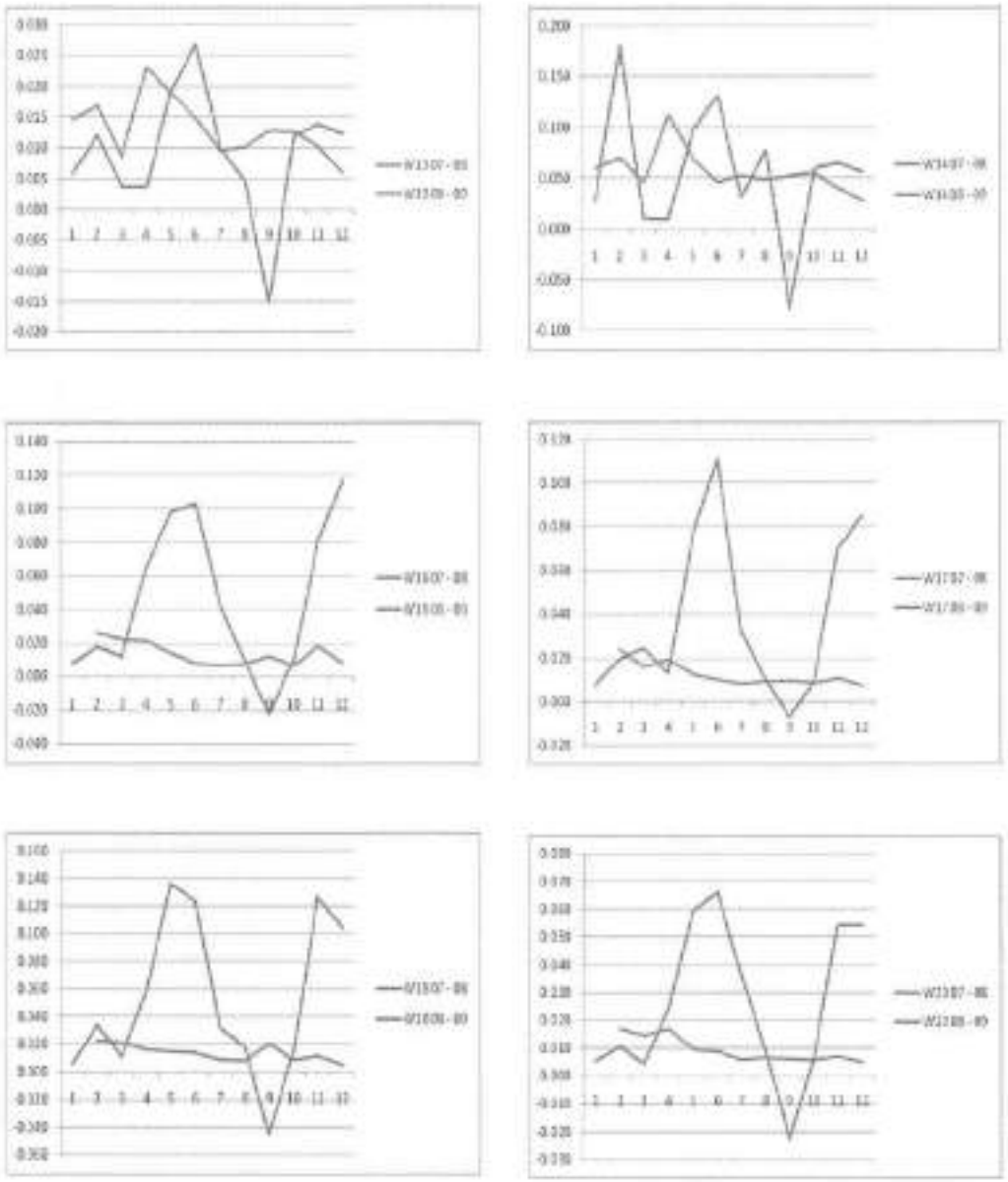

Figure 4.27 Comparison of seepage velocity before and after de-silting (Continued)

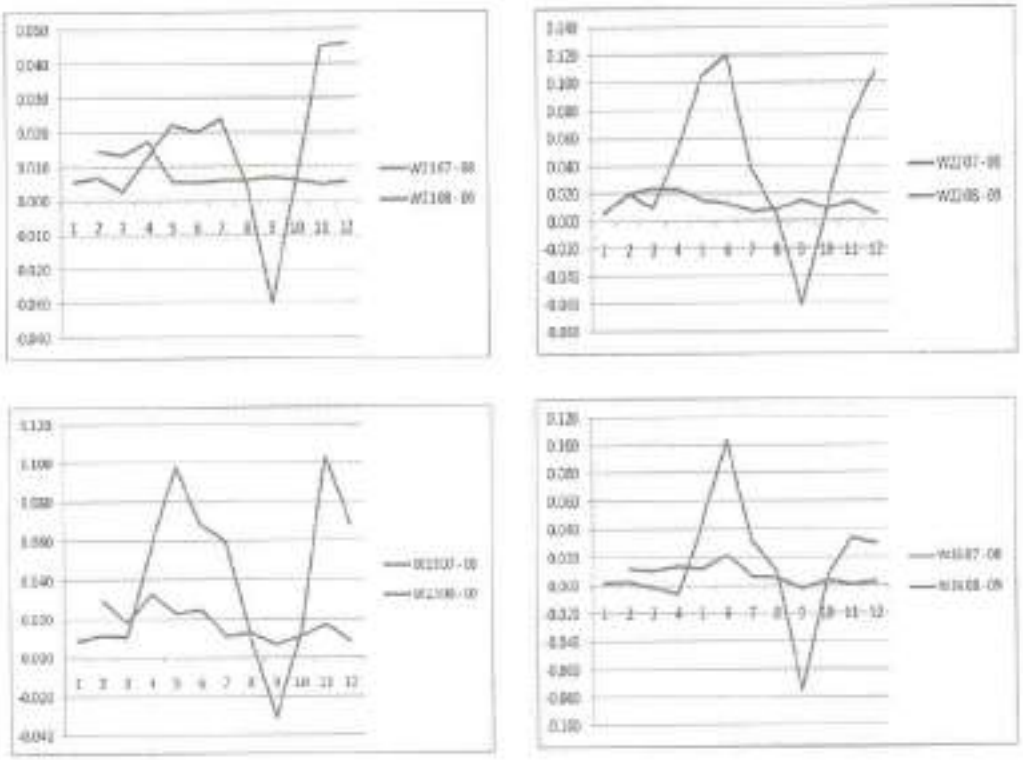

Figure 4.27 Comparison of seepage velocity before and after de-silting

Seepage velocity was higher during 2008-2009 than 2007-2008, that too during September to December, 2008. This is observed from the figure 4.27.

4.6 Summary

Ponpadi tank's present capacity is 1.2 Mm^3 which supports groundwater aquifer system in its command area. Here the aquifer is multilayer which are recharged through seepage flow from the tank and vertical movement of water leakage from one aquifer to other aquifer. Area of cultivation depends on the above quantum of water that tank contains for a particular time. Based on the above information, farmers are planning and cultivating their lands. Ponpadi tank supply channel has to be properly maintained and the tank bed has to be de-

silted in order to increase its capacity and also recharging capacity. The Sengulam tank capacity is 0.3 Mm^3 which gets filled two to three times in a year. Hence the groundwater potential is under steady state that supports two crop in a year. Here all the wells are open well, constructed in a weathered zone. If the tank bed is de-silted, periodically there is a possibility to improve its groundwater potential. Based on the hydrologic and hydraulic analysis of the Ponpadi tank system and Sengulam tank system, it was very well understood that tank and groundwater aquifer in the command area are very well interconnected. Hence a detailed study on the tank, command area and their interconnectivity are analysed were carried out in the forth coming chapter.

CHAPTER 5

TANK BED CHARACTERISTICS AND ITS RECHARGE CAPACITY

This phase of the project concentrates on the delineation of the highly permeable zone in the tank bed in order to improve the recharging capacity of the tank which is one of the objectives of the on going INCID (Indian National Committee on Irrigation and Drainage) Research project. In that project two tanks were selected already whose hydraulic and hydrologic characteristics were studied. In order to locate the place for de-silting in a tank bed in the selected tanks a preliminary survey was carried out inside the tank. Methodology adopted for this objective is shown in Figure 5.1. A four stage methodology was formulated which is given below.

- Geophysical Survey
- Infiltration Test
- Soil Texture Analysis
- Permeability Analysis

Each step of the methodology is explained in detail the following sections. Delineation of permeable zone in the project sites and its soil texture classification, permeability and the infiltration rate is discussed in the following chapter.

Initially geophysical survey is conducted to identify the permeable zone. After identifying the zone infiltration test is conducted at different depths to identify as to what depth the tank is to be de-silted. The soil samples collected at different depths and locations are used to estimate the tank bed characteristics and also analysed in the laboratory to estimate the co-efficient of permeability. The permeability values were also estimated by using a hydraulic properties software, which were compared with the laboratory values. Based on the above analysis the recharge behavior of the tank bed is estimated and the suitable zone for de-silting was delineated.

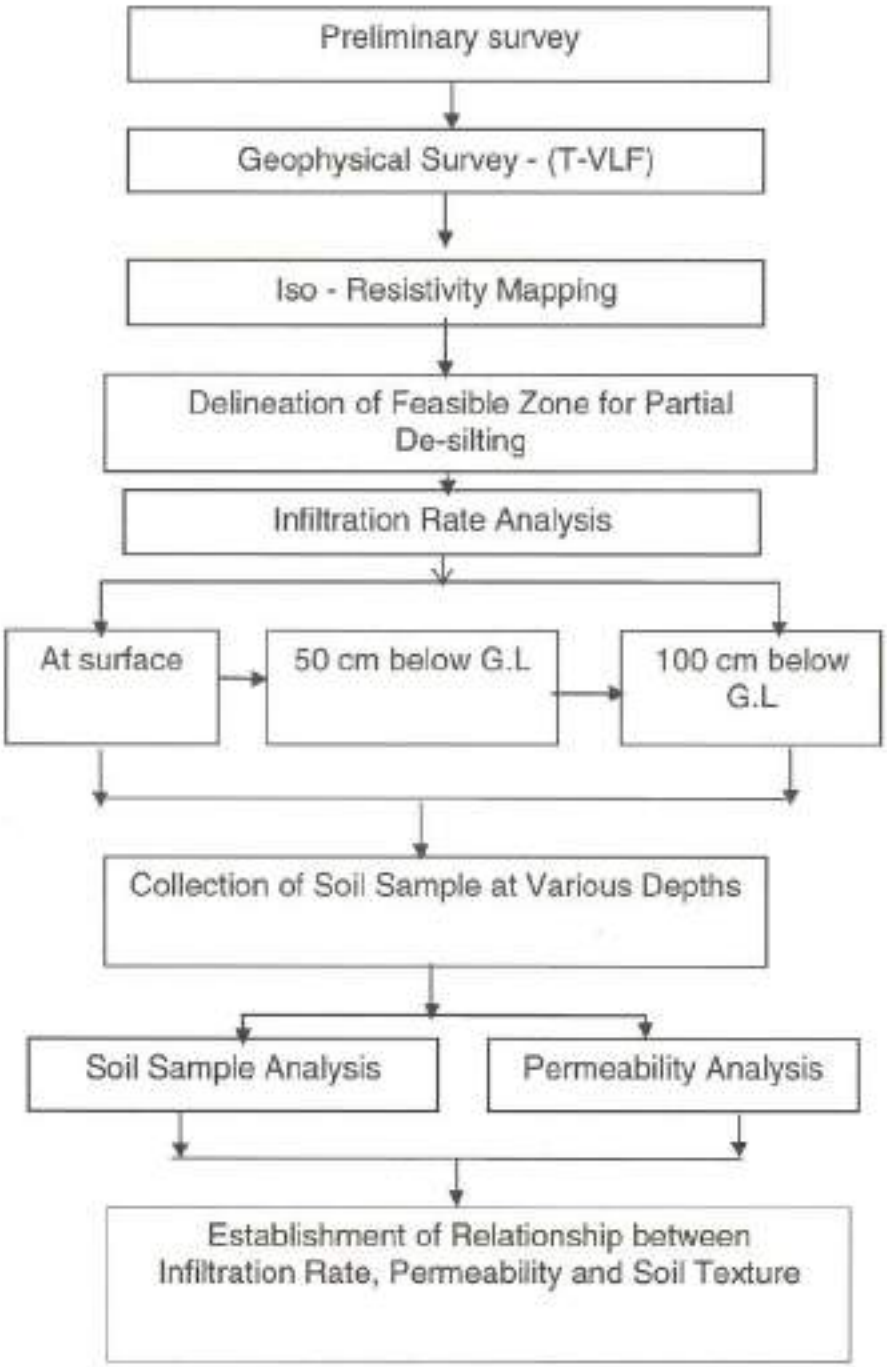

Figure 5.1 Steps followed to Delineate the Feasible zone for Partial De-silting

5.1 GEOPHYSICAL SURVEY

Geophysical survey refers to the systematic collection of geophysical data for spatial studies. Generally two methods of investigation are employed in the electrical resistivity method of traversing.

(i) Surface geophysical methods called profiling

(ii) Subsurface geophysical methods called depth sounding

5.1.1 Surface Profiling and Subsurface Depth Sounding

Surface profiling is used to detect subsurface changes in horizontal direction is carried out along a series of parallel lines and resistivity contour map of the area showing iso-resistivity lines can be prepared which will indicate high permeable or high resistivity zone that helps to identify the aquifer formation. Here the electrode separation is kept constant and the center of the electrode spread is moved from one station to another station to have the same constant electrode separations. As such the resistivity and seismic methods are widely employed and are relatively cheap. Subsurface depth sounding is to detect vertical changes. Here the center of the electrode spread remains fixed and the spacing between the electrodes is progressively increased until the maximum required depth is reached. Electrical resistivity surveys are generally used for preliminary exploration of larger areas. The interpretation based on such survey is confirmed by test drilling. There are mainly two common system of electrode arrangement one is Wenner system and the other is Schlumberger system.

In this project electromagnetic technology based instrument called Terra Very Low Frequency system (T-VLF system) made in France has been used. In the case of electrical methods, current is injected directly into the

ground, while in electromagnetic methods, currents are induced in the ground by the passage of electromagnetic waves. A simple example of an electromagnetic instrument is a metal detector, which is able to detect highly conductive metal objects buried at shallow depths. The same principles are used on a larger scale involving more powerful, well-calibrated instruments to map more subtle contrasts in electrical conductivity from the surface to depths of tens, hundreds or even thousands of meters.

5.1.2 Terra Very Low Frequency (T-VLF) System

The T-VLF (Terra Very Low Frequency) is the most widely used system which makes use of the energy of distant powerful radio transmitters in the 15-25 kHz range that operate in different countries. In radio technology terms these frequencies are known as VLF. The T-VLF (Terra Very Low Frequency) source is operating at a single well-defined frequency. It is lightweight and fast to use by a single operator (Figure 5.2). However the method is sensitive to effects of variations in the near-surface resistivity (i.e. within the top few meters) which can lead to numerous measurements of apparent resistivity.

Figure 5.2 T-VLF System

Figure 5.3 shows the behavior of electric and magnetic field from a VLF radio antenna in which E_x and E_z are the electric field components and H_y is the magnetic field component. This technique is especially useful for mapping steeply dipping structures such as faults, fracture zones and areas of mineralization. The time needed for one measurement is only 1 min, and one person can survey several line-kilometers in a day. It has basically a disadvantage because the apparent resistivity obtained cannot give information about layering.

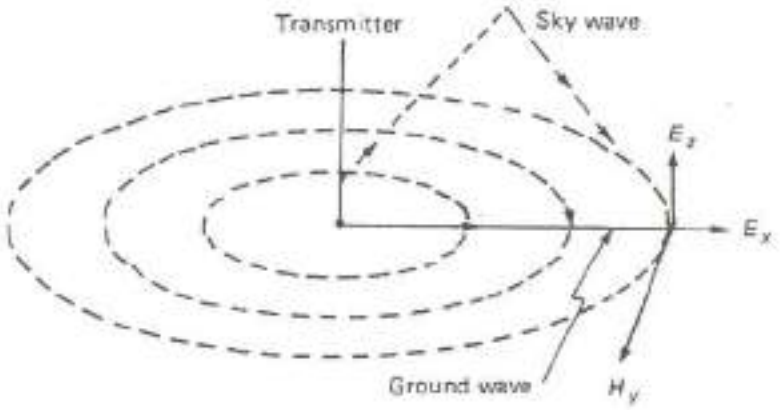

Figure 5.3 Behavior of Electric and Magnetic Field from a VLF Radio Antenna

5.1.3 Principle of Operation

VLF techniques measure the perturbations in a plane wave radio signal (15-30 kHz) emanating from one of several world-wide radio transmitters used for submarine communications. VLF falls in the broad category of electromagnetic (EM) methods of geophysics. The primary field (the transmitted radio signal) causes eddy currents to be induced in conductive geologic units or structures. Faraday's principle of electromagnetic induction tell us that any oscillating magnetic field (e.g., the radio wave) will produce an electric field and hence an electric current in a

conductive media. Those eddy currents in turn create a secondary magnetic field which is measured by the VLF receiver. The secondary or perturbed field may be phase shifted and oriented in a different direction than the primary field depending on the shape or geometry of the conductor, the orientation of the conductor, and the conductivity contrast with the surrounding material (e.g., the host rock).

The instrument measures both the primary and secondary fields together. All VLF instruments measure two components of the magnetic field or equivalently the "tilt angle" and elasticity of the field. Some instruments also measure the third magnetic component and the electric field. The electrical field is measured by inserting two probes in the ground, spaced about 10 meters apart, and measuring the potential difference at the transmitter frequency. The electric field provides additional information about the overburden thickness and conductivity.

5.1.4 Limitation of VLF

VLF is used primarily as a reconnaissance tool to identify anomalous areas for further investigation. Weaknesses of the method include

- VLF measurements are sensitive to "interference" from pipelines, utilities, fences, and other linear conductive objects.
- Interpretation is generally qualitative in nature; quantitative modeling requires a high data density and a well constrained model.
- VLF transmitters are subject to outages for scheduled or unscheduled maintenance. Unfavorable conditions may compromise the quality of the data.

5.1.5 Delineation of Permeable Zone

Terra Very Low Frequency (T-VLF) survey was carried out at two study places namely Ponpadi tank and Sengulam tank. At Ponpadi tank, T-VLF survey was started at 25 m from the tank bund to a distance of 220 m at an interval of 10m longitudinally. Similarly resistivity survey was carried out parallel to the previous one. Its apparent resistivity was noted and documented. Here, its depth of penetration of magnetic field is 5m.The total surveyed area was 2400 square meter. It is found that apparent resistivities in most of the locations were zero to three as shown in Figure 5.4. Resistivity contours were drawn to find out the highly permeable zone. Similarly the survey was conducted at Sengulam tank bed from sluice two to Sluice three to a distance of 200 m. At every 10 m interval apparent resistivity was noted. The total surveyed area was 5200 square meter. Figure 5.5 shows the longitudinal variation of resistivity at Sengulam tank bed.

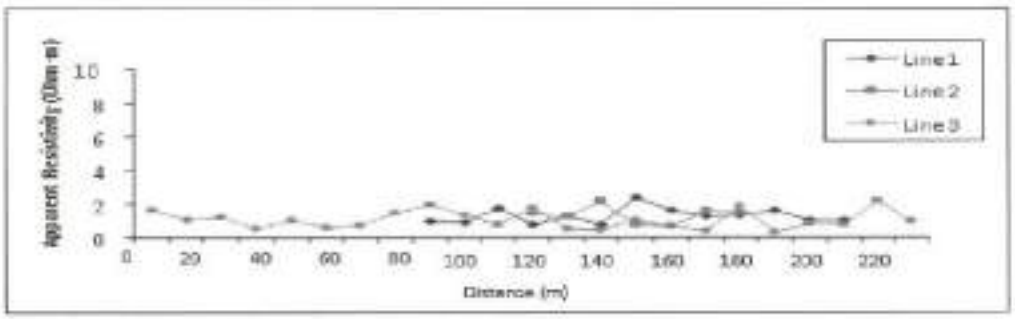

Figure 5.4 Longitudinal Variation of Resistivity at Ponpadi Tank Bed

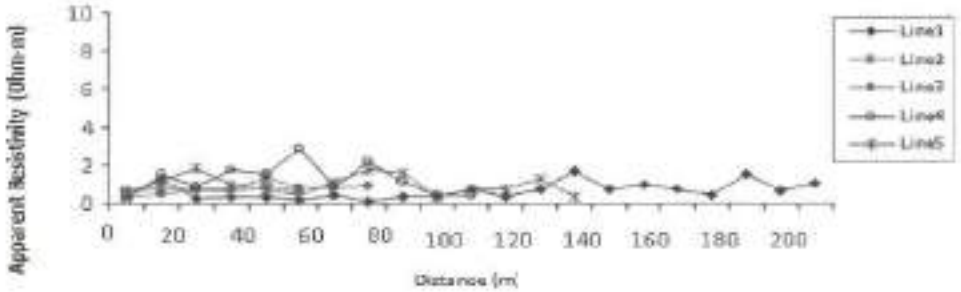

Figure 5.5 Longitudinal Variation of Resistivity at Sengulam Tank Bed

5.1.6 Iso-Resistivity Mapping

The data of the electromagnetic survey was used for the preparation of the iso-resistivity map of the Ponpadi and Sengulam tank bed. Iso-resistivity map display the lateral variation in the subsurface geology of the area. The area with low resistivity value indicates the occurrence of relatively good conductors while those with high value indicate poor conductors. The iso-resistivity map details the distribution of resistance at five meter depth. Figure 5.6 shows the iso-resistivity map for Ponpadi tank where the apparent resistivity lies between 0.84 Ohm-meter to 1.78 Ohm-meters. From the Iso-resistivity map and the observed litholog of nearby wells the geology of the area is decided in which less than one Ohm-meter indicates highly weathered and saturated genesis and greater than one Ohm-meter (1 Ohm-meter to 1.78 Ohm-meter) indicates the sandy layer up to a depth of five meter below the tank bed. Hence the area of permeable zone at Ponpadi tank for de-silting is calculated as 1910 square meter, out of surveyed area of 2400 sq.m. Similarly for Sengulam tank the Geology of the area is decided from the Iso-resistivity map and the observed litholog of nearby wells. Figure 5.7 shows the iso-resistivity map for Sengulam tank where the apparent resistivity lies between 0.04 Ohm-meter to 2.92 Ohm-meter in which greater than two Ohm-meter indicates Rock out crop (Hard rock); less than one Ohm-meter indicates unweathered granite with water filled joints and between one Ohm-meter to two Ohm-meter indicates the sandy layer up to a depth of five meter below the tank bed. The area of permeable zone at Sengulam tank for de-silting is calculated as 2353 square meter out of survey area of 5200 sq.m. Hence the apparent resistivity between 1- 2 ohm-meters is considered as the permeable zone for conducting infiltration test.

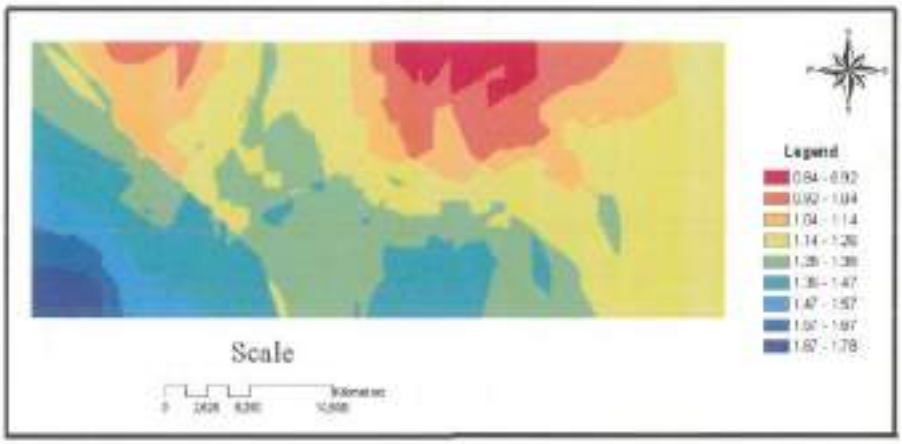

Figure 5.6 Iso-Resistivity Map of Ponpadi Tank

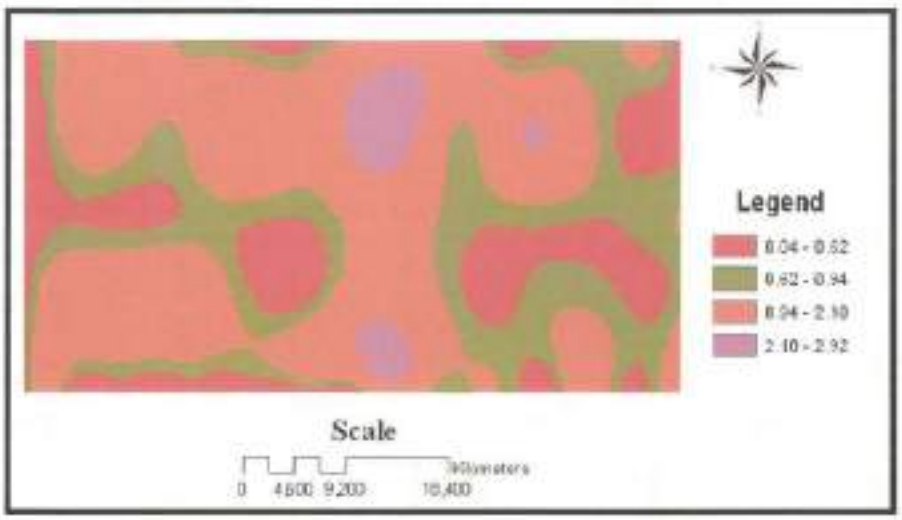

Figure 5.7 Iso-Resistivity Map of Sengulam Tank

5.2 INFILTRATION RECHARGE SYSTEM

Infiltration is the process by which water enters the soil. It separates water into two major hydrologic components - surface runoff and subsurface recharge. Infiltration rate usually shows a sharp decline with time from the start of the application of water. The constant rate approached after a

sufficiently large time is referred to as the Steady-infiltration rate. Infiltration Capacity is the maximum amount of water that is being absorbed by the soil. Infiltration capacity reduced by Surface compaction, fines blocking pores and frost action which is increased by cracks and fissures. Figure 5.8 shows the formation of a recharge mound below a recharging basin. Infiltration test was carried out with the help of Double ring infiltrometer as shown in Figure 5.9.

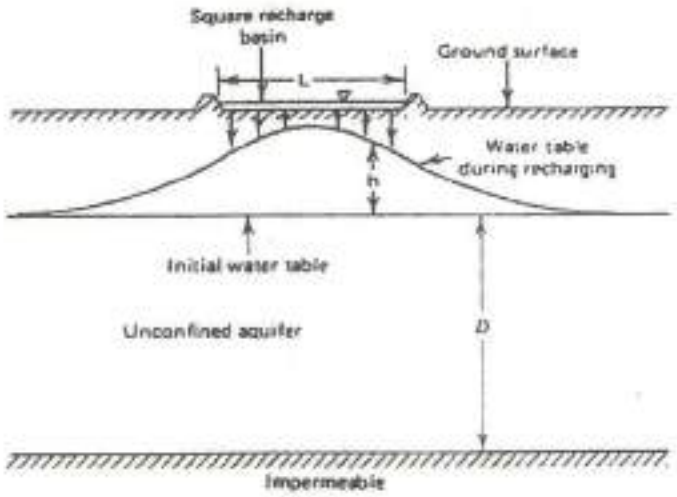

Figure 5.8 Infiltration Recharge System

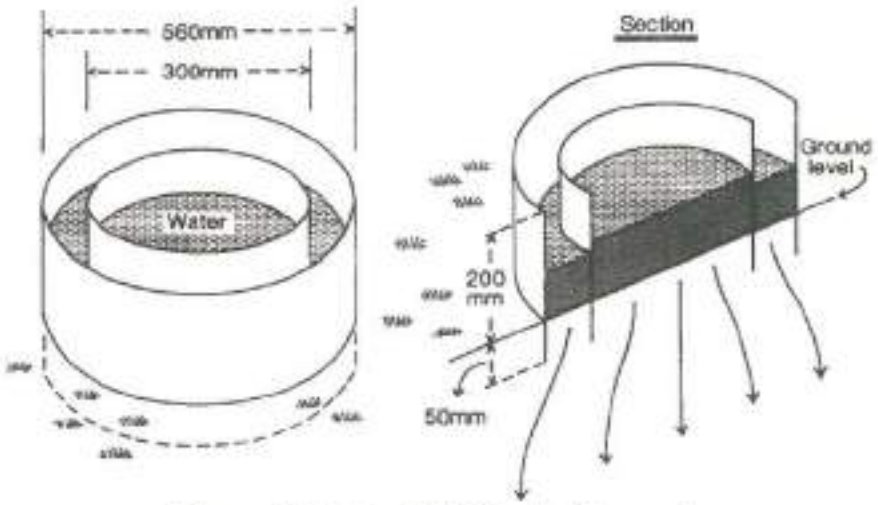

Figure 5.9 Double Ring Infiltrometer

- While in Sengulam tank bed, the infiltration rate is low at surface as compared with the infiltration rate at 50 cm depth as shown in Figure 5.15. The average infiltration rate is 0.50 cm per hour at surface, 1.32 cm per hour at 50 cm depth and 1.42 cm per hour at 100 cm depth. Below 100 cm depth out crop of rock is seen.

- The catchment area of the Sengulam tank is agriculture land. Hence there is a chance of movement of black cotton soil into the tank. At surface of Sengulam tank clay is the dominant factor and at 50 cm depth clay loam and sandy loam are detected. Hence Sengulam tank needs removal of 50 cm silt to increase recharge capacity of the tank.

Figure 5.10 Infiltration Test at Surface

Figure 5.11 Infiltration Test at 50 cm Depth below Ground Level

5.2.1 Infiltration Rate Analysis

In order to decide to what depth one should de-silt the tank bed, the infiltration test was conducted at different locations and depths. The same was carried out at surface, 50 cm, 100 cm and 150 cm depth below the tank bed at both the project site with the help of Double Ring Infiltrometer. Figure 5.10 and 5.11 show the infiltration test at surface and 50 cm below ground level. Figure 5.12 and 5.13 show the infiltration test location at Ponpadi and Sengulam tank. Table 5.1 and 5.2 shows the infiltration rate of Ponpadi and Sengulam tank bed.

- In Ponpadi tank bed infiltration rate is high at surface in all the locations considered as compared with the infiltration rate at 50 cm depth below tank bed as shown in Figure 5.14. The reason is catchment area of the Ponpadi tank is surrounded by hill hence during monsoon period surface flow takes directly from the hill towards tank .Hence there is a chance of settling of coarser particles in the tank. At the surface of the Ponpadi tank silty clay is the dominant factor while in 50 cm depth clay is the dominant factor. Generally infiltration rate is high for silty clay as compared with clay. Hence the surface of the Ponpadi tank has high infiltration rate. It was found that the average infiltration rate of Ponpadi tank is 0.82 cm per hour at surface, 0.22 cm per hour at 50 cm depth and 1.08 cm per hour at 100 cm depth.

- It was found that there is change in soil profile from 50 cm depth to 100 cm depth whose infiltration rate is 1.08 cm/hr which was reduced to 0.08 cm/hr at 150 cm depth below tank bed. It is concluded that there is a permeable formation at 100 cm below tank bed. Hence Ponpadi tank needs removal of 100 cm silt to increase recharge capacity of the tank.

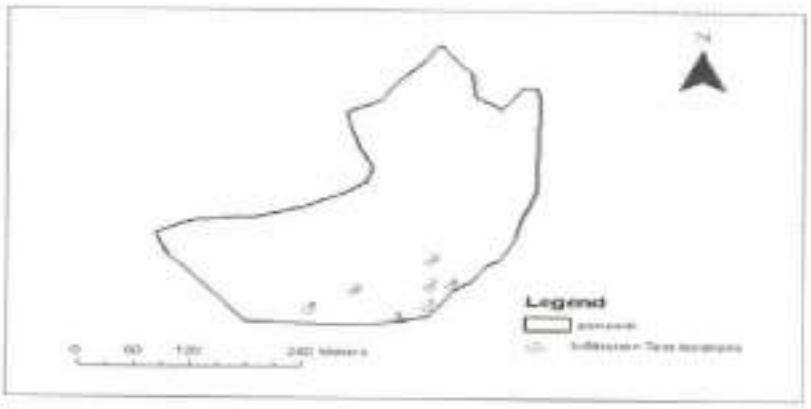

Figure 5.12 Location Map of Infiltration Test of Ponpadi Tank

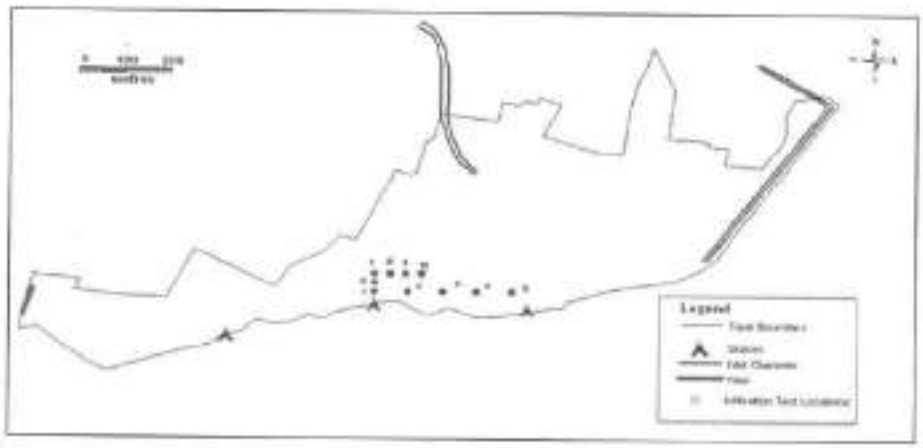

Figure 5.13 Location Map of Infiltration Test of Sengulam Tank

Table 5.1 Infiltration Rate of Ponpadi Tank Bed

Infiltration Rate (cm/hr)				
Location	**Surface**	**50 cm depth**	**100 cm depth**	**150 cm depth**
1	0.78	0.23	-	-
2	0.81	0.12	1.08	0.08
3	1.25	0.04	-	-
4	0.39	0.18	-	-
5	0.64	0.42	-	-
6	1.09	0.34	-	-

Table 5.2 Infiltration Rate of Sengulam Tank Bed

Infiltration Rate (cm/hr)			
Location	**Surface**	**50 cm depth**	**100 cm depth**
1	0.17	3.25	1.80
2	0.58	2.92	-
3	0.93	0.09	-
4	1.18	0.6	-
5	0.23	1.13	-
6	0.20	Rock	-
7	0.54	Rock	-
8	0.85	0.61	-
9	0.16	1.81	1.05
10	0.20	0.11	-

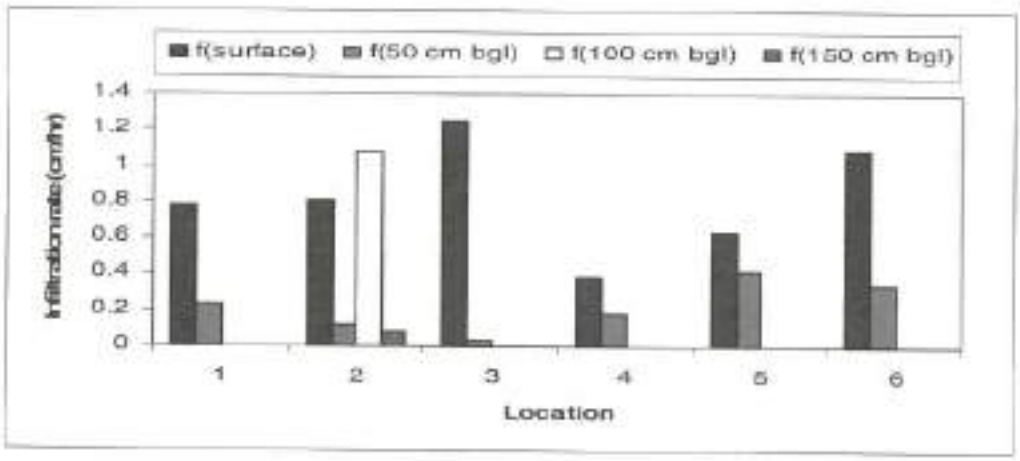

Figure 5.14 Infiltration Rate at Various Location and Depth of Ponpadi Tank

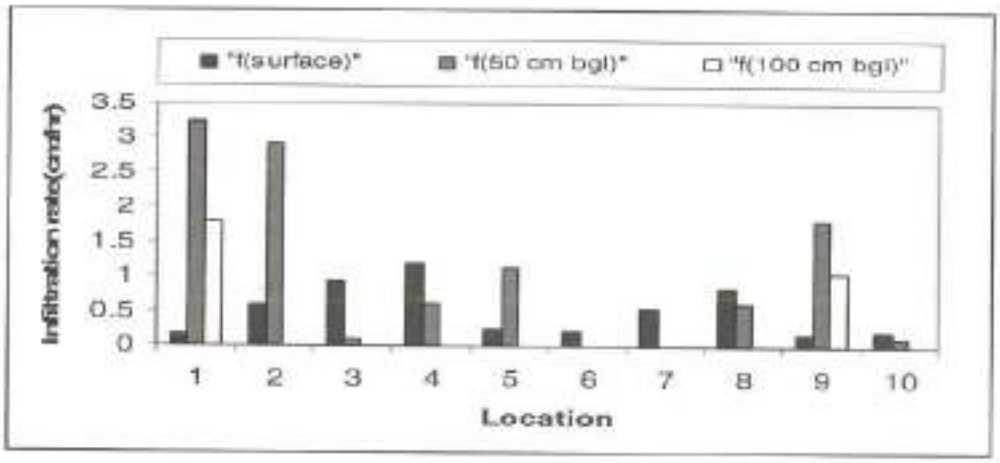

Figure 5.15 Infiltration Rate at Various Location and Depth of Sengulam Tank

5.3 SOIL TEXTURE TRIANGLE

Soil texture is a soil property used to describe the relative proportion of different grain sizes of mineral particles in a soil. Soil texture classification is based on the fractions of soil separates present in a soil. A soil texture triangle as shown in Figure 5.16 is used to classify the texture of a soil. The sides of the soil texture triangle are scaled for the percentages of sand, silt, and clay. Clay percentages are read from left to right across the triangle. Silt is read from the upper right to lower left and Sand is read from lower right towards the upper left portion of the triangle. The intersection of the three sizes on the triangle gives the texture class. For example, if we have a soil with 20 percent clay, 60 percent silt, and 20 percent sand it falls in the "silt loam" class. Soil texture analysis was carried out by the use of quartz glass jar as shown in Figure 5.17. The percent sand is the depth of the sand divided by the depth of the total soil. The percent silt is the depth of the silt divided by the depth of the total soil. The percent clay is 100 minus the percent sand plus silt.

Figure 5.16 Soil Texture Triangle

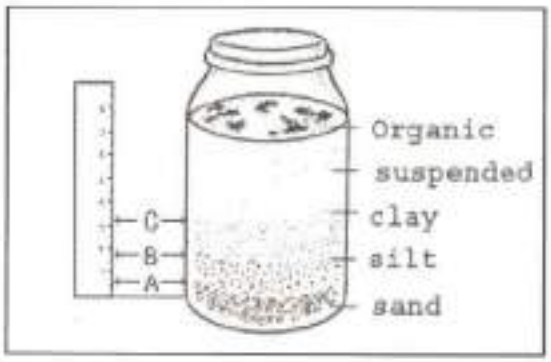

Figure 5.17 Soil Texture Analysis

5.3.1 Soil Texture Analysis

Three kilogram of soil sample was collected in a polythene bag at each location on both the tank bed where the infiltration test was done which is shown in Figure 5.18. Soil texture analysis was carried out by the use of quartz glass jar. Table 5.3 and 5.4 shows the soil texture at different location and depth of Ponpadi and Sengulam tank.

Table 5.3 indicates top layer is having silty clay at three locations, sandy clay at one location and clay at two locations. At 50 cm depth in all the locations it is clay, but at 100cm depth it is sandy clay and at 150 cm depth soil is 64 percent clay. Hence soil texture also confirms de-silting is needed for 100 cm at Ponpadi tank.

Table 5.4 indicates most of the soil texture at surface in the Sengulam tank is clay and it is sandy loam and clay loam at 50cm depth which is a favourable layer for de-silting.

Figure 5.18 Collection of Soil Sample at Various Location and Depth

Table 5.3 Soil Texture of Ponpadi Tank

PONPADI TANK						
Location	**Layer**	**Depth bgl (m)**	**Sand (%)**	**Silt (%)**	**Clay (%)**	**Soil Texture**
1	1	0	14.28	**42.86**	42.86	silty clay
	2	0.5	39.32	11.03	**49.65**	Clay
2	1	0	15.74	41.02	**43.24**	silty clay
	2	0.5	12.36	15.19	**72.45**	Clay
	3	1	**71.78**	0	28.22	sandy clay loam
	4	1.5	34.35	1.65	**64**	Clay
3	1	0	18.75	**40.97**	40.28	silty clay
	2	0.5	3.45	**84.19**	12.36	silty loam
4	1	0	32.75	7.25	**60**	Clay
	2	0.5	38.85	6.53	**54.62**	Clay
5	1	0	22.45	29.55	**48**	Clay
	2	0.5	32.15	20.93	**46.92**	Clay
6	1	0	**55.45**	13.43	31.12	sandy clay loam
	2	0.5	**45.46**	9.62	44.92	sandy clay

Table 5.4 Soil Texture of Sengulam Tank

SENGULAM TANK						
Location	**Layer**	**Depth bgl (m)**	**Sand (%)**	**Silt (%)**	**Clay (%)**	**Soil Texture**
1	1	0	39.13	13.04	**47.83**	Clay
	2	0.5	**78.32**	5.14	16.54	Sandy Loam
	3	1	**63.33**	13.33	23.34	Sandy Clay Loam
2	1	0	22.34	17.84	**59.82**	Clay
	2	0.5	**73.67**	8.49	17.84	Sandy Loam
3	1	0	23.34	**40.4**	36.26	Clay Loam
	2	0.5	45.42	5.12	**49.46**	Sandy Clay
	3	1				Rock
4	1	0	20	39.88	**40.12**	Clay
	2	0.5	**39.79**	20.96	39.25	Clay Loam
	3	1				Rock
5	1	0	40.25	12.29	**47.46**	Clay
	2	0.5	**42.12**	23.88	34	Clay Loam
	3	1				Rock
6	1	0	42.5	10.1	**47.65**	Clay
	2	0.5				Rock
	3	1				Rock
7	1	0	24.32	17.34	**58.34**	Clay
	2	0.5				Rock
	3	1				Rock
8	1	0	23.32	**39.43**	37.25	Clay Loam
	2	0.5	**39.45**	23.55	37	Clay Loam
	3	1				Rock
9	1	0	40.45	7.32	**52.33**	Clay
	2	0.5	33.25	**34.1**	32.65	Clay Loam
	3	1	**47.26**	20.46	32.28	Sandy Clay Loam
10	1	0	41.26	8.92	**49.82**	Clay
	2	0.5	**52.45**	1.72	45.83	Sandy Clay

5.4 HYDRAULIC CONDUCTIVITY

Saturated hydraulic conductivity is a quantitative measure of a saturated soil's ability to transmit water when subjected to a hydraulic gradient. Intrinsic permeability (k) is a quantitative property of porous material and is controlled slowly by pore geometry. It is the soil's hydraulic conductivity after the effect of fluid viscosity and density are removed. It is calculated as hydraulic conductivity (K) multiplied by the fluid viscosity divided by fluid density and the gravitational constant. Figure 5.19 shows the relationship between flux and hydraulic gradient. The sandy soil yields a higher flux (is more conductive) than the clay soil at the same hydraulic gradient. The soil with the steeper slope (the sandy soil) has the higher hydraulic conductivity. Hydraulic conductivity (or slope "K") defines the proportional relationship between flux and hydraulic gradient. Hydraulic conductivity (K) is the slope that defines the relationship. The dotted lines show that at equal hydraulic gradients, soils with higher conductivity have higher flux.

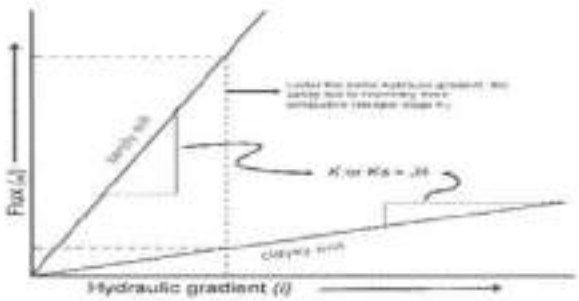

Figure 5.19 Relationship between Flux and Hydraulic Gradient

5.4.1 Estimation of Coefficient of Permeability

The experimental setup is shown in Figure 5.20. It works under the principle of falling head Permeameter. The advantage of the falling-head method can be used for both fine-grained and coarse-grained soils. The soil

sample is first saturated under a specific head condition. The water is then allowed to flow through the soil without maintaining a constant pressure head. The coefficient of permeability is given by

$$K = \frac{2.3aL}{At} \log_{10}\left(\frac{h_0}{h_1}\right) \tag{5.1}$$

Where

K	=	Coefficient of permeability
a	=	cross sectional area of stand pipe
A	=	cross sectional area of soil sample
L	=	length of the soil sample
t	=	time taken to head falls from h_0 to h_1
h_0, h_1	=	initial head, final head

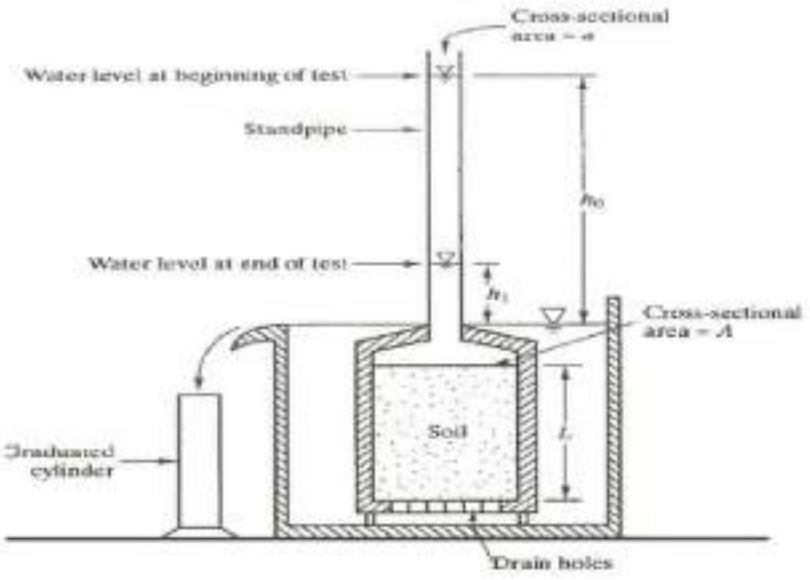

Figure 5.20 Falling Head Permeameter

5.4.2 Observed Hydraulic Conductivity

Saturated hydraulic conductivity of the Ponpadi and Sengulam tank bed soil was estimated with the falling head Permeameter in the laboratory as

shown in Figure 5.21. It was found that in Ponpadi tank the average saturated hydraulic conductivity is 0.42 cm per hour at surface 1.83 cm per hour at 50 cm depth and 0.91 cm per hour at 100 cm depth. Hence saturated hydraulic conductivity is high at 100 cm depth of Ponpadi tank bed as compared with 50 cm depth as shown in Table 5.5. While in Sengulam tank the average saturated hydraulic conductivity is 0.42 cm per hour at surface, 1.83 cm per hour at 50 cm depth and 0.91 cm per hour at 100 cm depth. Hence the same is high at 50 cm depth at Sengulam tank bed as compared with the surface as shown in Table 5.6. In Sengulam tank rock is visible at two locations in 50 cm depth and at eight locations in 100 cm depth.

Table 5.5 Permeability of Ponpadi Tank

Permeability(cm/hr)				
Location	**Surface**	**50 cm depth**	**100 cm depth**	**150 cm depth**
1	3.72	0.29	-	-
2	2.58	0.64	4.92	0.05
3	3.91	-	-	-
4	0.24	0.17	-	-
5	0.83	0.77	-	-
6	3.21	0.8	-	-

Table 5.6 Permeability of Sengulam Tank

Permeability(cm/hr)			
Location	**Surface**	**50 cm depth**	**100 cm depth**
1	0.27	6.96	1.0
2	0.84	4.05	-
3	1.09	0.21	-
4	1.0	0.84	-
5	0.19	0.81	-
6	0.22	-	-
7	0.33	-	-
8	0.02	0.48	-
9	0.17	1.1	0.82
10	0.10	0.21	-

Figure 5.21 Experimental Setup - Falling Head Permeameter

5.5 COMPUTED HYDRAULIC CONDUCTIVITY

Pedosphere has developed software to estimate the saturated hydraulic conductivity obtained from the soil texture of the soil. Figure 5.22 shows the hydraulic properties software. The software works on the principle of Saxton *et al.* (1986) equation (Hand book of hydrology, second edition). The percent of clay and sand are entered in the software to obtain saturated hydraulic conductivity. The saturated hydraulic conductivity obtained from hydraulic properties software is compared with the values obtained from the falling head Permeameter. It was observed that the difference was approximately 30 percent between the observed and computed hydraulic conductivity. This is because the soil taken from the bed is different from the one which is used to develop the software. The tank bed soil is changing every year based on its land use pattern in the catchments, rainfall intensity and the position where the tank lies. It means some tanks lie next to the hilly region or may be in the middle or tail reach.

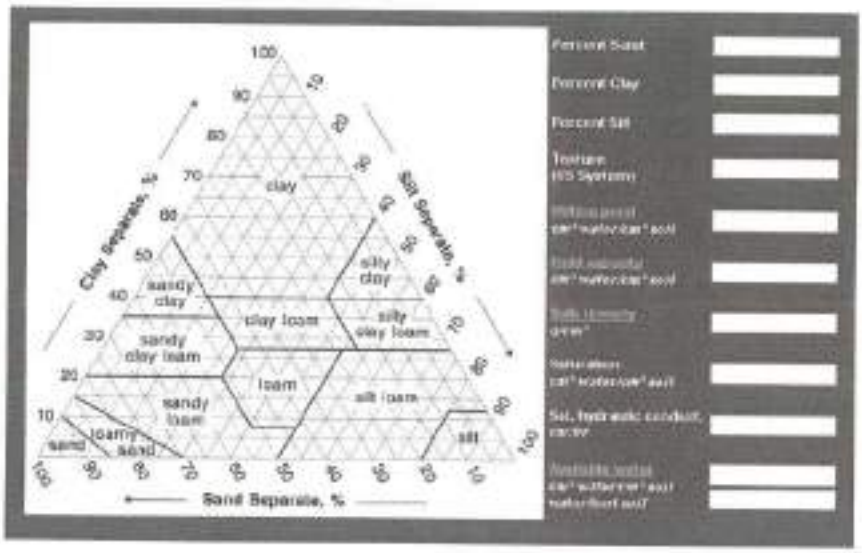

Figure 5.22 Hydraulic Properties Software

5.5.1 Analytical Method

Saxton *et al.* (1986) developed soil texture based relationship is given in Equation 5.2. His equation is based on soil texture and degree of saturation. Based on the equation he developed hydraulic conductivity curves as shown in Figure 5.23 to estimate saturated hydraulic conductivity. Limitations of Saxton's equation is which applicable only for soils with a clay content between 5 percent and 60 percent by weight and sand content of more than 5 percent by weight. Hence to suit the equation for a tank bed soil, Saxton et al equation was modified so that the difference between the observed and computed values will be within a limit.

Saxton et al equation is

$$K = k\,[\exp\,[\beta + \gamma(sa) + (\delta + \xi\,(sa) + \Phi(cl) + \lambda\,(cl)^2\,/\theta)]] \qquad (5.2)$$

Where

$k = 2.778 * 10^{-6}$ m/s

$\beta = 12.012$

$\gamma = -0.0755$

$\delta = -3.895$

ξ = 0.03671

Φ = -0.1103

λ = $8.8546 * 10^{-4}$

K = saturated hydraulic conductivity

sa = percents by weight of sand in the soil

cl = percents by weight of clay in the soil

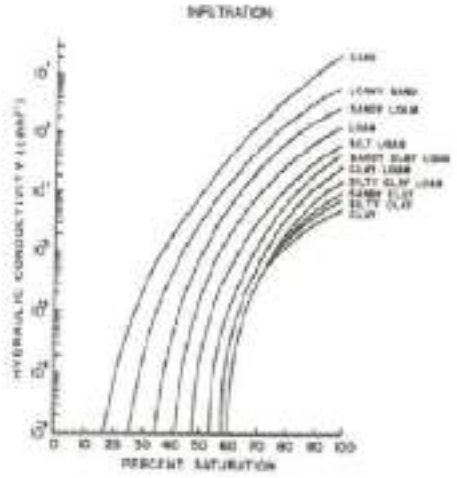

Figure 5.23 Hydraulic Conductivity Curves Classified by Soil Texture

5.5.2 Modified Saxton Equation

Saxton *et al.* (1986) equation was modified with respect to percentage of sand and clay present in a soil sample collected at various locations and depth in Ponpadi and Sengulam tank bed that is given in Equation 5.3.

$$K=\exp\{SA-CL-6.5(CL)^2\}\text{cm/hr} \quad (5.3)$$

Where

SA = percents by weight of sand in the soil

CL = percents by weight of clay in the soil

While developing the equation thirteen observed permeability values were used to calibrate the equation. The same equation was used to compute permeability for the remaining permeability data. It was found that in most of the locations observed and computed permeability was differed. Hence Equation 5.3 was again modified as given in Equation 5.4 which is a function of percent by weight sand and silt present in the soil.

$$K = [\exp\{SI\} + 33(SA)^2 - 24(SA) + 3.5] \text{ cm/hr} \qquad (5.4)$$

Where

SA = percents by weight of sand in the soil

SI = percents by weight of silt in the soil

Equation 5.4 was used to compute permeability for the entire 34 samples collected and compared with observed permeability as shown in Figure 5.23. It was found that the regression coefficient (R^2) was 0.7712. Hence sandy clay loam data were removed and a graph between observed and computed permeability was drawn for the remaining soil type. The regression coefficient was increased to 0.9334 as shown in Figure 5.24. Hence it is concluded that Modified Saxton Equation 5.4 is not applicable to sandy clay loam and sandy clay type soil. It indicates once soil texture is known its permeability will be estimated using Modified Saxton Equation 5.4.

A computer program (C++) was developed for computing saturated hydraulic conductivity by the use of modified equation in which one can easily obtained saturated hydraulic conductivity by entering the percent of sand and silt in the program as given below

```
//*To find the value of K*//
#include<iostream.h>
```

```
#include<math.h>
Void main ()
{
Float si,sa,k;
cout<<"Enter the value of si:";
cin>>si;
cout<<"Enter the value of sa:";
cin>>c;
K = [exp (si] + (33*sa*sa) – (24*sa) +3.5];
cout<<"Result k is "<<k;
}
```

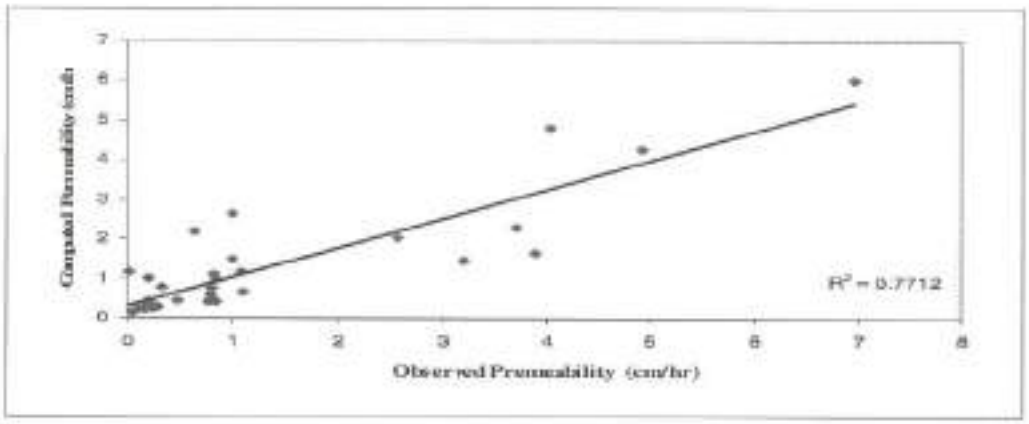

Figure 5.24 Validation of Modified Saxton Equation for all the Samples Collected

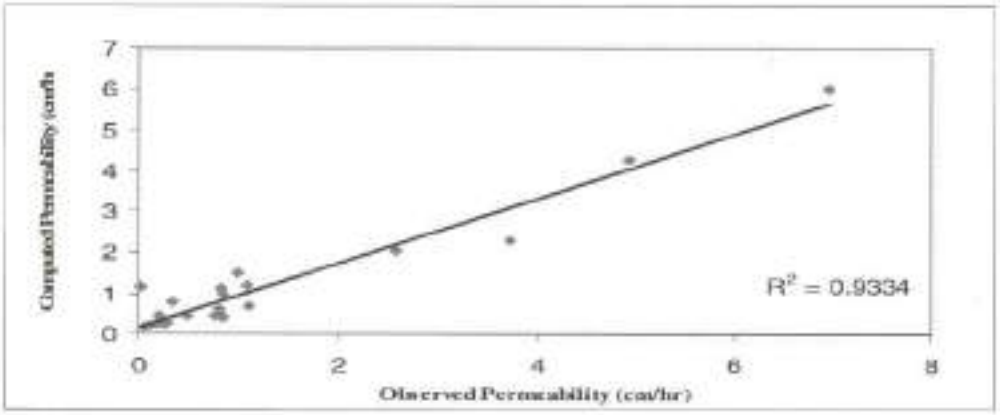

Figure 5.25 Validation of Modified Saxton Equation for all the Samples Collected except Sandy Clay and Sandy Clay Loam

5.6 ESTABLISHMENT OF RELATIONSHIP BETWEEN SOIL TEXTURE, PERMEABILITY AND INFILTRATION RATE

It is aimed to establish a relationship between observed permeability and observed infiltration rate for the different soil texture which was taken from two project sites Ponpadi and Sengulam tanks. Figure 5.25 shows the graph between observed infiltration rate and observed permeability for different soil texture.

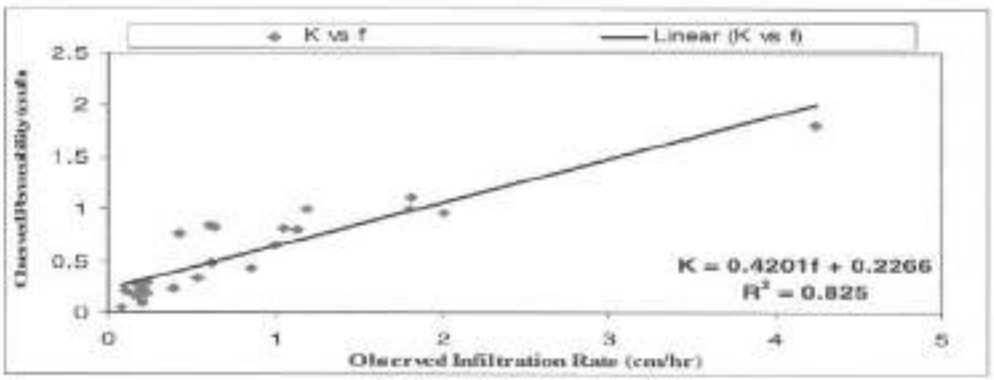

Figure 5.26 Relationship between Infiltration Rate and Hydraulic Conductivity

Empirical equation for computing infiltration rate if permeability is known is given in Equation 5.5

$$f = \frac{(K - 0.226)}{0.4201} \tag{5.5}$$

Where

f = Infiltration Rate (cm/hr)

K = Coefficient of Permeability (cm/hr)

Above empirical equation is not suitable for sandy soil. Since most of the tank bed soil is dominated by clay and silt. Two relationships were established one is Modified Saxton equation (Equation 5.4) and the other one is permeability is a function of infiltration rate (Equation 5.5). With the help of above said two equations one can estimate permeability and infiltration rate if the soil texture of the soil is known. Equation 5.5 is used to estimate infiltration rate. This computed infiltration rate is compared with observed infiltration rate whose R^2 value is 0.9659 which is shown in Figure 5.26. In addition the infiltration rate data collected during June 2009 is plotted in the same graph as shown in Figure 4.18. Infiltration rate is approximately three times higher than the infiltration rate observed during September 2008 which is shown in Figure 5.26. Hence the sandy clay loam soil is not suitable for computing infiltration rate from soil texture.

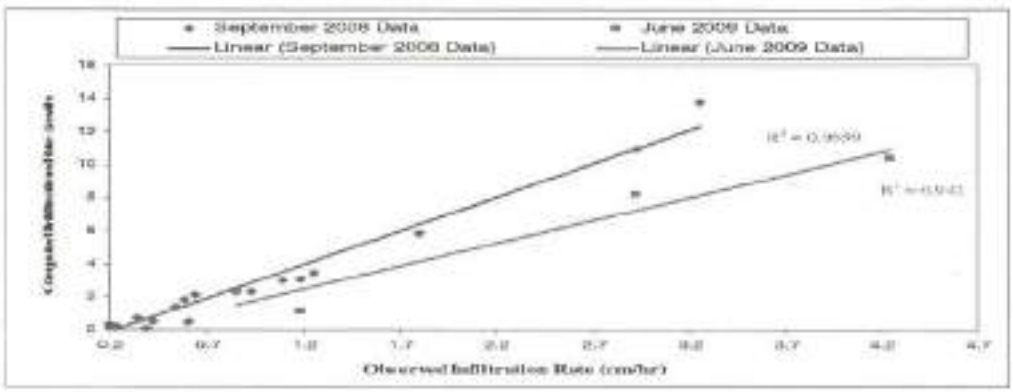

Figure 5.27 Comparison of Observed and Computed Infiltration Rate of Clay, Silty Clay and Clay Loam

From the above discussion one can conclude no need to do infiltration test at different locations and different depths of the tank bed and also no need to do permeability test in the laboratory. Once the soil texture is known for a tank bed then with the help of modified Saxton equation Permeability can be estimated. Substituting this computed permeability into the empirical relationship as given in Equation 5.5 infiltration rate can be estimated for different soil texture. Computed permeability and infiltration rate can be cross checked with one or two places of the tank bed.

5.7 STRATEGY FOR DE-SILTING

i. The deepest portion of the tank is to be selected where the water stays for a longer period of time in which siltation is more.

ii. Geophysical survey is to be conducted in the deepest portion of the tank to delineate the permeable zone.

iii. In that permeable zone infiltration test is to be carried out at different locations and depth.

iv. Soil samples are to be collected to determine permeability and soil texture.

v. Based on the soil texture, infiltration rate and permeability the depth of de-silting can be decided.

vi. If the infiltration rate is very less at 50 cm and 100 cm depth below tank bed level, then bore whole test has to be carried out with the help of hand auger.

vii. Collect soil samples at different layers and carry out soil sample analysis to determine the soil texture and

permeability in which one can easily determine at what depth the soil profile is permeable

viii. If infiltration is less even at 100 cm depth, recharge pits can be a viable option, water can be diverted to these pits and recharge capacity of the tank can be enhanced effectively.

5.8 PARTIAL DE-SILTING OF SENGULAM TANK

Based on TVLF survey and Infiltration test the area for partial de-silting at Sengulam tank was demarcated that is shown in figure 5.28. The partial de-silting work was carried out using one JCB and three tractors as shown in photograph 5.1. The work was scheduled for five days during 23rd to 27th September 2008 comprising of 44 working hours. The area of de-silting was 1395 Sq. m and the average removal depth was 0.61 m. The volume of silt removed was 846 m^3. The silt thus removed was used in raising the level of the bund between sluice 3 and sluice 1 and also used for strengthening the side slopes of the bund especially at weaker portions between sluice 2 and surplus weir. Certain portion of the silt was taken by the farmers for their agricultural lands.

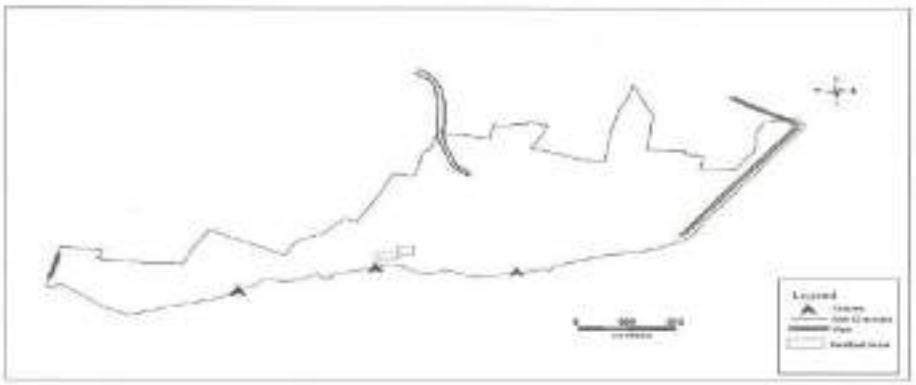

Figure 5.28 Partial De-silting Portion of Sengulam Tank

Photograph 5.1 Partial De-silting at Sengulam Tank

5.9 SUMMARY

Artificial recharge of groundwater is the movement of water through soil and aquifers provides a means of geo-purification of water. An integrated study covering the aspect of tank bed recharge is a crucial requirement of the present day. The present work is an attempt in this direction. Apart from geo-physical survey, the study also takes an account of infiltration test, soil texture analysis, and permeability analysis for identification of suitable sites for tank bed recharge. In this study, an attempt is made to provide a frame work for the characterization and mapping of subsurface profile for delineating highly permeable zone. To obtain detail information on these subsurface profiles, apparent resistivity data were acquired along the two tank bed which runs parallel and perpendicular to the axis of the tank bed.

The acquired data were processed with Arc GIS software and iso-resistivity maps are created. Highly permeable zone was delineated from the iso-resistivity map and infiltration tests were conducted in these highly permeable zone. This is to ascertain that to what depth the de-silting has to be carried out. Soil samples are collected from these places and soil texture and

permeability tests were carried out in the laboratory. Saxton equation is used to compute the permeability which was compared with the observed permeability. Since the match between the observed and computed was not good Saxton equation was modified to suit to the tank bed soil. It is observed that the modified Saxton Equation is suitable for all be types of soil except sandy soil. An empirical relationship between the infiltration rate and the permeability was obtained in which permeability is a function of infiltration rate. With the help of modified Saxton Equation (5.4) and empirical relationship (5.5) one can compute permeability and infiltration rate if soil texture is known. The conclusions derived after detailed analyses are presented in the following section.

The primary conclusion drawn from this study is summarized below

- From the geo-physical survey it is observed that in Ponpadi tank the area of permeable zone for de-silting is about 1910 square meter, in Sengulam tank the area of permeable zone is about 2353 square meter.
- In Ponpadi tank infiltration rate is high at surface (0.82 cm/hr) in all locations when compared with infiltration rate at 50 cm depth (0.22 cm/hr). It is found that there is a change in soil profile at 100 cm depth.
- In Ponpadi tank, clay is found at 50 cm to 100 cm depth, below 100 cm depth sandy clay is found, hence it can be further concluded that de-silting has to be carried out up to a depth of 100 cm in the delineated highly permeable zone.
- In the case of Sengulam tank it is observed that the infiltration rate is low at surface (0.51 cm/hr) as compared

with the infiltration rate obtained at 50 cm depth (1.50 cm/hr).

- In Sengulam tank, surface layer is dominated with clay and subsurface is dominated by sandy loam and clay loam is, hence it can be further concluded that de-silting can be carried out up to a depth of 50 cm in the delineated highly permeable zone.

- From laboratory permeability tests it is observed the value of permeability is higher for soil samples collected at 100 cm depth (4.92 cm/hr)in Ponpadi tank. Whereas in case of Sengulam tank it is observed that permeability value is higher for soil samples collected at 50 cm depth (1.83 cm/hr).

- It can be concluded that the methodology adopted in this study is an effective way for delineating the permeable zone of tank bed.

CHAPTER 6

ESTIMATION OF AQUIFER PARAMETERS THROUGH WELL DILUTION TECHNIQUE

6.1 GENERAL

The most commonly adopted method for determination of aquifer parameter is time consuming that requires specific setup. Tracer tests are used to trace the path of flowing water. Conservative tracers are used for groundwater studies which moves with the same velocity as the groundwater and its concentration is affected only by hydrodynamic dispersion. Tracer tests are generally regarded as being the most reliable and efficient means of gathering subsurface hydraulic information. Tracers are useful tools for defining aquifer parameter necessary for groundwater studies characterization and remediation such as recharge rates, well capture zone analysis, preferred flow path, volume and quality of water and susceptibility to contamination.

6.2 REQUIREMENT OF GROUNDWATER TRACER

A groundwater tracer can be any substance which is naturally, accidentally, or intentionally introduced into a groundwater system. Some tracers are more effective than others under certain conditions and there is no one universally accepted tracer that can be used under all conditions. Therefore, a tracer must be selected which will meet the most important requirements of the study objective and usually requires a compromise between study objective and tracer selection. The choice of a particular tracer depends upon the property that needs elucidation. If water is to be traced, then

a conservative solute is the best choice. The general requirements of an ideal tracer are listed as follows:

i. A tracer must be capable of quantitative measurement at very low concentrations;

ii. A tracer's introduction to the environment and its subsequent withdrawal must not modify the naturally occurring transport phenomenon;

iii. A tracer should be inexpensive and readily available, and analytical costs should be reasonable;

iv. A tracer should not be present in appreciable background concentrations in the natural water;

v. A tracer should not create a health hazard or interfere with later investigations;

vi. A tracer must be capable of transporting in the environment to which it is introduced in the same manner as the naturally occurring water;

vii. A tracer must not be sorbed by the material through which it is coming in contact;

The use of tracer has substantially increased our understanding of groundwater flow and transport mechanism. Well dilution technique that has definite advantages over the above methods has been under-used in Indian subcontinent. Objectives of this chapter is to estimate groundwater velocity, hydraulic conductivity and dispersion coefficient by using tracer and pumping test analysis. The goal of this chapter was achieved through following steps that is shown in flow chart.

i. Well Dilution Studies
ii. Soil Analysis
iii. Permeability Test

6.3 WELL DILUTION TECHNIQUE

Two types of well dilution techniques were adopted in the study area to estimate the aquifer parameter. They are single well dilution technique and two well dilution techniques.

6.3.1 Single well Dilution Technique

The basic theory and experimental details of single well tracer dilution technique are well established. The technique involves introduction of known quantity of tracer in a suitable well and monitoring of tracer concentration over a time period. Diagrammatic representation was shown in Figure 6.1. The filtration velocity can be estimated using the following relationship using the Equation 6.1.

$$V_f = \frac{\pi r}{2\alpha t} \ln \frac{C_o}{C} \qquad (6.1)$$

Where,

V_f	-	Filtration velocity in m/day
r	-	Internal radius of the well in meter
Co and C	-	Tracer concentration at time t = 0 and at time t
α	-	Correction factor to eliminate the distortion of the ground water flow lines caused by the presence of well

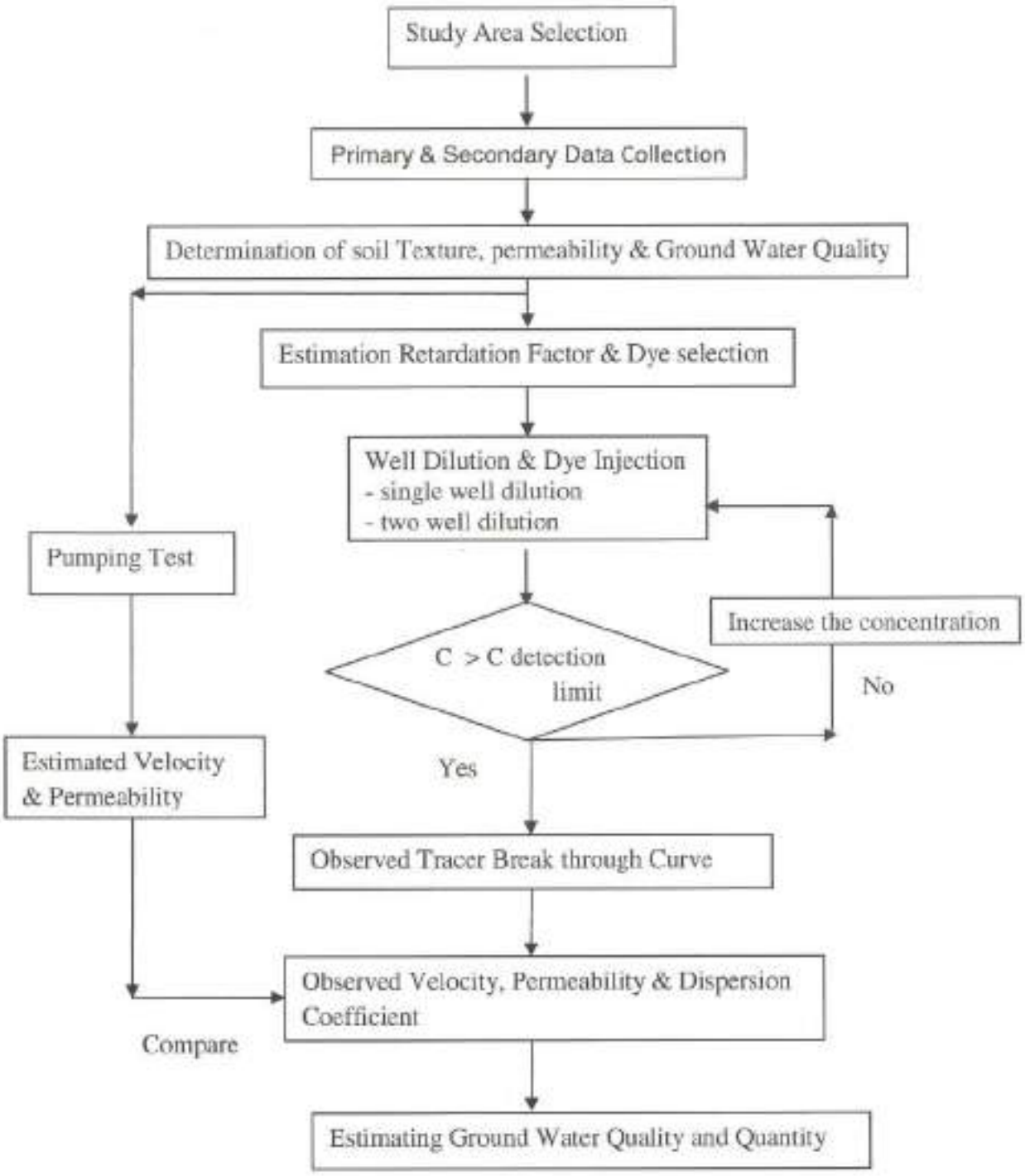

Methodology to Estimate Aquifer parameters through Well Dilution Techniques

The borehole distortion factor between 0.5 and 4; and 2 for an open well. By knowing the hydraulic gradient the permeability can be calculated by using Darcy's Law using the Equation 6.2

$$V_f = KI \tag{6.2}$$

Where,

K - Hydraulic Conductivity in m^2/s

I - Hydraulic gradient in metre

From the above experiment the concentration at various time was known. Graph of C/C_0 versus t, was plotted. The value of t at C/C_0 was 0.16 and 0.84 was noted from the graph. The filtration velocity was estimated from the above Equation 6.1. Finally the dispersion coefficient was obtained by the Equation 6.3.

$$D_L = \frac{1}{8}\left[\frac{(z-\bar{v}t_{0.16})}{\sqrt{t_{0.16}}} - \frac{(z-\bar{v}t_{0.84})}{\sqrt{t_{0.84}}}\right]^2 \tag{6.3}$$

Where,

D_L - Dispersion coefficeint in m^2/day,

Z - Distance at which dispersion was measured in metre

$t_{0.16}$ and $t_{0.84}$ – time at concentration at $C/C_0 = 0.16$ and $C/C_0 = 0.84$

$\bar{V}$ – Filtration velocity in m/day

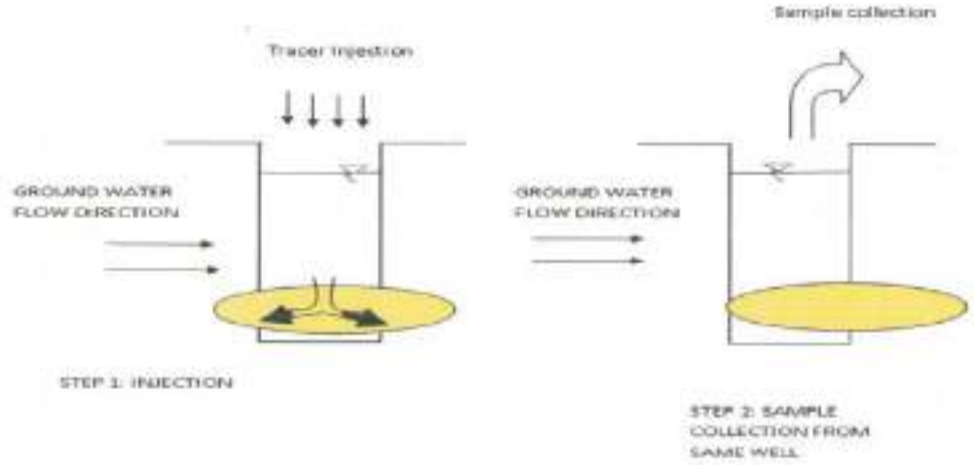

Figure 6.1 Diagrammatic Representation of Single Well Dilution

6.3.2 Two well Dilution Technique

The two well dilution techniques were injecting tracer in one well and monitoring in the other well at downstream of the injected well by natural and forced gradient.

Natural Gradient

Two well dilution techniques by natural gradient in monitoring the tracer concentration in the downstream well. The tracer moves in its natural gradient and not by pumping. The tracer break through curve was obtained. The concentration at various time intervals was noted in the well at downstream. Analyzing the resulting tracer break through curve, dispersion coefficient and dispersivity was estimated by Equation 6.4.

$$c(r,t) = \frac{M}{4\pi t B n \bar{v} \sqrt{\alpha_L}} \exp\left[-\frac{(r-vt)^2}{4D_L t}\right] \qquad (6.4)$$

Where,

M - Injected mass of tracer per unit section in kg

$\bar{V}$ - Velocity in m/s

α_L - Longitudinal Dispersivity in metre

B - Aquifer thickness in metre

n - porosity

x - Radial distance between two wells in metre

D_L - Longitudinal dispersion coefficient in m^2/s

Forced Gradient

The Method consists of injection of the tracer into one well situated within the drawdown cone caused by pumping well and subsequent measurement of the tracer concentration in the water abstracted from the neighboring well as a function of time. Diagrammatic Representation was shown in Figure 6.2. The tracer break through curve was monitored till the end recovery. Analyses of the resulting tracer break through curve yields dispersion coefficient and dispersivity. The one dimensional Dispersion equation was given in Equation 6.5 and 6.6.

$$c(r,t)=\frac{\Delta M}{2Q\sqrt{\pi\alpha_L vt^3}}\exp\left[-\frac{(r-vt)^2}{4D_L t}\right] \quad (6.5)$$

$$D_L = \alpha_L \, v \quad (6.6)$$

Where,

ΔM - Injected mass of tracer per unit section in kg

V - Velocity in m/s

α_L - Longitudinal Dispersivity in meter

D_L - Longitudinal dispersion co efficient in m^2/s

Q - Pumping rate of the well in m^3/s

r - Radial distance between two wells in meter

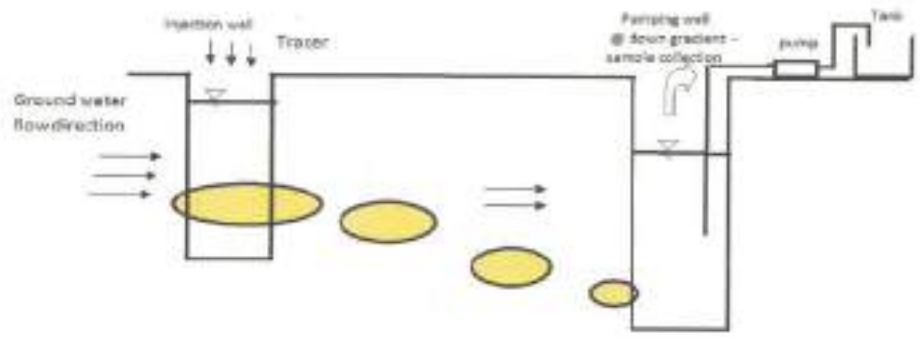

Figure 6.2 Diagrammatic Representation of Two Well Dilution

6.4 INSTALLATION OF BOREHOLE IN THE FIELD

To conduct tracer study seven bore holes as shown in figure were installed in seven location at the depth of around 2.5 m. Figure 6.3 shows the block diagram of the borehole location. Experiments were conducted with Sulpho Rhodamine-B and NaCl to estimate filtration velocity, permeability and dispersivity were calculated from filtration velocity.

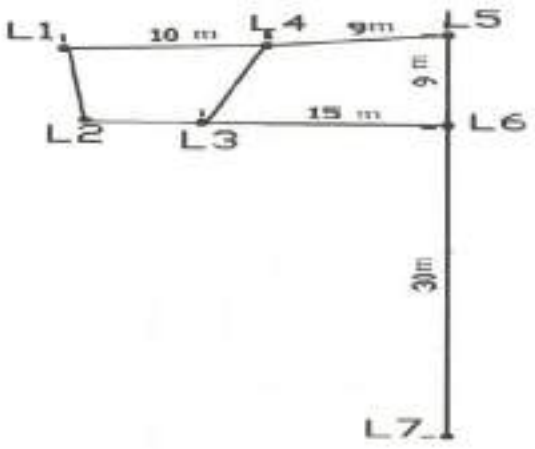

Figure 6.3 Block Diagram of Borehole Location at the Depth of 2 m

6.4.1 Single Well Dilution

A Known quantity of organic dye or chemical tracer was injected instantaneously into the borehole and the borehole was monitored continuously. Four experiments were carried out with Sulphorhodamine B (organic Tracer) and common salt NaCl (Chemical tracer).

Experiment 1 Single Well Dilution with SulphorhodamineB

Experiment 1 was Single well dilution study with SRB was done by two trials. One was with the concentration of 2500 ppb of 1000 ml and other was with 250 ppb concentration of 100 ml.

a. Trial 1

The solution of 2500 ppb concentration of one litre was poured instantaneously in the borehole L4. The water sample from the borehole L4 was collected from the time t= 0 to the time t days until the background concentration was attained. The concentration of the water samples collected from the borehole L4 was measured using the Fluorescent Spectrometer. The details of the single well dilution in borehole L4 was shown in Table 6.1. The concentration of Sulphorhodamine B in L4 was reduced to 39 ppb in 8580 min. The initial concentration C_0 was 465 ppb. By using the Equation 6.1 and 6.2 average filtration velocity estimated was 0.06 m/day and permeability estimated was 5.02 m/day.

Table 6.1 Details of Single Well Dilution in L4 by SRB

Date	Time at sample taken	Time 't'(min)	Concentration (ppb)	Filtration velocity (m/day)
09-04-2011	10:30	0	465	-
09-04-2011	15:00	270	437	0.05
10-04-2011	09:30	1410	364	0.05
10-04-2011	15:35	1775	347	0.04
11-04-2011	10:30	2880	311	0.05
11-04-2011	15:00	3150	270	0.05
12-04-2011	10:00	4290	216	0.05
12-04-2011	13:30	4470	196	0.05
13-04-2011	09:30	5670	165	0.05
13-04-2011	15:00	6000	151	0.06
14-04-2011	09:00	7080	101	0.06
14-04-2011	16:00	7500	86	0.08
15-04-2011	10:00	8580	39	0.06

Figure 6.4 shows the graph for C/C_0 versus t for single well dilution in L4 using Sulphorhodamine B as tracer explained in experiment 1, trial 1. From the Figure 6.4 at $C/C_0 = 0.16$, t = 7800 min and $C/C_0 = 0.84$, t = 900 min. By using the Equation 6.3 the dispersion co efficient estimated was 0.28 m^2/day and the dispersivity estimated was 7.1 m.

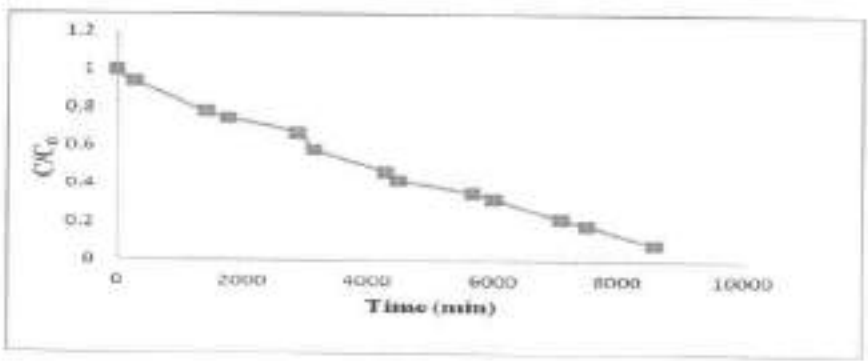

Figure 6.4 Single Well Dilution in L4 by SRB

b. Trial 2

The solution of 250 ppb concentration of 100 ml was poured instantaneously in the borehole B1. The water sample from the borehole B1 was collected from the time t= 0 to the time t days until the background concentration in attained. The concentration of the water samples collected from the borehole B1 was measured using the Fluorescent Spectrometer. The details of the single well dilution in borehole B1 was shown in Table 6.2. The concentration of Sulphorhodamine B in B1 was reduced to minimum of 36 ppb in 1448 min. By using the Equation 6.1 and 6.2 filtration velocity estimated was 0.05 m/day and permeability estimated was 4.9 m/day.

Table 6.2 Details of Single Well Dilution in B1 by SRB

Date	Time at sample taken	Time 't'(min)	Concentration ppb	Filtration velocity (m/day)
11-02-2011	17:37	0	203	-
11-02-2011	16:30	53	192	0.05
12-02-2011	8:00	823	92	0.04
12-02-2011	09:00	923	87	0.04
12-02-2011	09:25	948	84	0.04
12-02-2011	10:00	983	80	0.04
12-02-2011	10:30	1013	77	0.04
12-02-2011	11:10	1128	74	0.04
12-02-2011	11:38	1188	67	0.04
12-02-2011	12:10	1248	61	0.04
12-02-2011	12:30	1268	56	0.05
12-02-2011	13:30	1328	49	0.05
12-02-2011	14:38	1396	45	0.05
12-02-2011	15:30	1448	36	0.05

Figure 6.5 shows the graph for C/C_0 versus t for single well dilution in L4 using Sulphorhodamine B as tracer explained in experiment 1, trial 2. From the Figure 5.12 at $C/C_0 = 0.16$, t = 5000 min and $C/C_0 = 0.84$, t = 250 min. By using the Equation 6.3 the dispersion co efficient estimated was 0.3 m^2/day and the dispersivity estimated was 7.5 m.

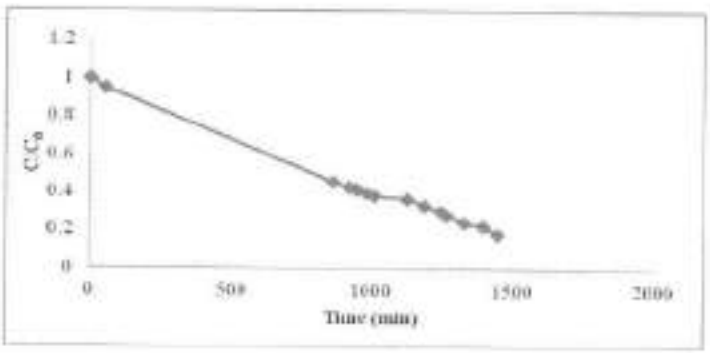

Figure 6.5 Single Well Dilution in B1 by SRB

Experiment 2 Single Well Dilution with NaCl

Experiment 2 was Single well dilution study with NaCl was done by two trial. One was with the concentration of 400 g of NaCl was diluted in the water sample and other was with 200 g of NaCl was diluted in the water sample.

a. Trial 3

400 g of NaCl was diluted in the water sample from the study area and it was poured instantaneously in the borehole L1. The borehole L1 was monitored continuously until the background was obtained. The water samples were collected from the borehole L1 at different times. The electrical conductivity of the water samples are measured in the laboratory. The details of the single well dilution in borehole L1 was shown in Table 6.3. The concentration of NaCl in L1 was reduced to background concentration of 1990 µs/cm in 10865 min. By using the Equation 6.1 and 6.2 average

filtration velocity estimated was 0.04m/day and permeability estimated was 3.36 m/day.

Figure 6.6 shows the graph for C/C_0 versus t for single well dilution in L1 using NaCl as tracer explained in experiment 2, trial 1. From the Figure 6.6 at $C/C_0 = 0.16$, t = 9400 min and $C/C_0 = 0.84$, t = 350 min. By using the Equation 6.3 the dispersion co efficient estimated was 0.45 m^2/day and the dispersivity estimated was 11.5 m.

Table 6.3 Details of Single Well Dilution in L1 by NaCl

Date	Time at sample taken	Time 't'(min)	Concentration EC (µs/cm)	Filtration Velocity (m/day)
20-03-2011	15:45	0	7,100	-
20-03-2011	16:15	30	7,100	0.02
21-03-2011	12:40	1255	6,360	0.02
21-03-2011	16:40	1495	5,200	0.03
22-03-2011	09:45	2520	4,950	0.03
22-03-2011	12:45	2700	4,900	0.04
22-03-2011	15:45	2880	4,850	0.04
23-03-2011	09:50	3965	4,620	0.04
23-03-2011	12:00	4685	4,110	0.04
23-03-2011	16:00	4925	3,890	0.04
24-03-2011	09:00	6065	3,620	0.04
24-03-2011	15:00	6425	3,390	0.04
25-03-2011	09:00	7505	2,900	0.04
25-03-2011	16:00	7925	2,710	0.04
26-03-2011	09:00	8945	2,580	0.04
26-03-2011	16:00	9365	2,440	0.04
27-03-2011	09:00	10385	2,110	0.04
27-03-2011	16:00	10865	1,990	0.04

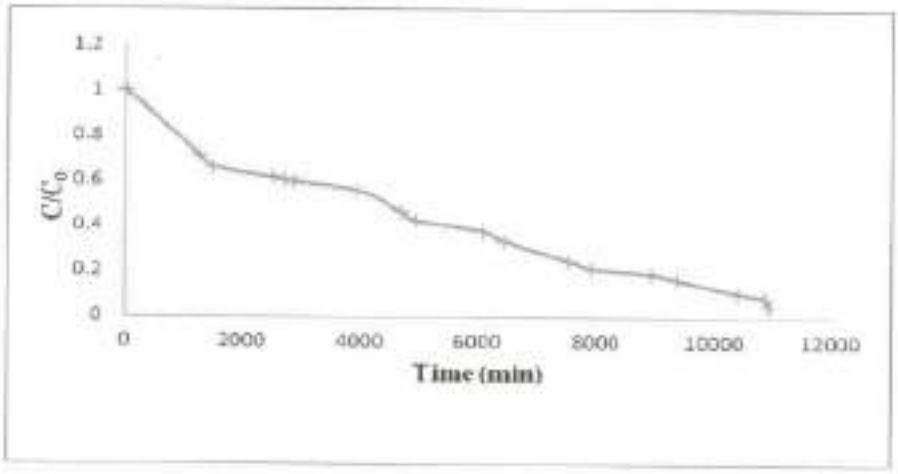

Figure 6.6 Single Well Dilution in L1 by NaCl

b. Trial 4

200 g of NaCl was diluted in the water sample from the study area and it was poured instantaneously in the borehole L6. The borehole L6 was monitored continuously until the background was obtained. The water samples are collected from the borehole L6 at different times. The EC of the water samples are measured in the laboratory. The details of the single well dilution in borehole L6 was shown in Table 6.4. By using the Equation 6.1 and 6.2 average filtration velocity was 0.04 m/day and permeability was 3.3 m/day.

Figure 6.7 shows the graph for C/C_0 versus t for single well dilution in L6 using NaCl as tracer explained in experiment 4. From the Figure 5.14 at $C/C_0 = 0.16$, t = 5672 min and $C/C_0 = 0.84$, t = 650 min. By using Equation 6.3 the dispersion co efficient estimated was 0.31 m^2/day and the dispersivity estimated was 10.6 m.

Table 6.4 Details of Single Well Dilution in L6 by NaCl

Date	Time at sample taken	Time 't'(min)	Concentration EC µs/cm	Filtration Velocity (m/day)
21-03-2011	11:28	0	5,320	-
21-03-2011	12:25	57	5,290	0.05
21-03-2011	12:53	85	5,250	0.05
21-03-2011	13:25	117	5,270	0.04
21-03-2011	13:55	147	5,240	0.04
22-03-2011	09:52	1344	4,200	0.04
22-03-2011	13:00	1532	4,120	0.04
22-03-2011	16:00	1712	4,080	0.03
23-03-2011	10:00	2792	3,700	0.03
23-03-2011	16:00	3152	3,420	0.03
24-03-2011	10:00	4232	2,820	0.03
24-03-2011	15:00	4532	2,510	0.03
25-03-2011	10:00	5672	2,100	0.03
25-03-2011	15:10	5982	1,950	0.03

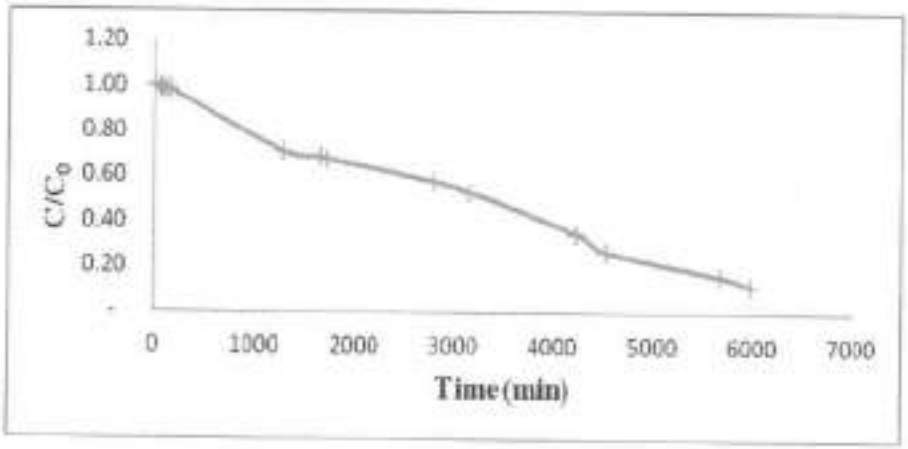

Figure 6.7 Single Well Dilution in L6 by NaCl

The groundwater tracers such as SRB and NaCl are used to estimate the observed velocity using the single well dilution technique. The

filtration velocity was estimated by using the Equation 6.1. The permeability was estimated by using the Equation 6.2, by using the hydraulic gradient 0.011. The details of the average filtration velocity and average dispersion coefficient obtained by the single well dilution technique were shown in Table 6.5.

Table 6.5 Estimated Filtration Velocity, Dispersivity and Dispersion Coefficient by Single Well Dilution Technique

Groundwater Tracer	Sulphorhodamine B	NaCl
Filtration Velocity m/day	0.05	0.04
Permeability m/day	4.76	3.82
Dispersivity in m	11.5	10.6
Dispersion coefficient m^2/day	0.45	0.31

6.4.2 Two well Dilution

Two well dilution was carried out by tow methods such as natural gradient and forced gradient method. NaCl was used as a chemical tracer to estimate dispersivity and dispersion coefficient

Experiment 3 Two Well Dilution by Natural Gradient

200 grams of NaCl was diluted in the water sample in the study area. The solution was poured in L6 and the bore well L6 and L7 was monitored. The distance between the bore wells was 30 m. The L7 was located downstream of L6. It was assumed that constant linear velocity for a uniform saturated groundwater flow field exists and that the tracer was

conservative. A break through curve was obtained in the L7 bore well. The tracer break through curve was shown in Figure 6.8. The detail of the break through curve was shown in Table 6.6. The time to peak in the break through curve was 4300 min and the time of first arrival was 1470 min.

Table 6.6 Details of Two Well Dilution Technique by Natural Gradient

Date	Time at sample taken	Time 't'(min)	Cl (mg/l)
19-03-2011	10:15	0	2,452
19-03-2011	12:33	138	2,460
19-03-2011	14:44	269	2,460
19-03-2011	15:37	322	2,460
19-03-2011	16:15	360	2,462
20-03-2011	10:45	1470	2,463
20-03-2011	12:52	1597	2,475
20-03-2011	15:58	1783	2,486
21-03-2011	11:53	2978	2,514
21-03-2011	12:20	3005	2,520
21-03-2011	12:56	3041	2,525
21-03-2011	13:28	3073	2,527
21-03-2011	13:58	3103	2,529
22-03-2011	09:55	4300	2,593
22-03-2011	15:55	4660	2,568
23-03-2011	10:00	5745	2,533
23-03-2011	15:00	6045	2,519

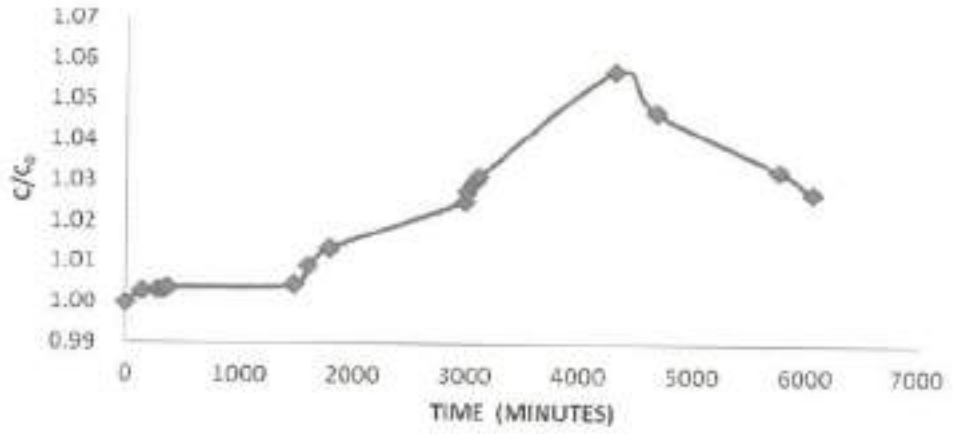

Figure 6.8 Two Well Dilution Technique by Natural Gradient

By using the Equation 4.8 and 4.10 the dispersion co efficient and dispersivity was calculated. The dispersion co efficient was 0.43 m^2/day and the longitudinal dispersivity was 13.5 m.

Experiment 4 Two Well Dilution By Forced Gradient

Borehole L5 was used as the source borehole whereas L4 was used as the abstraction borehole. Water was abstracted from L4 at a rate of 1.5 lpm for 2.5 hour (until a steady-state gradient existed between L4 and L5). The distance between the two bore wells was 9 m. 500 gram of NaCl was diluted in the water sample in the study area and it was poured in the source bore well L5. Bore well L4 was abstracted from the time t = 0. The tracer Break through curve was obtained and the peak was obtained at 120 minutes. The time of first arrival was at 50 minutes. The details of the Two well dilution at forced gradient was shown in Table 6.7. The Break through curve was shown in Figure 6.9.

Table 6.7 Details of Two Well Dilution Technique by Forced Gradient

Time in Minutes	Discharge Q (LPM)	Cl (mg/l)
0	0	2,227
2	5	2,227
5	12.5	2,227
10	25	2,243
20	50	2,269
40	100	2,385
50	125	4,121
60	150	4,780
80	200	7,003
100	250	8,499
120	300	9,002
130	325	8,320
140	350	6,996
150	375	5,152

By using the Equation 6.5 and 6.6 the dispersion co efficient and dispersivity were calculated. The dispersion co efficient was 0.61 m^2/day and the longitudinal dispersivity was 15.3 m.

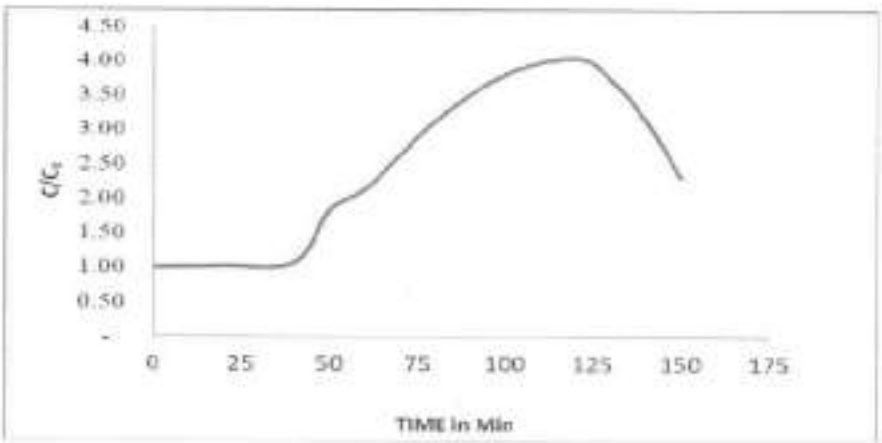

Figure 6.9 Two Well Dilution Technique by Forced Gradient

By analysing the tracer break through curve in two well dilution technique by natural gradient and forced gradient dispersion coefficient and dispersivity estimated was shown in Table 6.8.

Table 6.8 Estimation of Dispersivity and Dispersion Coefficient by Two Well Dilution Technique

Groundwater Tracer Break through	Natural Gradient	Forced Gradient
Velocity m/day	10.05	108
Dispersivity in m	13.55	15.31
Dispersion coefficient m^2/day	0.43	0.61

6.4.3 Permeability Estimation at Lab scale

The soil samples were collected from the command area and the permeability was estimated by falling hand permeameter, particle size distribution and pumping test.

(i) Falling Head Permeability Test

The diameter of the mould was 0.1 m and the length of the mould was 0.127 m. The soil samples collected from the study area was filled in the mould in three layers and compacted. The mould was connected with the falling head permeability apparatus as shown in Figure 5.8. The permeability estimated from the falling head permeability test was 3.45 m/day.

(ii) Particle Size Distribution

Particle size distribution study was carried out in the laboratory. The D_{10} size was obtained as 0.074 mm. Grading curve of aquifer was plotted

in Figure 5.9. The permeability estimated from the particle size distribution was **4.65 m/day.**

(iii) Pumping Test

The pumping test was performed in the wells located in the study area. It involved the measurement of the draw down with respect to time. From pumping test data the aquifer parameters were calculated.

As a result of pumping test data, the following aquifer parameters were obtained.

i) Permeability.

ii) Specific yield.

iii) Specific capacity.

6.4.4 Permeability

M. Kumaraswamy method is method used for estimating the permeability for large diameter wells located in hard rock area, unconfined aquifer of the study area. M. Kumaraswamy mathematical equation defining the inflow into a well in hard rock areas to determine permeability is,

$$w = \frac{\frac{a}{D}\ln\sqrt{\frac{1+d_2/D}{1-d_2/D}} - \ln\sqrt{\frac{1+d_1/D}{1-d_1/D}}}{t_R}$$

Where,

W = Hard Rock Permeability(m/day)

a = Cross Sectional Area(m^2).

D = Static Water Column(m)

d_1 = Water Column when pumping stopped.(m)

d_2 = Water Column at t_R minutes(m)

t_R = Time Taken For Recuperation (min)

6.4.5 Specific Capacity

A formula of Slichter has been used to determine the specific capacity based on the recovery performance of the dug wells. Slichter's formula is expressed as a linear function of time and a logarithmic function of drawdown. The formula given by Slichter to determine specific capacity is,

$$C' = 2.303 \frac{A}{t'} log_{10} \frac{S1}{S2} .(m^2/hr)$$

C' - specific capacity(m^2/min)

A - cross sectional area of the well (m^2).

t' - time after pumping stops (hr).

S1 - drawdown at time pumping stops (m).

S2 - water level to be recuperated.(m)

6.4.6 Specific Yield

The formula given by Slichter to determine specific yield is,

$$C = 2.303 \frac{A}{t'} log_{10} \frac{S1}{S2}$$

C - specific yield

A - cross sectional area of the well (m^2).

t' - time after pumping stops (hr).

S1 - drawdown at time pumping stops (m).

S2 - water level to be recuperated.(m)

6.4.7 Aquifer Parameter Estimation

In the command area six wells were selected for pumping test to determine the permeability, specific yield and specific capacity. The principle behind the pumping test is to pump the water from the well at constant discharge and the drawdown in the well has to be measured. The recovery is also measured after the pumping is stopped. These measured data were substituted in an appropriate equation to calculate the hydraulic characteristics of an aquifer .

Before carrying out pumping test preliminary studies are carried out by electrical resistivity survey, secondary data which involves the geological formation of the subsurface type and thickness of the aquifer zones. The pumping test were carried out in the well 5, well 6, well 13, well 14, well 16, well 17.

Diameter of the well = 7m.

Area of cross section of the well(A)= $38.4 m^2$

Duration of pumping = 348 minutes.

Drawdown in the well when pumping stopped(S1)= 2.81 m.

Duration of recovery test(t) = 120 minutes=2 hr

Residual draw down at time 't' when pumping stops=1.38 m.

Water level to be Recuperated(S2)= 1.5m.

Specific Capacity

The formula given by Slichter to determine specific capacity is,

$$c' = 2.303 \frac{A}{t'} log_{10} \frac{S1}{S2}$$

$$c' = 2.303 \frac{38.465}{2} log_{10} \frac{2.8}{1.5}$$

$$= 12.06(m^2/hr)$$

Specific Yield

The formula given by Slichter to determine specific yield is,

$$c = \frac{2.303}{t'} \log_{10} \frac{S1}{S2}$$

$$c = \frac{2.303}{2} \log_{10} \frac{2.8}{1.5}$$

$=0.31 m^3/hr/m^2/$per metre drawdown.

Permeability

Diameter of the well=7m.

Cross sectional area of the well(a)=38.4 m^2.

Static water column(D)= 7m.

Water column when pumping stopped(d_1)=4.1 m.

Water column at t_R minutes(d_2)=5.5 m

Time taken for recuperation = 120min.

$$w = \frac{38.4}{7} \frac{\ln\sqrt{\frac{1+5.5/7}{1-5.5/7}} - \ln\sqrt{\frac{1+4.1/7}{1-4.1/7}}}{120}$$

= 26.18 m/day.

During pumping test in well 16, two near by wells were pumped. While the pumping test were carried out in the other wells . the pumping in the near by wells may influence the pumped well. This may be the reason for the increase in the Hydraulic conductivity of the pumped well.

Table 6.9 Aquifer Parameters Calculated Through Pumping Test

	Well 13	Well 14	Well 17	Well 5	Well 16	Well 6
Diameter of the well(m)	7	9	9	8	7	8
Area of cross section of the well(m^2)	38.4	63.5	63.5	50.2	38.4	50.2
Duration of pumping(min)	451	190	418	260	348	220
Drawdown in the well(m)	3.3	1.8	2.9	2.1	2.8	1.7
Duration of recovery test(min)	152	120	120	130	120	120
Water level Recuperated at t,min(m)	1.6	0.5	0.9	0.7	1.3	1.0
Water column when pumping stops (m)	4.6	5.1	4.6	4.8	4.1	5.2
Water column Recuperated at t,min(m)	6.37	5.6	5.6	5.5	5.5	5.9
Specific capacity(m^2/hr)	10.05	10.33	11.79	9.39	12.06	22.27
Specific yield	26 %	16 %	18 %	18 %	31 %	44 %
Hydraulic conductivity (m/day)	4.64	4.89	5.82	4.61	6.55	5.7

In well 6 it is observed that the specific yield and specific capacity is high. It is inferred that the well 6 is located in the highly weathered or fractured zone obtained through pumping test is higher than the Hydraulic conductivity of weathered rock. This may be attributed by the presence of fractured zone below the weathered zone might have contributed some portion of water to wells from the second layer.

SUMMARY

The hydraulic conductivity estimated by the three methods shown in Table 6.10 were in the same range of 3.5 to 5.5 m/day. Hydraulic conductivity given by the public works department was in the range of 0.5 to 2.5 m/day. Average specific capacity and specific yield of the aquifer are 12.7 m^3 per hour per unit draw down and 26 percent.

Hydraulic conductivity is a quantitative measure of a saturated soils ability to transmit water where subjected to a hydraulic gradient. It is the property of the soil with which the pores of a saturated soil permit water movement. Hydraulic conductivity is an important property because it is used to calculate the flux in a groundwater aquifer for any hydraulic gradient.

Table 6.10 Hydraulic conductivity Estimated by conventional Methods

Method	Hydraulic Conductivity m/day
Well Dilutions Method	3.82 to 4.76
Permeameter test	3.45
Particle size distribution	4.65
Pumping test	4.6 to 6.5
Public Works Department Report	0.5 to 2.5

CHAPTER - 7

ESTIMATION OF TANK AND AQUIFER INTERACTION THROUGH GEOELECTRICAL STUDIES

7.1 GENERAL

Geophysics has reached a place of vital importance to the scientific development and protection of the world's precious, groundwater supply, this method provide rapid and effective techniques for groundwater exploration and aquifer interaction. The resistivity of the material depends on many factors such as groundwater quality, saturation, aquifer lithology and porosity. This technique is widely used to determine depth, boundaries and location of an Major limitation aquifer, when ground in of this method is when subsurface formation exist with homogeneities and anisotropy. Although various geophysical techniques are being applied to explore groundwater resources, the electrical resistivity method proves the most powerful and cost affective. This chapter aims to know the interaction between tank and the groundwater aquifer of the command area as shown in the flow chart

Objectives of this chapter are

1. To evaluate tank and surrounding aquifer charactersistics;
2. To establish relationship between geo-electric parameters and aquifer properties;
3. To evaluate tank and aquifer interaction;

Above said objectives were attained through following steps

i. Resistivity Survey to measure aquifer resistivities in the command area;
ii. Establishment of relationship between geo-electric and aquifer hydraulic parameters;
iii. Collection and analysis of water samples;

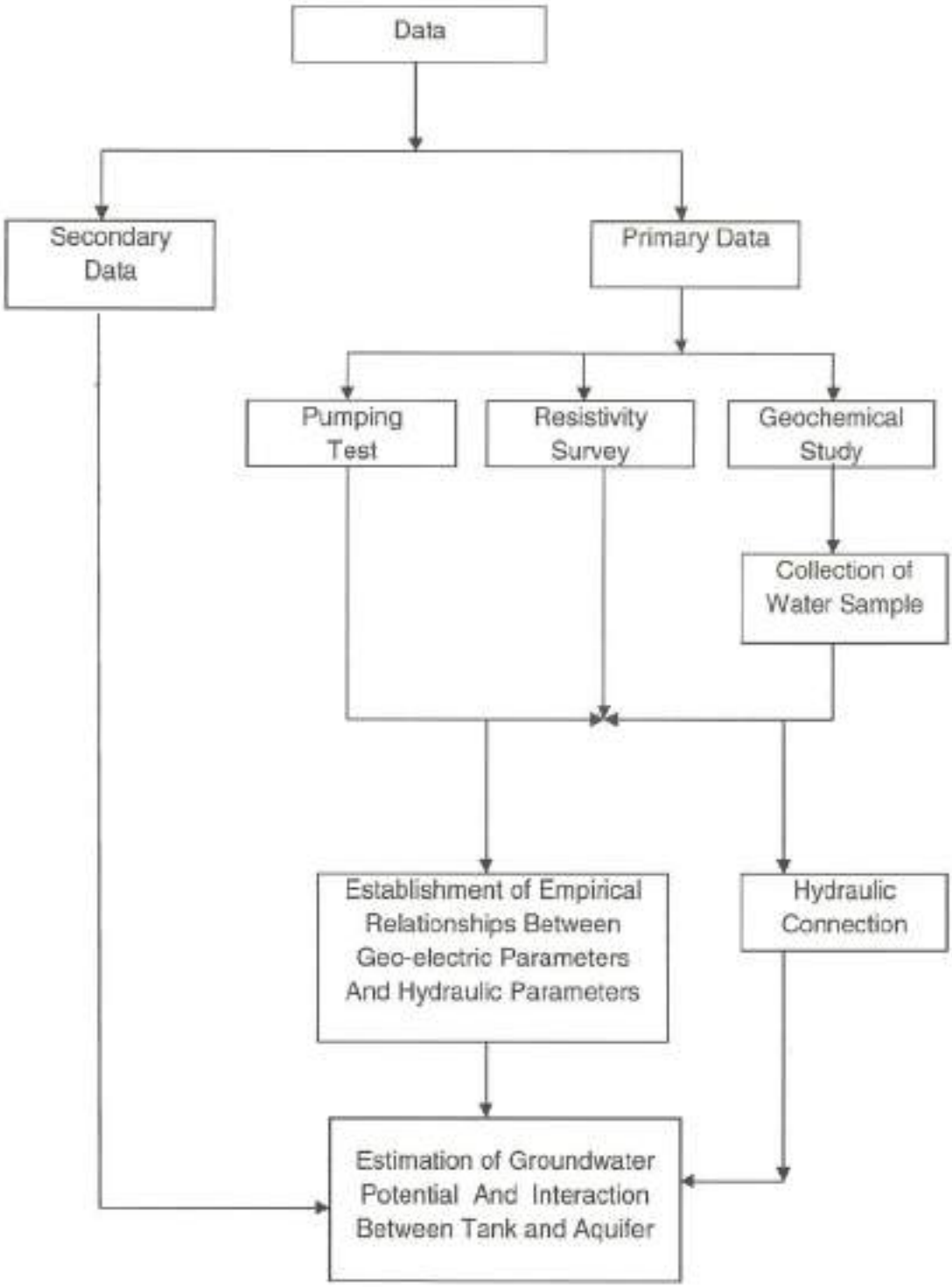

Flow chart for Tank and Aquifer Interaction

7.2 RESISTIVITY MEASUREMENTS

The apparent resistivity values are measured and true resistivity transverse resistance, longitudinal unit conductance are calculated as explained below,

7.2.1 Apparent Resistivity

The apparent resistivity for a measured resistance is given by,

$$\rho_a = \pi \frac{(L/2)^2-(b/2)^2}{b} R, \quad L >> b$$

$$\rho_a = \frac{\pi L^2}{4b} R, \quad \text{if} \quad L > 5b$$

7.2.2 True Resistivity

The apparent resistivity value is interpreted to obtain the true resistivity of the sub-surface layers by the inverse slope method. The linear plot is done between (AB/2) on X-axis and [(AB/2)/ρa] on Y-axis. Then the plotted point is joined with the best fitting straight line segments. Each segment represents one subsurface layer. The Inverse Slope of each line segment directly gives the true resistivity of the subsurface layer. The intersections of the line segments is multiplied with (2/3) to get the depths to the interfaces.

7.2.3 Longitudinal Unit Conductance

It is the ratio between the thickness of the aquifer (m) and the resistivity of the aquifer (ρ).

$$S=h/\rho$$

7.2.4 Transverse Resistance

It is the product of the thickness of the aquifer (m) and the resistivity of the aquifer(p)

$TR = h/\rho$

7.2.5 Formation Factor

It is calculated using the aquifer resistivity(ρ) and the water resistivity of the formation($\rho\omega$) using the Archies law(Archie,1942)

$FF = \rho / \rho_\omega$ ρ_ω = resistivity of water.

The water resistivity will be calculated using the following equation.

ρ_ω = 10000/ electrical conductivity of water.

The aquifer hydraulic parameters hydraulic conductivity, transmisivity are estimated from resistivity measurements as explained below,

7.3 Geoelectric Parameters Estimations

The geophysical investigation employed in this study was electrical resistivity survey. This study used ABEM resistivity meter SAS 1000 using the inverse slope method true resistivity values were obtained. The true resistivity values were used to interpret the lithology of the subsurface formation with the support of litholog information which was collected from institute for water studies, Public Work Department (PWD),

7.3.1 Electrical Resistivity Survey

The electrical resistivity method adopted in this study was Schlumberger array. In this Schlumberger array four electrodes (C_1, C_2, P_1, P_2) were placed along a straight line symmetrically over centre point. C_1 and C_2 are the current electrodes. P_1 and P_2 are the potential electrodes. The separation between potential electrodes was kept small when compared to the current electrode separation. In this study the maximum current electrode spacing kept over a point O is 100m and the maximum potential electrode spacing kept over a point is 20m. The corresponding current and potential electrode spacing followed in this study is presented in the Table 7.1.

Table 7.1 Corresponding Potential and Current Electrode Spacing

Potential electrode spacing over a point 'O'	Current electrode spacing over a point 'O'
0.5m	1.5m-10m
2m	10m-50m
5m	50m-100m
10m	100m

7.3.2 Inverse Slope Method

The Schlumberger sounding apparent resistivity values were interpreted using the inverse slope method to get the true resistivity values of the sub surface layers. The linear plot was drawn between (AB/2) on X-axis and $\{(AB/2)/\rho_a\}$ on Y-axis. Then the plotted point is joined with the best fitting straight line segments. Each segment represents one subsurface layer. The Inverse Slope of each line segment directly gives the true resistivity of the subsurface layer. The intersections of the line segments is multiplied with

(2/3) to get the depths to the interfaces. while interpreting the apparent resistivity values, negative slopes are encountered near by the locations tank bund 2 and inside the tank 2. The apparent resistivity values were interpreted by the inverse slope method that is presented through following figures 7.1 to 7.17.

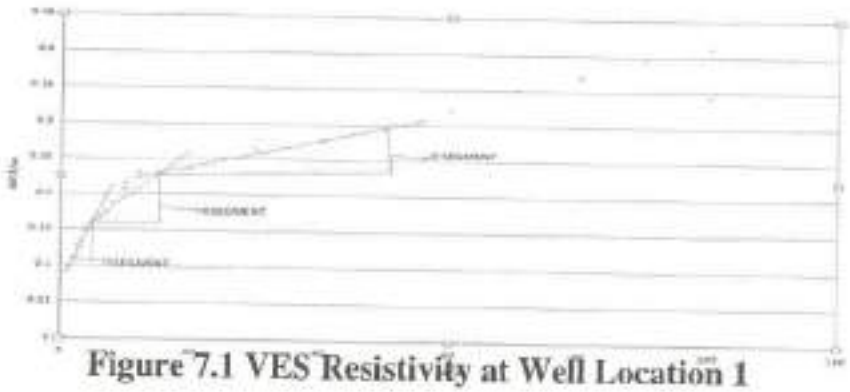

Figure 7.1 VES Resistivity at Well Location 1

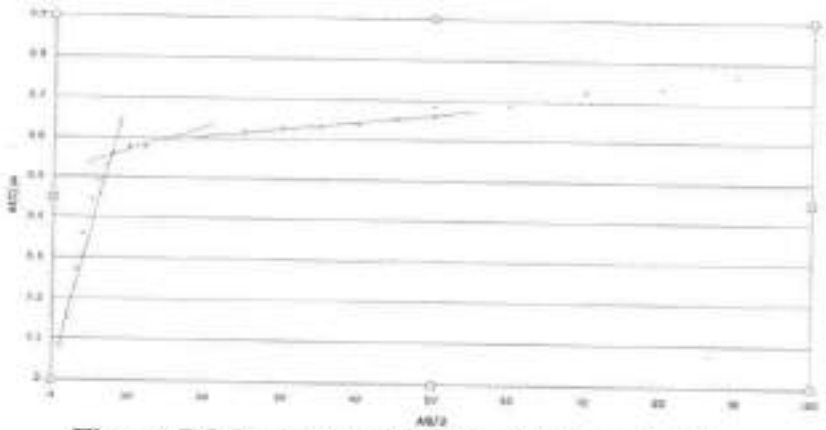

Figure 7.2 VES Resistivity at well location 2

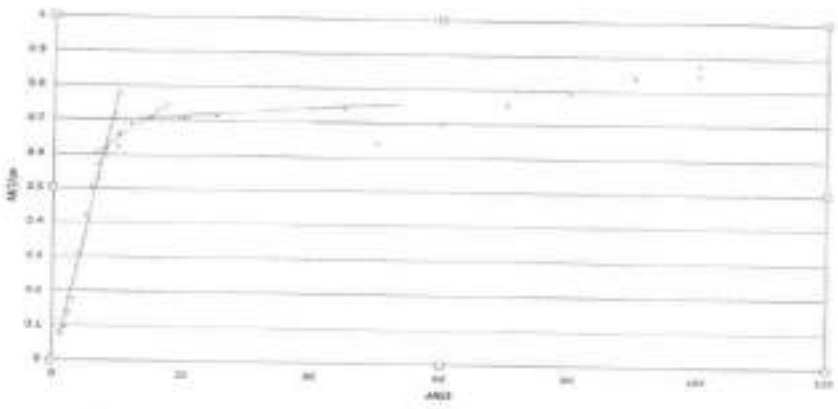

Figure 7.3 VES Resistivity at Well Location 5

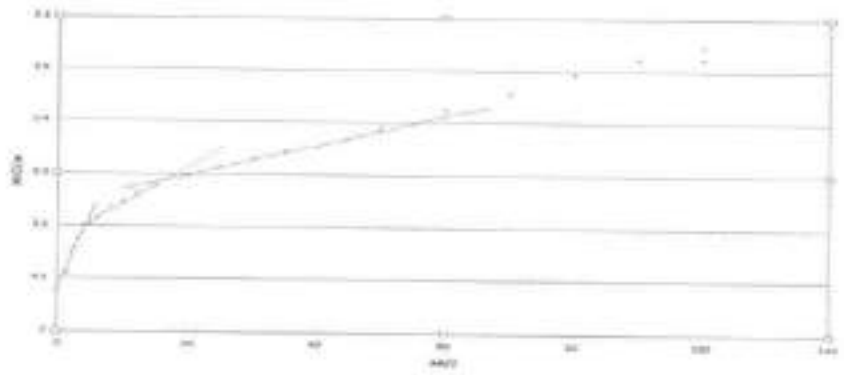

Figure 7.4 VES Resistivity at Well Location 6

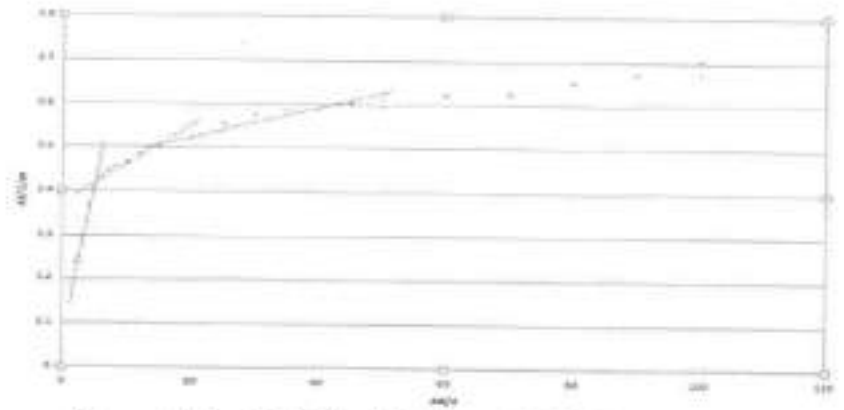

Figure 7.5 VES Resistivity at Well Location 8

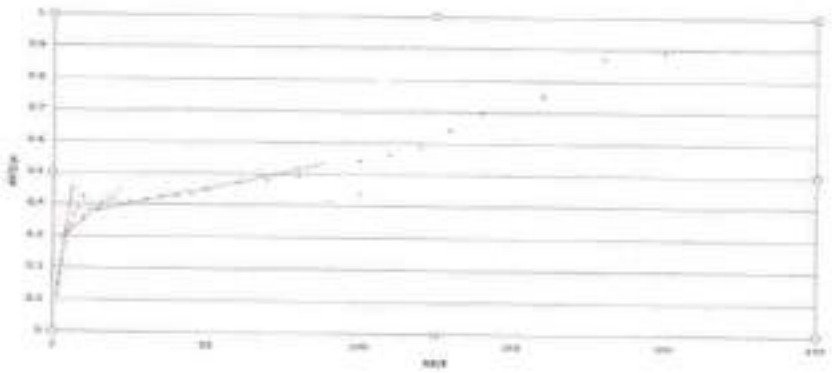

Figure 7.6 VES Resistivity at Well Location 9

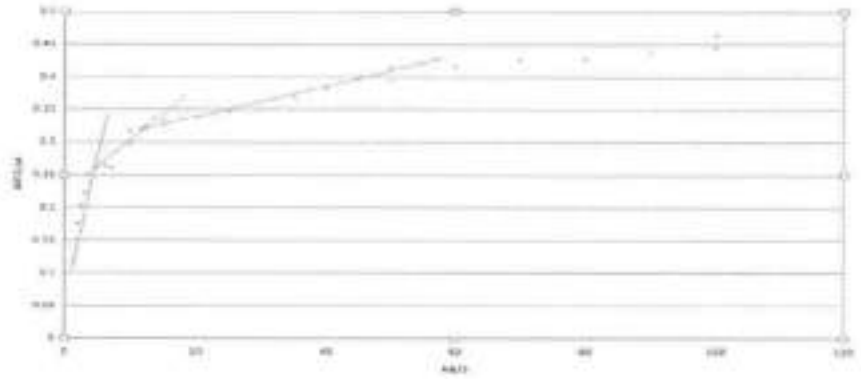

Figure 7.8 VES Resistivity at Well Location 10

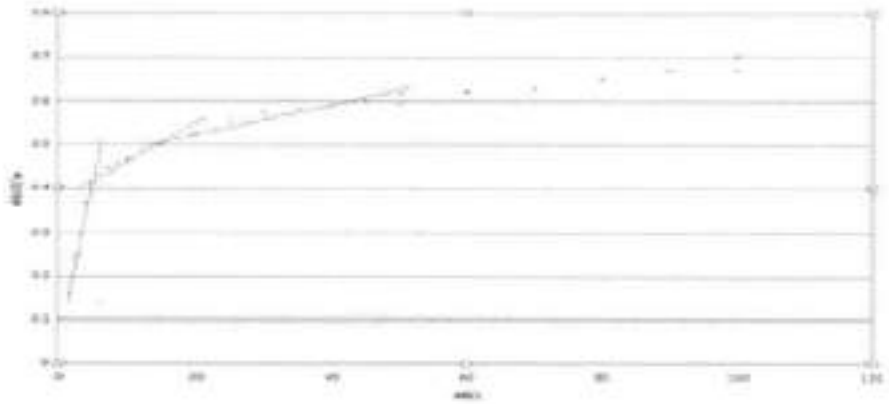

Figure 7.9 VES Resistivity at Well Location 12

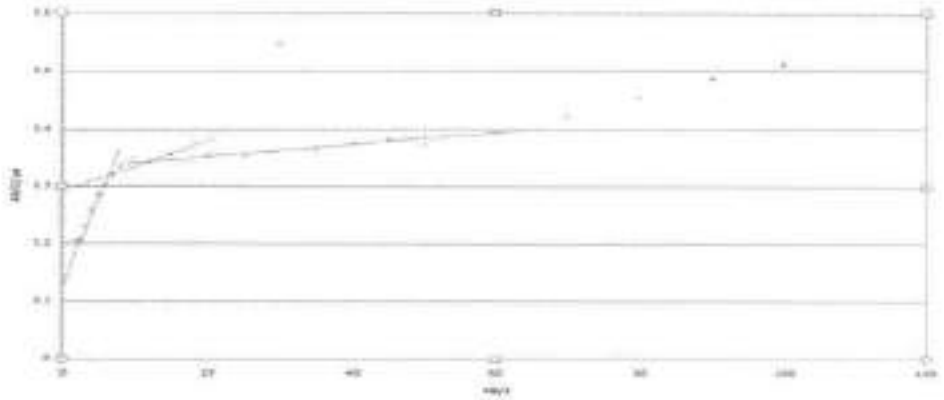

Figure 7.10 VES Resistivity at Well Location 13

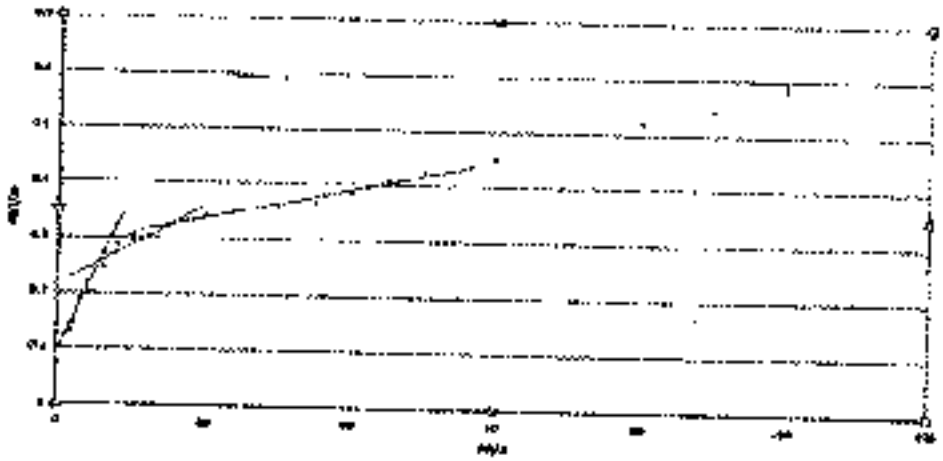

Figure 7.11 VES Resistivity at Well Location 14

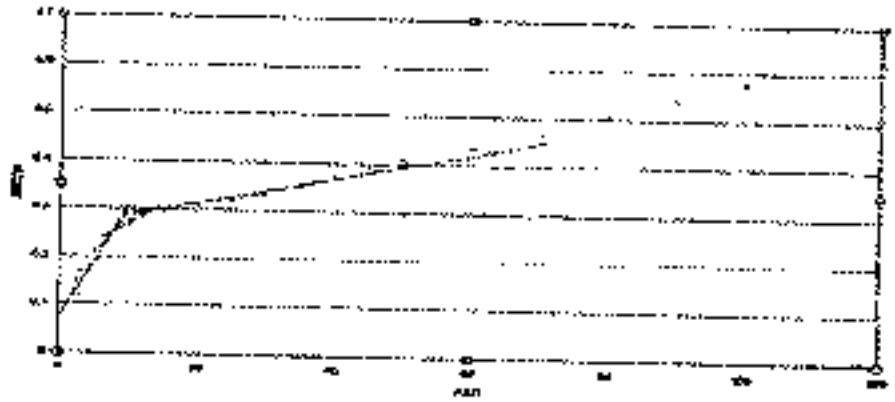

Figure 7.12 VES Resistivity at Well Location 17

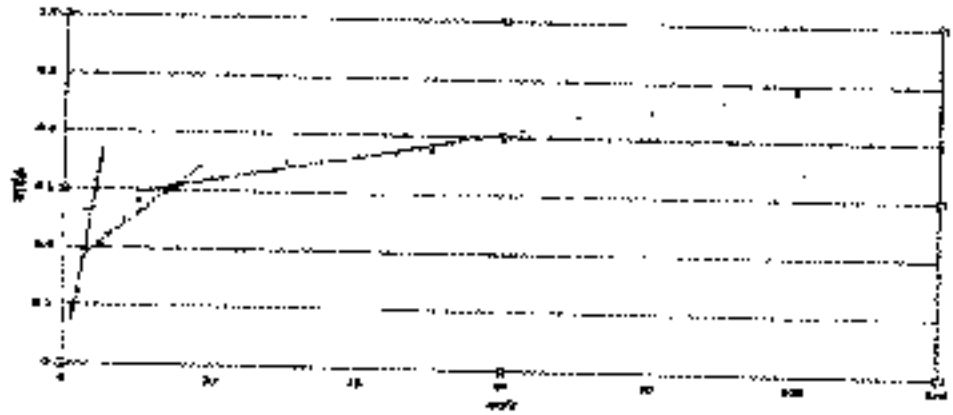

Figure 7.13 VES Resistivity at Well Location Near tank bund 1

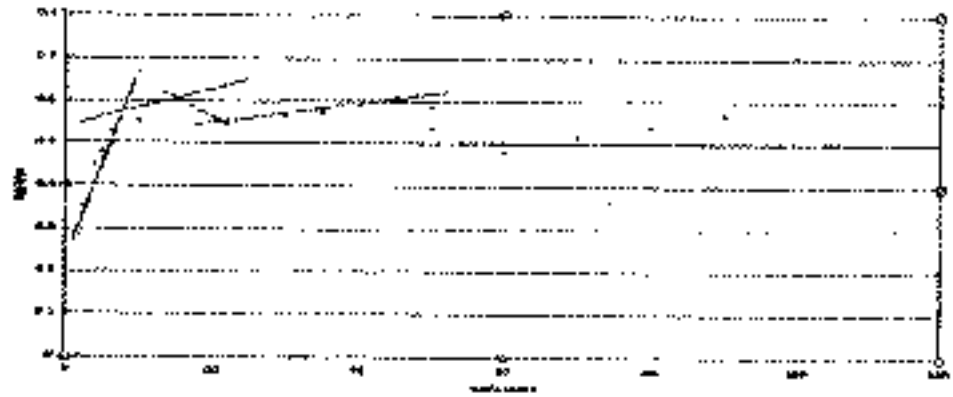

Figure 7.14 VES Resistivity at Well Location Near Tank Bund 2

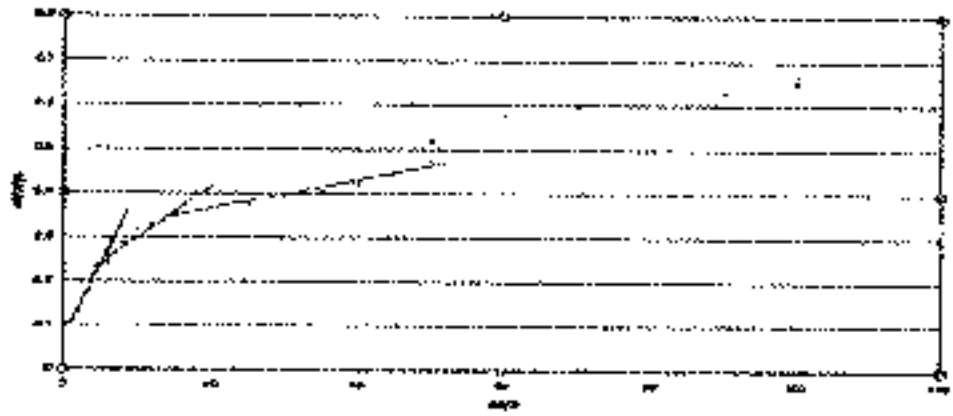

Figure 7.15 VES Resistivity at well Location Near Tank Bund 3

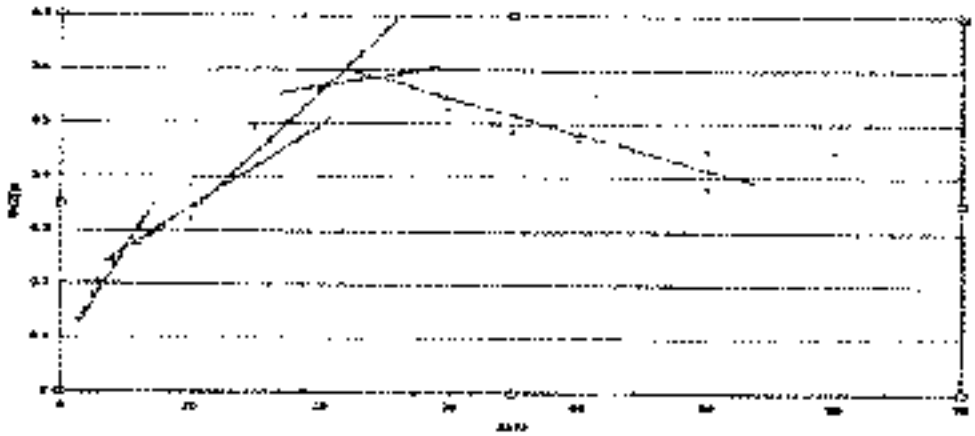

Figure 7.16 VES Resistivity at Location Inside The Tank 1

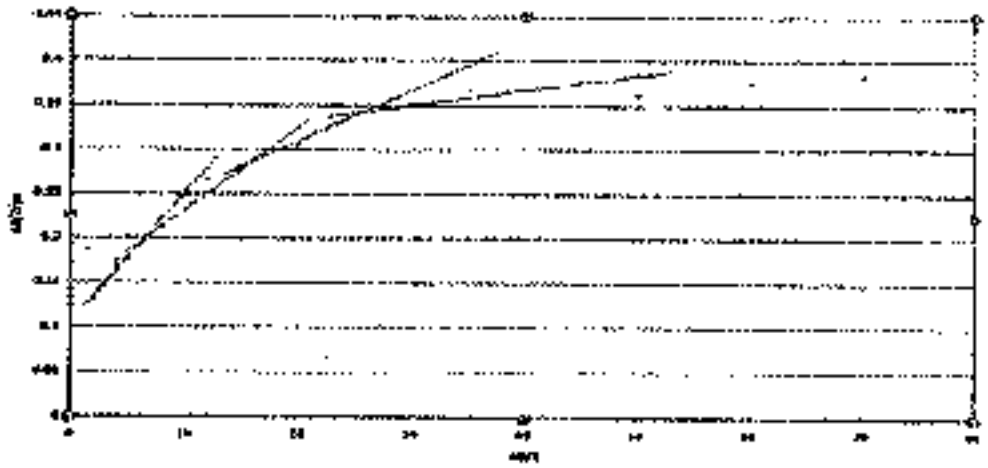

Figure 7.17 VES Resistivity at Location Inside the Tank 2

The instrument is traversed over a certain distance in the well station 1. When the potential electrode spacing i.e.,(AB/2) is kept at a distance, then the depth of penetration is generally taken as one third of AB. Similarly the AB/2 distance varies and also the depth of penetration also varies. From the inverse slope method , following true resistivity values are obtained for three layers in the well station 1. Similarly it is also obtained for various other VES locations in the study area.

7.3.3 Model Calculation for Calculating True Resistivity for Well 1

The inverse slope method adopted at the well location 1is calculated as follows,

I segment = $\frac{1}{\frac{\Delta V}{\Delta x}} = \frac{1}{\frac{0.000388}{2.5}} = 57.0$ ohm-m.

II segment = $\frac{1}{\frac{\Delta V}{\Delta x}} = \frac{1}{\frac{0.004968}{10}} = 144.8$ ohm-m.

III segment = $\frac{1}{\frac{\Delta V}{\Delta x}} = \frac{1}{\frac{0.000369}{2.035}} = 542.2$ ohm-m.

The results indicates that three layers of formation exist which was found through inverse slope method. The resistivities and depth to interfaces of three layers are 57.1, 144.7, and 542.6 ohm. m and 3..3, 6.7, and 23.3m respectively. Total depth of the weathered zone is almost 30 to 30m except at two locations well 9, well 13. It can be seen from the inverse slope graph that there is no ambiguity in joining the points that is evident in the figures 7.1 to figure 7.17. It is noted that the negative slope in the point of tank bund 2 and inside tank 1. It may be due to the inhomogeneties in the subsurface layers. The above mentioned procedure is followed for other well locations and that are given in table 7.2.

Table 7.2 Summary Of True Resistivity Values And Layer Thickness

Location	Layer resistivity 'ρ' in ohm-m				Layer thickness 'h' in ohm-m				Bed Rock depth (m)
	ρ_1	ρ_2	ρ_3	ρ_4	h1	h2	h3	h4	H
Well 1	57.0	144.7	542.6	---	3.3	6.67	23.3	---	33.3
Well 2	14.8	187.6	588.2	---	5.3	4.67	23.3	---	33.3
Well 5	12.1	74.5	730.9	---	5.3	4.67	23.3	---	33.3
Well 6	29.0	139.7	322.9	---	2.6	7.34	23.3	---	33.3
Well 8	53.3	91.9	248.1	---	4.6	5.34	16.6	---	26.6
Well 9	20.3	162.9	538.9	---	4.0	6.0	30.0	---	40.0
Well 10	24.3	115.1	418.9	---	3.3	4.6	25.3	---	33.3
Well 12	14.3	108.5	299.6	---	3.3	6.6	23.3	---	33.3
Well 13	34.1	171.4	1213.9	---	4.0	6.0	30.0	---	40.0
Well 14	33.9	104.3	306.6	---	3.3	6.6	23.3	---	33.3
Well 16	40.3	102.2	290.6	---	5.3	8.0	20.0	---	33.3
Well 17	43.3	126.9	308.9	---	5.3	2.6	25.3	---	33.3
Tank bund 1	14.8	97.1	475.4	---	2.6	7.3	20.0	---	30.0
Tank bund 2	22.8	163.3	Negative slope	382.3	5.3	4.6	---	16.67	30.0
Tank bund 3	31.3	83.4	322.9	---	3.3	6.6	20.0	---	30.0
Inside tank 1	26.1	61.5	42.99	220.6	3.3	4.6	5.3	3.33	16.6
Inside tank 2	66.2	101.0	172.1	565.5	4.0	5.0	7.6	16.67	33.3

7.3.4 Geo Electrical sections along AA' , BB' and CC'

Geo-electrical sections from north to south were carried out as shown in figure 7.18. This helps to conceptualize the aquifer formation in the study area. Geo electrical sections along AA' ,BB' and CC' are shown in figures 7.19 to 7.21 respectively.

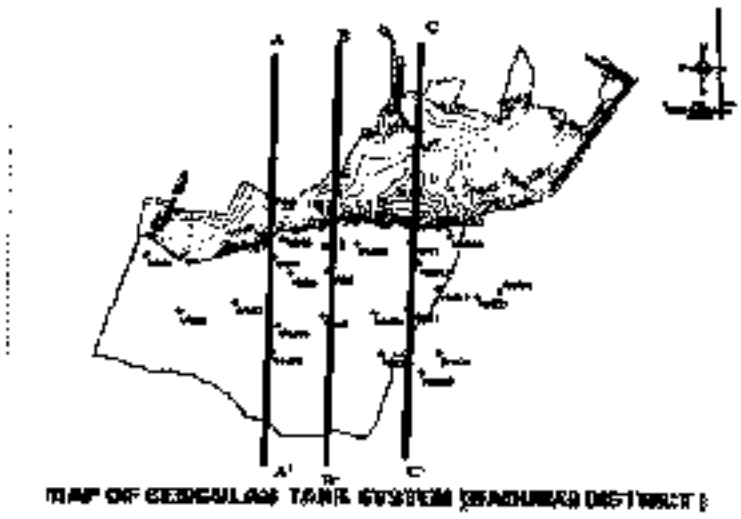

Fig 7.18 Wells lies along the straight line

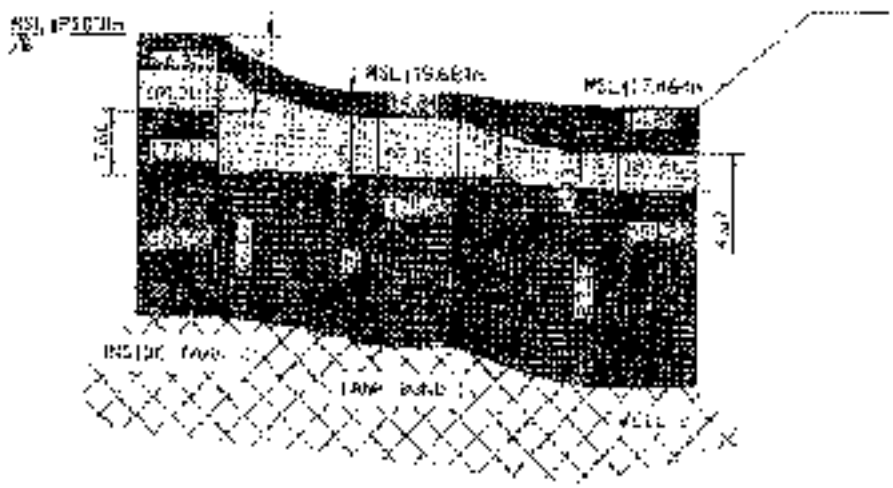

Figure 7.19 Cross Sectional View Along The Line AA'

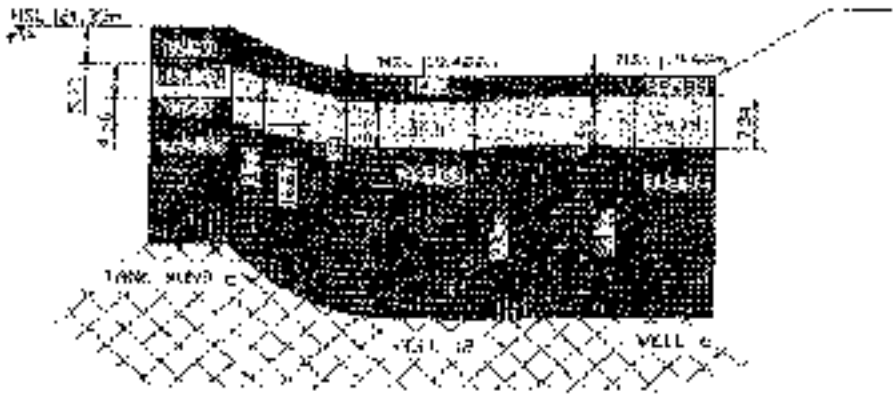

Figure 7.20 Cross Sectional View Along The Line BB'

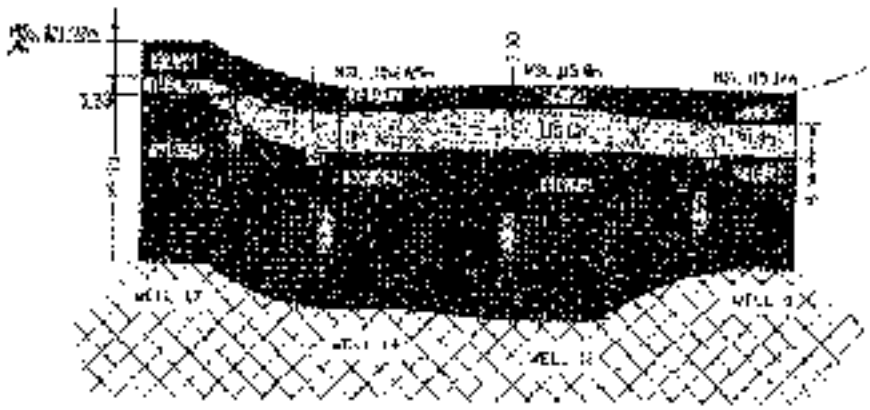

Figure 7.21 Cross Sectional View Along The Line CC'

The resistivities of different subsurface layers in the study area are encountered during investigation that are interpreted as follows,

Top soil< 65 ohm.m

Highly and semi-weathered granitic genesis- 70-180 ohm.m

Fractured and jointed granitic genesis-180-500 ohm.m

Hard massive bed rock> 500 ohm.m

The second layer and third layer is identified as the accumulation of groundwater. The open wells are constructed in second layer and the third

layer. The results obtained through the pumping test were found to be similar to the data obtained from the Institute of Water Studies.

7.3.5 Geo-electrical Parameters Estimation

The fundamental parameters to describe a geo-electric section are its true resistivity (ρ) and its thickness (h). In multilayered cases, the individual resistivities and the thickness of the layers are represented by ρ_1, ρ_2, ρ_3 and h_1, h_2 and h_3 respectively. From these fundamental parameters, other secondary geo-electric parameters namely longitudinal conductance(S), transverse resistance(TR) and anisotropy are obtained.

(a) Longitudinal Conductance(S).

It is the ratio of the resistivity values and thickness of the respective layers.

$$S_1 = \frac{h_1}{\rho_1}; S_2 = \frac{h_2}{\rho_2}; S_3 = \frac{h_3}{\rho_3}.$$

$$S_1 = \frac{2.32}{57.096} = 0.0583 \text{(Siemens)}$$

$$S_2 = \frac{6.67}{144.71} = 0.0460 \text{(Siemens)}$$

$$S_3 = \frac{23.23}{542.60} = 0.0429 \text{(Siemens)}$$

The total longitudinal conductance is,

$$S = S_1 + S_2 + S_3.$$

$$S = 0.0583 + 0.0460 + 0.0429 = 0.1472 \text{(Siemens)}$$

(b) Transverse Resistance(*TR*)

It is the product of the resistivity values and thickness of the aquifers.

$TR1 = h_1\rho_1$; $TR2 = h_2\rho_2$; $TR3 = h_3\rho_3$;

$TR1$=3.33*57.096=190.12 ohm.m^2

$TR2$ =10*144.71=965.21 ohm.m^2

$TR3$=23.33*0.0429=12658.885 ohm.m^2

The total transverse resistance is,

$TR = TR1 + TR2 + TR3$

TR =190.12+965.21+12658.885= 13814.25(ohm.m^2)

(c) Formation Factor

FF=$\rho/\rho\omega$

$\rho\omega$= resistivity of water.

$\rho\omega$ = 10000/ electrical conductivity of water.

ρ=687.31 ohm.m

Electrical conductivity of water= 1310 µs/cm.

$\rho\omega$ = 10000/1310

Formation factor for well 1 = 687.31/7.6355 = 90.01(no.unit)

For the calculation of formation factor the second and third layers are considered to get the aquifer resistivity. The summary of longitudinal conductance, transverse resistance for all the three layers is presented below the table 7.3 and table 7.4 respectively.

Table 7.3 Summary of Longitudinal Conductance

SL. NO.	Wells	Longitudinal Conductance(S)(siemens)				
		Layer 1	Layer 2	Layer 3	Layer 4	Total
1	Well 1	0.0583	0.0460	0.0429	----	0.1472
2	Well 2	0.3581	0.0248	0.0396	----	0.4225
3	Well 5	0.437	0.0626	0.0319	----	0.5315
4	Well 6	0.0914	0.0525	0.0722	----	0.2161
5	Well 8	0.0873	0.0580	0.0671	----	0.2124
6	Well 9	0.1961	0.0368	0.0556	----	0.28851
7	Well 10	0.1367	0 040	0.0604	——	0 2371
8	Well 12	0.2328	0.0614	0.0778	----	0.372
9	Well 13	0.1171	0.0349	0.0247	----	0.1767
10	Well 14	0.0986	0.0639	0.0760	——	0.2791
11	Well 16	0.1321	0.0782	0.0688	——	0.2791
12	Well 17	0.1229	0.0210	0.0819	——	0.2258
13	Tank Bund 1	0 1792	0.0755	0.0420	----	0.2967
14	Tank Bund 2	0.2339	0.0285	0.0397	0.0435	0.3456
15	Tank Bund 3	0.1060	0.0799	0.0619	——	0.2478
16	Inside Tank 1	0.1273	0.0785	0.1239	0.0150	0.34471
17	Inside Tank 2	0.0604	0.0495	0.0445	0.0294	0.1838

Table 7.4 Summary of Transverse Resistance

Sl. No.	Wells	Transverse Resistance ($ohm.m^2$)				
		Layer 1	Layer 2	Layer 3	Layer 4	Total
1	well 1	190.1	965.2	12658.8	----	13814.2
2	well 2	79.3	876.3	19605.7	----	20561.3
3	well 5	64.9	348.1	17053.9	----	17467.1
4	well 6	77.3	1025.7	7533.7	----	8636.8
5	well 8	248.1	491.0	4133.3	----	4872.8
6	well 9	81.5	977.9	16169.5	----	17229.0
7	Well10	81.0	921.0	13963.9	----	14966.0
8	Well 12	47.6	724.1	6991.7	----	7763.5
9	Well 13	136.5	1028.7	36417.3	----	37582.5
10	Well 14	113.0	695.8	7155.0	----	7963.9
11	Well 16	215.0	817.6	5813.8	----	6846.4
12	Well 17	231.1	339.0	7825.4	----	8395.5
13	Tank bund 1	39.4	713.3	9508.6	----	10261.3
14	Tank bund 2	121.5	763.9	278.6	6373.7	7537.8
15	Tank bund 3	104.5	556.2	6458.4	----	7119.2
16	Inside tank 1	87.1	287.3	229.1	734.7	1338.3
17	Inside tank 2	264.9	505.0	1318.4	9427.9	11516.2

It is noted that the longitudinal conductance is seems to be unique through out the study area. High longitudinal conductance values are noted in well 5, and well 2. The transverse resistance is not unique throughout the study area and it varies widely. High transverse resistance is noted in well 2,

well 5, well 9 and well 13. The formation factor which is obtained from water resistivity is presented in Table 7.5.

Table 7.5. Summary of Formation Factor for Wells

Well Name	Electrical Conductivity(μs/cm)	Water Resistivity(ohm.m)	Formation Factor
Well 1	1310	7.6	90.0
Well 2	1800	5.5	139.6
Well 5	2140	4.6	172.3
Well 6	1900	5.2	87.9
Well 8	1390	7.1	47.2
Well 9	1750	5.7	122.8
Well 10	1690	5.9	90.2
Well 12	1450	6.8	59.1
Well 13	2120	4.7	293.6
Well 14	2250	4.4	92.4
Well 16	1890	5.2	74.2
Well 17	1270	7.8	55.3

The formation factor is noted to be high in well 2, well 5, well 9 and well 13 where transverse resistance is also found to be high in this wells.

7.4 ESTABLISHMENT OF EMPIRICAL RELATIONSHIP BETWEEN RESISTIVITY PARAMETERS AND AQUIFER HYDRAULIC PARAMETERS

Step-1 The relationship was established between the formation factor and Hydraulic conductivity ;

Step-2 The relationship was established between the aquifer resistivity and Hydraulic conductivity ;

Step-3 with these relationships, aquifer parameters at unknown location was deduced. Then these parameters were validated;

Pumping tests were carried out in six wells which were used for establishing the empirical relationship.

7.4.1 Relationship between Geo-electric parameters and Aquifer parameters

In the study area the relationship is established between geo-electric parameters and aquifer parameters. The pumping tests have been carried out for 6 wells in the study area. The relationship between geo-electric and aquifer parameters are established for 5 well data and 1 well data are utilized for validation purpose. With this relationship if the resistivity values of the area are known then the aquifer parameters can be obtained.

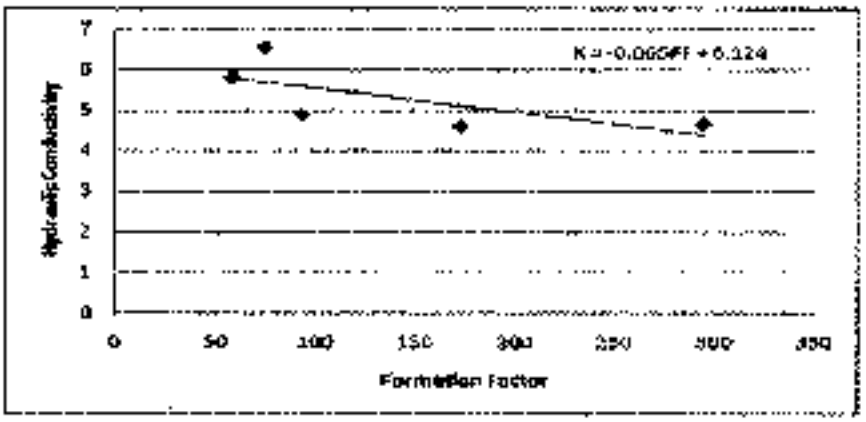

Figure 7.21 Relationship Between Formation Factor and Hydraulic conductivity

Validation

Observed Hydraulic conductivity for well 6 through pumping test = 5.73 m/day.

Calculated Hydraulic conductivity for well 6 from the linear relationship obtained = 5.23 m/day.

The observed Hydraulic conductivity and the calculated Hydraulic conductivity are found to be identical.

7.4.2 Relationship between Apparent Resistivity and Hydraulic Conductivity

Similarly the relationship is also established between the apparent resistivity(ρ) and Hydraulic conductivity (K). Well 16 data is used for the validation purpose. The empirical relationship between formation factor and Hydraulic conductivity is shown in the figure 7.22

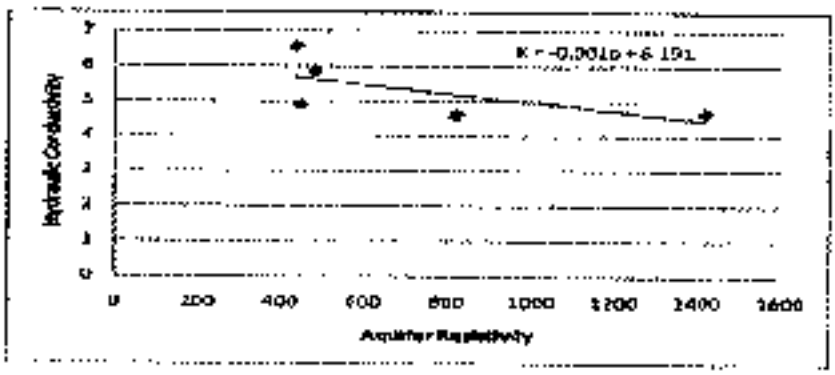

Figure 7.22 Relationship Between Resistivity and Hydraulic conductivity

Validation

Observed Hydraulic conductivity for well 16 through pumping test = 5.723 m/day.

Calculated Hydraulic conductivity for well 16 from the linear relationship obtained = 5.69924 m/day.

The observed Hydraulic conductivity through pumping test and the calculated Hydraulic conductivity from the linear relationship are found to be identical.

7.5 Geochemical Analysis

Water samples were collected from the tank and the wells every month and analysed for hardness, TDS, Calcium and Chloride to verify the hydraulic connection between the tank and surrounding aquifer system. This

connectivity was compared with the interaction obtained through aquifer hydraulic parameters. The geochemical analysis data are shown in table 7.6

Table 7.6 Geochemical Analysis of Water Samples

	Electrical conductivity (µs/cm)	TDS	Chloride (mg/l)
Well 1	1310	838.4	259.9
Well 2	1800	1152	422.3
Well 3	1840	1177.6	442.3
Well 4	1850	1184	434 8
Well 5	2140	1369.6	527.3
Well 6	1900	1216	510.2
Well 7	1170	748.8	259.9
Well 8	1390	889.6	272.4
Well 9	1750	1120	527.3
Well 10	1690	1081.6	384.8
Well11	1620	1036.8	372.3
Well 12	1450	928	322.4
Well 13	2120	1356.8	497.3
Well 14	2250	1440	582.3
Well 15	1950	1248	512.2
Well 16	1890	1209.6	384.8
Well 17	1270	812.8	284.9
Well 18	1280	819.2	227.4
Tank	1390	889.6	234.9

7.6 Tank and Aquifer Interaction

The geophysical survey has been carried out inside the tank and in the command area downstream of the tank. Same geological setting exists all over the study area. There is a continuity in the geological formation of the tank and its downstream aquifer. Since there is a very good connectivity the aquifer has been recharged as soon as tank gets filled up Geochemical parameters such as TDS and Cl were also showed similar values inside and downstream of the tank. There is not much variation in the amount of chloride, TDS in the water inside and in the command area. Thus the

continuity between the tank and aquifer were also confirmed by the geochemical studies.

7.7 SUMMARY

Vertical Electrical Sounding (VES) were carried out in 17 location both inside the dank and in the command area. Twelve VES were carried out in the command area, three closer proximity of the tank bund and two inside the tank. All VES data showed similar readings throughout the study area expect one or two places that may be due to the inhomogeaties of the subsurface soil layer. From the VES data and information the geological formation is continuous from the tank to the groundwater aquifer in the command area. First layer is the soil, the second and third layers are weathered and fractured aquifer which are potential zones fro groundwater tapping. The resistivities of the second and third layer ranges 65-180 ohm-m and 180-500 oh-m respectively. Open wells were dug in the second and third layer. Empirical relationship between geo-electric parameters and aquifer parameters were established. From the relationship unknown location aquifer parameters can be determined at detail study on the tank, aquifer in the command area and their interaction were evaluated through Electro Magnetic survey (TVLF), Geophysical Survey, Well dilution method and conventional methods such as pumping test, soil texture analysis and permeameter test. These studies provided qualitative information on tank-aquifer nexus. To get exact quantitative information about seepage rate from tank to aquifer that was studied through tracer study before and after de-silting in the next chapter.

CHAPTER – 8

EVALUATION OF SEEPAGE RATE THROUGH TRACER STUDY

A tracer is a matter carried by ground water which will give information concerning the direction of movement, velocity of the water and potential contaminants which might he transported by the water. The study of tracer can help to determine hydraulic conductivity, porosity, dispersivity, chemical distribution coefficient and other hydro geologic parameters. A tracer can be entirely natural such as the heat carried by hot spring water, fuel oil from a ruptured storage tank. A tracer should travel with the same velocity and direction as the water and does not interact with solid material; a tracer should be non toxic. It should be relatively inexpensive, easily detected with widely available and simple technology. The tracer should be present in concentration well above background concentration of the same constituent in the natural system which is being studied. Finally the tracer itself should not modify the hydraulic conductivity or other properties of the medium being studied.

Artificial tracers are different environmental tracer. Environmental tracers are substances that occur naturally in the environment or are released in advertently to the environment through human activities. In subsurface hydrology the most commonly used, environmental tracer are isotopes of Hydrogen (^{2}H and ^{3}H), Oxygen (^{18}O) and Chlorine (^{36}Cl and ^{37}Cl), but many other isotopes and synthetic chemical have been used as well.

Obviously an ideal tracer does not exist. Because of the complexities of the natural system together with the large number of requirements for the tracer themselves, the selection and use of tracer is almost an art. The numbers of possible tracer which can be used in groundwater are thousand in number if all tracer constituents together with stable isotopes and radionuclides are considered. More practical tracers are water temperature, yeast, bacteria, Lycopodium spores, ions, organic acids, dyes and radioactive tracers. All tracers have strengths and limitation that affect their usefulness in specific situation. Multiple tracers are frequently used simultaneously to overcome these limits and satisfy practical objectives.

8.1 TYPES OF ARTIFICIAL TRACERS

Many different types of human applied tracers called artificial tracers, are used in the subsurface hydrology and are reviewed and compiled in several publications. For completeness, a brief summary of these tracers are summarized below in the Table 8.1

Table 8.1 Artificial Water Tracer Analytic Techniques, Advantages, Disadvantages, and Pertinent References (from Boron Isotopes as an Artificial Tracer, 2006)

Tracers	Analytic Technique	Advantages	Disadvantages	Reference
Inorganic Ions (eg. Bromide, chloride, boron, others	Ion chromatography, Atomic absorption, ion-selectivity; electrode, titration, electrical conductivity	Inexpensive, easily obtainable, ease of sampling and analysis, conservative, stable	High background, toxicity, density flow, coagulate clay minerals, reducing aquifer permeability	Behrens et al.(2001); Jalbert et al(2000)

Dyes (eg uranine, eosin, rhodamine WT, fluorescein, and others)	Fluorimetric methods (filter fluorometer, spectrofluorimeter)	Inexpensive, easily obtainable, low background, ease of sampling	Large mass required, degradation, sorption, density flow, toxicity, permitting	Behrens et al,(2001) Jalbert et al(2000), Pang et al, (1998)
Biological (eg, bacteria, bacteriophages, viruses)	Microscope, colony counting	Inexpensive, low background	Special sample collection and preparation, decay, sorption, and pore size exclusion, Quality assurance/quality control	Keswick et al (1982), Pang et al, (1998), Rossi et al(1988)
Difluorobenzoates	High performance liquid chromatography, ion chromatography, gas chromatography,	Inexpensive, easy detection	Interference from inorganic anions and organic constituents, toxicity, permitting, sorption, degradation	Plummer et al (2000), Jaynes(1994)
Radionuclides (e.g. ^{3}H, He, Ar, Kr, Cl, Si, Sr, and others)	Mass spectrometry, scintillation counting	Dating of old ground water (100 years), intrinsic, stable, no sorption, anthropogenic input	Expensive, specialized analytic techniques, half- live (> 1 to 1000s of years), large sample volumes, initial values problem, permitting, radiation hazards	Plummer et al (2000), Smethie et al (1992)
Noble gases (eg. Xe, Ne, Ar, He, and Kr)	Mass spectrometry, gas chromarography	Stable, nonreactive, no sorption, excess air formation	Expensive, large sample volumes, few laboratories capable of analysis, moderate sampling complexity	Cook and Herczeg (2000), Davisson et al (1998)

Stable isotopes (e.g. Boron-10 and Boron-11, oxygen -18 and deuterium, sulfur -34, and others)	Mass spectrometry	Relatively inexpensive, low analytic detection limits, intrinsic or artificial, case of sample collection	Specialized analytic technique	Cook and Herczeg (2000), Plummer et al. (2000) Dyer and Caprara (1997)

8.1.1 Temperature

Well injection of water with a temperature different from the ambient water temperature allows detection of the thermal pulse with spatially and temporally resolved temperature measurements. Temperature tracing is useful for locating high-permeability zones in an aquifer, providing the temperature differences between injected and background water are small to avoid significant changes in density and viscosity of the fluid.

8.1.2 Isotopes

Common isotopes used as tracers in subsurface hydrology are the stable isotopes ^{2}H, ^{13}C, ^{15}N, ^{18}O and ^{34}S and the radioactive-isotopes ^{3}H, ^{51}Cr, ^{60}CO, ^{82}Br, and ^{131}I. Radioactive isotopes are superior to other tracers because at very small concentration it can be measured. It requires very special equipment for their determination. All process is complicated. It is rather expensive, specialized techniques and radiation hazards. Currently used short lived isotopes are ^{75}S with a half life of 119.7 days. Deuterium ($^{2}H_2O$) at low concentration is considered as the most ideal water tracer. It needs sophisticated instrumentation for chemical analysis and quantification.

8.1.3 Inorganic Anions

In addition to deuterium, Cl^- and Br^- are considered almost ideal conservative tracer for water movement. These anions rarely sorb to soil

particles, and often chloride and bromide move faster than the average water molecule. Anions like PO_4^{3-} or F^- sorb to the solid phase by ligand exchange and are less affected by anion exclusion; but, because of strong sorption, these anions are unsuitable as hydrological tracers. Iodide sorbs to some degree to soil minerals, has a low oxidation potential and oxidizes under aerobic condition, limiting its use as a water tracer.

Compared with F^-, Cl^-, I^- and NO_3^- the bromide ion is the most suitable human applied tracer in field studies. Nitrate is subjected to chemical transformations, and Cl^- occurs in large quantities in soils and aquifers. The concentrations of bromide in natural water are approximately 300 times smaller than those of chloride. The toxicity of bromide is low and unless an excessive amount is applied, no toxicological problem should arise. On the basis of bromide toxicity data, proposed a quality criterion of 1mg L^{-1} of ground water. Below this concentration, chronic toxicological effects on aquatic organism should be nonexistent.

8.1.4 Fluorocarbon

Chlorofluorocarbons (CFCs), which have been released to the environment by human activities since the 1940's, are classified as environmental tracers. CFCs were also proposed as human- applied tracers and were considered useful because they were nonreactive, were resistant to breakdown, and had low toxicity, however, CFCs were linked to the destruction of the stratospheric ozone layer, and therefore they should not be used as human- applied hydrological tracers anymore.

8.1.5 Sulfur Hexafluoride

Sulfur Hexafluoride (SF_6) can be used as a gas phase and liquid phase tracer. SF_6 is a nontoxic, colorless, odorless gas with density of 6.602 g/

l, melting point of -50.75°C, vapor pressure of >1000 kPa for temperature > 0°C, and water solubility ranging from of 33.2 mg/l at 29.6°C to 74.0 mg / l at 2°C

Anthropogenic emission of SF_5 to the environmental began in 1953. Because of its persistence and stability in the environment, SF_5 has been a useful environmental tracer in atmospheric investigation and groundwater dating

8.1.6 Ethanol, Benzoate, and Fluorobenzoates

Ethanol and benzoate (benzoic acid) were found to be useful conservative tracers for ground water movement. In a series of recharge and injection experiments both organic compounds moved like bromide. Benzoate, particularly because of its excellent sensitivity to spectrophotometry, was recommended as an excellent groundwater tracer. Benzoate and benzenesulfonic acid have also been used as geothermal ground water tracers.

Difluorobenzoates are nonreactive and are associated with inexpensive analyses and low detection limits. However inorganic anions and organic constituents can interface with analytic techniques and little toxicity information is available. In summary, benzoates and fluorobenzoates are useful tracers that migrate under most p^H conditions found in solid and aquifers, similarly to bromide. Under low pH conditions mobility usually decreases. Sorption and transport of fluorobenzoates can be affected by organic carbon, clay and iron oxide content.

8.1.7 Spores and Particles

Solid and colloidal particles have been used frequently as tracers, particularly to investigate the hydrology of Karst regions. Chaff has been reported that spores were one of the earliest hydrological tracers. Clubmoss

spores have also been used as tracers in karstic regions. The spores of Lycopodium clavatum are nearly spherical, have a diameter of approximately 30 µm, and have a density slightly higher than that of water. Spores can be dyed with different colors and can therefore serve as multiple tracers. Sampling and detection of the spores is, however, rather cumbersome because water sample must be filtered and spores must be quantified by microscopy.

Synthetic colloidal particles are used to investigate colloid transport and colloidal process in porous media. Synthetic microspheres are available in a variety of sizes and surface properties and can be stained with fluorescent dyes.

8.1.8 Microorganisms

Yeast, bacteria, and viruses have been proposed and used as hydrological tracers. Some decades ago, bacteria and viruses were considered conservative tracers; however, researchers now know that microorganisms interact with the solid phase in aquifers. Nevertheless, bacteria and viruses can serve as indicators of ground water contamination. In karstic regions, microorganism can serve as useful tracers for detecting flow pathways and flow connections. Biological tracer bacteria require special sample preparation and experience decay and/or sorption. Some larger bacteria may experience pore size exclusion retarding transport.

8.1.9 Dyes

Dyes have proven to be powerful tracers. Dyes can be directly observed or indirectly detected by a water sample analysis. The most commonly used dyes in ground water hydrology are fluorescent, allowing detection at very low concentrations. Dyes consist of relatively large organic molecules and, as such interact to some degree with the solid matrix in soils

and aquifers. A variety of dyes are available as hydrological tracers. A particular dye is chosen based on the specific purpose of the tracing experiment. Various classes of dye tracers and its characteristics are discussed below.

8.2 CLASSIFICATION OF DYES

Dyes are usually classified either by their chemical structure or by their method of application. These two grouping systems are referred to as chemical and colorisuc classification, respectively. The most comprehensive catalogue of dyes is the Color Index, which lists information on several thousands of different dyes, including chemical structures, selected physical and chemical properties.

Of the commonly used fluorescent dyes, fluorescein was widely used earlier in nineteenth century and it is visibly detected in low concentration but has very poor stability under sunlight. In United states and Japan were accessing fluorescent dye for quantitative tracing work in surface water they adopted the equally fluorescent dye Rhoda mine B. In the various types of dye the most widely used dyes for groundwater studies are orange florescent dye.

Subsequently Sulpho Rhodamine B (CI 45100) is introduced which is although resistant to adsorption, it is comparatively expensive and is later replaced by the cheaper dye Rhodamine WT which was developed specifically for tracing work. Reynolds (1966) used the green dye Pyranine (CI 59040) for tracing percolation water because it was very resistant to adsorption. Blue fluorescent dyes Pyranine, Lisamine FF and Amino G acid are also used for water tracing. Names of the dyes, colour Index no, generic name are given in the table 8.2 (Smart and Laid law, USGS report).

Table 8.2 **Generic Name, Excitation Emission Maxima, Minimum detectable Concentrations of the tracer Dyes (from P.L.Smart and Laid law 1977)**

Name of dyes	Colour Index no	Generic Name	Maximum excitation (nm),	Maximum Emission (nm)	Background reading, † scale units 0 - 100	Minimum detectability, ‡ (ppb)
Blue Fluorescent Dyes						
Amino G acid			355 (310)	445	19.0	0.51
Photine CU		CI fluorescent brightener 15	345	435 (455)	19.0	0.36
Green Fluorescent Dyes						
Fluorescein	45350	CI acid yellow 73	490	520	26.5	0.29
Lissamine FF	56205	CI acid yellow 7	420	515	26.5	0.29
Pyranine	59040	CI solvent green 7	455 (405)	515	26.5	0.087
Orange Fluorescent Dyes						
Rhodamine B [c,d,f,h]	45170	CI basic violet 10	555	580	1.5	0.01
Rhodamine WT[h]			555	580	1.5	0.013
Sulphorhodamine B[e,f]	45100	CI acid red 52	565	590	1.5	0.061

Fluorescent dyes are organic chemicals that absorb light from the ultraviolet part of the spectrum are molecularly energized and emit light at a longer wave length range. Each dye has different excitation and emission wavelength. Table 8.2 gives excitation and emission wavelength of the various dyes and also its Generic Name. It is also found that orage fluorescent dyes are least detected in the background.

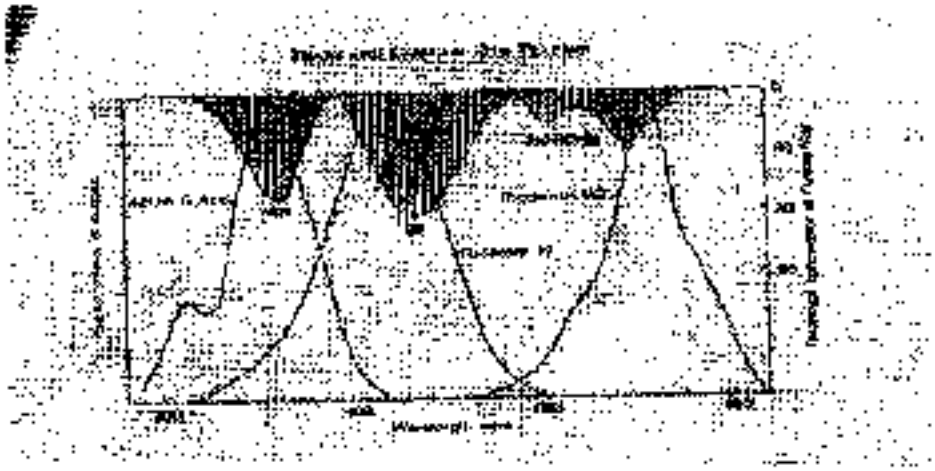

Figure 8.1 Excitation Spectra of Amino G acid, Lissamine FF, and Rhodamine WT

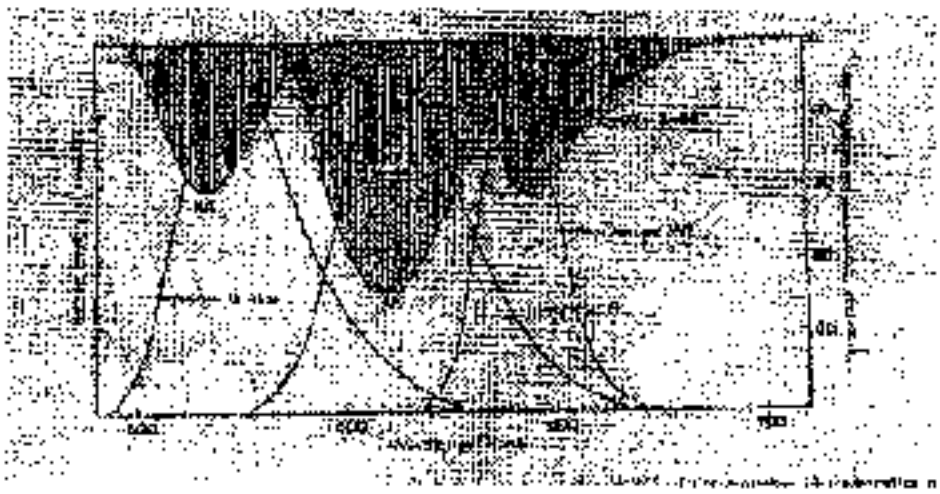

Figure 8.2 Emission Spectra of Amino G acid, Lissamine FF and Rhodamine WT

Figure 8.1 and Figure 8.2 gives excitation and emission spectra of amino G acid, lissamine FF, and Rhodamine WT. When the tracer dye is applied in the field for groundwater studies, the loss of dye may occur due to adsorption with soil, reaction with chemical such as oxidation of dye by chlorine or oxygen. Adsorption is one of the limiting factors for the suitability of a dye tracer. It is very important to evaluate the adsorption character of the dye in the soil.

8.2.1 Factors Affecting Dye Fluorescence

Many factors such as temperature, pH, Salinity, Chlorine, Suspended solids, Sediments and Background fluorescence are affecting dye concentrations that are discussed below.

(i) Temperature

Fluorescence intensity varies inversely with temperature though this rate depends on the dye. The experimental data, consisting of fluorescence reading at a number of different temperatures were fitted by a curve of the form. The fluorescence of the rhodamine dyes and photine CU are significantly affected by temperature variation, and correction may therefore be necessary in quantitative studies. It will often be simpler to prepare a calibration curve at a selected room temperature and continue to use this room temperature for all analysis when continuous monitoring work is being carried out in the field it is relatively simple to take occasional discrete sample for later laboratory analysis. These may be used to check the continuous record and also to correct for the both machine and sample temperature difference from the value used during calibration.

(ii) pH

The fluorescence dyes vary with respect to change in pH. No significant problem with lissamine FF and sulpho rhodamine B, rhodamine B,

rhodamine WT fluorescence is affected to significant extent below pH of five. Amino G acid, fluorescein and photine CU are affected below six. Some correction should be considered in water with a pH lower than these values. Pyranine shows excessive variation in fluorescence with pH changes in the range normally encountered in natural waters. There are two possible reasons for the response of fluorescent dyes to pH changes, ionization and structural changes. The dyes examined are anionic (except rhodamine B which is cationic) and as pH decreases, the acid functional groups become protanated. This affects the degree of resonance in the molecule and reduces the amount of fluorescence. The change will be instantaneous and directly related to dissociation constant of the dye. For carboxylic group's dissociation occurs between pH four and six compared with pH six to seven and half for phenolic group and below pH five for sulphonate groups. Thus the dyes having sulphonate acid group remain fluorescent to lower pH values, as is exemplified by lissamine FF and sulpho rhodamine B.

(iii) Salinity

High salinities affect tracer's performance. Feuerstein and Selleck (1963) reported that sulpho rhodamine B, rhodamine B were only slightly affected by chlorosities of up to 18 g/l but that there was a marked effect for fluorescein. Furthermore the effect of the salt was not instantaneous, a gradual decay occurring over a period of up to 300 hours.

(iv) Chlorine

There was a progressive loss of fluorescence which was independent of dye concentration and most rapid at high chloride residuals, though no single rate could be obtained for a given residual because of the continuous loss of chlorine from the sample. For short duration tests at normal chlorine dosage there will not be a significant reduction in the fluorescence of

Rhodamine B or Rhodamine WT but for duration over two hour apparent dye losses must be taken into consideration.

(v) Background Fluorescence

An apparent or real fluorescence background in water sample taken for dye analysis can cause several problems in tracer studies. It may mask very low concentrations of the tracer or cause apparent recoveries to be in excess of 100% in quantitative work. The two major source of background are natural and suspended sediment and natural fluorescence.

(vi) Suspended Sediment

The presence of suspended sediment raises apparent background fluorescence and reduces the effective dye fluorescence because of light adsorption and scattering by sediment particle. It is reported that there was a reduction in fluorescence of a dye solution for sediment concentration of up to 1000 mg/l above this concentration, adsorption of the tracer onto the sediment may become an experimental problem. The effect was found to be independent of dye concentration. The blue emission wavelength is clearly affected much more than the green and orange. Fine white sediment may in fact increase apparent fluorescence even at sediment concentration which is very turbid, while this is never the case with dark-colored sediments. In most cases, if the suspended sediment is allowed to settle out for a period of 10 - 20 hours, substantially correct dye concentration may be obtained.

(vii) Natural Fluorescence

The cause of natural fluorescence has frequently been wrongly described by the fluorescence of algae, especially chlorella, and to other natural plant pigment. The majority of algae and phytoplankton contain the

green pigment chlorophyll, which has a strong red fluorescence peaking at 650nm. Clearly this will cause very little fluorescence interference even when the orange filter combination is used. Some red algae do contain phycoerythrin which has a fluorescence maximum at 580 nm coincident with the rhodamine B emission peak. However, it has been widely recognized that the background fluorescence at green wave band is many times stronger than that at the orange, which is rarely a major problem. There fore it may be concluded that the algae pigment are not an important cause of background fluorescence.

Most natural water contain dissolved and colloidal matter which when it is sufficiently concentrated produces a marked yellow or brown coloration. This material consists of complex polymeric hydroxyl-carboxylic and aromatic acid, which frequently contain known fluorescent structures. Emission maxima occur at wavelength from 420nm to 520nm for natural water and at 400nm for pulp mill effluent; in all cases the fluorescence was strong. In recent work has shown that the total organic carbon (TOC) concentration in a range of polluted and natural correlated linearly with fluorescence measured over a wide wave band between 400 nm and 600 nm.

The blue and green background values are much higher than the orange. The variation is due to both between site variation caused by difference in the water source and temporal variation at a site caused by storm flow. Highly variable values are found for soil water surface run off from clay soil and river receiving sewage or agricultural effluent, while lower values are obtained from groundwater bodies sample in pumping wells and springs.

Because of the high background at the green and blue wavelengths the sensitivity of the analysis for these dyes has been reduced. The apparent increased discrimination of a high sensitivity filter combination is negated by the corresponding increase in the variability of the background. Attempts to

separate background from dye fluorescence by physical and chemical technique have proved unsuccessful because of the chemical similarity of the compound producing the background to the dye itself. Thus a through knowledge of the range of background variation is required when green and blue fluorescent dyes are being used. This is rarely necessary for the orange dye because of the much lower background reading.

(viii) Non Adsorptive Dye Loss

a. Photochemical Decay

When compound absorb light energy, the molecule becomes excited and raised to a higher energy state. Fluorescence is caused when the molecule revert to the lower energy state by the emission of light. The high energy state will also take part in chemical reaction more readily than the base state; thus as compound fluorescence they often decompose owing to oxidation and other chemical changes. The rate of this decay will depend on the energy of the incident light beam. Thus photochemical decomposition is dependent in both light intensity and wavelength, UV light causing more rapid decomposition than longer wavelength.

It is very difficult to obtain photochemical decay rates which have direct application to field condition because decomposition is dependent on dye concentration and light intensity. Photochemical decay is expressed in the form $F = F_i \exp^{-kt}$ where F_i is the initial fluorescence at time t and k is the decay coefficient. The decay rates are very high for fluorescein, which rapidly loses its fluorescence under bright sunlight condition. Sulpho Rhodamine B is less affected than rhodamine B but lissamine FF appears to be an order of magnitude better than these two. The rate presented probably represented maximum values for field condition, where water depth and turbidity will considerably reduce the average light intensity.

The very fast decay of photine CU under all light conditions precludes its use as a quantitative water tracer. This also applies to fluorescein, which was previously thought to be reasonably stable. The orange fluorescent dyes exhibit low photochemical decay rates such that no correction will be required for tests of up to one week in a duration. It is significant that the difference between the decay rates for a six hours exposure to sunlight and six hours exposure to artificial light becomes progressively higher for dyes absorbing at shorter wavelength. The ratio varies from three to four times for the orange dyes to over 40 times for blue dyes, as would be expected gives the much greater ultraviolet abdsorption of blue dyes together with the significant ultraviolet content of sunlight. Amino G acid has a low photochemical decay rate compared with other blue fluorescent dyes.

b. Chemical Decay

Chemical decay vigorous agitation of dye solution may cause reduction in fluorescence even under dark condition. A systemaric study of this effect experienced considerably experimental difficulties. Finally concluding that rhodamine B was more susceptible than rhodamine WT or sulpho rhodamine B to this type of decay. No significant loss for the dyes over a three day period of agitation or after a similar period with oxygen bubbling through the sample.

c. Bio Degradation

The susceptibility to biodegradation of the tracer dye is significant in biologically hostile environments, like activated sludge system. Bio degradation was small in a high rate sewage oxidation pond effluent, over the one hour period used for equilibration. Rhodamine B in a sample which contained a large algae population showed no measurable decrease in fluorescence over a period of four days. Experiments on the biodegradation of

these tracers using biologically active material are difficult to conduct because the relative magnitudes of adsorption and biodegradation losses are not known. Furthermore the populations present are not stable through time and very high background values may be encountered. Data for adsorption on two different components of a mixed liquor, sub samples of which had been sterilized before addition of the dye. The marked difference between the curve for the sterilized and live sub sample indicates that there was a significant non adsorption loss, which properly represent biodegradation of the dye. Certainly other dyes are known to be biodegradable in both aerobic and non aerobic system including optical brighteners similar to photine CU. Therefore for tracing work in system with large population of micro organism it is that biodegradation will be a significant cause of dye loss. In the majority of surface water it will be unnecessary to consider biodegradation of the tracer dyes because bacterial population will be very much lower than those used in these experiments.

(ix) Adsorptive Dye Loss

Consequently a large number of laboratory experiment, such as batch technique elution method and a column method have been reported, because of the variation in dye concentration equilibration time. Adsorption of dye onto sediment surface is mainly irreversible and therefore a high resistance to adsorption is of paramount important for a dye tracer. However, because of the variation in dye concentration equilibration time, experimental technique and the sediments used, it has proved difficult to extend the result of one study to those of more recent studies on newly introduced tracer.

- Adsorption of dyes at high sediment concentration is considerably less than at low sediment concentration.

- They also conducted experiment on organic and inorganic sediments. Organic phases such as sawdust, humus, heather were tend to adsorb more than inorganic phases such as clay, limestone, orthoquatzite for both rhodamine WT and fluorescein. Sulphorhodamine B was observed to be more resistant to adsorption on organic materials.

- Adsorption losses were found on the glass bottle which was not encountered in the dye rhodamine WT. Since rhodamine B is cationic which is attracted by the most solid surface. Hence samples are to be stored in polythene botules.

(x) Toxicity

Two aspects of dye toxicity are important. First possible deleterious effect on aquatic and marine life. Second the limitation which should be considered where human consumption of the labeled water is a possibility. Rhodamine B concentration sufficiently high to be a problem are so transient under normal field application, because of rapid dilution following injection that the dye will not cause any ill effects to aquatic life.

8.3 FLUORESECENCE SPECTROSCOPY

Fluorescence spectroscopy is a type of electromagnetic spectroscopy which analyse fluorescence of a sample. It involves using a beam of light usually Ultraviolet light that excites the electrons in molecules of certain compounds and cause them to emit light of a lower energy. Devices that measure fluorescence are called fluorometers. In a typical experiment, the different frequencies of fluorescent light emitted by a sample are measured, holding the excitation light at a constant wavelength. This is called an emission spectrum. An excitation spectrum is measured by recording a

number of emission spectra using different wavelengths of excitation light. There are two general types of instruments exist which are Filter fluorometer – The filter based to isolate the incident light and fluorescent light. Spectrofluorometers–Diffraction grating monochromators used to isolate the incident light and fluorescent light.

Working Principle

In both types, the light from an excitation source passes through a filter or monochromators and strikes the sample. A portion of the incident light is absorbed by the sample and some of the molecules in the sample fluoresce. The fluorescent light passes through a second filter or monochromators and reaches a detector which is usually placed at 90° to the incident light beam to minimize the risk of transmitted or reflected incident light reaching the detector.

Various light source may be used as excitation source, including lasers, photo diodes and lamps; Xenon arcs and mercury vapor lamps in particular. A laser only emits light of high irradiance at a very narrow wavelength interval, typically under 0.01 nm, which makes an excitation monochromators or filter unnecessary. The disadvantage of this method is that the wavelength of a laser cannot be changed by much. A mercury vapor lamp is a line lamp meaning it emits light near peak wavelength. By contrast, xenon arc has a continuous croission spectrum with nearly constant intensity in the range from 300 800 nm and a sufficient irradiance for measurements down to just above 200 nm.

Filters and/or monochromators may be used in fluorimeters. A monochromator transmits light of an adjustable wavelength with an adjustable tolerance. The most common type of monochromator utilizes a diffraction grating, that is, collimated light illuminates a grating and exits with a different

angle depending on the wavelength. The monochromator can then be adjusted to select which wavelengths to transmit. For allowing anisotropy measurement the addition of two polarization filters are necessary: One after the excitation monochromators or filter, and one before the emission monochromators or filter. As mentioned before, the fluorescence is most often measured at a 90° angle relative to the excitation light as shown in figure.8.3

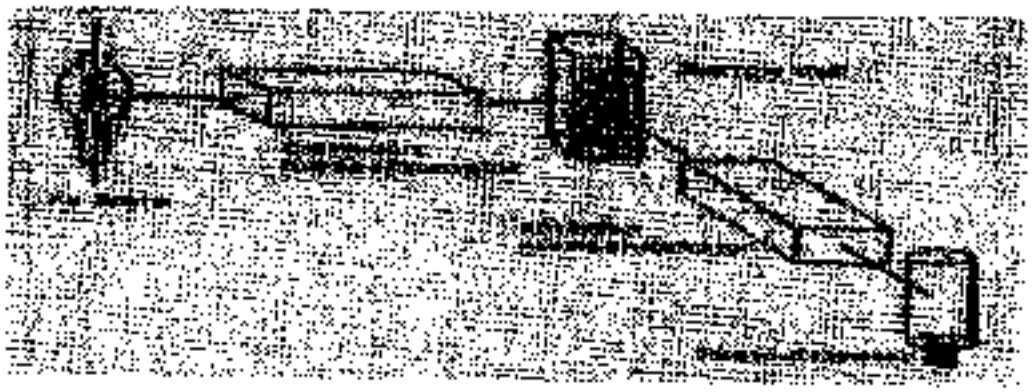

Figure 8.3 **Schematic of a fluorometer with 90° geometry utilizing a Xenon light source (form Fluorescence Spectroscopy, 2009)**

This geometry is used instead of placing the sensor at the line of excitation light at a 180° angle in order to avoid interference of the transmitted excitation light. No monochromators is perfect and it will transmit some stray light, which is light with other wavelength than the targeted. An ideal monochromators would only transmit light in the specified range and have a high wavelength independent transmission when measuring at a 90° angle, only the light scattered by the sample causes stray light. This result in a better signal to noise ratio, and lowers the detection limit by approximately wavelength as the incident light, where as in Raman scattering light changes wavelength usually to longer wavelengths. Raman scattering is the result of virtual electronic state induced by the excitation light. From this virtual state, the molecules may relax back to vibrational level other than the vibration

ground state. In fluorescence spectra, it is always seen at a constant wave number difference relative to the excitation wave number e.g. the peak appears at a wave number 3600 cm^{-1} lower than the excitation light in water. Other aspects to consider the inner filter effects these include reabsorption. Reabsorption happens because another molecule or part of a macromolecule absorbs at the wavelengths at which the fluorophore emit radiations. The result is that the intensity of the excitation light is not constant through out the solution. Resulting, only a small percentage of the excitation light reaches the fluorophores that are visible for the detection system. The inner filter effect changes the spectrum intensity of the emitted light and they must therefore be considered when analyzing the emission spectrum of fluorescent light.

Fluorescence Spectrophotometer

Model F 2000 fluorescence spectrophotometer contains a Xenon lamp and filled with a gas which is at about 9atm at ordinary temperature and 30atm after ignition. Applied voltage to the Xenon lamp is about 90 V while the power switch is kept ON and a high voltage of 30 KV in the moment LAMP START button is pressed.

After completion the coarse and fine adjustment, the performances of the instrument were checked out. For the instrument normal operation the sensitivity is to be checked. After power up the following performance were carried out for more than 30 minutes. This instrument is capable of automatically measuring a Raman spectrum of water and determining noise at a Raman Peak and calculating the sensitivity. An excitation wavelength of 350 nm is measured automatically, and the noise at a peak wavelength in the Raman spectrum is to be checked. For this complete measurement, instruments take the time of about 12 minutes. If either of above allowable limits are exceeded, following steps are to be followed.

i. If the cell is contaminated and produces background emission, sensitivity cannot be checked correctly. The cell must be handled carefully.

ii. If distilled water contains impurities, the Raman spectrum may be deformed as exemplified in figure 8.4. If it is impossible to obtain an S/N ratio of 2000 or higher in such a case, we measure the spectrum once again with distilled water having higher purity

iii. S/N ratio is degraded if the light source is not adjusted to its optimum position

Figure 8.4 **Raman Spectrum Affected by Impurities (from Instruction Manual for Model F - 2000 Fluorescence Spectrophotometer)**

Figure 8.5 **Optical System Configurations (from Instruction Manual for Model F - 2000 Fluorescence Spectrophotometer)**

Figure 8.5 shows the optical system configuration of the model F 2000. The radiation coming from the Xe lamp is converged at entrance slit S1 of the excitation monochromators through lenses L1 and L2. Only the light dispersed by the excitation concave grating (excitation beam) enters exit slit S2. The excitation beam from exit slit S2 is reflected by concave mirror M1 and the slit into two by the beam splitter BS. O one of two excitation beam goes to the monitor detector for its measurements. And the other beam (most of excitation) passing through BS is converged to the sample cell through lens L3.

The fluorescence coming out of the sample is restricted into entrance slit S3 of the emission monochromators through lenses L4 and L5. The fluorescence dispersed by the emission concave grating passes through exit slit S4 and is converged at the photomultiplier via concave mirror M2 for intensity measurement. The emission slit serves also as a shutter to protect the photomultiplier. It automatically closes upon opening the lid of sample compartment.

8.4 SELECTING DYE FOR INJECTION

Selecting a particular dye for water tracing is based on the quality of water draining underground, nature of background concentrations of the tracers and the separability of dye from the background fluorescence, detectability and toxicity at low concentrations, availability or complexity of equipment needed to detect the dyes, availability and cost of a particular dye. Generally, no dye is 100 percent conservative, either they are sorbed onto clay or lost due to chemical decay. Thus, loss due to adsorbtion can influence the selection of a dye. The level of background fluorescence can effect the selection of a dye. Infact, determination of background levels needs to be adopted as the first step in most traces because this provides a standard for comparison of dye recovered.

Because some fluorescent dyes decay on exposure to ultraviolet light, the dyes are less than ideal if the water being traced repeatedly sinks and rises and flows along the surface. Smart and Laidlaw (1977) reported that the photochemical decay rates are very high for fluorescein, which rapidly loses its fluorescence under bright sunlight conditions. Quinlan (1987a) also reported that optical brighteners and fluorescein are very susceptible to photochemical decay especially in low concentrations. An evaluation of cost and availability of a particular dye involves factors that can be unique to a particular user. Therefore, these factors are not discussed here.

After going through literature on dyes, it is found that

- Lissamine FF is extremely stable and resistance to adsorption losses which is 9 times more expensive than rhodamine WT. This dye is superior and is recommended as the best quantitative tracer of the three green dye

- Blue and green wavelengths fluorescence is significantly present in the nature. Hence multiple injections are needed to over come the background fluorescence. Therefore orange dye such as rhodamine B, rhodamine WT and sulpho rhodamine B are preferred. Rhodamine B and rhodamine WT are three times as fluorescent as sulpho rhodamine B and will therefore label a larger volume of water per unit weight. Rhodamine B suffers enormous losses due to adsorption on many surfaces. Rhodamine WT exhibit moderate resistance. Sulpho rhodamine B is not readily adsorbed by humus, it suffers significant losses on mineral surfaces. Although rhodamine B appears to be most economical tracer because of its very large (0.7) adsorption losses it is less preferred. Rhodamine WT the second cost effective dye has no serious disadvantages although it was not the most conservative tracer of those examined.

Sulpho rhodamine B is resistant to adsorption but it is more expensive than rhodamine WT.

- Even through rhodamine WT and sulpho rhodamine B are advantageous, it is expensive and not available in the market. Hence in this project rhodamine B dye was used whose colour index number is 45170 whose excitation wavelength is 555 nm and emission wavelength between 570 and 580 nm. To over come the adsorption losses more amount of rhodamine B were applied more than required.

8.5 SELECTING QUANTITY OF DYE FOR INJECTION

Having selected a particular dye, the next step is to select the optimum quantity of dye for injection. The quantity of dye to be injected is selected in order to provide a detectable amount of dye at the recovery point, but the concentration should remain below visible levels. The quantity of dye used for injection is generally based on the estimated flow conditions, the distance of the trace, and the peak dye concentration expected at the recovery point. To some extent, the quantity of dye will vary depending on the nature of the injection point. For example, if the dye can be added to water draining directly into an open swallet, less dye will be required than if the dye must infiltrate through soil and unconsolidated material in the bottom of the aquifer.

Selecting the optimum amount of dye for qualitative tracing is a matter of experience. The amounts may be adjusted to depending on the initial results. Quantum (1870) suggested for qualitative tracer under moderate flow condition, one pounds of fluorescein per straight line mile of tracer up to a maximum of five pounds. Alley and fletcher (1976) present a

monograph for selecting the quantity of fluorresein to be injected. If the ground water flow system is in fractured zones, and then the equation is

$$Wd = 1.478 \sqrt{DQ/V}$$

Wd weight of fluorescein dye in kg to be injected

D straight line distance in km from injection point to recovery point

Q discharge at the resurgence in cubic meters per second; and

V estimated velocity of ground water flow in meters per hour

For this equation, the velocity of ground water flow is the most difficult to estimate because it depends on the nature of the conduits and the hydrologic condition at the time of the tracer. There fore, initial dye tracing needs to be attempted under medium base flow condition for a study area, subsequent tracer under extreme flow condition are needed to better define the flow condition are needed to better define the flow variation. Other methods was used to quantity dye requirement by EPA (1.999) was given below. In this formula a target concentration of 10 micrograms per liter (ppb) was assumed in the circulation cell and dye recovery of only one percent. A conservative estimate of dye loss of 99 percent (1 percent recovery) were used to account for adsorption, attenuation and degradation of dye in the aquifer.

The equation for calculation of dye volume is

$$\text{Dye volume} = \frac{\text{(Final concentration) * (Water volume to be Dyed)}}{\text{(Dye concentration) (Dye specific gravity)}}$$

Assume volume of water dyed is 1699 cubic meter and final concentration is 10 micrograms per liter. The specific gravity of rhodamine WT, 20 percent solution is 1.19; the specific gravity of fluorescein, 7.5 percent solution is to 50.

For rhodamine WT 20 percent solution

$$\text{Dye volume required} = \frac{(1*10^{-9})\,(1,699,200\ \text{lit})}{(0.2)\,(1.19)}$$

$$= 0.0714 \text{ liters}$$

Since only one percent recovered;

100 * dye volume = 100 * 0.0714

=7.1 litres of Rhodamine WT 20 percent solution is required

For fluorescein 7.5 percent solution

$$\text{Dye volume required} = \frac{(1*10^{-8})\,(1,699,200\ \text{lit})}{(0.075)\,(1.050)}$$

$$= 0.2158 \text{ litres}$$

Since only one percent recovered;

100 * dye volume = 100 * 0.2158

= 21.6 litres of fluorescein 7.5 percent solution is required

Hence for a 1,699 m^3 of water, the minimum required quantity of dye is 21.6 litres at fluorecein and 7.2 litres of rhodamine WT.

8.5.1 Dye Handling Procedures

In order to simplify dye injection when using powder such as Rhodamine B, especially during windy conditions, the powder can be mixed with water before going to field. The dye solution is directly poured into the tank in order to lessen dye loss due to photochemical decay or absorption by organic debris at the surface. While mixing and injecting the dye, extreme care needs to be taken to avoid contaminating the area around the injection point. Such contamination can lead to a false positive trace and erroraneous interpretations. To lessen the possibility of contamination, long sleeve rubber

or disposable, plastic gloves needs to be worn during all handling operations. Ideally, care needs to be taken to ensure that dye collection devices are not handled by the same person that handled previously the dye. Different people need to handle each task. The tracer needs to be stored and transported to the injection site safely and carefully.

Rhodamine B normally comes from the manufacturer as a 20 percent concentration in containers. Overtime, some dye may settle out of solution, therefore before the dye is withdrawn from the container, the contents needs to be thoroughly mixed to ensure that the dye is appropriately mixed.

8.6 DYE RECOVERY EQUIPMENT AND PROCEDURE

The dye may be recovered by passive dye detectors consisting of packets of activated charcoal suspended in all ground water sampling points. The detectors or packet of activated coconut charcoal are left in places for 1 to 5 days. Carbon bugs are retrieved and sealed in a plastic bag and returned to the laboratory in a light tight case. This is keeping in refrigerator to decrease bacterial action that could reduce fluorescence. The charcoal is elutriated in an alcohol solution and visually checking for the concern dye colour. The maximum colour intensity develops almost immediately upon addition of the elutriant and then slowly decreases. Dye concentration can be confirmed by instrumental analysis of the elutriant. This provides qualitative information of dye detection.

8.6.1 Calibration Procedure

Filter fluorometer or fluorescence spectro fluorometer measure the intensity of light at a selected wavelength from a water sample containing a fluorescent substance. The intensity of fluorescence is proportional to the

amount of fluorescent substance present. The fluorescent spectro fluorometers are to be calibrated for a dye recovery data acceptable for quantitative analysis.

The preparation of calibration standards is basically the processes of step by step reduction of the dye solution until concentration that are expected during dye recovery are reached. This reduction is generally known as serial dilution. Precise measurements of the initial volume of dyes and added diluent in each step of the procedure are necessary to prepare a set of standards for an accurate calibration of the instrument. For rhodamine B, 20 percent solution, three serial dilutions are required to obtain concentration on the order of 100 ppb. In each step, the preceding concentration becomes the new initial concentration. This third dilution 100 ppb needs to be retained in quantity as a working solution and is used for further dilution if standards below 100 ppb are needed. The use of the working solution eliminated the necessity to perform complete serial dilution each time the instrument is calibrated so long as the same dye lot is being used. The same working solution needs to be used through out an investigation as long as all dye used from same dye lot. The working solution needs to be sealed and stored out of light when not in use. Distilled water is used for calibrating the instrument to zero background. The instrument is to be checked with temperature equilibrated solution before the final measurement for all dye samples.

Five mg of rhodamine B powder was mixed with one liter of distilled water to get a working solution of 1 ppm or 1000 ppb concentration. 100 ppb working solution was prepared from 1000 ppb solution 10 ml of 1000 ppb diluted with 90 ml of distilled water to get 100 ppb. In the same manner 1, 2, 4, 8 and 10 ppb rhodamine B working solution were prepared. These known concentration dye samples were kept in a instrument which

provides intensity in nm. Using above concentration and intensity calibration curve is drawn as shown in figure 8.6

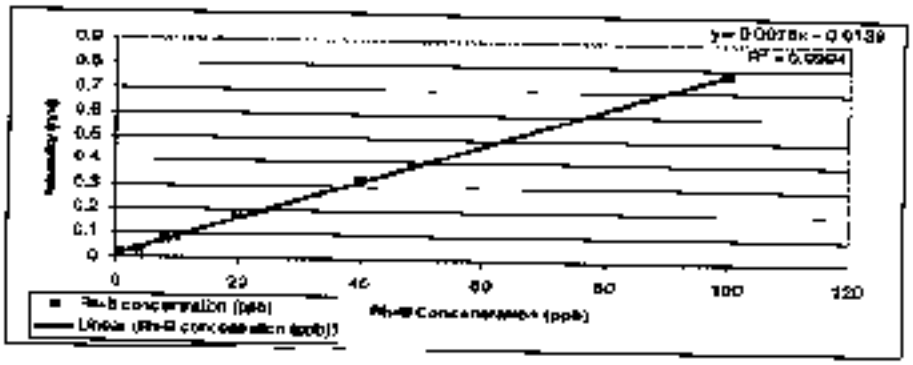

Figure 8.6 Calibration Curve for 1 – 100 ppb

The best fit curve gives an equation to calculate unknown concentration that is taken from the field

Best fit equation

Intensity (y) = 0.0076x + 0.0139

Whose $R^2 = 0.9994$

x represent concentration in ppb

y represents intensity in nm

$$\text{Concentration } (x) = \frac{\text{Intensity } (y) - 0.0139}{0.0076}$$

Similarly 1 ppb to 1000 ppb best fit calibration curve were drawn as shown in figure 8.7

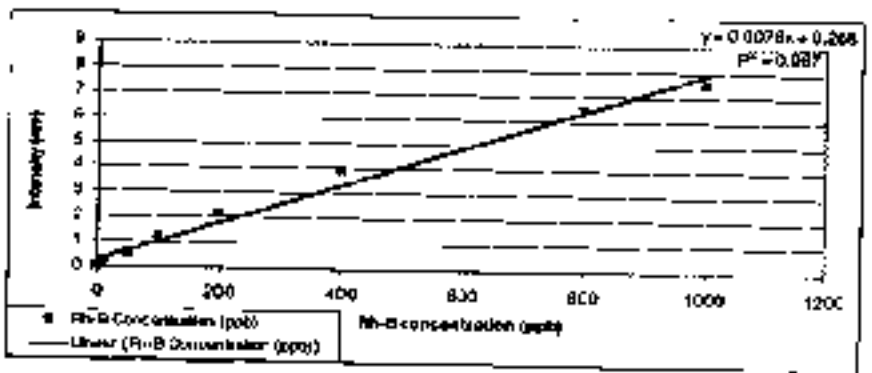

Figure 8.7 Calibration Curve for 1 – 1000 ppb

The regression equation for the above said values is

Intensity (y) = 0.0076x + 0.268

R^2 = 0.987

x - Rhodamine B concentration in ppb

y - Intensity in am

When ever the ground water samples were analysed in the instrument, the instrument will be calibrated then unknown sample intensity were measured and then rhodamine B concentration were calculated from the regression equation.

8.7 QUANTITATIVE DYE TRACING

Quantitative dye tracing consist of the injection of a known quantity of dye and the measurement of the concentration of the over time, at a particular ground water discharge point such as a spring or well. Determination of dye recovery requires measurement of both dye content and ground water discharge. These measurements are made at each dye resurgence site that was identified as being hydraulically connected to injection location by previous qualitative tracer tests. Water samples were collected and the dye content of each sample is measured with properly calibrated fluorometer or fluorescent spectrometer. These data are plotted against time to produce a dye recovery break through curve (time concentration). Typical dye recovery curve is shown in figure 8.8. This figure was taken from USEPA report October 1988. It represents the dye injection in a sinking stream and sampled at 11500 feet from the injection site.

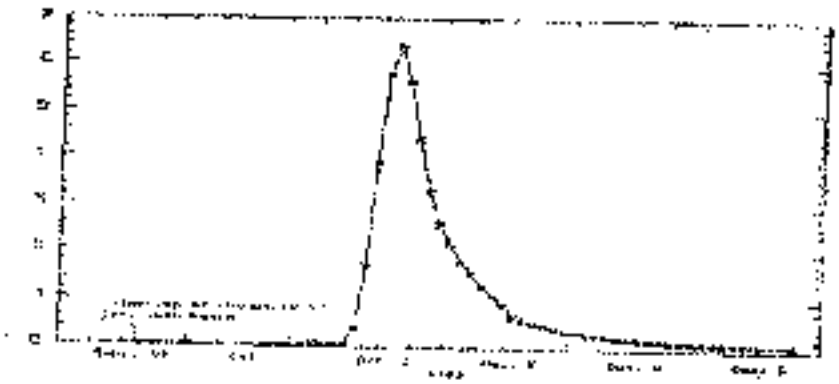

Figure 8.8 Typical Dye Recovery Curve

Quantitative dye tracing can be performed to determine potential contaminant transport characteristics, such as persistence, dispersion rate and concentration. Quantitative dye tracer tests are more labor intensive and required more sophisticated equipment and techniques than qualitative dye tracing because the objective is to define dye concentration variation during passage of the dye cloud rather than simply to determine if the dye appeared at a particular spring or well.

The shape and magnitude of the dye recovery curve is determined by (1) the quantity of dye injected (2) the characteristics of the dyes (3) discharge at the resurgence (4) rate of dispersion of the dye and (5) the cross sectional mining of the dye before arrival at the sampling point. The apparent shape of the dye recovery curve can also be affected by the sampling interval.

Analysis of the dye recovery curve provides insight into the flow characteristics of the aquifer such as the effective time of travel between a swallet and the resurgence and the velocity of groundwater flow. Additional analysis of the recovery curve and discharge measurement may be used to provide estimates of peak concentration duration and dispersion. Because these data may be related to the velocity and dispersion of a potential groundwater pollutant.

Rhodamine B is one of the traditional fluorescent water tracing dye. It is relatively cheap. It is detected visually and measured by appropriate fluorometric equipment. Visually the dye appears as a bright dark red to magenta. It has the lowest rates of decomposition. Its fluorescence yield is temperature dependent. Its solubility is 50 g/l. However, the solubility in acetic acid solution is ± 400 g/l. Chlorinated tap water decomposes rhodamine B. Rhodamine B solutions adsorb on to plastics and should be kept in glass. Rhodamine B is suspected to be carcinogenic in California. But in New Jersey, it was stated that there is limited evidence of carcinogenicity in laboratory animal and no evidence at all in humance. Rhodamine B excitation and emission spectra are shown in figure 8.9

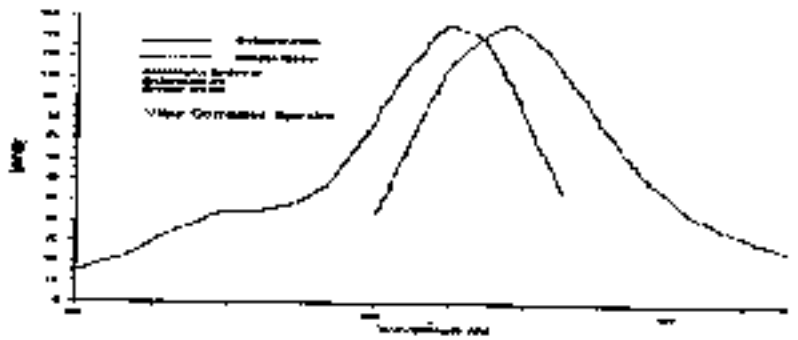

Figure 8.9 Excitation and Emissions spectra of Rhodamine B dye

8.8 APPLICATION OF RHODAMINE B IN FIELD

After calibrating the fluorescent spectrophotometer and studying the behavior of the rhodamine B, it was decided to apply the rhodamine B in the project area Sengulam Tank at Viruthunagar and Ponpadi Tank at Thiruthani. Rhodamine B was applied in the Sengulam tank during March 2008 which was not applied in the Ponpadi tank during 2008. Since rhodamine B dye was not available in the market. But in the year 2009, rhodamine B was applied in both the tanks during February 2009 which explained below in depth.

Rhodamine-B powder was mixed with water and known concentration solution (stock solution), were prepared and checked for its emission wavelength in the fluorescent spectrophotometer. It was excited at 555 nm and the rhodamine B fluoresence was emitted between 571 to 573 nm wavelengths. The lower most detectability of the instrument is 0.1ppb and maximum 1000 ppb.

8.8.1 Rhodamine B application in Sengulam Tank - Year 2008

Rhodamine B study was conducted during February 2008. During that time the tank storage was154000 m^3. Initially it was planned to use very low concentration (5 ppb) of rhodamine B in the Sengulam tank water. For 5 ppb concentration volume of dye required is given below

$$\text{Volume of dye} = \frac{5 * 10^{-3} * 0.154 * 10^{9} \text{ lit}}{200 \text{ gm/lit}}$$

$$= 3850 \text{ liters}$$

$$\sim 800 \text{ gm of rhodamine B}$$

800 gm of rhodamine B powder was mixed with 1600 liters of tank water and poured through out the tank in order to have uniform distribution of dye. Then with help of stick it was mixed very well with tank water. Tank water and groundwater samples were collected for ten days before addition of dye to determine back ground fluorescence. On an average natural fluorescence of 8 ppb were detected between the wave length 613 and 615 nm. This may be due to presence of algae and phytoplankton in the sample reported by Feuerstein and selleck (1963). Similarly samples were collected daily after addition of a dye in a tank. Tank water had rhodamine B fluorescence for some days that too at very low concentration. But even after five days, rhodamine dye ions were not detected in the pumping wells which

were considered for the study. Hence it was planned to try at 16 ppb concentration of rhodamine B dye on 5th March 2008.

$$\text{Volume of dye required} = \frac{16 * 10^{-3} * 0.154 * 10^{9}}{200}$$

$$= 12320 \text{ lit}$$

$$\sim 2500 \text{ gm of rhodamine B}$$

This 2500 gm of rhodamine B was mixed with 5000 liters of tank water which was sprayed over the tank water surface. Water sample were collected from the tank and pumping wells. The schedule of dye application and recovery were given in table 8.3.

Table 8.3 Schedule for Dye Study in the year 2008

Duration	Sample Collection	Purpose
20/1/08 to 15/2/08	Collection of tank water and well water	To study natural fluorescence existence
15/2/08	Rhodamine B of 800 gm applied with 1600 liters of tank water	To estimate the groundwater velocity
16/2/08 to 28/2/08	Collection of tank water and ground water	Dye was not detected
5/3/08	Rhodamine B of 2500 gm applied with 5000 liters of tank water	Re application of rhodamine B
6/3/08 to 14/3/08	Water sample collected daily	Rhodamine B was detected in one day in most of the wells
18/3/08 to 2/4/08	Water sample collected once in two days	Rhodamine B was detected till 18.3.08. After that natural fluorescence was alone detected due to continuous raining of 217 mm from 15.3.08 to 23.3.08
7/4/08 to 27/4/08	Water sample collected once in three days	Natural fluorescence alone was detected
May, June, July	Water sample collected once in 15 days	Natural fluorescence alone was detected

Since rhodamine B was emitted at 571 – 573 nm wavelength range, the fluorescent spectrophotometer was adjusted for photometry option in which calibration curve was saved which provides directly rhodamine B fluorescence. For every day sample analysis emission wavelength was verified and then the entire sample were analysed. Samples were collected for 26 days from 6.03.08 to 3.07.08 while doing sample analysis; there was a sudden raise in fluorescence in the tank water on 16.03.08 and in the well water on 23.03.08. Then it was found that this peak fluorescence emitted at a wavelength 621 to 627 nm. This change in fluorescence and wavelength was due to continuous rainfall during 15.03.08 to 23.03.08 that amounts to 217 mm that is given below in table 8.4.

Rain water was analysed for its fluorescence and wavelength. It was found that rainwater had 110 ppb to 153 ppb emitted at 554 nm to 630 nm wavelength. Hence after 15.03.08 rhodamine B fluorescent was not found in tank water and ground water. Therefore the graphs are drawn between 6.03.08 to 15.03.08 and discussed below.

- Tank natural fluorescence was 12.4 ppb before rhodomine B dye application which was observed at 614 nm wavelength. It was observed that the rhodamine B fluorescence in the Sengulam Tank was 29.1 ppb one day after the dye application. It was decreasing steadily as shown in figure 8.10. Due to heavy rainfall of 217 mm, rhodamine B was lost in the tank water after 9th day of dye application.

- After 9th day, it was found that no rhodamine B was found in the tank water. It had only natural fluorescence which was emitted at 614 to 617 nm wavelength which was exclusively due to rainfall. Natural fluorescence variation is shown in figure 8.11

Table 8.4 Rhodamine B and Natural fluorescence at Sengulam Tank water during 2008

DATE	Rainfall (mm)	Day	Tank water RF (ppb) at 571 nm	Tank water NF (ppb)	Remarks
06/3/08		1	29.1	12.4	At 614 nm
07/3/08		2	26.8	0	
08/3/08		3	22.3	0	
09/3/08		4	26.1	0	
10/3/08		5	27.7	0	
11/3/08		6	11.9	0	
12/3/08		7	6.5	0	
13/3/08		8	5.9	0	
14/3/08		9	7.2	0	
15/3/08	6.8	10	-	-	
16/3/08	50.4	11	0	32.9	At 621 nm
17/3/08	2.8	12	-	-	
18/3/08	46.2	13	0	29.6	
19/3/08	17.4	14	-	-	
20/3/08	15.4	15	-	-	
21/3/08	52.6	16	-	-	
22/3/08	19.2	17	-	-	
23/3/08	6	18	0	25.1	
27/3/08		22	0	20.7	
30/3/08		25	0	18.1	
02/4/08		28	0	17.3	
07/4/08		33	0	25.4	
10/4/08		36	0	26.9	
14/4/08		40	0	13.7	
17/4/08		43	0	10.5	
20/4/08		46	0	10.7	
24/4/08		50	0	10.6	
27/4/08		53	0	16.8	
02/5/08		58	0	14.8	
30/5/08		86	0	10.5	
02/6/08		89	0	14.8	
03/6/08		90	0	3.9	
Total	216.8				

*** RF – Rhodamine B fluorescence NF – Natural fluorescence**

- Rhodamine B fluorescence was detected in most of the well in one day after dye application except the wells W1, W2 and W3 which lies below the sluice 1 as shown in table 8.5.
- First day arrival concentration was minimum compare to the break through concentration.
- Average break through concentration was 3.7 ppb which were detected between 2 and 9 days as shown in table 8.5.

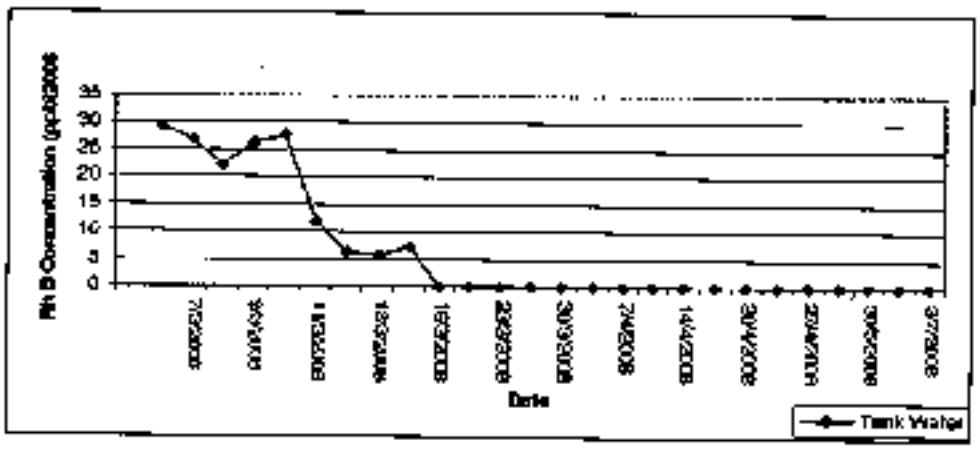

Figure 8.10 Rhodamine B fluorescence in the Sengulam Tank during 2008

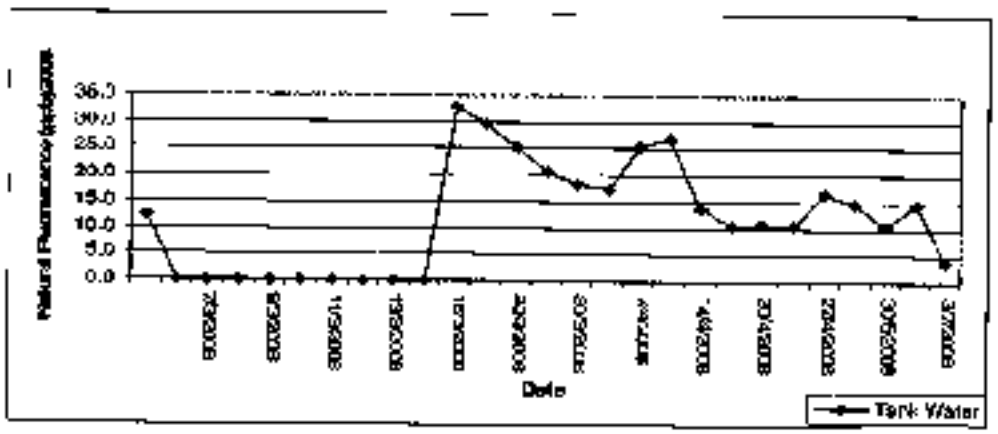

Figure 8.11 Natural fluorescence in the Sengulam tank during 2008 after rainfall

- After 18.3.08 (13th day) rhodamine B was not detected in any one of the wells. But natural fluorescence were found at 614 to 617 nm in all the wells from 23.3.08 (18th day) as shown in figure 6.12. Natural fluorescence was ranging between 12 ppb and 3.3 ppb

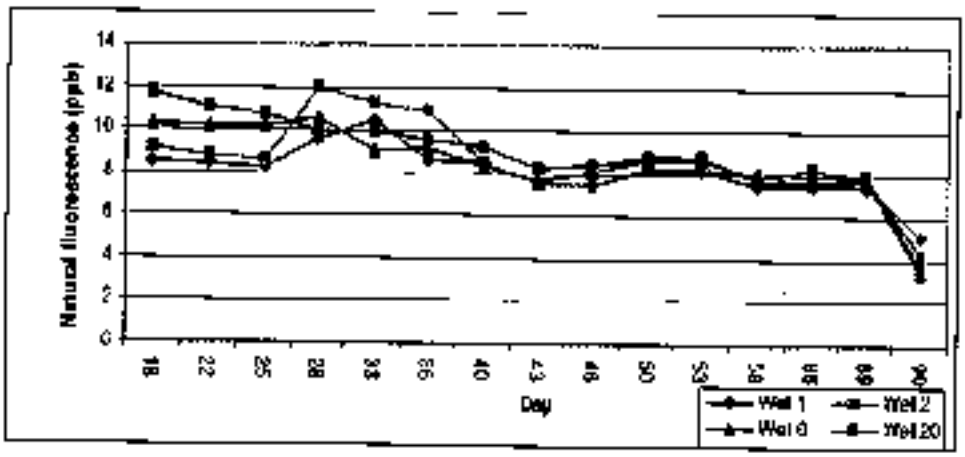

Figure 8.12 Comparison of Natural fluorescence in Sengulam wells during 2008

Table 8.5 Analysis of Rhodamine B fluorescence detection in the Sengulam Tank during 2008

Wells	Distance from the bund (m)	Area Contribution (sq km)	No of days of conc. detection	Date of First Rh-B Detection	Day of First arrival (th Day)	Arrival Conc. (ppb)	Date of Break through	Peak found on (th Day)	Peak Conc. (ppb)	Velocity (m/day)
W1	49.10	0.024	9	8/3/08	3	0.20	11/3/08	6	4.00	8.2
W2	152.8	0.085	8	9/3/08	4	2.40	11/3/08	6	4.80	25.5
W3	163.6	0.039	5	9/3/08	4	0.20	11/3/08	6	5.90	27.3
W4	67.90	0.015	7	6/3/08	1	2.90	6/3/08	1	2.90	67.9
W5	29.70	0.008	10	6/3/08	1	0.70	10/3/08	5	4.00	5.9
W6	131.0	0.016	6	6/3/08	1	1.60	6/3/08	1	1.60	131.0
W7	281.2	0.030	11	6/3/08	1	0.40	11/3/08	6	3.60	46.9
W8	152.1	0.018	9	6/3/08	1	1.40	14/3/08	9	5.80	16.9
W9	66.00	0.011	9	6/3/08	1	3.20	14/3/08	9	4.00	7.3
W10	82.30	0.018	10	6/3/08	1	1.80	6/3/08	1	1.80	82.3
W11	49.70	0.012	8	6/3/08	1	1.80	6/3/08	1	1.80	49.7
W12	109.1	0.014	8	6/3/08	1	0.70	6/3/08	1	1.80	109.1
W13	198.0	0.017	10	6/3/08	1	1.00	13/3/08	8	3.40	24.8
W14	38.30	0.034	7	6/3/08	1	0.40	11/3/08	6	4.50	6.4
W16	298.4	0.018	10	6/3/08	1	3.10	12/3/08	7	3.10	42.6
W17	367.3	0.086	7	6/3/08	1	3.20	6/3/08	1	3.10	367.3
W18	287.9	0.023	3	6/3/08	1	0.20	14/3/08	9	3.20	32.0
W19	406.5	0.059	11	6/3/08	1	2.70	12/3/08	7	5.90	58.1
W20	459.2	0.058	7	6/3/08	1	1.20	7/3/08	2	4.10	229.6
W21	401.8	0.064	7	6/3/08	1	1.30	7/3/08	2	3.80	200.9
W22	257.3	0.018	8	6/3/08	1	2.90	7/3/08	2	5.70	128.7
W23	255.4	0.024	9	6/3/08	1	0.40	12/3/08	7	1.30	36.5
W24	261.2	0.074	8	6/3/08	1	1.70	9/3/08	4	4.80	65.3
Total			**187.0**		**31.0**	**35.4**		**107.0**	**84.9**	**1770.0**
Average			**8.1**		**1.3**	**1.5**		**4.7**	**3.7**	**77.0**

Velocity Determination

Groundwater velocity was calculated based on the well distance from the tank bund and the breakthrough concentration as given below.

Velocity = Distance from the tank bund / Day of Break through Concentration

$$v = x / t \text{ m/day}$$

Wells were classified with respect to distance from the tank bund such as 150 m, 300 m and 450 m which may be expected to behave similar.

- Even though the wells W1, W4, W5, W6, W8, W9, W10, W11, W12 and W14 are lying at proximity of 150 m which had different velocity as shown in table 8.6. For example wells W1 and W11 are having different velocity of 8.2 and 109.1 m/day even though both lie same distance from the tank bund.

Table 8.6 Wells in the proximity of 150m from the bund

Well No	Distance from tank bund (m)	Break through conc. (ppb)	Velocity (m/day)	Velocity (cm/sec)
W 5	30	4.0	5.9	0.007
W14	38	4.5	49.7	0.058
W1	49	4.0	8.2	0.009
W11	50	1.8	109	0.126
W9	66	4.0	7.3	0.008
W4	68	2.9	67.9	0.079
W12	109	1.8	198	0.229
W10	82	1.8	82.3	0.095
W6	131	1.6	131	0.152
W8	152	5.8	16.9	0.02

- Similarly wells W23 and W22 had very high velocity of 36.5 and 128.7 m/day as shown in table 8.7

Table 8.7 Wells in the proximity of 300m from the bund

Well No	Distance from tank bund (m)	Break through conc. (ppb)	Velocity (m/day)	Velocity (cm/sec)
W2	153	4.8	25.5	0.03
W3	164	5.9	27.3	0.031
W13	198	3.4	24.8	0.028
W23	255	1.3	36.5	0.042
W22	257	5.7	128.7	0.149
W24	261	4.8	65.3	0.076
W7	281	3.6	46.9	0.054
W18	288	3.2	32.0	0.037
W16	298	3.1	42.6	0.049

- At the same time, ground water velocity was examine 201 m/day in the well 20, even though it lies at 460 m from the tank bund as shown in table 8.8.

Table 8.8 Wells in the proximity of 450m from the bund

Well No	Distance from tank bund (m)	Break through conc. (ppb)	Velocity (m/day)	Velocity (cm/sec)
W17	367	3.1	287.9	0.333
W21	402	3.8	128.7	0.149
W19	407	5.9	65.6	0.076
W20	460	4.1	200.9	0.233

- Average number of day's rhodamine B detected 8.1 days

  Average first concentration detection 1.5 ppb

Average breakthrough day	4.7 days
Average break through concentration	3.7 ppb
Average seepage velocity	77 m/day / 0.09 cm/sec

8.8.2 Rhodamine B application in Sengulam Tank - Year 2009

In the year 2009, background fluorescence was measured for more than fifteen days before application of rhodamine B. Background fluorescence was found at 613 to 614 nm in the range of 3 to 4 ppb which is given in table 8.9

Table 8.9 Natural fluorescence & TDS in Sengulam Tank during 2009

Well No	Wavelength (nm)	Intensity (ppb)	TDS (ppm)
W1	613	2.98	917
W2	613	2.96	831
W3	613	3.03	711
W4	613	3.28	503
W5	614	3.42	439
W6	614	3.18	377
W7	614	3.11	462
W8	614	3.18	276
W9	614	3.06	217
W10	615	3.07	212
W11	614	3.22	248
W12	614	3.24	259
W13	614	3.31	384
W14	614	3.83	244
W15	613	4.35	113
W16	613	4.25	397
W17	614	4.32	348
W18	617	3.7[illegible]	380
W19	617	3.07	157
W20	614	3.04	604
W21	614	3.16	301
W22	614	3.44	379
W23	614	3.573	1070
W24	613	3.176	1240

Sengulam tank storage was approximately calculated from the depth versus storage curve 0.09 Mm^3 ie 90000 m^3 on 21.02.09. In the year 2008 very less rhodamine B fluorescence with limited number of days were detected. It was thought that it may be due to lesser quantity of rhodamine B application ie 16 ppb. Hence in the year 2009 it was planned to apply approximately at 30 ppb rhodamine B fluorescence

Hence

$$\text{Volume of dye required} = \frac{30 * 10^{-3} * 0.09 * 10^{9}}{200}$$

$$= 13500 \text{ lit}$$

$$= 2700 \text{ gm of rhodamine B powder.}$$

Dye application was carried out on 21.02.09 at 3.30 pm at sengulam tank. To be on higher side 3000 gm of rhodamine B was mixed with 6000 liters of tank water which was poured over the tank water at more than 30 locations. Water samples were collected from the tank and analysis schedule in shown in table 8.10.

As Sengulam Tank was poured with 3000 gm of rhodamine B, it had 75 ppb rhodamine B fluorescence after 1st day of dye application as shown in figure 8.13 which was slowly decreasing and becomes zero on 13.03.08. This was due to rainfall of 148.5 mm from 13.03.09 to 16.03.09 as given in the table 8.11. From 13.03.09, natural fluorescence was emitted at wavelength 540 to 560 nm whose values were very high as shown in figure 8.14.

Table 8.10 Schedule for dye study in the year 2009

Duration	Sample Collection	Purpose
02/2/09 to 21/02/09	Collection of tank water and Well water	To study natural fluorescence existence
21/02/09 at 3.30 pm	Rhodamine B of 3000 gm applied with 6000 liters of tank water	To estimate Groundwater velocity and zone of influence of the tank on command area wells
22/02/09 to 28/02/09	water samples collected daily	Rhodamine B was detected in 6 wells on 28/02/09. Rhodamine B was detected in 12 wells during early days. Rhodamine B was detected in 6 wells on 4/03/09. Rhodamine B was detected continuously till 13/03/09.
02/3/09 to 9/03/09	Water samples collected once in two days	Rhodamine B was continuously detected in most of the wells
10/03/09 to 23/03/09	Water samples collected once in three days	Rhodamine B was detected till 13/03/09. On 13/03/09 there was a heavy rainfall was there which was continued till 16/03/09. Due to this rainfall of 149 mm, the tank water was diluted and rhodamine B was not detected in the tank water and well water
28/03/09 to 16/04/09	Water samples were collected once in a week	Natural fluorescence were alone detected at 540 to 560 nm
29/04/09 to 24/05/09	Water samples were collected once in fifteen days	Natural fluorescence were alone detected at 540 to 560 nm
01/06/09	Water samples were collected monthly once	Natural fluorescence were alone detected at 540 to 560 nm

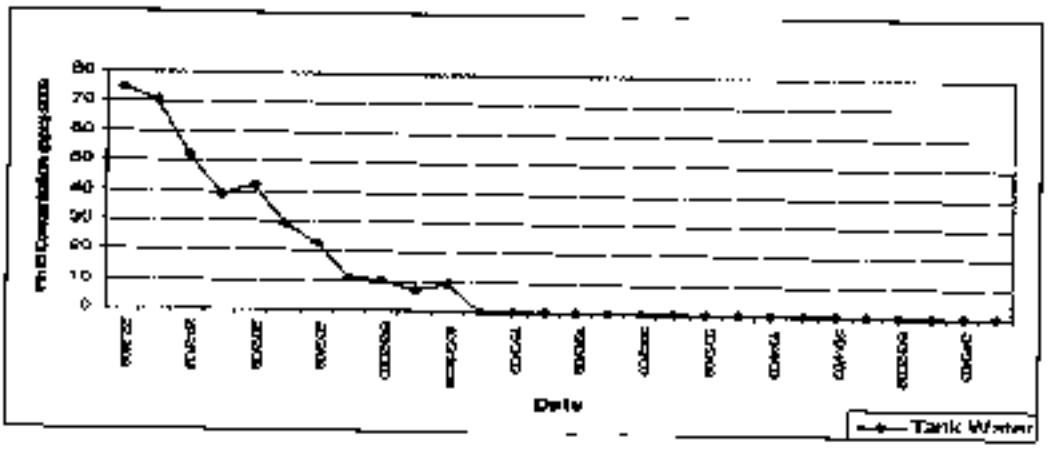

Figure 8.13 Rhodamine B fluorescence in the Sengulam Tank in the year 2009

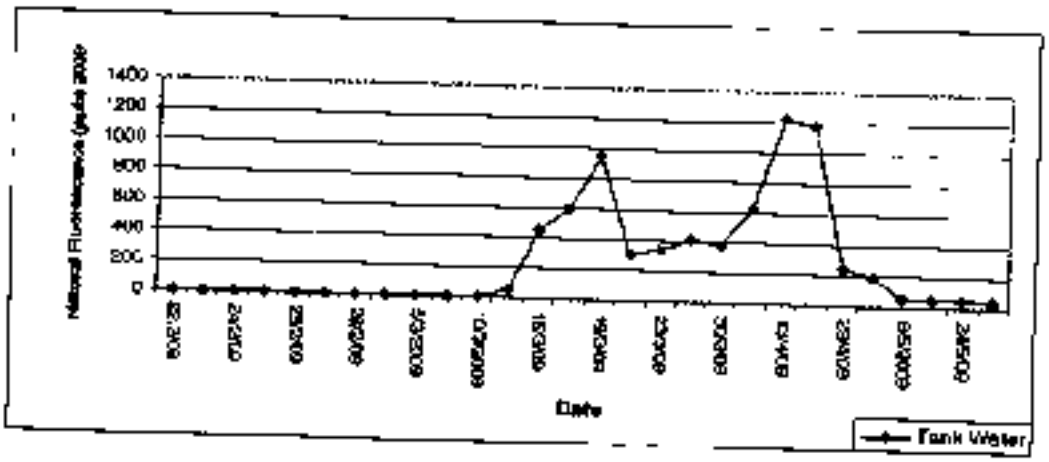

Figure 8.14 Natural fluorescence in the Sengulam Tank in the year 2009

Table 8.11 Rhodamine B and Natural fluorescence in the Sengulam tank during 2009

Date	Rainfall (mm)	Day	Tank water RF (ppb) at 571 nm	Tank water NF (ppb)
22/2/09		1	74.7	0
23/2/09		2	70.7	0
24/2/09		3	51.7	0
25/2/09		4	39.1	0
26/2/09		5	41.9	0
27/2/09		6	28.9	0
28/2/09		7	22.6	0
04/3/09		11	11.2	0
05/3/09		12	10.1	0
09/3/09		16	7.3	0
10/3/09		17	9.5	0
13/3/09	87.2	20	0	50.4
14/3/09	27.3	21	-	-
15/3/09	16.8	22	0	456.1
16/3/09	17.2	23	-	-
17/3/09		24	-	-
18/3/09		25	0	598.2
19/3/09		26	0	949.5
21/3/09		28	0	306.1
23/3/09		30	0	335
28/3/09		35	0	406.1
30/3/09		37	0	379.8
08/4/09		46	0	629.6
13/4/09		51	0	1228.6

16/4/09		54	0	1181.6
29/4/09		67	0	242.5
04/5/09		72	0	186.2
08/5/09		76	0	49.2
15/5/09		83	0	52.8
24/5/09		92	0	55.3
01/6/09		100	0	43.6
Total	148.5			

*** RF – Rhodamine B fluorescence NF – Natural fluorescence**

Table 8.12 First Detection Day of Rhodamine B

Wells	Day of Detection
W4 and W10	1st day
W21	1st day with 0.1 ppb
W3 and W12	just detected on 2nd day with 0.1 and 0.4 ppb
W1, W 9, W14, W19, and W2	5th day
W 5, W7, W8, W18 and W24	7th day
W 2, W6, W11, W22 and W23	11th day

Even though rhodamine B of 3000 gm was poured which was more than the year 2008, delayed dye detection was found. It is due to very less storage which did not provide enough head to drive the rhodamine B to the command area wells. Most of the wells received rhodamine B after 7 days that too sudden increased pumping by the farmers in the sengulam tank command area wells. This heavy pumping developed trough in the wells which might have invited the rhodamine B in to the wells after 7 days as shown in table 8.12

Rhodamine B was not detected after 13.03.09. Very high natural fluorescence were found in the wells as shown in figure 8.15 which were detected between 540 to 560 nm wave length. This natural fluorescence may

be due to soil and plant extracts washed out by the rainwater and tank water after rainfall. Table 8.13 gives the information about the rhodamine B first arrival day and concentration, break through day, break through concentration and ground water velocity.

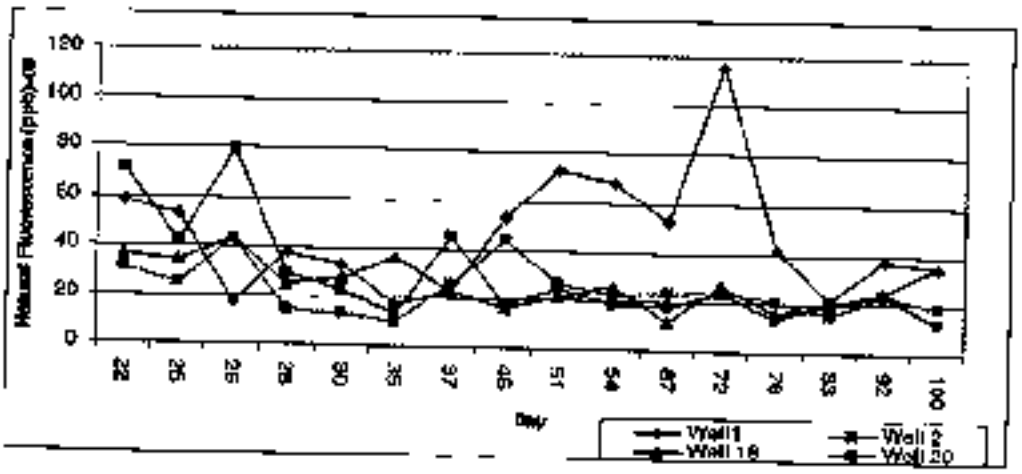

Figure 8.15 **Comparison of Natural fluorescence in Sengulam wells during 2009**

Table 8.13 **Analysis of Rhodamine B fluorescence detection in the Sengulam Tank during 2009**

WELLS	Distance from the bund (m)	Area Contribution (sq km)	No of days of conc. detection	Date of First Rh-B Detection	Day of First arrival (th Day)	Arrival Conc. (ppb)	Date of Break through	Peak found on (th Day)	Peak Conc. (ppb)	Velocity (m/day)
W1	49.1	0.024	7	26/2/09	5	0.7	13/3/09	20	2.4	2.46
W2	152.8	0.085	5	04/3/09	11	1.8	09/3/09	16	2.3	9.55
W3	163.6	0.039	7	23/2/09	2	0.1	04/3/09	11	6.5	14.87
W4	67.9	0.015	6	22/2/09	1	2.3	04/3/09	11	4.5	6.17
W5	29.7	0.008	6	28/2/09	7	2.4	05/3/09	12	7.5	2.48
W6	131.0	0.016	6	04/3/09	11	6.8	05/3/09	12	7.0	10.92
W7	281.2	0.030	7	28/2/09	7	1.3	10/3/09	17	7.5	16.54
W8	152.1	0.018	7	28/2/09	7	2.3	13/3/09	20	5.8	7.61
W9	66.0	0.011	8	25/2/09	4	2.9	10/3/09	17	5.5	3.88
W10	82.3	0.018	7	22/2/09	1	0.9	10/3/09	17	8.6	4.84
W11	49.7	0.012	6	04/3/09	11	2.7	10/3/09	17	6.6	2.92
W12	109.1	0.014	8	23/2/09	2	0.4	05/3/09	12	8.1	9.09
W13	198.0	0.017	6	27/2/09	6	1.8	10/2/09	17	4.3	11.65

W14	38.3	0.034	7	26/2/09	5	1.9	05/3/09	12	8.7	3.19
W16	298.4	0.018	6	22/2/09	1	0.1	05/3/09	12	9.3	24.87
W17	367.3	0.086	6	27/2/09	6	0.8	05/3/09	12	3.5	30.61
W18	287.9	0.023	6	28/2/09	7	0.1	04/3/09	11	4.0	26.17
W19	406.5	0.059	7	25/2/09	4	1.6	10/3/09	17	6.8	23.91
W20	459.2	0.058	6	26/2/09	5	2.8	10/3/09	17	3.6	27.01
W21	401.8	0.064	7	22/2/09	1	0.1	04/3/09	11	8.9	36.53
W22	257.3	0.018	5	04/3/09	11	1.8	13/3/09	20	2.8	12.87
W23	255.4	0.024	5	04/3/09	11	2.0	05/3/09	12	2.3	21.28
W24	261.2	0.074	6	28/2/09	7	1.2	05/3/09	12	3.5	21.77
Total			147.0		133.0	38.8		335.0	130.1	391.2
Average			6.4		5.8	1.7		14.6	5.7	14.4

Rhodamine B detection was entirely different during 2008 and 2009 which is explicitly seen in the figure 8.16a to 8.16w and also in the table 8.14

Major Findings of Rhodamine behaviors in the Sengulam tank;

- Natural fluorescence was detected at 613 nm during 2008 and 2009 before dye application;
- After rainfall natural fluorescence was detected at 612 - 627 nm during 2008 and 540 - 560 nm during 2009;
- Fluorescence of rainwater was detected at 554 – 630 nm wavelength;
- Detection of rhodamine B is not a function of the distance of the well from the source alone. It is dependent on type of soil, distribution of fractures. Mainly it depends on tank water head and pumping pattern in a command area wells. Rhodamine B was detected in one day during most of the wells during 2008. At the same time it was detected 7 to 11 days in most of the wells during 2009. This is because 2008 storage during dye application was 0.154 Mm^3 and 0.09Mm^3 during 2009. This is also very clearly seen in velocity of ground water during 2008 and 2009.

- Average velocity during 2008 was 77 m/day;
- Average velocity during 2009 was 14 m/day;
- No day rhodamine B was detected with injected concentration;

Average break through rhodamine B detection in the year 2008 was 3.5 ppb out of 16 ppb and in the year 2009, 5.4 ppb out of 33 ppb. Dye recovery was 22 percent in the year 2008 and 16 percent in the year 2009.

Rhodamine B was lost mainly by soil adsorption. Some losses might have taken by sunlight adsorption, variation in temperature Rhodamine was least resistant to soil adsorption.

- More no of days, detection was found in the year 2009 than 2008 since 3000 gms for 0.09 Mm^3 and 2500 gm for 0.154 Mm^3 during the year 2009 and 2008 respectively.

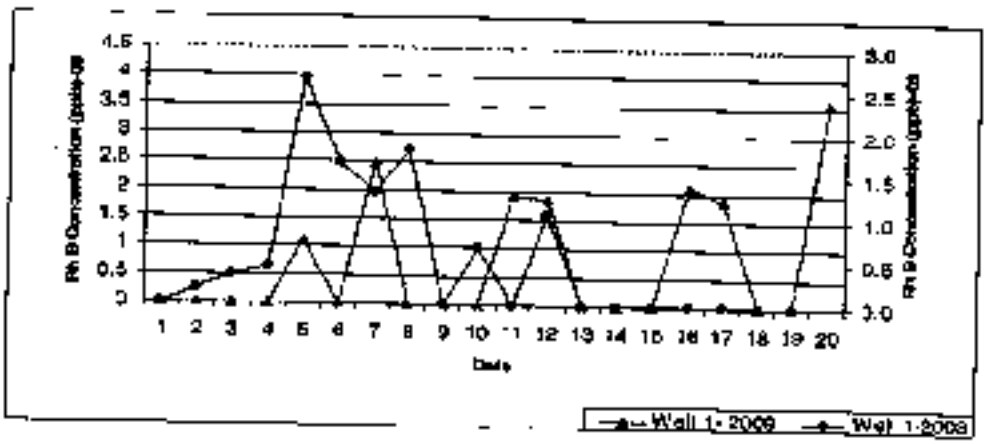

Figure 8.16a Comparison of Rhodamine B fluorescence between 2008 & 2009 in Well 1

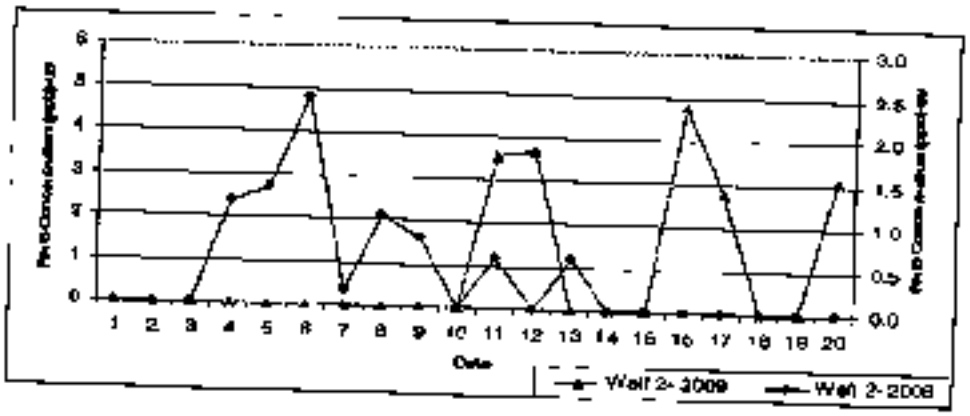

Figure 8.16b Comparison of Rhodamine B fluorescence between 2008 & 2009 in Well 2

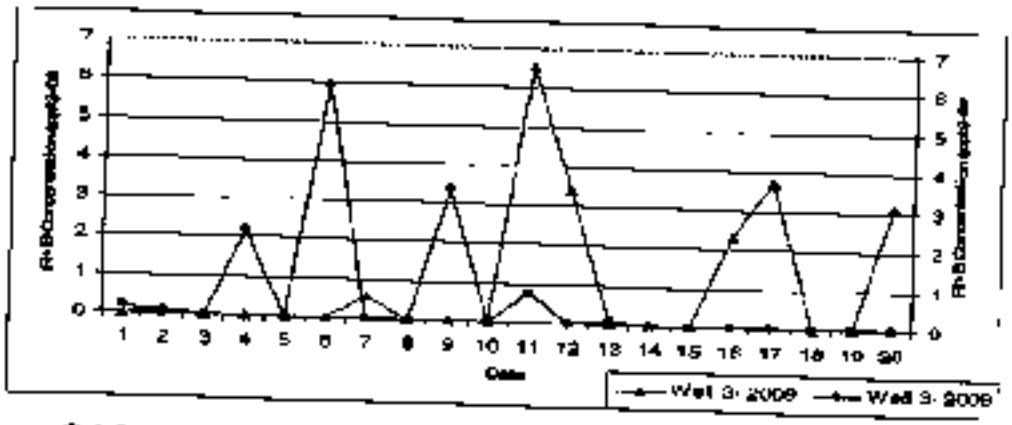

Figure 8.16c Comparison of Rhodamine B fluorescence between 2008 & 2009 in Well 3

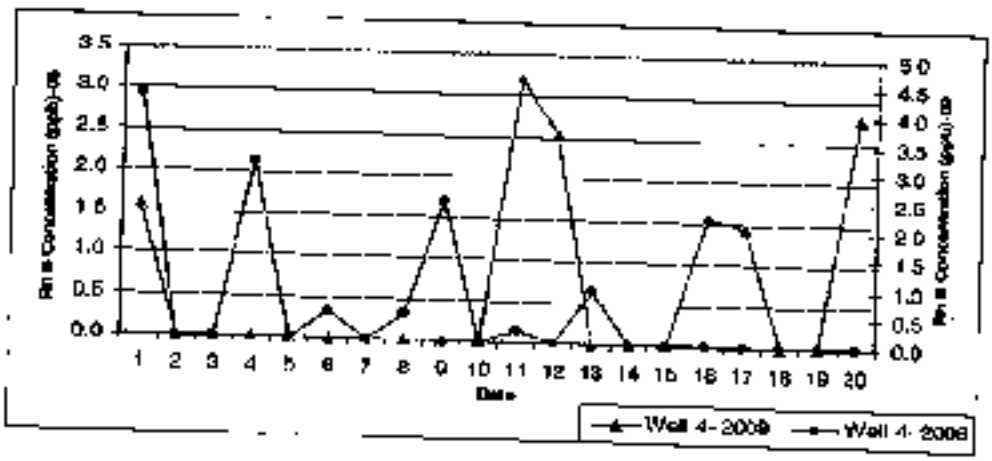

Figure 8.16d Comparison of Rhodamine B fluorescence between 2008 & 2009 in Well 4

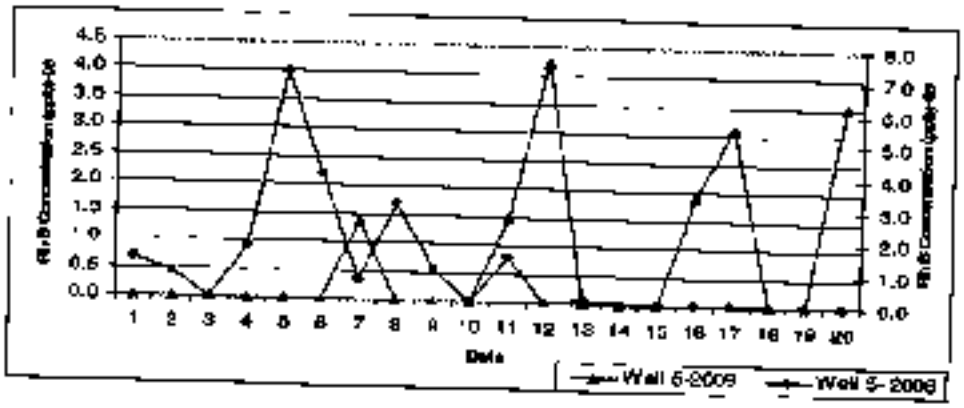

Figure 8.16e Comparison of Rhodamine B fluorescence between 2008 & 2009 in Well 5

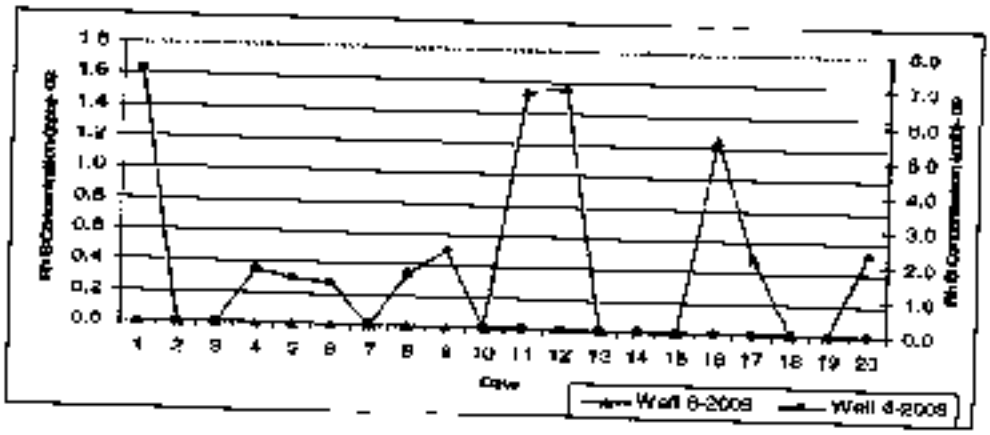

Figure 8.16f Comparison of Rhodamine B fluorescence between 2008 & 2009 in Well 6

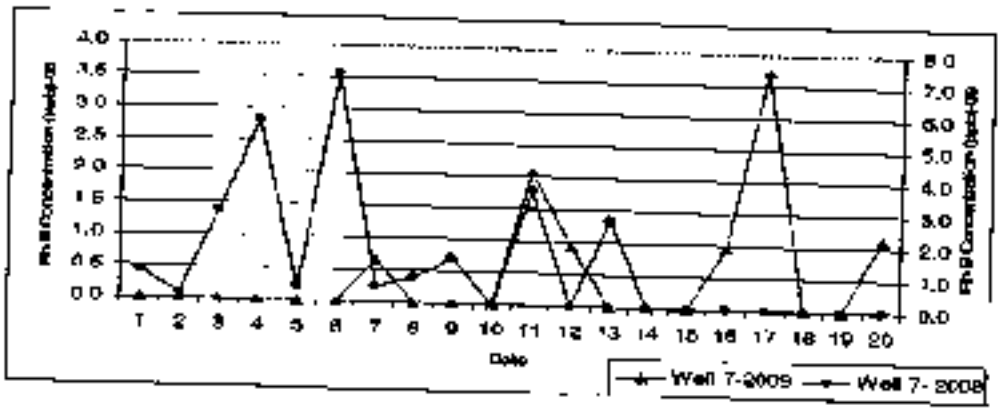

Figure 8.16g Comparison of Rhodamine B fluorescence between 2008 & 2009 in Well 7

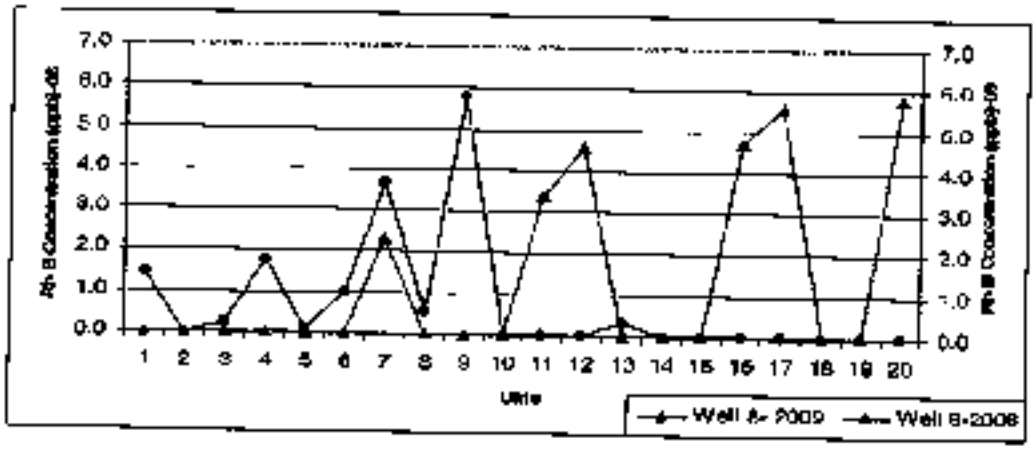

Figure 8.16h **Comparison of Rhodamine B fluorescence between 2008 & 2009 in Well 8**

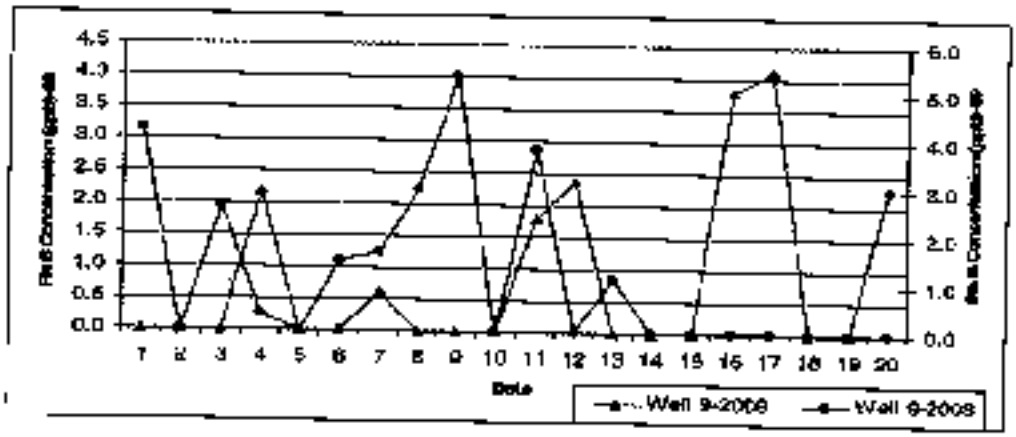

Figure 8.16i **Comparison of Rhodamine B fluorescence between 2008 & 2009 in Well 9**

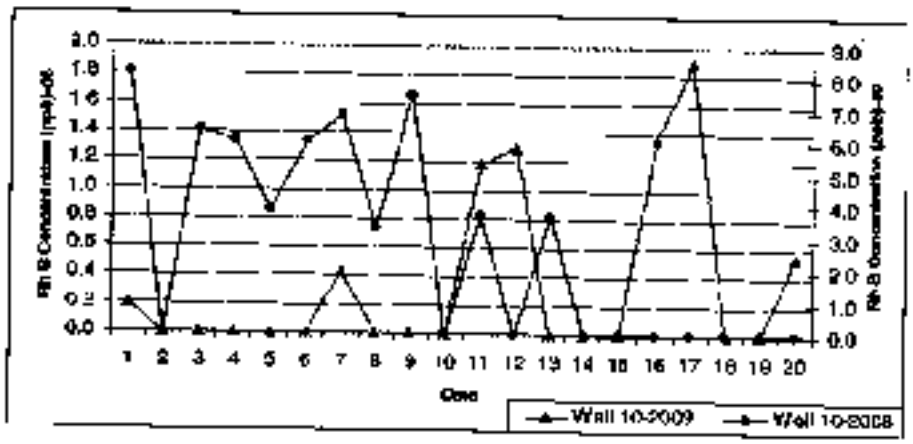

Figure 8.16j **Comparison of Rhodamine B fluorescence between 2008 & 2009 in Well 10**

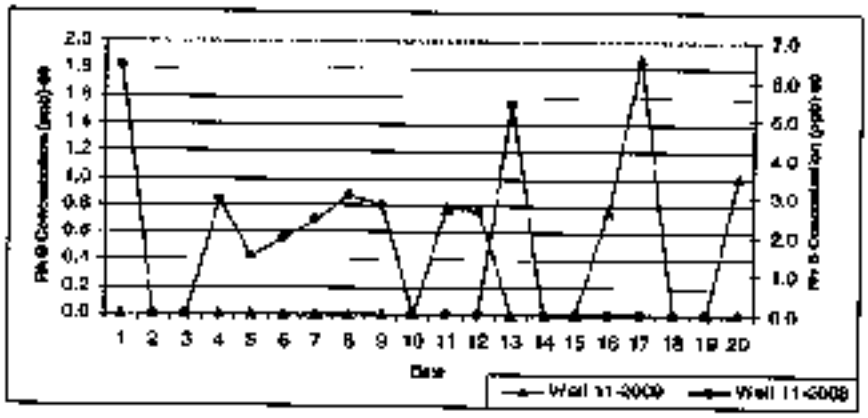

Figure 8.16k Comparison of Rhodamine B fluorescence between 2008 & 2009 in Well 11

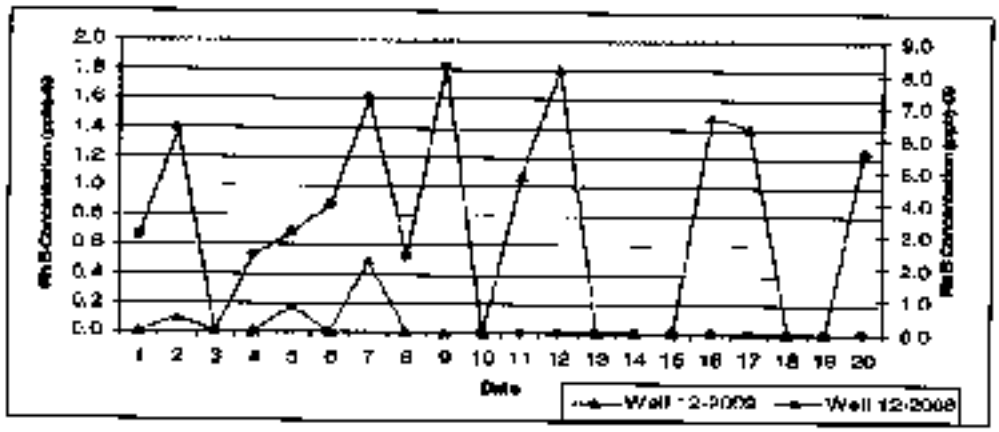

Figure 8.16l Comparison of Rhodamine B fluorescence between 2008 & 2009 in Well 12

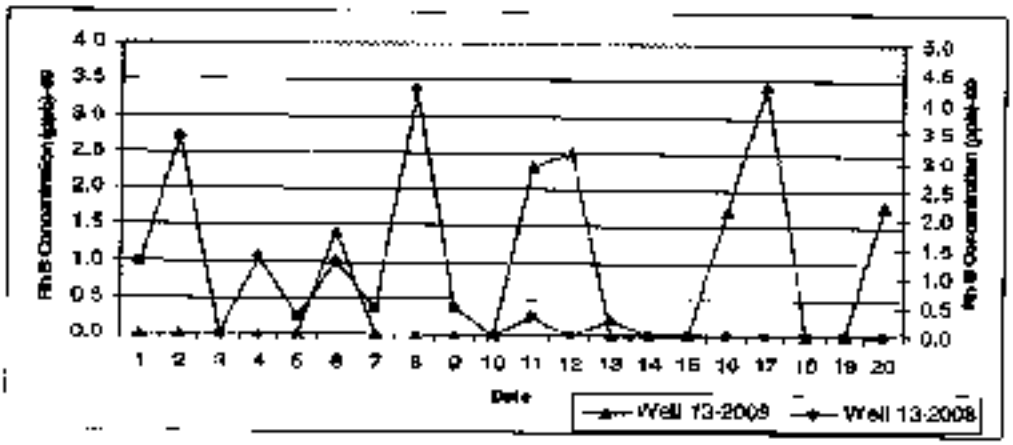

Figure 8.16m Comparison of Rhodamine B fluorescence between 2008 & 2009 in Well 13

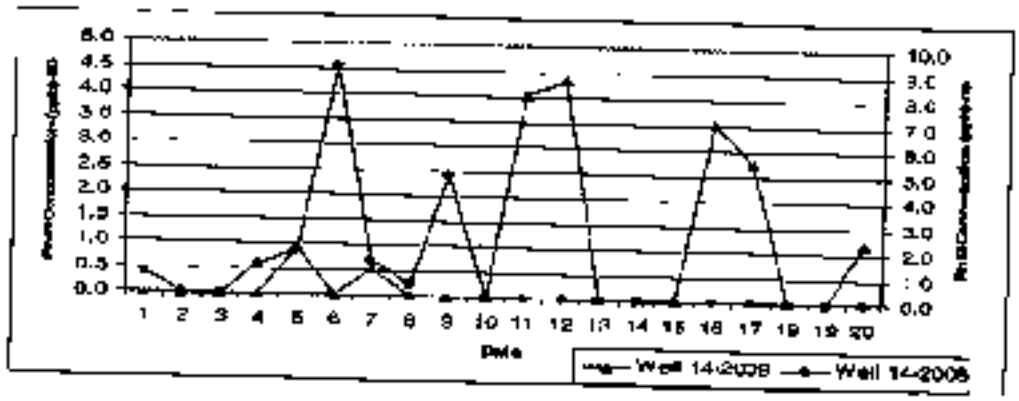

Figure 8.16n **Comparison of Rhodamine B fluorescence between 2008 & 2009 in Well 14**

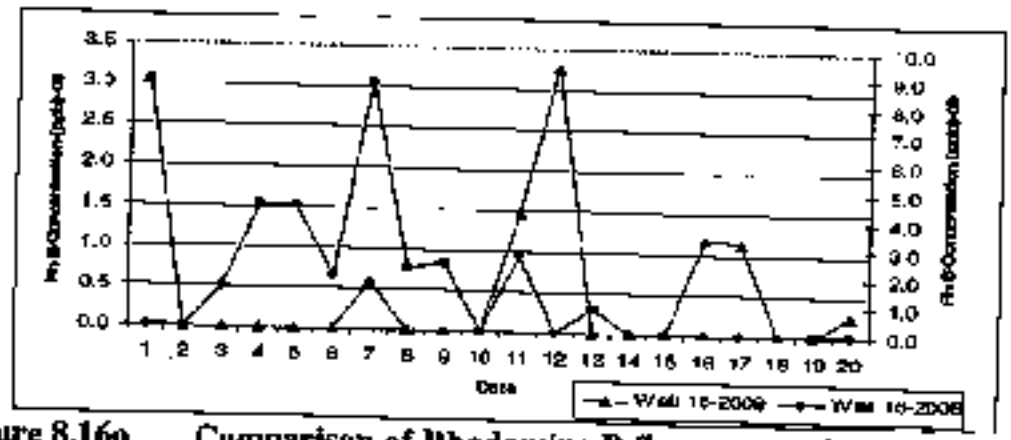

Figure 8.16o **Comparison of Rhodamine B fluorescence between 2008 & 2009 in Well 16**

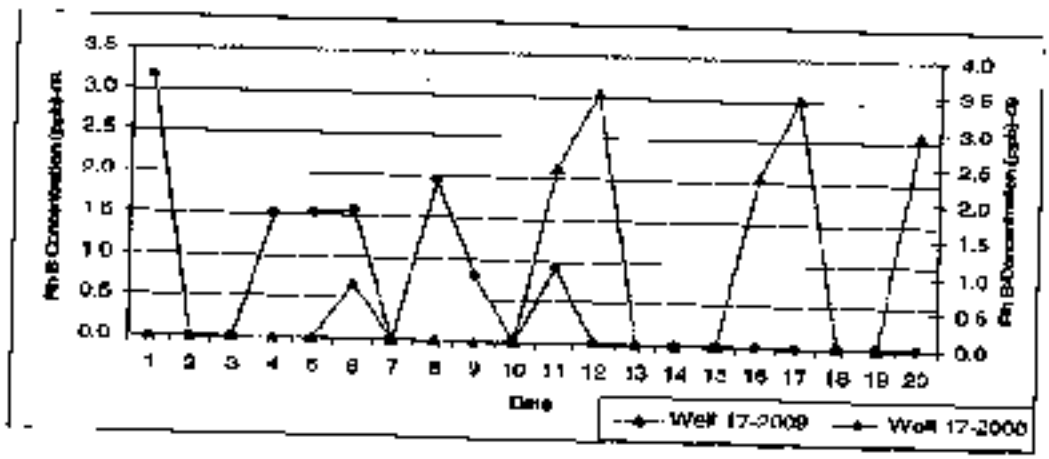

Figure 8.16p **Comparison of Rhodamine B fluorescence between 2008 & 2009 in Well 17**

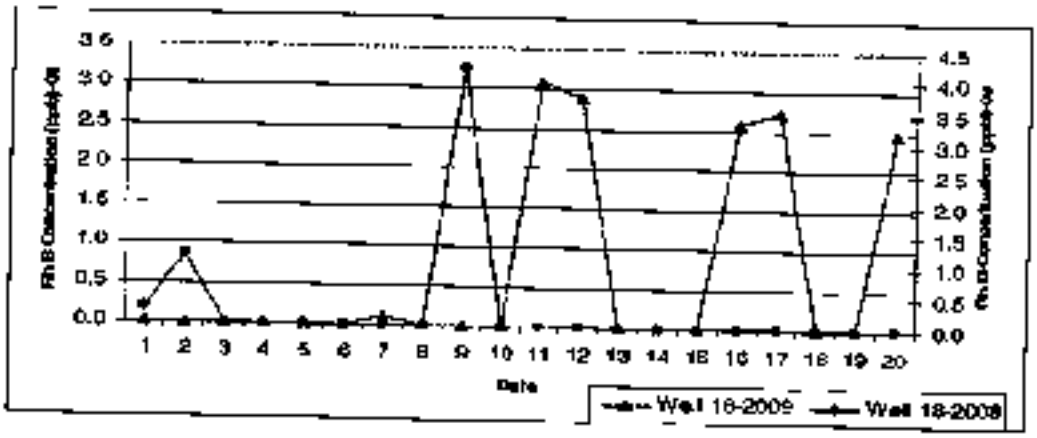

Figure 8.16q Comparison of Rhodamine B fluorescence between 2008 & 2009 in Well 18

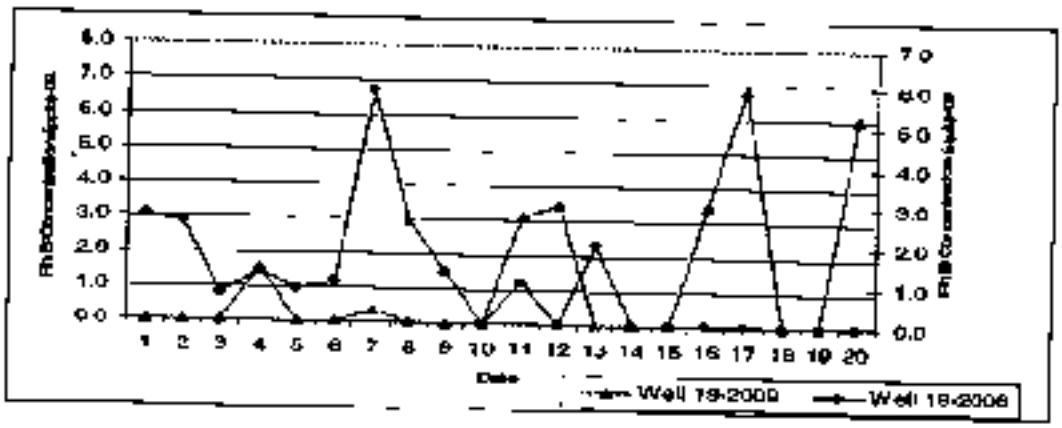

Figure 8.16r Comparison of Rhodamine B fluorescence between 2008 & 2009 in Well 19

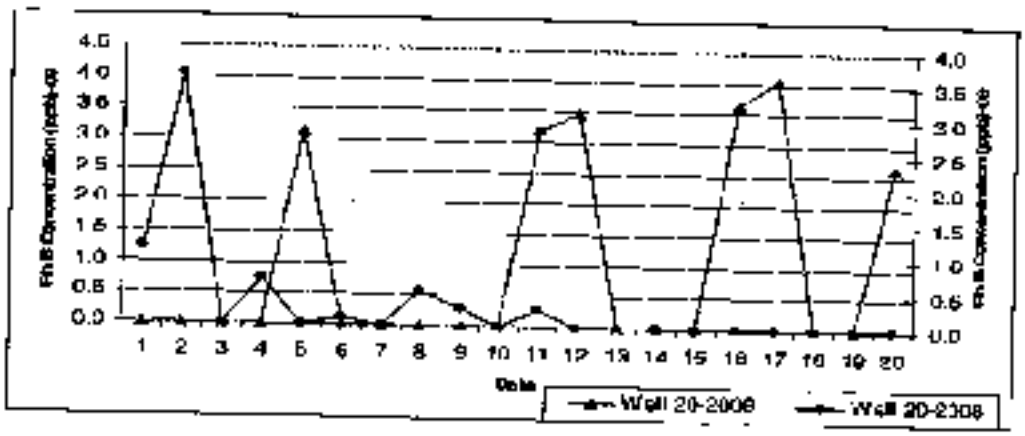

Figure 706 8.16s Comparison of Rhodamine B fluorescence between 2008 & 2009 in Well 20

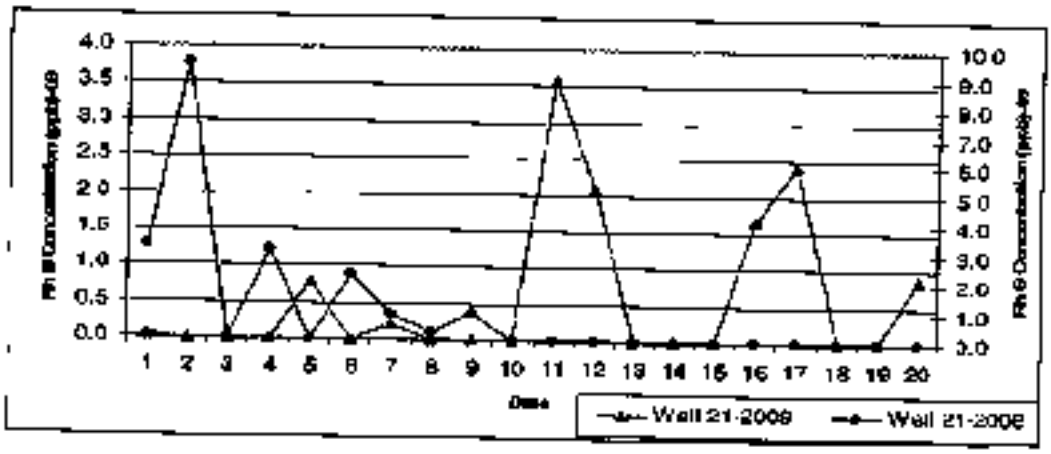

Figure 8.16t Comparison of Rhodamine B fluorescence between 2008 & 2009 in Well 21

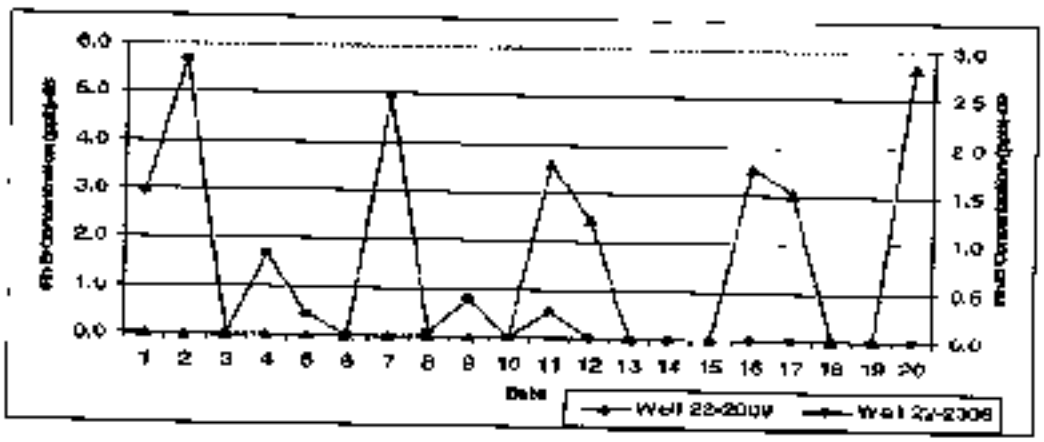

Figure 8.16u Comparison of Rhodamine B fluorescence between 2008 & 2009 in Well 22

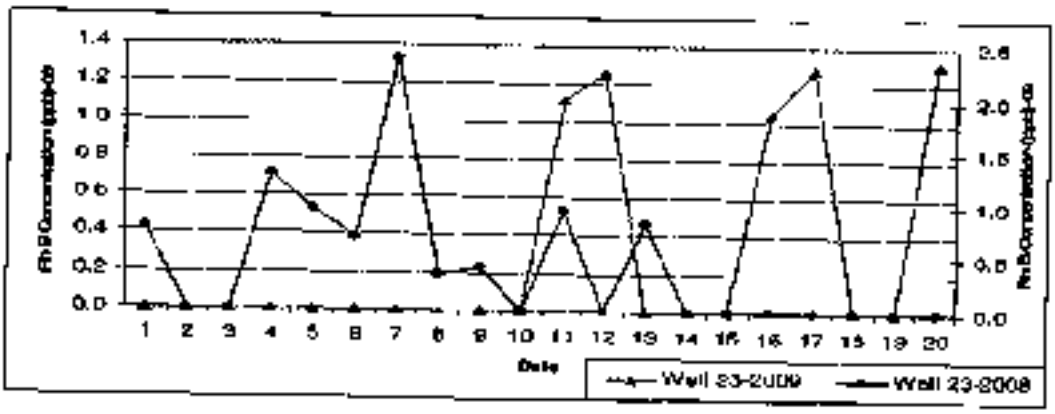

Figure 8.16v Comparison of Rhodamine B fluorescence between 2008 & 2009 in Well 23

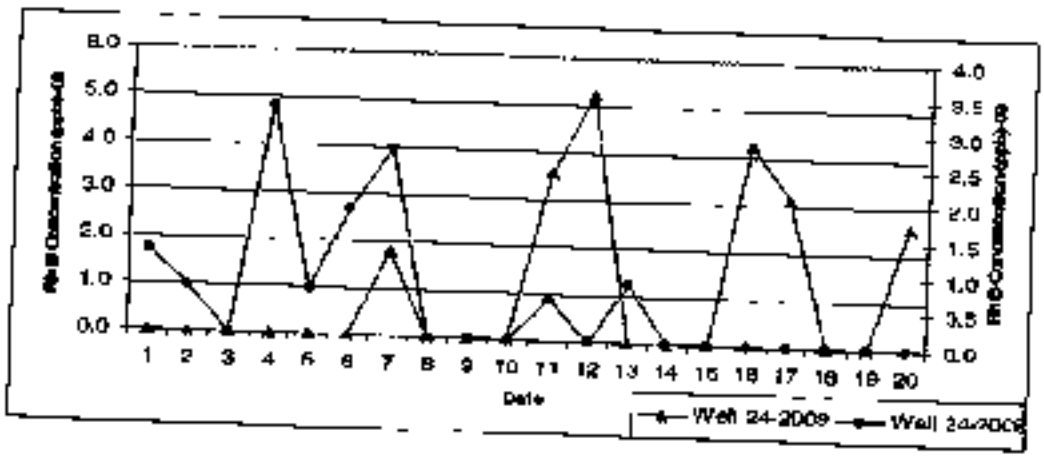

Figure 8.16w **Comparison of Rhodamine B fluorescence between 2008 & 2009 in Well 24**

Table 8.14 Comparison of ground water velocity between the year 2008 and 2009

Wells	Distance from the bund (m)	Area Contribution (sq km)	No. of days of conc. Detection - 2008	No of days of conc. Detection - 2009	Day of First arrival (th Day)-2008	Day of First arrival (th Day) - 2009	Arrival Conc. (ppb)-2008	Arrival Conc. (ppb)-2009	Peak found on (th Day)-2008	Peak found on (th Day)-2009	Peak Conc. (ppb)-2008	Peak Conc. (ppb)-2009	Velocity (m/day)-2008	Velocity (m/day)-2009
W5	29.7	0.008	10	6	1	7	0.70	2.4	5	12	4.0	7.5	5.9	2.5
W14	38.3	0.034	7	7	1	5	0.40	1.9	6	12	4.5	8.7	6.4	3.2
W1	49.1	0.024	9	7	3	5	0.20	0.7	6	20	4.0	2.4	8.2	2.5
W11	49.7	0.012	8	6	1	11	1.80	2.7	1	17	1.8	6.6	49.7	2.9
W9	66.1	0.011	9	8	1	4	3.20	2.9	9	17	4.0	5.5	7.3	3.9
W4	67.9	0.015	7	6	1	1	2.90	2.3	1	11	2.9	4.6	67.9	6.2
W10	82.3	0.018	10	7	1	1	1.80	0.9	1	17	1.8	8.6	82.3	4.8
W12	109.1	0.014	8	8	1	2	0.70	0.4	1	12	1.8	8.1	109.1	9.1
W6	131.1	0.016	6	6	1	11	1.60	6.8	1	12	1.6	7.0	131.0	10.9
W8	152.1	0.018	9	7	1	7	1.40	2.3	9	20	5.8	5.8	16.9	7.6
W2	152.8	0.085	8	5	4	11	2.40	1.8	6	16	4.8	2.3	25.5	9.6
W3	163.6	0.039	5	7	4	2	0.20	0.1	6	11	5.9	6.5	27.3	14.9
W13	198.1	0.017	10	6	1	6	1.00	1.8	8	17	3.4	4.3	24.8	11.6
W22	257.3	0.018	8	5	1	11	2.90	1.8	2	20	5.7	2.8	128.7	12.9
W23	255.4	0.024	9	5	1	11	0.40	2.0	7	12	1.3	2.3	36.5	21.3

W24	261.2	0.074	8	6	1	7	1.70	1.2	4	12	4.8	3.5	65.3	21.8
W7	281.2	0.030	11	7	1	7	0.40	1.3	6	17	3.6	7.5	46.9	16.5
W18	287.9	0.023	3	6	1	7	0.20	0.1	9	11	3.2	4.0	32.0	26.2
W16	298.4	0.018	10	6	1	1	3.10	0.1	7	12	3.1	9.3	42.6	24.9
W17	367.3	0.086	7	6	1	6	3.20	0.8	1	12	3.1	3.5	367.3	30.6
W21	401.8	0.064	7	7	1	1	1.30	0.1	2	11	3.8	8.9	200.9	36.5
W19	406.5	0.059	11	7	1	4	2.70	1.6	7	17	5.9	6.8	58.1	23.9
W20	459.2	0.058	7	6	1	5	1.20	2.8	2	17	4.1	3.6	229.6	27.0
Total			170.0	134.0			34.3	34.5	96.0	311.0	76.4	113.9	1757.7	325.5
Average			7.1	5.6			1.4	1.4	4.0	13.0	3.2	4.7	76.4	14.2

8.8.3 Rhodamine B application in Ponpadi Tank - Year 2009

Before applying rhodamine B in the Ponpadi tank, background samples were collected from the tank and wells over two weeks. For this about 31 wells were considered which contain both open wells, shallow and deep bore wells.

Natural Fluorescence

Natural fluorescence were found which were detected at different emission wavelength

- During September 2008, natural fluorescence were detected at 613 - 616 nm wavelength whose fluorescence were 10 to 15 ppb;
- Natural fluorescence was 3 to 4 ppb at 614 nm wavelength were detected during October 2008;
- During November 2008 it was 2 ppb at 614 nm wavelength;
- After (rainfall) monsoon ie. during December 2008 the natural fluorescence were detected at 560 nm wavelength. Its fluorescence ranged between 7 and 13 ppb;
- Before the application of rhodamine B the samples were collected continuously for fifteen days. In which no rhodamine B was detected. Natural fluorescence was detected at 550 to 560 nm wavelengths which are given below.

Wells	Intensity	Natural fluorescence (ppb)	TDS (ppm)
R1	0.036	2.9	423
R3	0.03	2.1	414
R4	0.029	1.97	412
R5	0.032	2.37	411
L1	0.028	1.84	541
L2	0.026	1.6	561
L4	0.03	2.1	570
L6	0.033	2.5	563
L7	0.049	4.6	710
L8	0.034	2.6	828
L9	0.036	2.89	826
P1	0.03	2.1	433

With this background information rhodamine B application was conducted at 3 pm on 15.02.09 after discussing with the farmers to get their consent. During that time the tank storage was 0.28 Mm^3 approximately which was one fourth capacity of the tank. Initially it was tried for 5 ppb concentration in the tank. For this 1400 gm of rhodamine was mixed with 2800 liters of tank water and poured into tank at various locations. On the same day of dye application 15.02.09, samples from the tank were collected from the tank at various locations and analyzed for rhodamine B fluorescence which was about 34.9 ppb Samples were collected daily from the tank which are given in table 6.15

Table 8.15 Rhodamine B Fluorescence in the Poupadi Tank in the First Trial

Date	Concentration (ppb)
15/02/09	34.9
16/02/09	22.91
17/02/09	11.6
18/02/09	6.2
19/02/09	5.9
20/02/09	4.1
23/02/09	3.1

After 23rd of February 2009 the rhodamine B fluorescence was below detection level in the tank water. Similarly samples were collected from the wells; no wells received the rhodamine B except few wells R1, R3, R4 and R5 that too with very less fluorescence of 1 to 3 ppb. Samples were collected daily from 16.02.09 to 2.03.09. Rhodamine B was not detected in any of the day except few wells very closer to the tank. This made us to re do the exercise on 3.03.09. Approximately about 4500 gm of rhodamine B was mixed with 9000 liters of water and poured into tank on 3.03.09. The sample from the tank was collected on the same day (3.03.09) of dye application at four locations which were about 86.9, 73 3, 114.6 and 81.7 ppb. The schedule of the rjodamine B application and collection were shown in table 8.16

Table 8.16 Schedule of rhodamine B study at Ponpadi tank during 2009

Duration	Sample Collection	Purpose
1/02/09 to 15/02/09	Sample was collected from the tank and wells	Natural fluorescence were detected at 555 to 560 nm wavelength
15/02/09	Rhodamine B of 1400 gm applied	Dye application at 3.00 pm
16/02/09	Water sample were collected from the tank and wells	Rhodamine B was not detected in the wells
16/02/09 to 2/03/09	Water sample collection	Rhodamine B was detected in very few wells R1, R2, R4 and R5
3/03/09	4500 gm of rhodamine B was applied	Dye application
4/03/09 to 23/05/09	Sample were collected once in two or three days	- Rhodamine B was detected at various wells till 21/3/09 - from 21/03/09 to 8/4/09 some of the wells received - After 8/04/09 no wells were detected with rhodamine B

Initial concentration of rhodamine B in the tank was high 47.1 ppb. On 4.03.09 which was got mixed and started reducing as shown in figure 8.12. After 37 days (23.03.09) of dye application, rhodamine B fluorescence

had become nil in the tank. From 13.04.09 natural fluorescence were detected at 555 to 560 nm wavelength which is shown in the figure 8.18

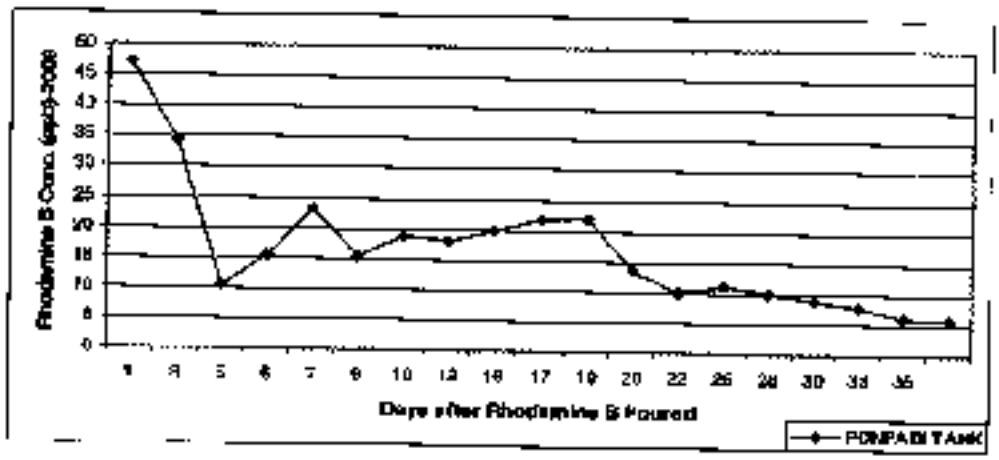

Figure 8.17 Rhodamine B fluorescence in the Ponpadi Tank during 2009

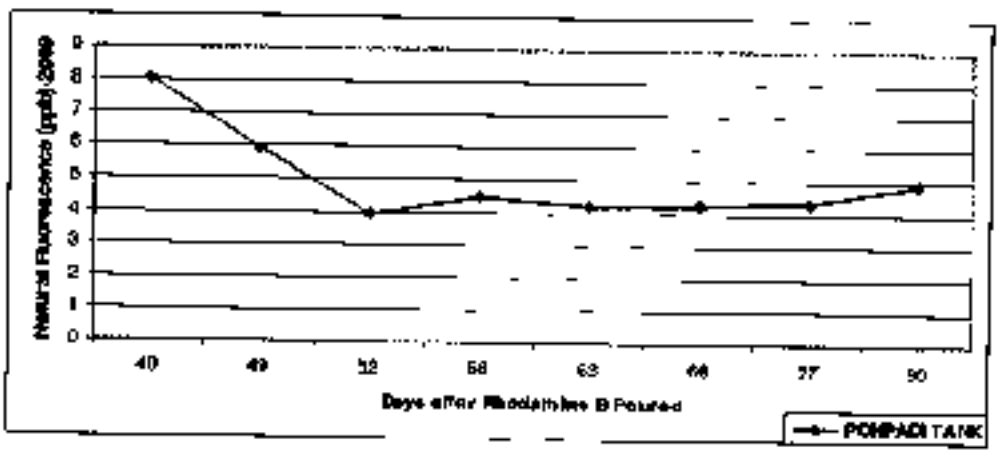

Figure 8.18 Natural fluorescence in the Ponpadi Tank during 2009

From next day (4/3/09) of rhodamine B application samples were collected from the tank and also from the selected wells such as R1, R3, R4, R5 L1, L2, L3, L4, L5, L6, L7, L8, L9, L12, L15, L16, L17, L21 P1, P2, P3, P4, P5, P6, P7 and P11

- Wells R1, R3, R4 and R5 received rhodamine B first day after dye application and continued to be detected for 20 days which ranged between 7 ppb and 1ppb as shown in figure 8.19. Above said wells are

lying very close to the tank to a distance of 54 to 95 m in which pumping was usually very less.

- Similarly rhodamine B was detected in one day in the wells L1 to L7 which were also open wells which are lying 130 m and 95 m from the tank bund as shown in figure 8.20 pumping in the wells L1 and L7 were 45 m^3/day during February and 25 m^3/day during February and March 2009 respectively as shown in table 8.18
- Rhodamine B was detected on 3rd day in the wells L4 and L6 which lies 233 m and 158 m from the tank bund as shown in figure 8.21.
- In the wells L2, L12, L15, and L16 rhodamine B was detected on 5th day whose distance from the tank bund was 422, 451, 452 and 473 m as shown in figure 8.22.
- Rhodamine B was detected on 3rd day in the wells L7 and L9 which is at a distance of 616 and 633 m from the tank bund as shown in figure 8.23.
- In the case of a well L17, the rhodamine B was detected on 9th day which lasted for few days with very less fluorescence well L17 is at a distance 866 m from the tank bund as shown in. In the well L21, rhodamine B was detected on 5th day as shown in figure 8.24.
- Wells P1, P2, P4, P5, P6, P7 and P11 are lying 231 m to 631 m from the tank bund whose well depths are 50 m to 105 m. Even though pumping in these wells were more, rhodamine B was detected only after 19 days that too for few days with very less fluorescence. Dye was not at all detected in the bore wells P5 and P11. P5 and P11 are deep wells which are located at a depth more than 100 m as shown in table 8.17
- Table 8.18 gives information about rhodamine B first arrival day and concentration, break through day, break through concentration and ground water velocity.

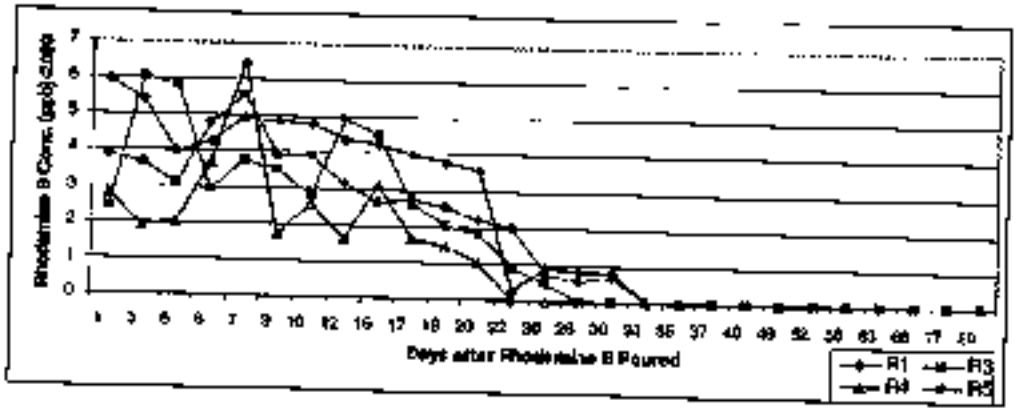

Figure 8.19 **Rhodamine B Detection in the Open wells of Ponpadi tank command area in the year 2009**

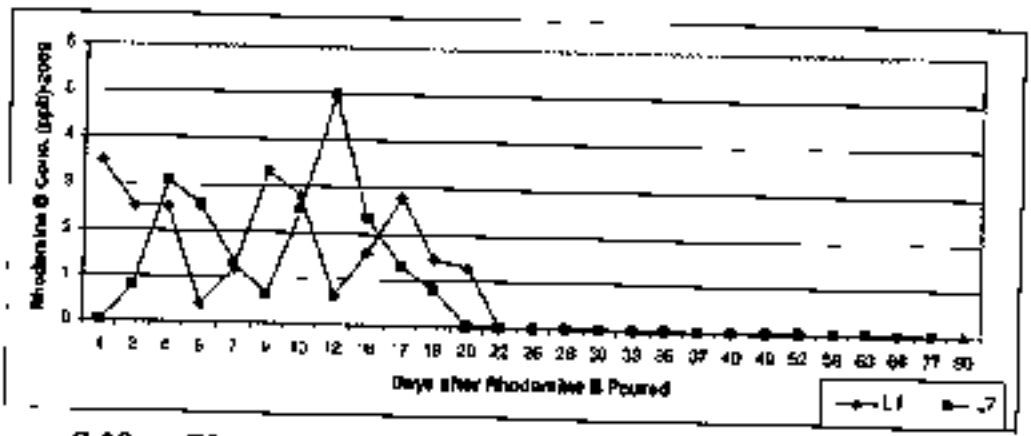

Figure 8.20 **Rhodamine B Detection in the shallow bore wells L1 & L7 of Ponpadi tank command area in the year 2009**

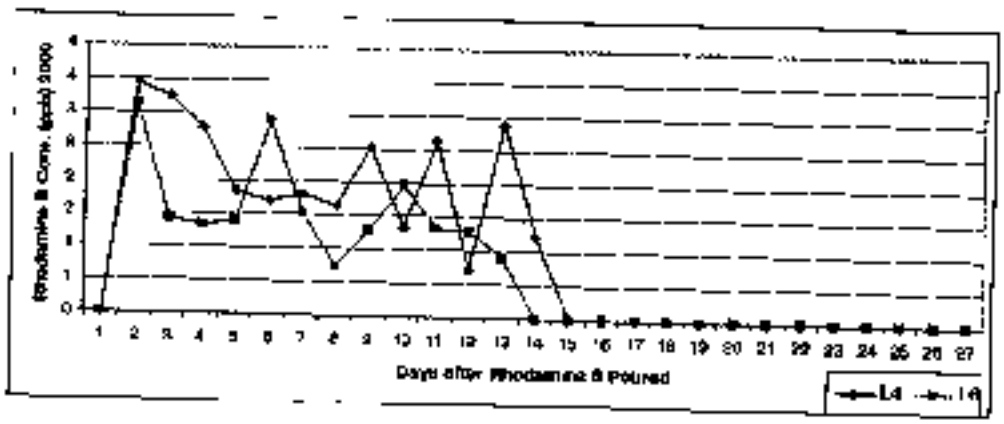

Figure 8.21 **Rhodamine B Detection in the shallow bore wells L4 & L6 of Ponpadi tank command area in the year 2009**

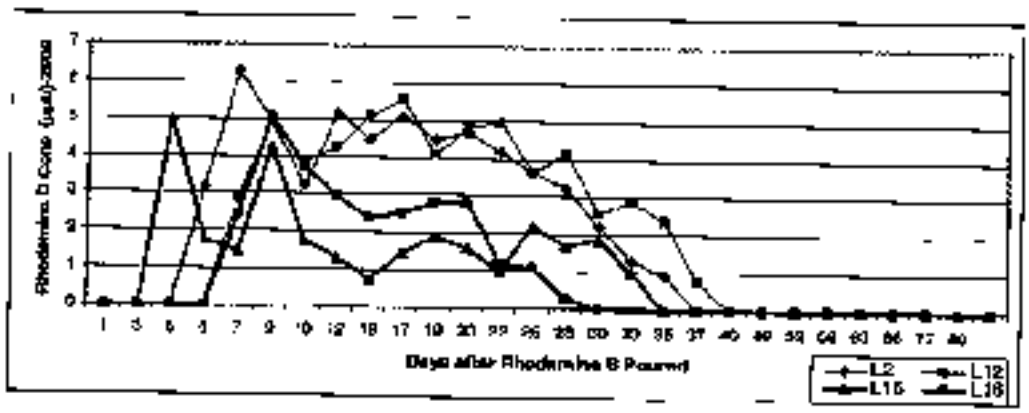

Figure 8.22 **Rhodamine B Detection in the shallow bore wells L2, L12, L15, and L16 of Ponpadi tank command area in the year 2009**

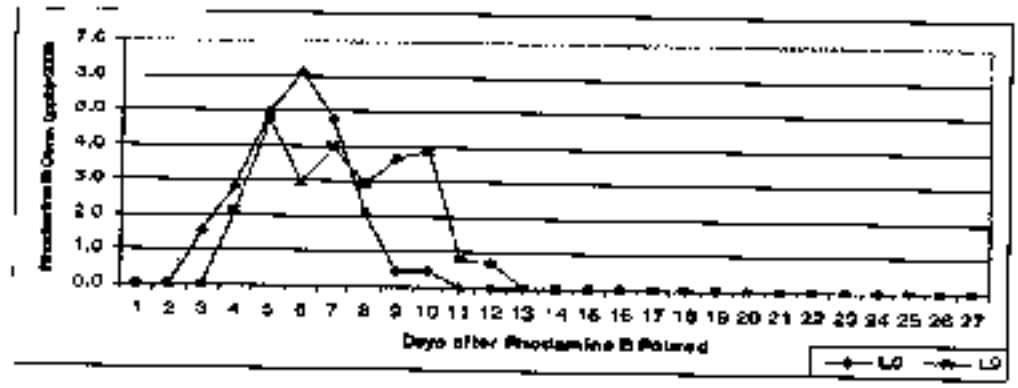

Figure 8.23 **Rhodamine B Detection in the shallow bore wells L8 & L9 of Ponpadi tank command area in the year 2009**

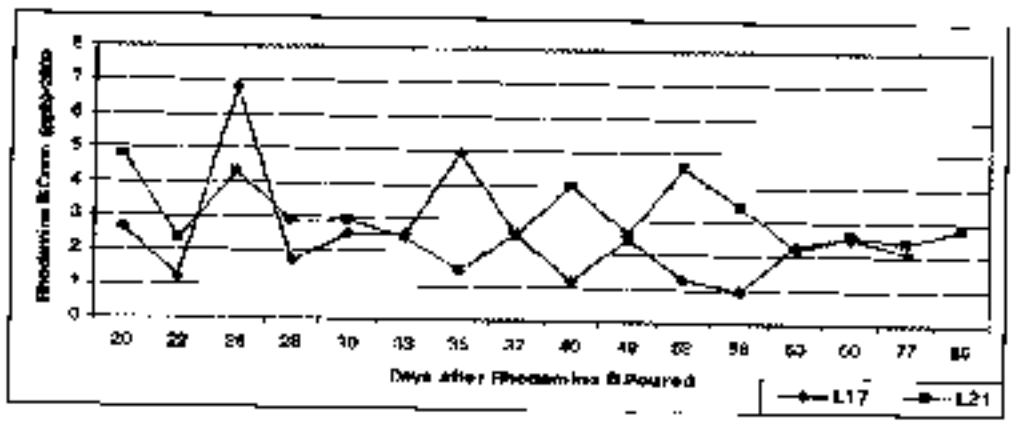

Figure 8.24 **Rhodamine B Detection in the shallow bore wells L17 & L21 of Ponpadi tank command area in the year 2009**

Table 8.17 Rhodamine B Detection in the Deep Bore wells

Date	Days	P1	P6	P2	P4	P7	P5	PI1
23/03/09	19		1.7					
24/03/09	20		1.3	1.1	0.2	0.9		
26/03/09	22	1.8	0.7	0.3	2.5			
30/03/09	26	1.3		0.6	0.7			

Table 8.18 Analysis of Rhodamine B fluorescence Detection in the Poupadi Tank during 2009

Wells	Distance from the bund (m)	Area Contribution (sq km)	No of days of conc. detection	Date of First Rh-B Detection	Day of First arrival (th Day)	Arrival Conc. (ppb)	Date of Break through	Peak found on (th Day)	Peak Conc. (ppb)	Velocity (m/day)
R1	94.60	54230	16	04/3/09	1	6.0	04/3/09	1	6	94.6
R3	80.50	64200	14	04/3/09	1	2.4	07/3/09	3	6	26.8
R4	88.60	63940	12	04/3/09	1	2.8	11/3/09	7	6.5	12.7
R5	54.30	64120	16	04/3/09	1	3.8	11/3/09	7	5.6	7.8
L1	129.5	99280	12	04/3/09	1	3.5	04/3/09	1	3.5	129.5
L2	422.2	11050	15	10/3/09	6	3.2	11/3/09	7	6.3	60.3
L4	233.6	12070	13	07/3/09	3	3.4	07/3/09	3	3.4	77.9
L6	158.3	45840	12	07/3/09	3	3.1	07/3/09	3	3.1	52.8
L7	95.60	65080	10	04/3/09	1	0.8	07/3/09	3	3.1	31.9
L8	616.3	13902	8	09/3/09	5	1.6	13/3/09	9	6.2	68.5
L9	633.2	14010	15	10/3/09	6	2.1	11/3/09	7	4.7	90.5
L12	451.8	11029	15	10/3/09	6	2.9	20/3/09	16	5.6	28.2
L15	452.7	37082	15	07/3/09	3	5.0	07/3/09	3	5	150.9
L16	473.7	37660	11	10/3/09	6	2.4	13/3/09	9	3.7	52.6
L17	865.9	28730	7	13/3/09	9	1.1	14/3/09	10	2.6	86.6
L21	279.4	19460	8	10/3/09	6	4.3	11/3/09	7	5.6	39.9
P1	231.1	96720	2	26/3/09	22	1.8	26/3/09	22	1.8	10.5
P2	414.6	10834	3	24/3/09	20	1.1	24/3/09	20	1.1	20.7
P4	374.7	69940	3	24/3/09	20	0.2	26/3/09	22	2.5	17.0
P5	506.5	15890	Nil	—		Nil			Nil	
P6	70.90	65260	3	23/3/09	19	1.7	23/3/09	19	1.7	3.7
P7	471.3	16210	1	24/3/09	20	0.9	24/3/09	20	0.9	23.6
P11	661.4	32950	Nil			Nil			Nil	
		Total	211		160.0	54.1		199.0	84.9	1086.9
		Average	10.0		7.6	2.6		9.5	4.0	51.8

Inference

i. As the wells R1, R3 R4 and R5 are very closer to the tank bund it has recovered rhodamine B with in one day. Even though pumping in these wells were not there.

ii. Other wells have L1, L2, L4, L6, L7, L8, L9, L12, L15, L16, L17 and L21 received rhodamine B depending upon its depth with respect to tank elevation, distance from tank bund and its pumping rate. If pumping is more those wells have received the dye with in one day as shown in the table 8.19

iii. Pumping was carried out in the open wells R4 and R5 only during January 2009 as shown in table 8.20

iv. Deep bore wells P1, P2, P4, P5, P6, P7 and P11 have received rhodamine B for limited days may be due to its depth

v. Since entire Ponpadi tank water was released on 1.04.09 by the fisher man, tank had very very little water.

vi. Even after release of water from the tank some of the wells were with rhodamine B fluorescence which may be due to the presence of rhodamine B in the command area which gets circulated with in it.

vii. Actual recovery in the wells are given in the table 8.21. recovery of rhodamine B was comparatively high 38 percent in the open wellss R1, R3, R4 and R5. Shallow borewells L1 to L21 were 27 percent and in deep borewells 10 percent.

Table 8.19 **Pumping rate at Ponpadi bore wells during February – April 2009**

Wells	Distance (m)	February		March		April	
		m^3/day	days	m^3/day	days	m^3/day	days
L1	130	45	19	28.5	15	25	13
L7	95	45	21	25	20	21	23
L4	233	54	24	33	20	33	23
L5/L6	158	53	24	34	8	26	24
L2	422	48	22	26	21	15	6
L12	452						
L15	453	29.3	18	20.6	15	15	10
L16	473						
L8	616	60	20	38	20	30	20
L9	633	68	23	46	24	31	25
L17	866	53	21	33	21	24	21
P1	231	48.3	23	28	21	24	24
P2	414	47	17	24	17	16	11
P4	375	41	16	32	22	18	22
P5	506	57	21	39	24	29	24
P6	71	45	21	25	20	21	23
P7	471	37	15	25	20	24	3
P11	661	61	22	44	20	29	20

Table 8.20 Pumping Rate at Ponpadi Open wells during February – April 2009

Wells	Distance (m)	February	March	April	Remarks
R1	95	Open Well	Open Well	Open Well	No pumping during February, March, April
R3	81				
R4	89	Bore Well	Bore Well	Bore Well	- Pumping was for 6 to 10 hrs during January 2009 - No pumping during February, March, April
R5	54				

Table 8.21 Percent Recovery of Rhodamine B from the Ponpadi Wells

Wells	Recovery	Remarks
R1	38	Open wells: Comparatively high percentage of recovery Average Recovery was 38 percent
R2	38	
R4	41	
R5	35	
L1	22	Open wells and shallow Bore well: Medium recovery of rhodamine B Average recovery was 27 percent
L2	39	
L4	21	
L6	19	
L7	19	
L8	39	
L9	29	
L12	35	
L15	31	
L16	23	
L17	16	
L21	35	
P1	11	Deep Bore wells: Least recovery of rhodamine B Average recovery was 10 percent
P2	7	
P4	16	
P6	11	
P7	6	

8.8.4 Findings from Dye Study

Most of the studies recommended to use at least three or more dyes to evaluate which is highly suitable for particular soil and water due to non availability of other dyes in the Indian market, Rhodamine-B alone used for groundwater tracing at both the study area sengulam Tank and Ponpadi Tank. Recovery was very less due to adsorption of dye on the soil matrix. Hence with the help of rhodamine – B study it was able to conclude that for different head of water in the tank, different zone of influence was observed. In order to have better results following steps are to be followed in any dye study.

There are five critical observations to successful ground water tracing.

(i) Selection of appropriate dyes and adequate quantities of dyes and water. The dyes and their performance are dramatically different from one another. (Never assume that a pound of one dye equals a pound of another).

(ii) Primary sampling reliance should be on activate carbon samples rather than on water samples.

(iii) Procedures should insure that no dye lost in samples prior to analysis;

(iv) Sample analysis instruments and methods should quantify dye concentration, distinguish among dyes and adequately deal with fluctuation in background and interference fluorescence.

(v) Good study designs require selection of appropriate dye introduction points.

Thomas Aley (2002) formulated 11 basic rules for ground water tracing studies called as "Rules to Dye By"

(i) Successful groundwater tracing can be conducted in a wide range of hydrogeologic settings. Bench test of dye performance under the conditions to be encountered are strongly recommended;

(ii) Background sampling and quantitative analysis of the samples is an important component of most professional grade groundwater traces. Many tracing investigations should have two or more rounds of background sampling prior to any dye introduction. Study should allow to change the type and quantity of dyes based upon the results of background sampling.

(iii) In most cases fluorescein is the most effective groundwater tracing dye. Eosine and rhodamine WT are commonly very effective and can be used concurrently with fluorescein inmany cases. Fluorescein should be used to encounter the most adsorptive surfaces. Rhodamine WT should be used to encounter the least adsorptive surfaces.

(iv) Use enough dye enough water and dyes which are appropriate to the conditios likely to be encountered. There are no general equation which will give quantity of dye. One seldom recovers most of the dye introduced because of losses to adsorptions, biological decompositions and other processes.

(v) Use dye introduction points which are appropriate to the questions to be addressed by the investigation in the case of surface water tracing. Utilize monitoring wells for dye introduction only when they are clearly appropriate.

(vi) Sample all the points at which the dye might discharge. Do through field work prior to dye introduction.

(vii) Sample for an adequate period of time. One approach for dealing with sampling duration is to recognize that tracer dyes are most effective in assessing preferential flow routes. Such flow routes provide relatively rapid water and dye transport; it such routes exist

between the dye introduction point and sampling stations then one should be able to estimate that one or more dye recoveries should occur prior to the end of a projected study period. Failure to recover the dye in that period should be view as evidence that the hypothetical preferential flow routes either do not exist or else are not integrated into a preferential flow system.

(viii) For most studies primary reliance should be on sampling with activated carbon samples and secondary reliance on grab samples of water. The use of both kinds of samples should be considered and will enhance the value of investigation.

(ix) Collect samplers and place new samplers at intervals frequent enough to ensure that dyes are not missed and that most or all of the dye recovered at a sampling station is not limited to only one sampling period. In most cases weekly intervals are adequate; more frequent sampling can be desirable during the first week or two after dye introduction consistent sapling intervals during a study are desirable;

(x) Good analysis for the tracer dye is essential for professional groundwater tracing. Thus study must establish. Credible detection thresholds for the various dyes based upon the analytical instrument, field experience and site specific leach ground sampling. Detection thresholds should be neither too high nor too low;

(xi) Groundwater tracing is fundamentally simple, yet it would hope that the person doing the work had experience has experience. Hence for future study fluorescein, Lissamine FF, Rhodamine WT and Sulpho rhodamine B are planned to buy. Until now it was came to know through Thomas Aley, OUL that one pound of Rhodamine WT cost Rs.

Through Fishers Scientific company

1 Gram of Sulphorhodamine B costs Rs.2700/-

1 Gram of Lissamine FF costs Rs. 9700/-

Above said dyes will be bought and studied its behavior on Sangulam and Ponpadi tank soil and water though column study in the CWR laboratory.

8.9 ADSORPTION CHARACTERISTICS OF THE ORGANIC TRACER DYES

While using the dye for groundwater study, one of the major problem is adsorption which is a limiting factor leads to loss of fluorescence dye. Due to sorption the recovery of dye at the final outcome is very low than the expected concentration. It is important to evaluate the adsorption characteristics and behaviour on subsurface. Batch study and column study were conducted with two different types of soil such as sandy soil and clay soil. Batch study was carried out to evaluate the behaviour of dye by varying the parameter such as dye concentration, soil, temperature and salinity. Column study was carried out, to analyse the dye adsorption and to determine adsorbed concentration in soil for all the three types of dyes. This section concentrated on

i. To compare the adsorption character for two widely used dye with different soil;

ii. To determine the parameter responsible for adsorption;
Steps followed are given below

- Soil Sample Analysis
- Selection of Dye
- Parameters Varation

- Batch and column study
- Dye Recovery
- Adsorption Coefficient Evaluation

Three different dyes such as Rhodamine B, Sulphorhodamine B and Fluorescein were chosen and used it in different soil that were collected from various places and also at sengulam tank bed. Sandy soil and clay soil were considered for the batch and column study

8.9.1 Calibration curve for Rhodamine B, Sulpho-Rhodamine B and Fluorescein

The calibration curve was prepared by measuring the known concentration that varying from 1ppb, 10 ppb, 100 ppb to 1000 ppb in fluorescence spectrophotometer for Sulphorhodamine B and Fluorescein. For rhodamine B the concentration vary from 1 ppb to 200 ppb. The Table 8.22 shows the intensity values for each concentration. Figures 8.25 to 8.27 shows the best fit graph for all the three dyes that has been taken for the study. These graphs were used to find the unknown concentration from the known value concentration.

Table 8.22 Intensity value for Sulphorhodamine B, Rhodamine B and Fluorescein

Concentration ppb	Intensity		
	SRB	Rhodamine	Fluorescein
1	0.02	0.088	0.63
2	0.034	0.156	0.711
4	0.053	0.294	1.006
6	0.073	0.456	1.116
8	0.094	0.619	1.261
10	0.116	0.736	1.902
20	0.325	1.283	2.723

40	0.557	2.049	5.518
60	0.915	2.844	6.938
80	1.119	3.639	9.456
100	1.426	4.26	11.35
200	2.123	6.845	20.56
400	3.345		32.91
600	4.523		46.38
800	5.359		54.95
1000	6.113		62.86

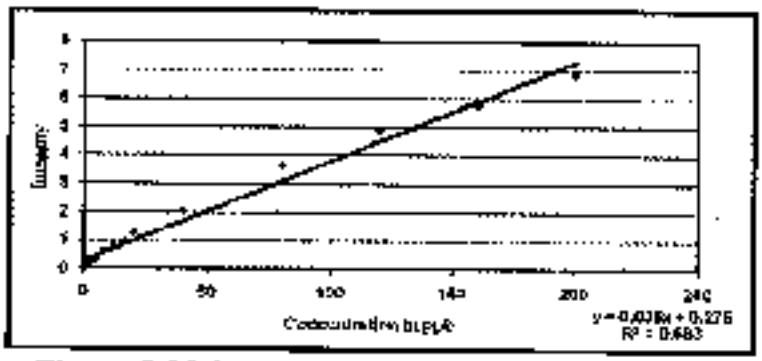

Figure 8.25 Standard Graph for Rhodamine B

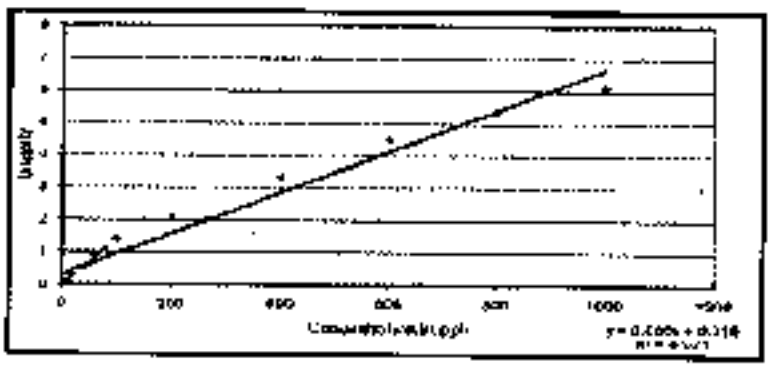

Fig 8.26 Standard Graph for sulforhodamine B

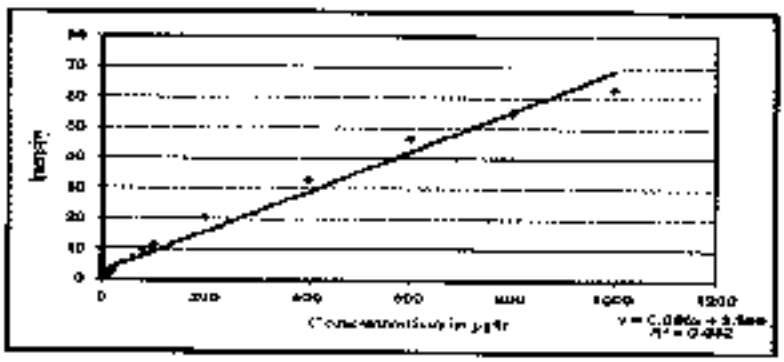

Fig 8.27 Standard Graph for Fluorescein

8.9.2 Batch study

Batch study was a preliminary study that conducted to evaluate the behaviour of dye under various parameters such as different water and dye concentration, decay chemical decay and sediment concentration using dyes. The concentrations varied from 100 ppb to 1000 ppb for sulphorhodamine B and Fluoresein and 20 ppb to 200 ppb of Rhodomine B.

i) Photochemical Decay

A dye loss has increased in surface water due to increase in water temperature or degradation by photochemical decay. Different concentration of 100 ppb to 1000 ppb was prepared in a beaker and placed in direct sunlight for five hours between 11.00 a.m to 4.00 p.m. Then the fluorescence magnitude was measured in spectrophotometer to identify the dye loss and it was shown in Figure 8.28 and 8.29 for recovery of dye concentration for three types of dyes. Due to photochemical decay the dye loss of dye for concentration of 200 ppb was shown below, the dye loss was up to 5 to 15% for Sulphorhodamine B, for Fluorescein 10 to 20% for 1000ppb and for rhodamine B 12% for 200 ppb. Of the three dyes fluorescein were highly affected by the sunlight.

Dyes	Reduction dye loss at 200 ppb
Rhodamine B	12%
Sulphorhodamine B	14%
Fluorescein	20%

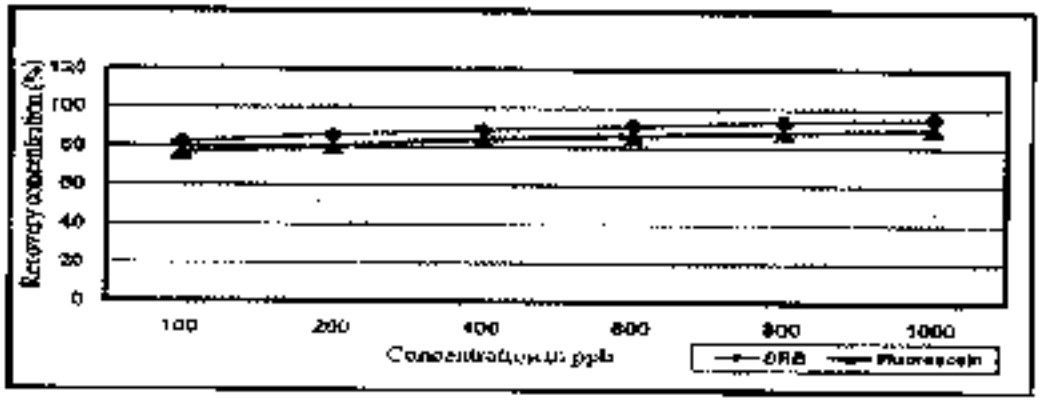

Figure 8.28 Photochemical Decay for Sulphorhodamine B and Fluorescein

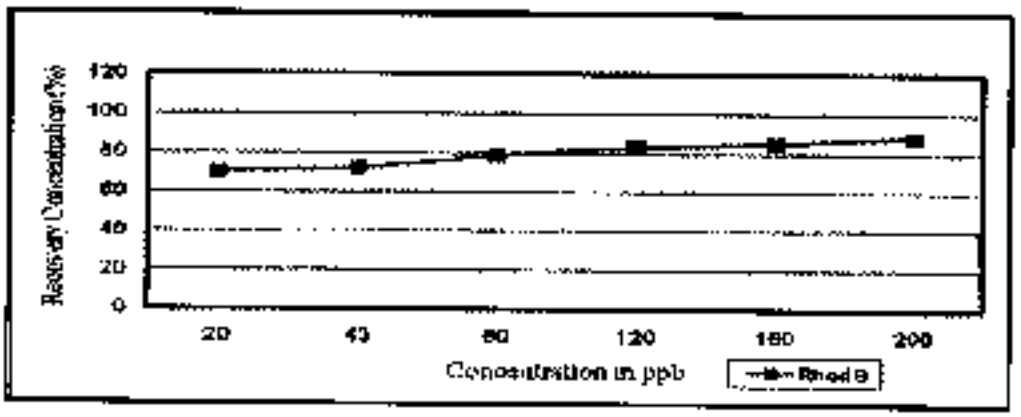

Figure 8.29 Photochemical Decay for Rhodamine B

ii) Chemical Decay

Feuerstein and Selleck (1963) and Watt (1965) have reported that vigorous agitation of dye solutions may cause reduction in fluorescence. Hence the dye solution were agitated for five days for different concentration and the graph was drawn for the average of five days and shown in Figure 8.30 and 8.31. It shows that there is no significant loss of dyes. The table shows the percent of dye loss at 200 ppb.

Dyes	Reduction dye loss at 200 (ppb)
Rhodamine B	9%
Sulphorhodamine B	6%
Fluorescein	4%

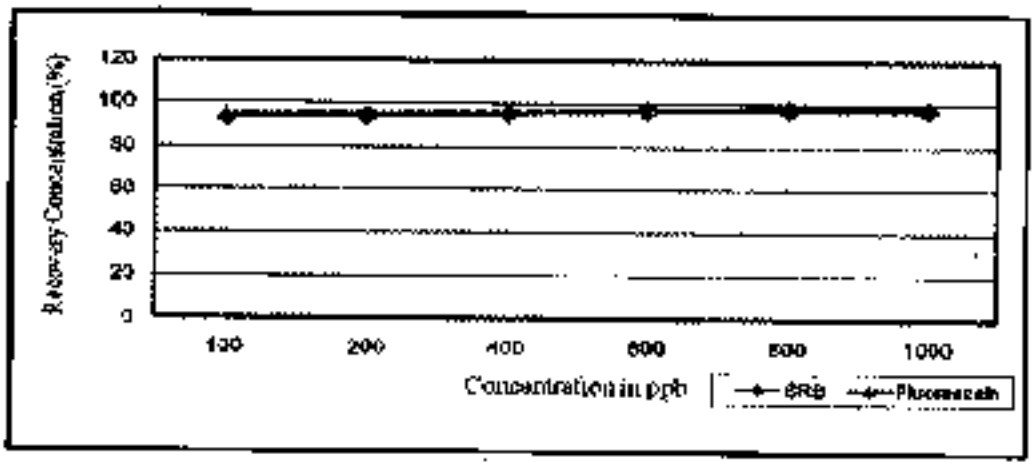

Figure 8.30 Chemical Decay for Sulphorhodamine B and Fluorescein

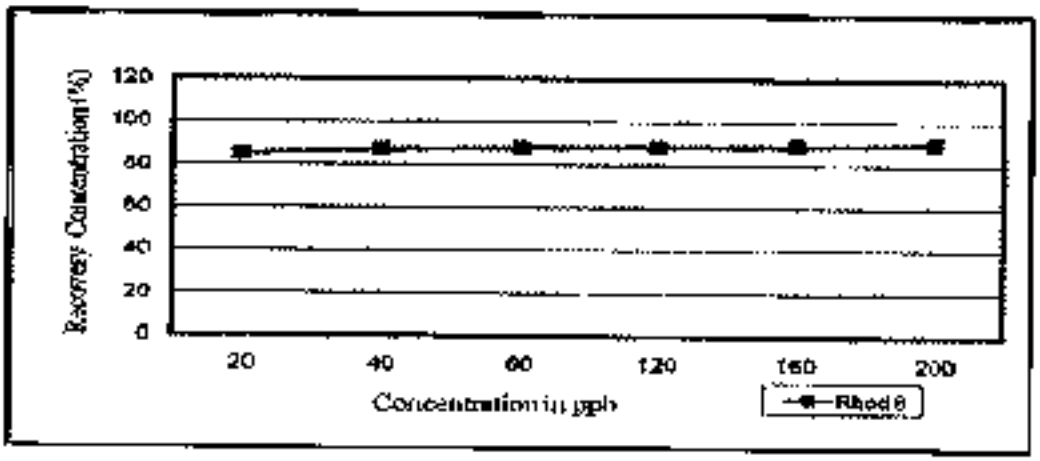

Figure 8.31 Chemical Decay for Rhodamine B

iii) **Salinity**

When tracer are being used in marine environment or in waste water, high salinities will be encountered which may affect tracer

performance. Waste water and tab water were used to evaluate the impact of salinity on dye concentration that prepared from 100 ppb to 1000 ppb. Waste water and tab water salinity were ranged from 380 mg/l and 450 mg/l and TDS of waste water was 1250 mg/l. Reduction of Sulphorhodamine B, Fluorescein and Rhodamine B dye by waste water and tab water were shown in Figures 8.32 to 8.35. The figures indicate that if salinity was more, dye loss was more. In addition dye loss was more for lower concentration. The table shows the reduction of dye loss at 200 ppb.

Dyes	Reduction dye loss at 200 ppb for Waste water	Reduction dye loss at 200 ppb for Tab Water
Rhodamine B	20%	23%
Sulphorhodamine B	10%	11%
Fluorescein	7%	6%

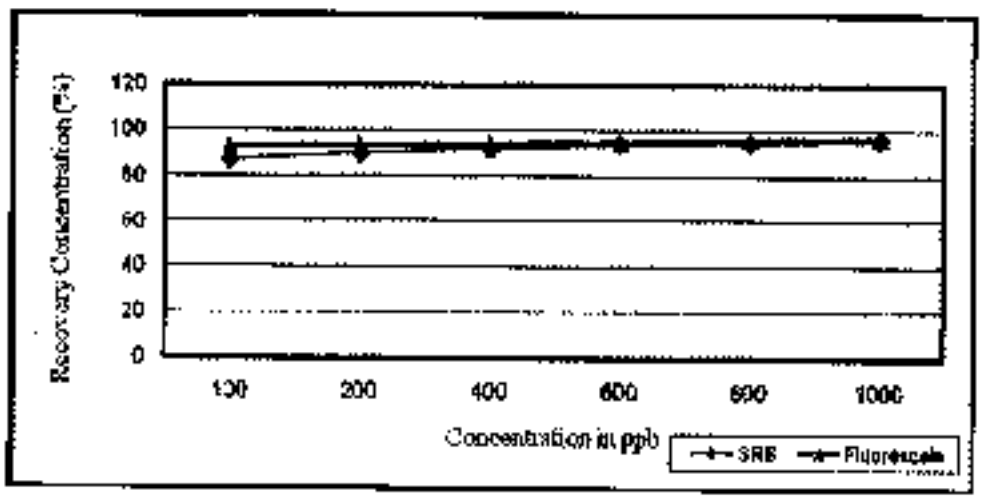

Figure 8.32 Batch Study with Waste Water for Sulphorhodamine B

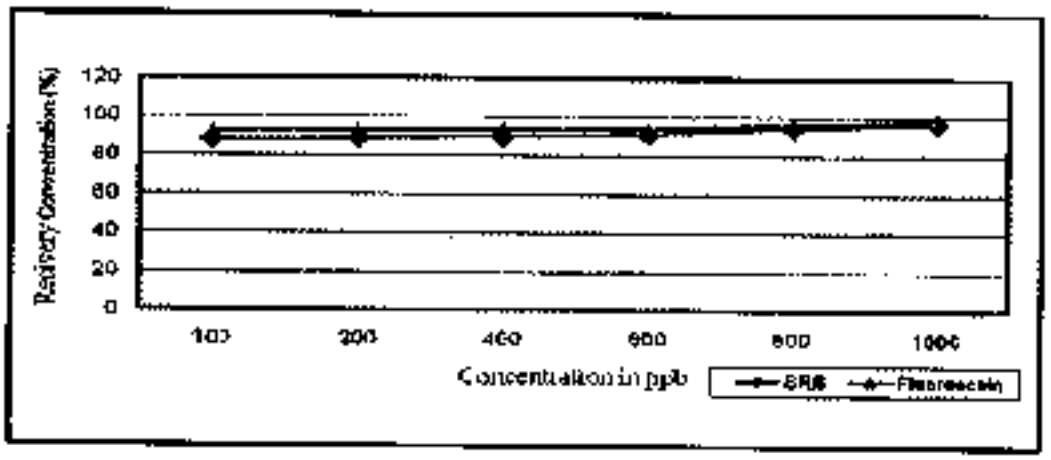

Figure 8.33 Batch study with Tap Water for Sulphorhodamine B and Fluorescein

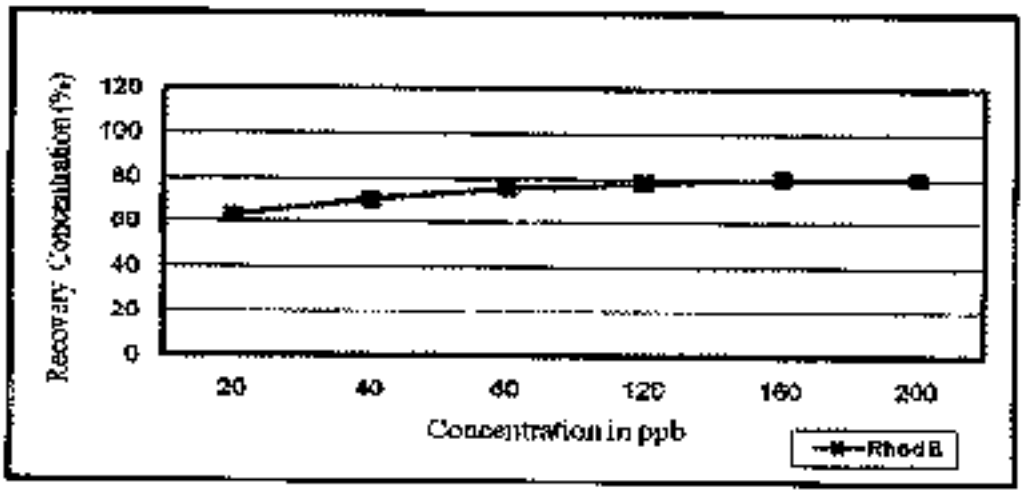

Figure 8.34 Batch study with Waste Water for Rhodamine B

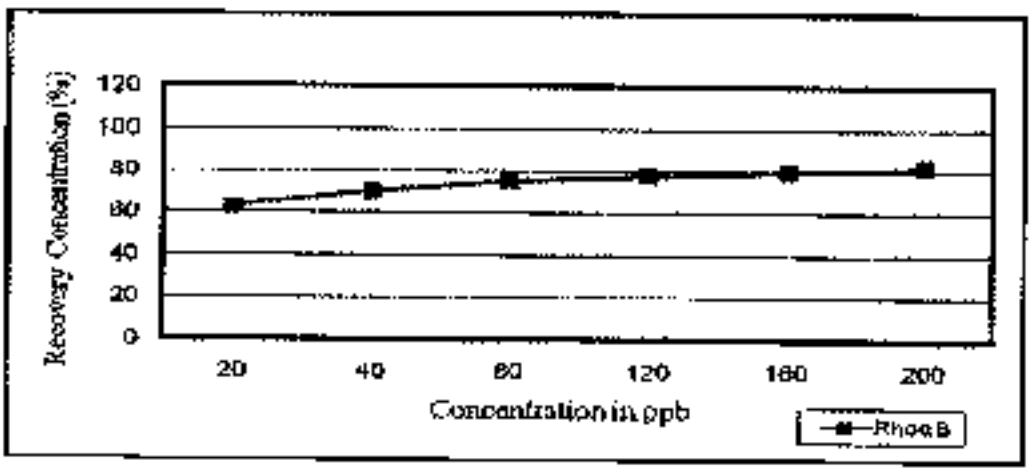

Figure 8.35 Batch study with Tap Water for Rhodamine B

iv) Sediment Concentration:

Smart and Laidlaw (1977) were found a marked decrease in the percentage of dye loss to adsorbing materials with increase in dye concentration. Batch study was conducted by varying the sediment weight for 100 ppb solution and tried for two different types of soil such as sand and clay. It showed that the fluorescence was affected as the clay concentration increases when compared with sand. When compared to Rhodamine B, Sulforhodamine B and Fluorescein had good resistance to adsorption in the sandy soil, as shown in Figure 8.36.

Figure 8.37 the Fluorescein had good resistance to adsorption of dye in clay soil when compare to other dyes such as sulphorhodamine B and rhodamine B. The percentage of concentration recovery for 100ppb was shown in the Table 8.23.

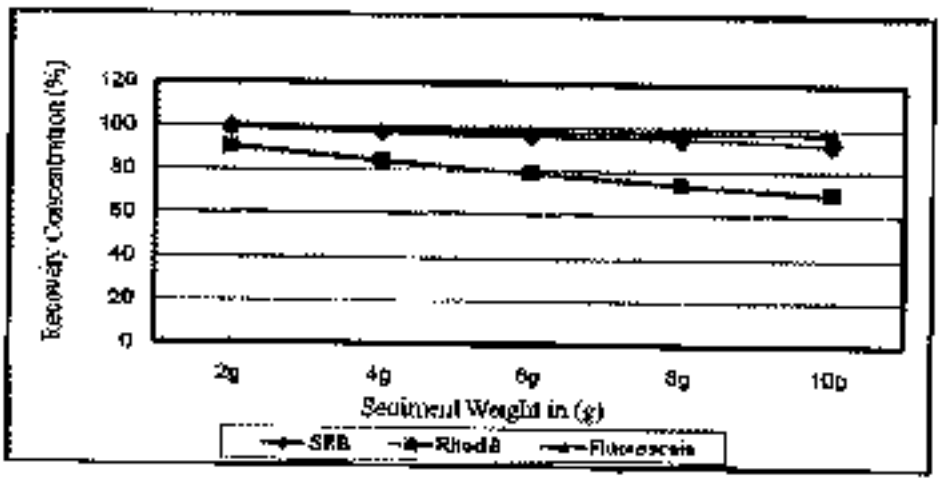

Figure 8.36 Batch study by varying the Sand Weight in gram

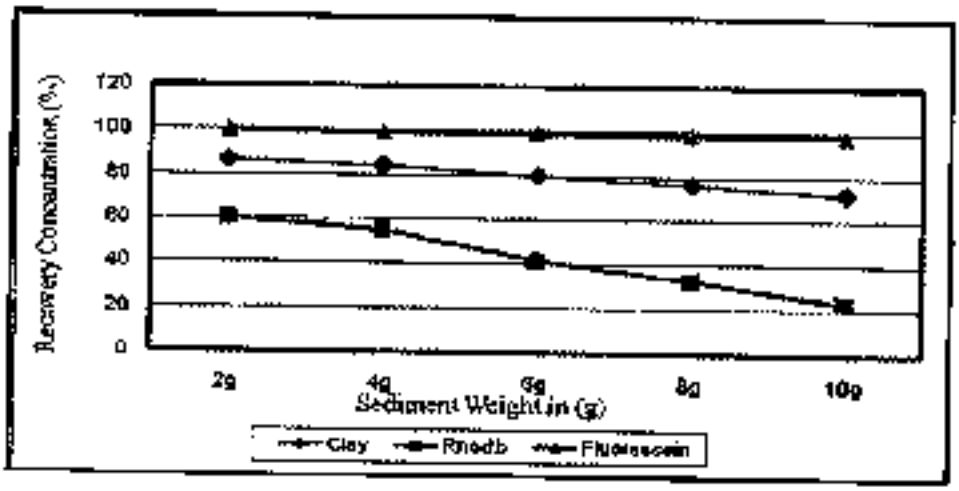

Figure 8.37 Batch study by varying the Clay Weight in gram

Table 8.23 Reduction of dye loss due to Salinity

Dyes	Reduction dye loss at 10g of Sandy Soil	Reduction dye loss at 10g of Clay Soil
Rhodamine B	30%	75%
Sulphorhodamine B	4%	20%
Fluorescein	2%	4%

8.9.2 Batch Study Results

The result of batch study that conducted was summarized below,

- Fluorescein was affected by photochemical decay when compare to rhodamine B and Sulphorhodamine B. Rhodamine B shows had good resistance to photochemical decay.
- There is no significant loss due to chemical decay. The dye loss was minimum for all three dyes.

- The dyes were affected due to salinity. if the dye study conducted in waste water then the reduction of dye loss will occur. Fluorescein had better resistance when compare to other dyes.

- Rhodamine B dye was highly adsorbed to soil when compare to Sulphorhodamine B and Fluorescein Fluorescein had good resistance to both the soil when compare to Sulphorhodamine B.

8.9.3 Soil column Experiment

After the batch study. the column experiment was carried out. Two columns were fabricated and filled with two types of soil sand and clay. Figure (fig 8.38) is the column setup for the experimental study.

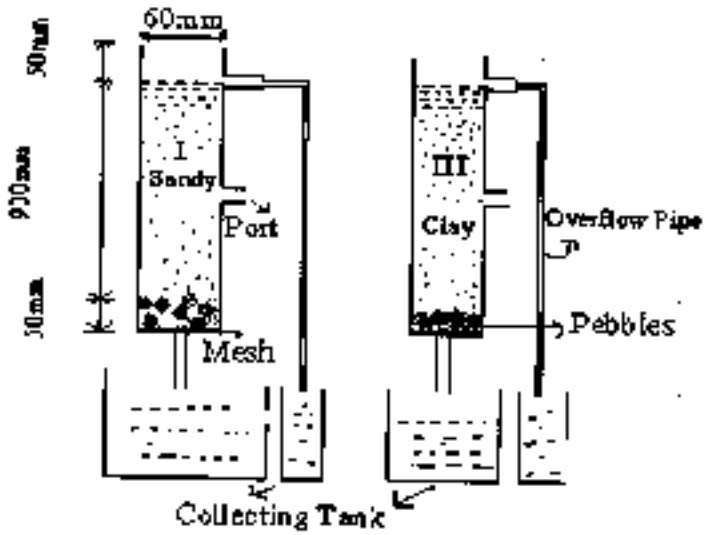

Figure 8.38 Soil Column Design

The columns were made with Acrylic and Rad an inner diameter of 6 cm and one metre length. Columns were provided with out lets to collect sample at the bottom and also it was equipped with sampling ports at different depth to obtain recovery soil and water samples. Two columns were filed with 50 cm sandy and clayey soil which were not compacted. The column was saturated with distilled water initially to remove suspended sediments three types of dyes were used at different dye concentration. The dye concentration

such as 20 ppb,200 ppb and 400 ppb were prepared and poured into the column manually at different time interval. Experiment was conducted for a period of four hours and samples were collected and analysed in the spectrophotometer.

i) **Adsorption of Rhodamine B**

- Rhodamine B was readily adsorbed to soil which was about 90 percent (181ppb was adsorbed) of 200 ppb concentration and 69 percent (275 ppb was adsorbed) of 400 ppb and 80 percent (16 ppb) of 20 ppb in a Sandy soil.
- Similarly 200 ppb Rhodamine B dye was passed through the clay soil column. The recovery was very minimum and adsorption was maximum that leads to clogging soil and no dye was recovered.
- The column was washed out with distilled water to determine the recovery was 121 ppb in the 200 ppb dye concentration and very little was recovered 20 to 30 percent in the 20 ppb dye concentration which are shown in figure 8.39 and figure 8.40.

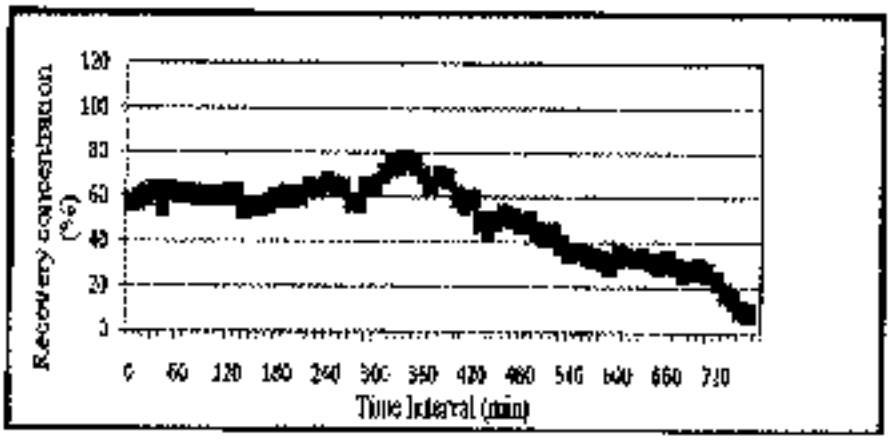

Figure 8.39 Recovery of Dye Concentration for 200 ppb

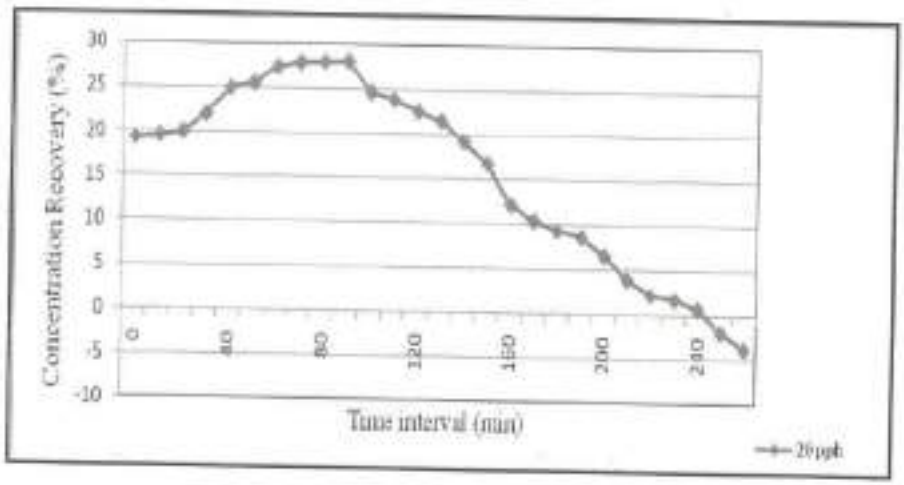

Figure 8.40 Recovery of Dye Concentration for 20 ppb

ii) Adsorption and Recovery of Sulpho Rhodamine Dye

- Here SR-B dye concentration of 1000 ppb, 100 ppb and 20 ppb was prepared and passed through sandy soil column at discrete time interval of ten minutes for four hours. Initially the dye adsorption was more than 80 percent in all the three dye concentration then slowly reduced which are shown in figure 8.41 to figure 8.43

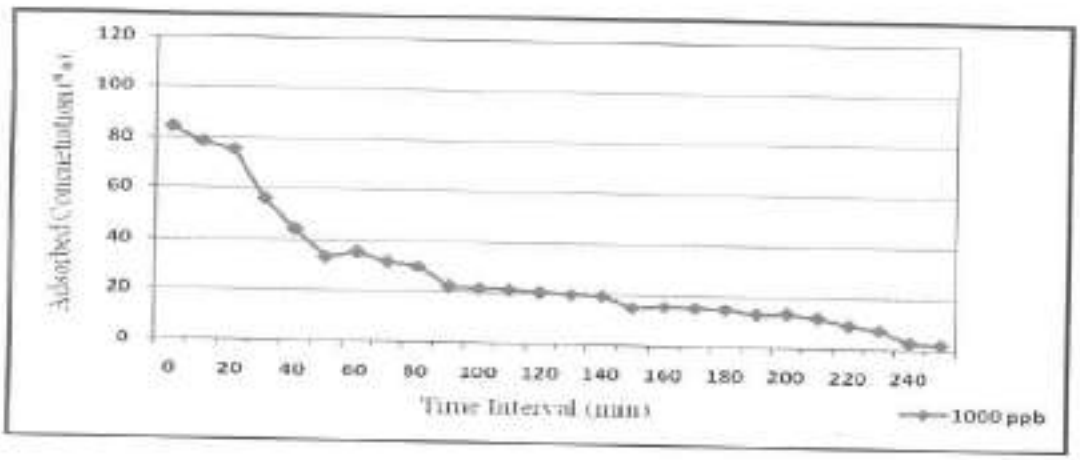

Figure 8.41 Percentage of Adsorbed Dye Concnetration for Sulphorhodamine B in sandy soil for 1000ppb

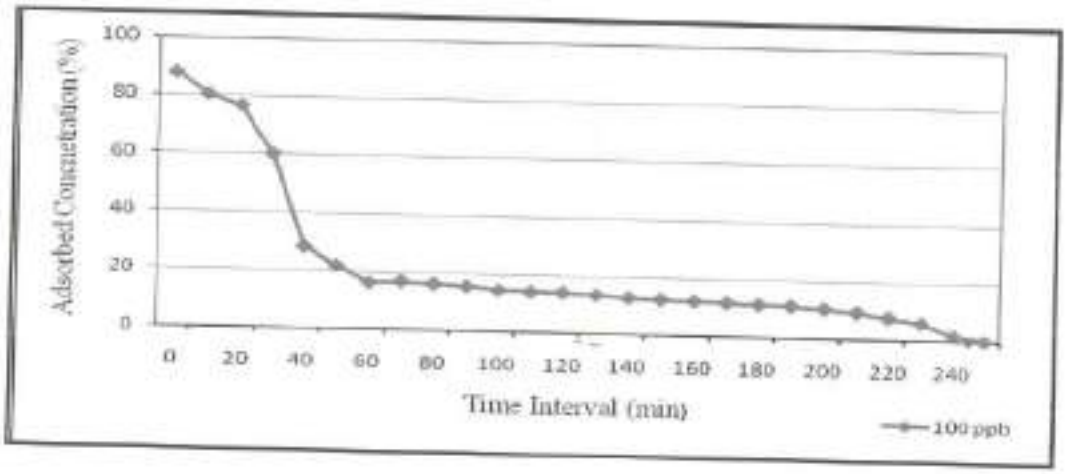

Figure 8.42 Percentage of Adsorbed Dye Concnetration for Sulphorhodamine B in sandy soil for 100 ppb

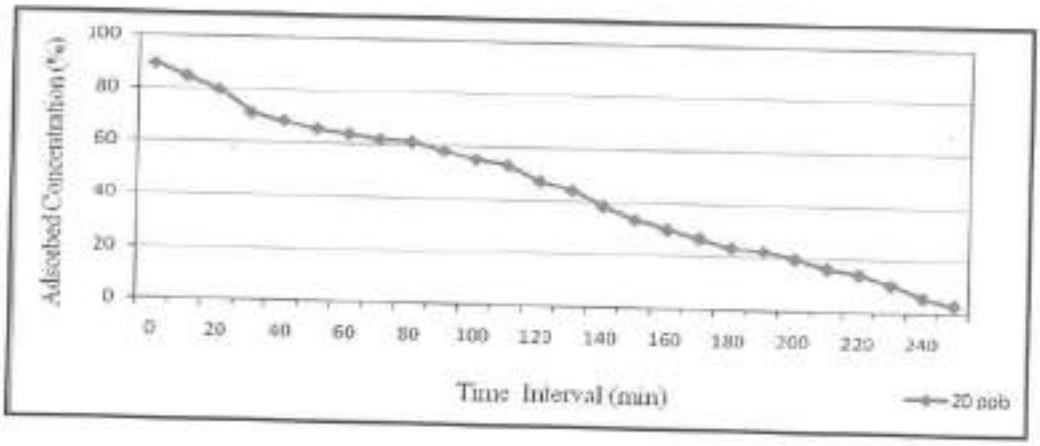

Figure 8.43 Percentage of Adsorbed Dye Concnetration for sulphorhodamine B in sandy soil for 20 ppb

➢ The adsorption of sulphorhodamine B to the sandy soil was relateively less compare to rhodamine B dye. Sulphorhodamine B had good resistance to adsorption sandy soil.

- Similarly SR-B dye of 1000 ppb, 100 ppb and 20 ppb were poured into the column filled with clayey soil for 8 hours. Recovery was carried out for five days to determine the recovery and retention of dye. Initially adsorption of 1000 ppb dye was 99 percent and

recovery was very minimum. Adsorption and recovery of SR-B dye were shown in figure 8.44 to figure 8.46

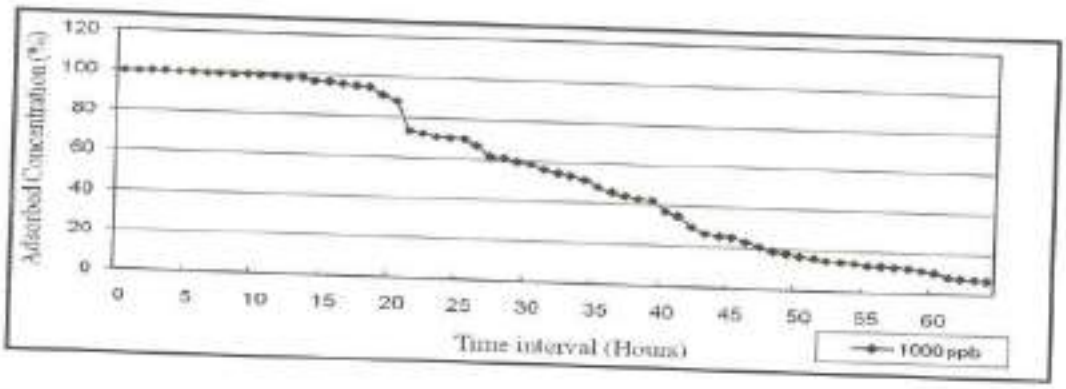

Figure 8.44 **Percentage of Adsorbed Dye Concnetration for Sulphorhodamine B in Clay soil for 1000 ppb**

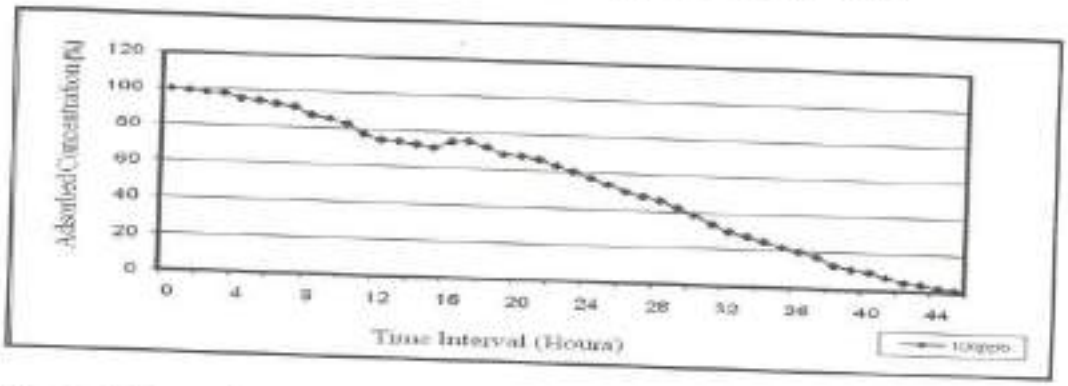

Figure 8.45 **Percentage of Adsorbed Dye Concnetration for Sulphorhodamine B in Clay soil for 100 ppb**

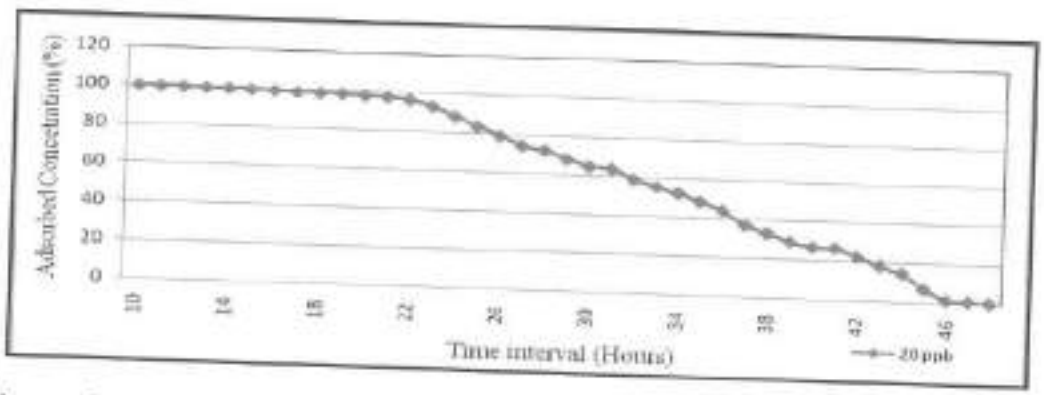

Figure 8.46 **Percentage of Adsorbed Dye Concnetration for Sulphorhodamine B in Clay soil for 20 ppb.**

iii) **Adsorption and Recovery of Fluorescein Dye**

- The problem that occurred with fluorescein dye was that it exist in soil and water naturally. Hence to determine background concentration of fluorescein, the sandy soil column was with distilled water and the samples were collected at different interval and measured background Fluorescein of 2 to 5 ppb was detected at 508 mm wavelength. Then 100 ppb and 20 ppb fluorescein dye solution were passed at constant flow rate through the sandy soil column. The recovery of dye concentration was higher than poured that is due to background fluorescein.

  - The fluoresein dye was not adsorbed onto the sandy soil and it showed good resistance to adsorption.

- Figure 8.47 and figure 8.48 show the recovery of fluorescein dye of 100 ppb and 20 ppb. These figures indicate that fluorescein was highly subjected to background. Fluorescence as it shows recovery concentration higher than initial concentrations.

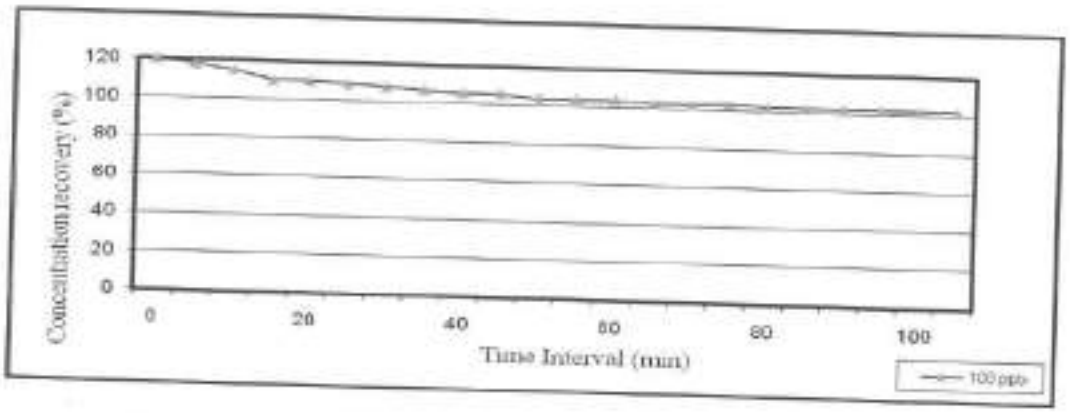

Figure 8.47 Recovery of Dye Concentration of Fluorescein for 100ppb

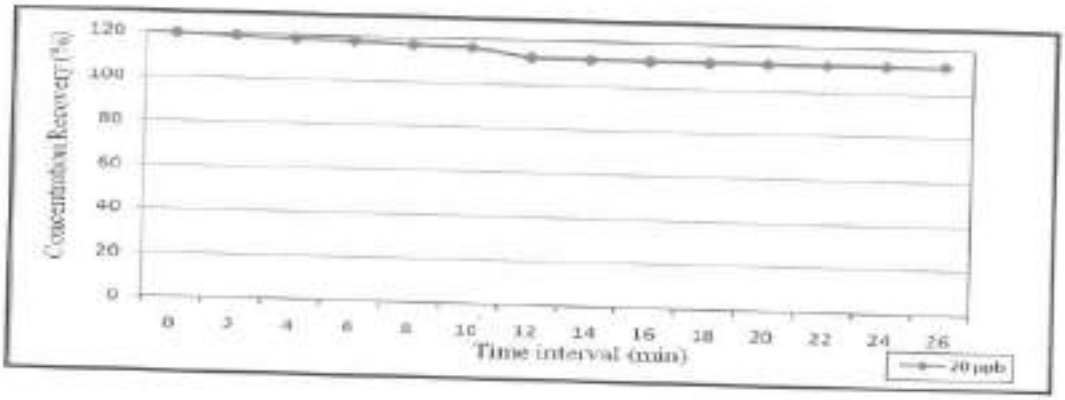

Figure 8.48 Recovery of Dye Concentration of Fluorescein for 20 ppb

- Fluorescein dye was poured into the clayey soil column of 30 cm depth and constant flow 60 cm. Was maintained to drive the dye to pass through clay soil. As the driving force was high the recovery of dye was also high. Clay soil is highly subjected to background fluorescence. Its recovery was shown in figure 8.49.

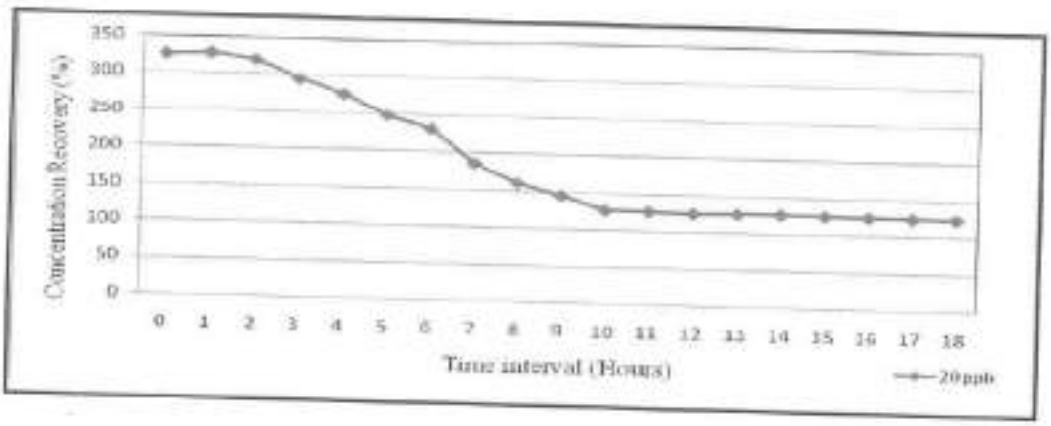

Figure 8.49 Percentage of dye concnetration recovery for Fluorescein

8.9.4 Adsorption Isotherm

Adsorption is usually described through isotherms, that is, the amount of adsorbate (dye) on the adsorbent (soil) as a function of its pressure (if gas) or concentration (if liquid) at constant temperature. The quantity adsorbed is normalized by the mass of the adsorbent to allow comparison of

different materials. An adsorptive on isotherm for a single gaseous adsorptive on a solid is the function which relates at constant temperature the amount of substance adsorbed at equilibrium to the pressure or concentration of the adsorptive in the gas phase. The data were fitted to freundlich adsorption isotherm were calculated and discussed. Freundlich Isotherm was explained below.

(i) Isotherm

Adsorption isotherm experiments were carried out by varying the sediment weigh for a concentration of 100ppb of 100ml solution. The amount of dye adsorbed onto the soil q_e (µg/g) was calculated using the following equation:

$$q = \frac{(C_i - C_e)*V}{M}$$

where C_i and C_e are the intial and equilibrium dye concentration (ppb) of dye respectively. V is the volume of the solution (L) and M is the weight of the sediment used (g). The percentage of dye removal (R%) was calculated using the following equation

$$R\ \% = \frac{C_i - C_e}{C_i} * 100$$

The effects of dye adsorbance at various situations were analyzed. The sediment weight was varied by keeping the dye concentration constant and the amount of dye adsorbed was measured by isotherm study.

- By keeping the dye concentration, the effects of dye adsorbed by varying the sediment weight were analyzed. The amount of dye adsorbed was measured by isotherm study.

- Rhodamine B was adsorbed more on to soil when compare to sulphorhodamines and Fluorescein

Rhodamine B	0.5 to 3.5 mg/g
Sulphorhodamine B	0.2 to 1.2 mg/g
Fluorecein	<0.04 mg/g

- Percentage of dye adsorbance was increases as the adsorbent dosage increases. When the sediment weight was 80g the percentage of dye adsorbed was

Rhodamine B	98%
SR-B	88%
Fluorescence	7%

- Therefore Fluorescein showed good resistance to adsorption.

- The effect of initial concentration adsorption was investigated by varying concentration ranging from 10 ppb to 100 ppb

Adsorption of	10 ppb	100 ppb
Rhodamine B	98%	88%
SR-B	98%	88%
Fluorescein	0	7%

(ii) Freundlich Isotherm

Adsorption was usually described through an isotherm that was the amount of adsorbate (dye) on the adsorbent (soil) as a function of its pressure or concentration at constant temperature. The quantity adsorbed was normalized by the mass of the adsorbent to allow comparison of different materials. An adsorptive on isotherm for a single gaseous adsorptive on a solid was the function which relates at constant temperature the amount of substance adsorbed at equilibrium to the pressure or concentration of adsorptive in the gas phase. The data were fitted to Freundlich adsoption

isotherm were calculated and discussed. The Equation 4.3 for the Freundlich Isotherm was given below.

$$\log \frac{x}{m} = \log k_d + {}^1/_n \log C_e$$

Where,

x - Quantity adsorbed in g/l

m - Mass of the adsorbent in g/l

C_e - Equillibrium concentration g/l

k_d and n are empirical constant for each adsorbent and adsorbate pair at a given temperature, which will be obtained from the intercepts and slope of the linear plots of log x/m verses log C_e. Retardation factor was given by the Equation 4.4.

$$\text{Retardation factor} = 1 + \frac{\rho_b k_d}{n}$$

Where,

ρ_d - Bulk mass density is in the range of 1.6 to 2 g/cc

n - Porosity

Equilibrium batch studies were conducted with clay soil as a sediment for isotherm study. In isotherm study three dyes Rh-B, SR-B and Fluorescein with 100 ppb concentration was used as absorbate. In which the weight of sediment was varied from 10 g, 20 g to 80 g for 100 ml of dye solution of 100 ppb concentration. The dye solution with sediments were shaken for several hours and dye concentration were measured for different time interval and were continued until the dye concentration reacts equilibrium. The initial and equilibrium concentration was measured and the mass of dye adsorbed was determined. Similarly the dye concentration varied

form 10 ppb, 20 ppb to 100 ppb at constant sediment of 40 g and media blank were measured for each isotherm study.

Based on the non linear data resulting from equilibrium sorption isotherm, Freundlich isotherm constants K_d and n were evaluated for three fluorescent dyes. The data log x/m and log C_e for different sediment weight and concentration were plotted in a graph and fitted to an isotherm equation. The constants n and K_d were determined from the slope and intercept values of the plot that shown in figure 8.50 a,b,c which represent the sorption isotherm for all the three dyes with varying media properties.

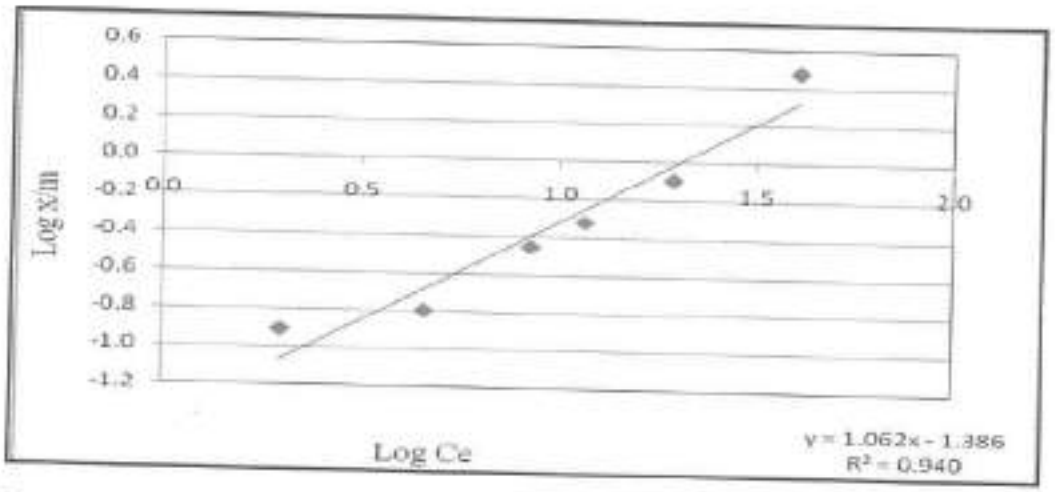

Figure 8.50 a **Plot of Log Ce Vs Log x/m for Rhodamine B dye sediment vary from 10 to 80g**

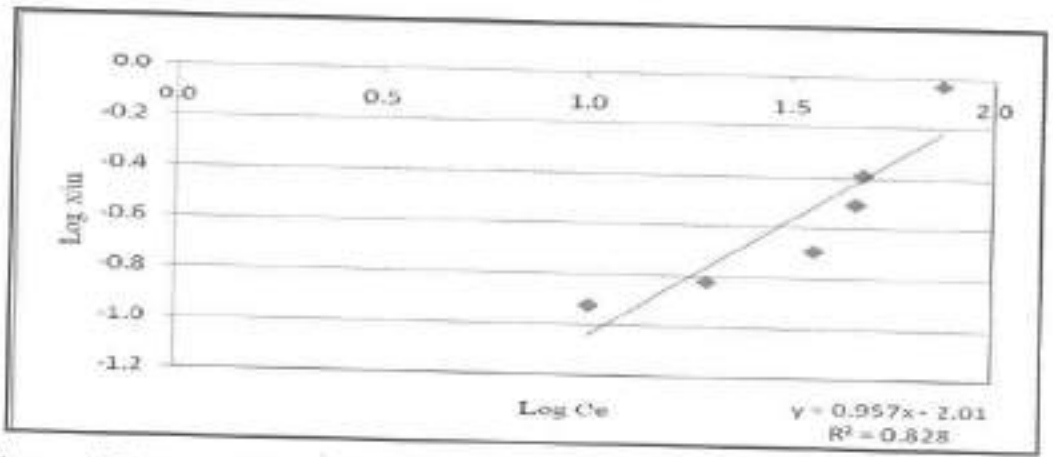

Figure 8.50 b **Plot of Log Ce Vs Log x/m for Sulphorhodamine B dye Sediment vary from 10 to 80g**

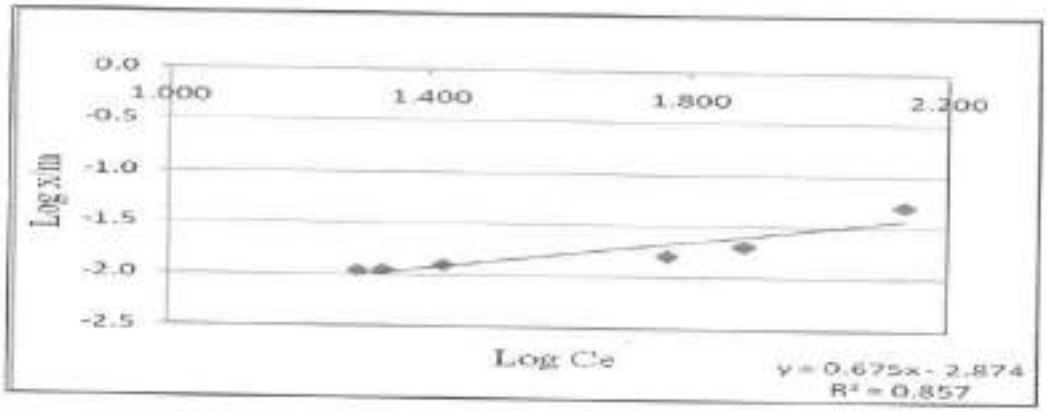

Figure 8.50 c **Plot of Log Ce Vs Log x/m for Fluorescein sediment vary from 10 to 80g**

Figure 8.51 a, b, c show the isotherm curve for different concentration rhodamine B, Sulphorhodamine B and Fluorescein dye.

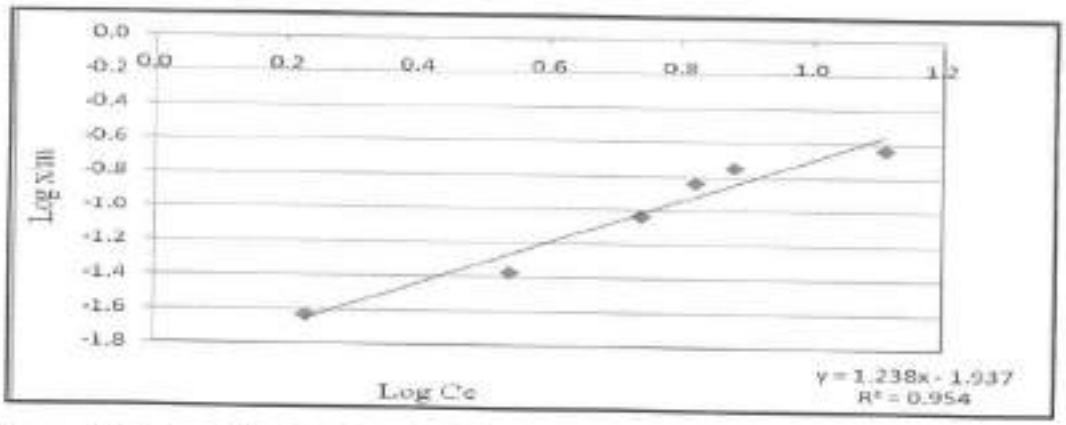

Figure.8.51 a **Plot of Log Ce Vs Log x/m for Rhodamine B of different Concentration**

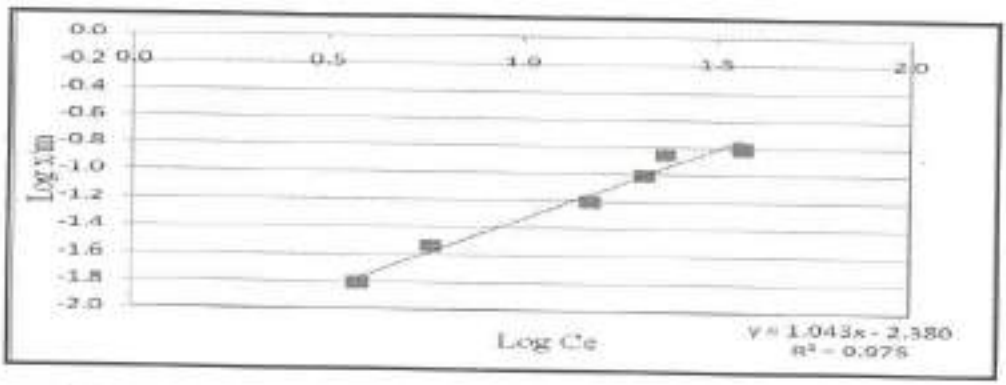

Figure.8.51b **Plot of Log Ce Vs Log x/m for three dyes of different Concentration**

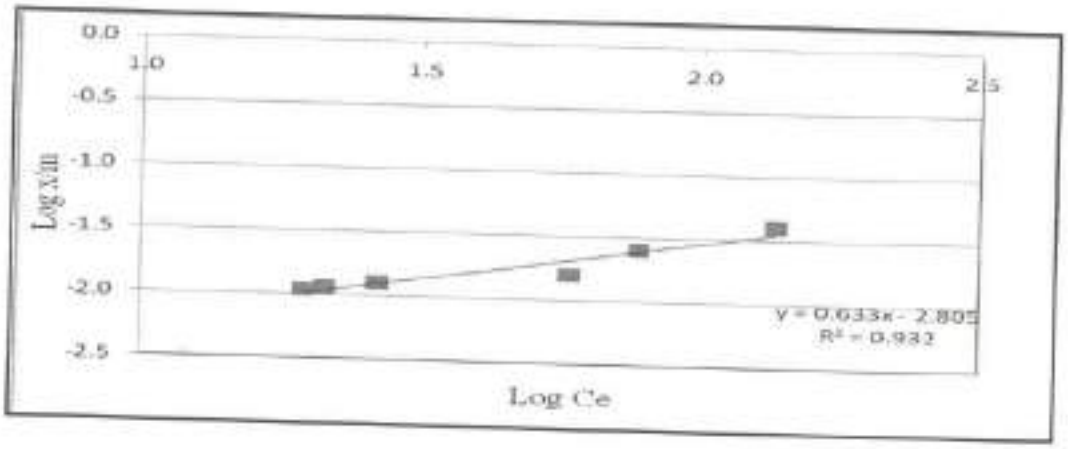

Figure.8.51 c Plot of Log Ce Vs Log x/m for three dyes of different Concentration

Table 8.24 and 8.25 shows the n and k values for the three types of dyes that taken from the slope and intercept value of graph.

Table 8.24 n and k Values for Three Types Dyes at Different Sediment Weight

Dyes	Slope	Intercept	n	K
Rhodamine B	1.062	-1.386	0.942	0.0411
Sulphorhodamine B	0.957	-2.01	1.045	0.00977
Fluorescein	0.657	-2.874	1.522	0.00133

Table 8.25 n and k Values for Three Types of Dyes at Different Concentration

Dyes	Slope	Intercept	n	K
Rhodamine B	1.237	-1.937	0.808	0.0115
Sulphorhodamine B	1.043	-2.380	0.958	0.0041
Fluorescein	0.633	-2.805	1.579	0.0015

Table 8.24 and 8.25 shows the n and k values for the three types of dyes. The author Sumanjit (2008) referred that the values of n greater than unity indicated that adsorption was less for the dye. The adsorption coefficient K value was minimum for fluorescein and Sulphorhodamine B when compare to rhodamine dye. Fluorescein had good resistance to adsorption for which the adsorption coefficient was minimum.

8.9.5 Characteristics of Soil properties Before and After the column study

The clay soil properties was tested before and after the column test with Rhodamine B and Sulphorhodamine B in which the adsorption was more to observe the cause of adsorption in soil and identify the changes in the soil properties and the result were shown in the Table 5.3

Table 8.26 shows the soil properties of clay soil that used for the column study. The pH of the rhodamine B clay soil was less when compare to Sulphorhodamine B clay soil. Bor Jier Shiau et.al (1993) represented that adsorption decreases with increase in pH. Sulphorhodamine B adsorb less When compare to rhodamine B but greater than original clay soil. The other metals were less than the original clay soil. The author Jari M mentioned hydroxyl group of dye also responsible for adsorption. If the dye had more number of hydroxyl group then the adsorption will be more. The adsorption was less for fluorescein dye which has one hydroxyl group and similarly Sulphorhodamine B has two hydroxyl group in which adsorption was less but greater than fluorescein.

Table 8.26 Soil Properties of Clay Soil Before and After the Column Test

Soil properties	Unit	Org soil	RB soil	SRB soil
Organic content in soil	%	0.40	0.33	0.35
Soil pH		7.06	7.65	8.45
Soil EC	mS/cm	0.121	0.06	0.03
Cationic Exchage Capacity	Meq/100g	18.33	16.32	14.97
Iron Available Fe	ppm	4.52	4.96	3.78
Copper Available Cu	ppm	2.94	2.72	2.56
Magnese Available Mn	ppm	14.59	10.09	9.34

8.9.6 Summary

This chapter concentrated to estimate seepage velocity through tracer study. Initially the various types of tracers and detection methods were studied. Then rhodamine – B applied in the sengulam tank, viruthunagar during February 2008. During that time the tank storage was 0.154 Mm^3. Initially it was planned to use very low concentration (5 ppb) of rhodamine B in the Sengulam tank water. Hence 800 gm of rhodamine B powder was mined with 1600 litres of tank water and poured throughout the tank in order to have uniform distribution of dye. Tank water and groundwater samples were collected daily. Even after five days, rhodamine B dye were not detected in the pumping wells which were considered for the study. Hence it was planned to try at 16 ppb concentration of rhodamine B dye on 5th March 2008. similar to earlier trial 2500 gm of rhodamine B mined with 5000 litres of tank water and sprayed over the tank water surface. Water samples were collected and analysed. The rhodamine B concentrating in the tank was 29.1 ppb after 24 hrs of dye application. After 9 days, rhodamine B concentration in the tank water concentraton was below detectable level.

i. Rhodamine – B fluorescence was detected in most of the wells after 24 hrs of dye application except the well W1, W2 and W3 which lies below the Sluice 1;

ii. Average break through concentration was 3.7 ppb which were detected between 2 and 9 days;

iii. After 13 days of dye application, rhodamine B was not detected in any one of the well.

iv. The seepage velocity during March 2008 was 0.007 cm/sec to 0.333 cm/sec;

v. Wells which were away from the tank received rhodamine B earlier than the nearer wells. This is attributed to interconnectivity of the tank and the aquifer and also low much pumping had carried out.

Sengulam tank had 0.09 Mm^3 on 21.02.2009 on which 3000 gm of rhodamine B at 30 ppb concentration prepared and poured on the surface of tank and samples were collected and analysed. Even though higher concentration of rhodamine B was poured during the year 2009 delayed dye detection was found. It is due to very less tank storage that did not provide enough had to drive the rhodamine – B to the command area wells. Most of the wells received rhodamine B after 7 days that too due to sudden and several pumping by the farmers.

- Rhodamine B detection in the wells were after 7 to 10 days in most of the wells during 2009;
- Average seepage velocity was 14 m/day which was less than the year 2008;

Tank study was conducted at Ponpadi tank on 23/02/2009 at very low concentration most of the rhodamine B lost by adsorption. Hence 4500 gm of rhodamine B mined with 9000 litres of tank water was pored into the

tank and mined well in order to have uniform distribution of dye on 03/03/2009. Average seepage velocity was 52 m/day.

Major findings are

i. Movement of rhodamine B is not only depends on the distance of well from the tank that depends mainly on tank water had and pumping pattern in the wells;

ii. No day rhodamine B was detected with injected concentration; This is attributed to soil adsorption plus sunlight adsorption and temperature;

iii. Seepage velocity estimated through tracer study was developed by datum head, forced hydraulic head due to pumping in the command area.

iv. Tracer study was able to conclude that for different head of water in the tank, different zone of influence was observed.

In addition, this chapter concentrated on adsorption of dye on the soil through batch and column study to evaluate the isotherm constant. This study has been done to decide how much quantum of dye is needed to be injected to get the targeted dye concentration in the observation point highly. Both Rhodamine -B and Sulpho Rhodaminne-B were adsorbed on to clay soil than sandy soil. The amount of dye adsorbed was very minimum for fluorescein. Hence Fluorescein was the suitable dye for groundwater tracing. However most groundwater studies used Rh-B and SR-B because it is available in the Indian chemical market and is also relatively cheaper.

CHAPTER 9

EVALUATION OF IMPACT OF PARTIAL DE-SILTING THROUGH NUMERICAL MODELING

9.1 GENERAL

In the earlier chapters the seepage rate from the tank, groundwater velocity, tank and groundwater nexus were evaluated through analytical methods and tracer studies. This chapter aims to evaluate the impact of partial de-silting on tank water seepage, groundwater velocity and groundwater potential through groundwater modeling.

9.2 GROUNDWATER MODELING

Groundwater modeling is the process of simulating the groundwater basin system which constitutes a groundwater model that is mainly mathematical in nature. Groundwater simulation can be defined as reproducing the essence of the system without reproducing the system itself. In the numerical groundwater modeling, a discrete solution is obtained with respect to both the time and space domains by using numerical approximations of the partial differential equation. Various numerical solution techniques are being used in groundwater modeling. Among them, the most used three approaches in groundwater modeling are Finite Difference Method, Finite Element Method, and the Analytical Element Method. All the

techniques have their own advantages and disadvantages with respect to availability, costs, applicability and required knowledge of the user.

9.3 APPLICATION OF GROUNDWATER MODELING

The objectives which can be achieved with the groundwater models for the optimum production and management of groundwater resources are such as

- To forecast water levels and effects on aquifer storage conditions with respect to space;
- To increase natural replenishment by selective pumping in the aquifer domain;
- To evaluate the rate of decline in groundwater table under the current withdrawal condition;
- To plan the best cropping pattern from a cost benefit point of view;
- To predict the spread of contaminants in polluted aquifers for the present scenarios;
- To determine the efficacy of the various remedial aquifer strategies;
- To estimate aquifer parameters involving transmissivity, hydraulic conductivity, storage coefficient, specific yield , longitudinal and transverse dispersion coefficients and zonal recharge in the flow domain;
- To assess the buildup of the groundwater head due to the construction of an aquifer barrier;
- To predict the sea water intrusion in coastal aquifers and planning of remediation strategies;

- To investigate the optimal well spacing for withdrawing groundwater from heterogeneous anisotropic aquifers;

9.4 TYPES OF MODELING APPROACH

There are two types of modeling approach based on their input and output variables. They are forward flow and transport model and inverse flow and transport model. In the forward flow and transport model the input will be the aquifer parameters such as hydraulic conductivity, dispersivity, storage and recharge and the output will be the head and concentration values. In the inverse flow and transport model the input will be the observed head and concentration values and output will be the aquifer parameters. The flow chart representing the forward and inverse flow and transport model is described in fig 9.1 and fig 9.2

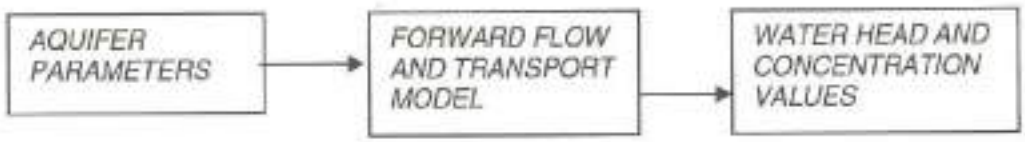

Figure 9.1 Forward flow and transport model

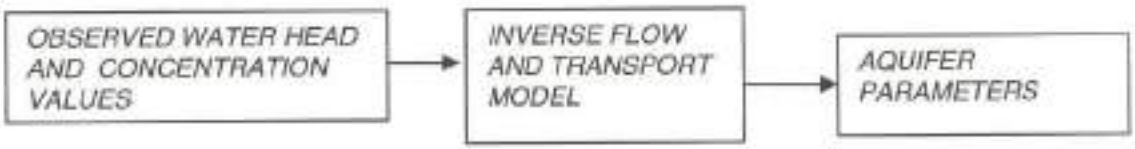

Figure 9.2 Inverse flow and transport model

9.4.1 Inverse Modeling

A groundwater flow model is a forward problem that predicts the unknown state of the system by solving the appropriate governing equation. An inverse model is the model which determines the unknown physical parameters and other conditions of the system by finding a good match between the observed and simulated variables. Inverse modeling is applied to estimate the hydraulic conductivity, transmissivity, storage coefficient,

specific yield, porosity, dispersivity, and aquifer recharge with adequate reliability. Inverse modeling can substantially improve the quality of groundwater models and yield results that are not readily available through trial and error methods. It also reduces the time required for obtaining the optimum value of the parameters. The benefit of inverse modeling is its ability to compute optimal values of the parameters, which produces the closest fit between the observed and simulated aquifer heads or solute concentration in the flow region. The inverse problem may result in less useful solutions due to an improper conceptual model, incorrect discretisation and poor convergence of the minimization algorithms.

9.5 STEP BY STEP PROCEDURE OF MODELING

The methodology for the project is shown in Fig 9.3. Various stages of the methodology are listed below,

i. Model Conceptualization

ii. Primary data and Secondary data Collection

iii. Input Data
   - Aquifer Properties
   - Initial and Boundary condition
   - Recharge and Discharge Rates

iv. Calibration and Validation

v. Parameter Estimation

vi. Scenario Prediction

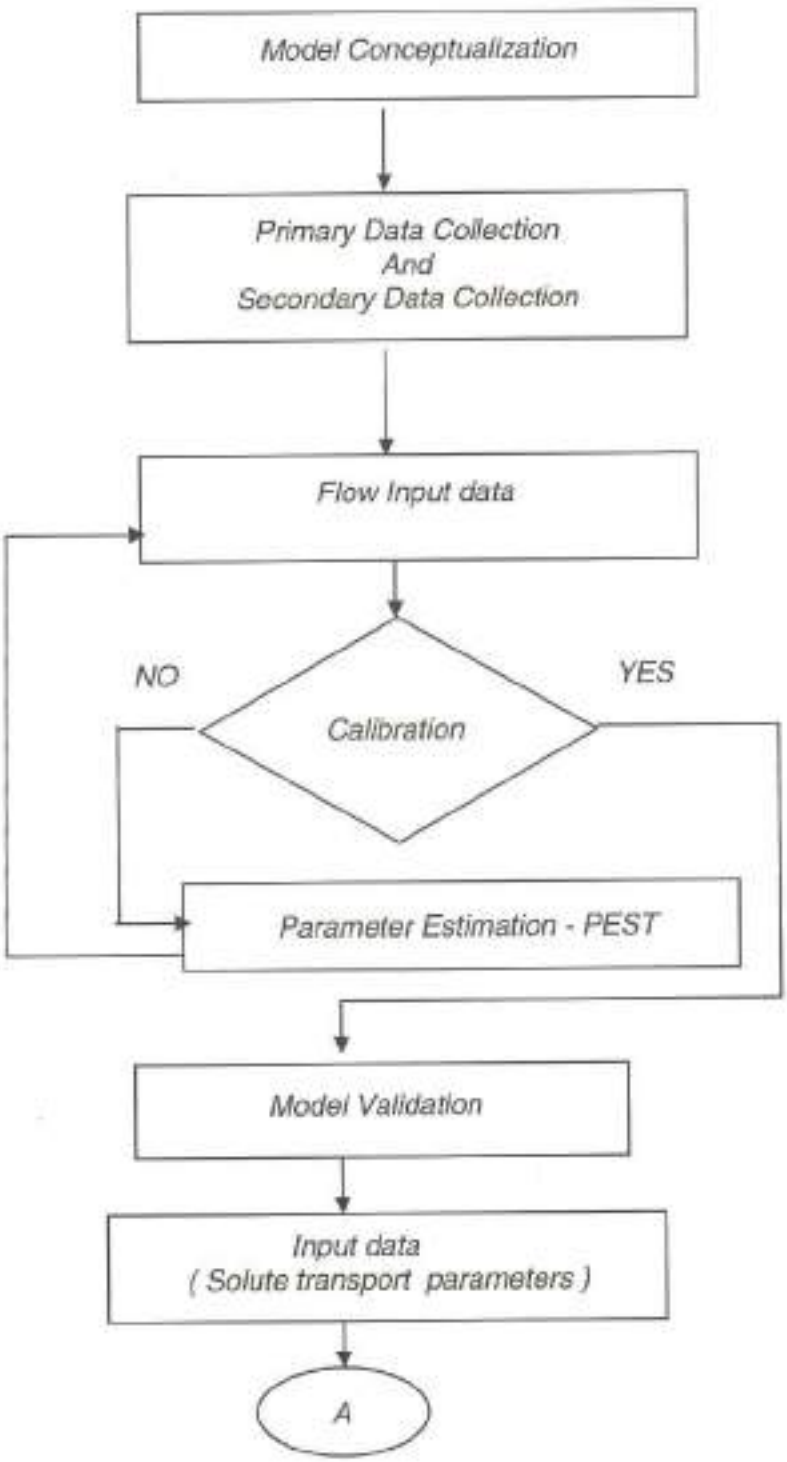
Model Conceptualization
Primary Data Collection
And
Secondary Data Collection
Flow Input data
NO
YES
Calibration
Parameter Estimation - PEST
Model Validation
Input data
(Solute transport parameters)
A

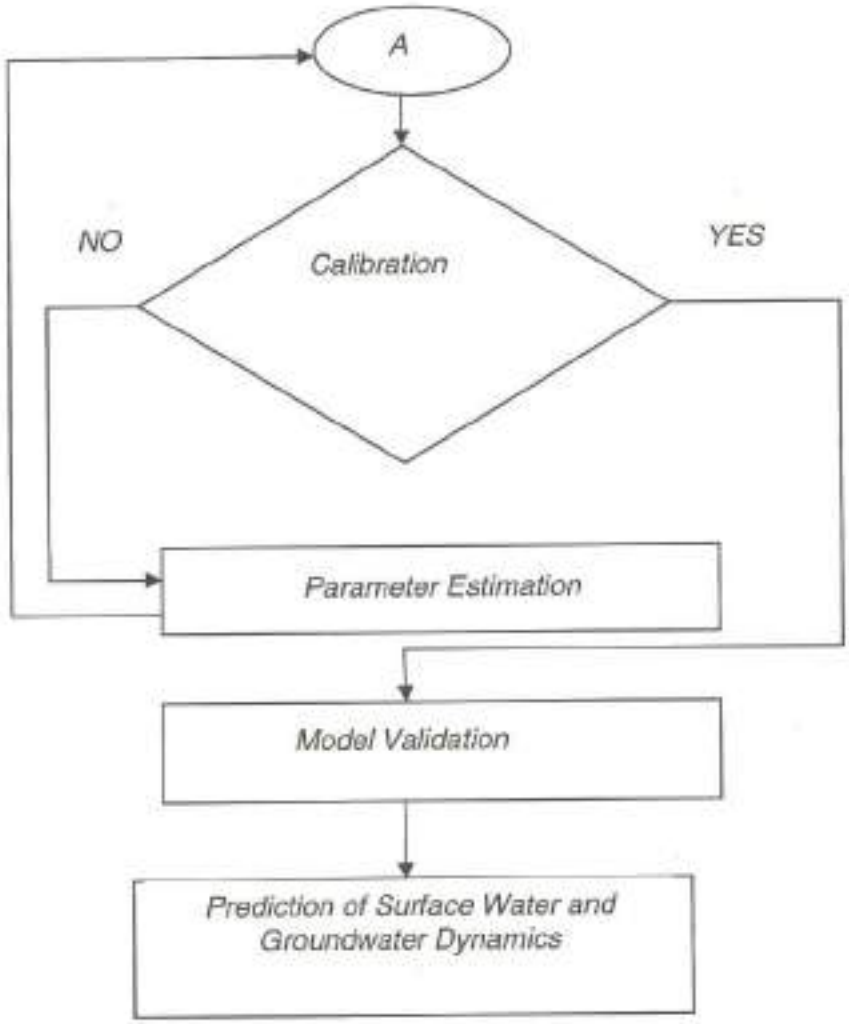

Figure 9.3 Methodology to Estimate the Impact of Partial De-silting

9.5.1 Model Conceptualization

Model conceptualization is the process in which data describing the field conditions are assembled in a systematic way to describe the groundwater flow and contaminant transport process at a site. The model conceptualization aids in determining the modeling approach and also helps to select the software to use. The model domain in shown in the fig 9.4

Figure 9.4 Model Domain

9.5.2 Primary and Secondary Data Collection

Primary data such as monthly tank water level, groundwater levels have to be collected from the field. The hydraulic conductivity and specific yield or porosity have been taken from the field evaluation and also from the Public Work Department. Monthly Rainfall data from nearby raingauge station and month discharge rates from the farmers. Through GPS survey and reduced level survey the tank bed levels and wells levels were collected. Geologic and hydro-geologic information were collected from the department and in the field.

9.5.2 Input Data to the Model

The input data given for groundwater modeling are as follows

(i) Elevation of the different layers in the aquifer system.

(ii) The bottom elevation of the model was assigned based on the weathered thickness.

(iii) Different boundary condition such as recharge boundary and constant head boundary and concentration boundary were given for the model which is shown in Fig 9.5.

(iv) Water head values and concentration levels of the chloride observed in the observation wells for all time periods.

(v) Pumping rates from all the pumping wells for all time periods.

(vi) Properties such as hydraulic conductivity, storage, longitudinal and transversal dispersivity, initial heads values. Hydraulic conductivity assigned for the layers is shown in Fig 9.6.

(vii) Initially longitudinal dispersivity of the model was taken as 0.31m.

(viii) The water level for all the wells collected during the first month was assigned as the initial head condition.

(ix) The concentration levels observed from all the wells during the first month were given for initial concentration condition.

(x) The size of the grid for the entire area is based on the total surface area of the study area.

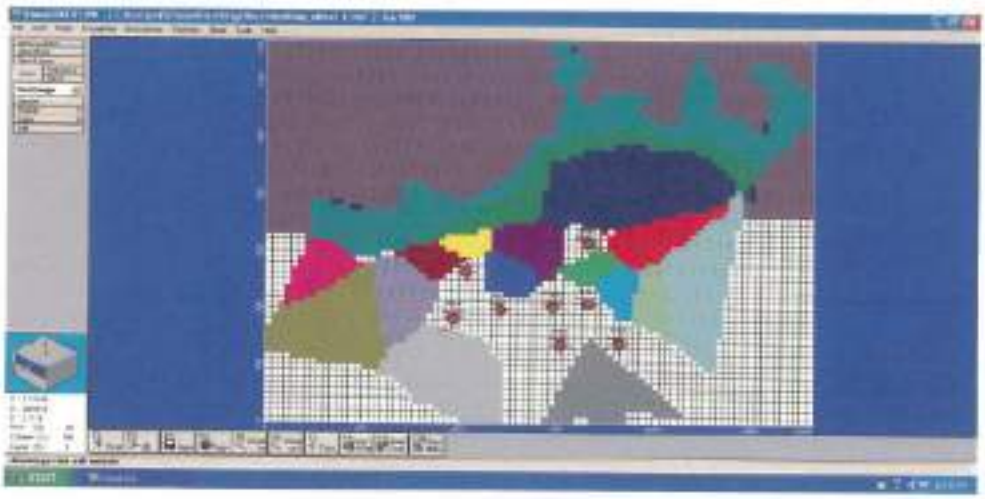

Figure 9.5 Schematic Diagram for Recharge Boundary

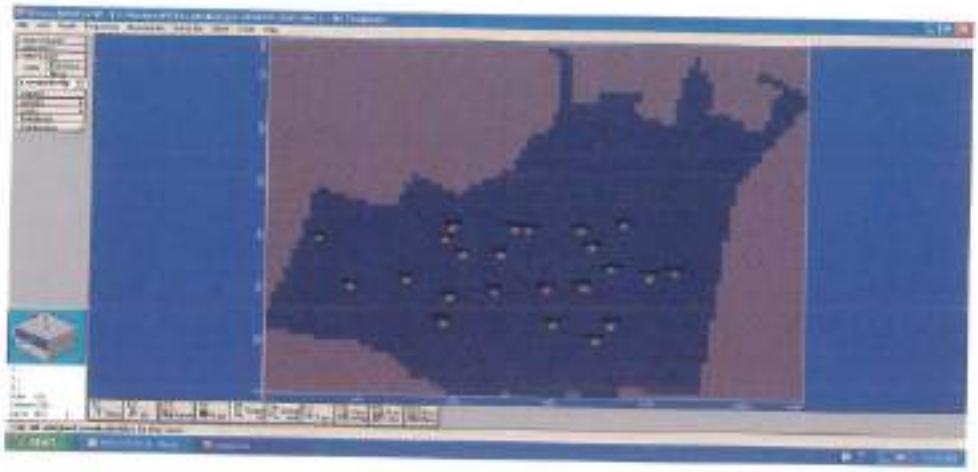

Figure 9.6 Schematic Diagram of Hydraulic Conductivity

9.5.4 Flow Model Calibration

The purpose of model calibration is to establish that the model can reproduce field measured heads and flow. Calibration was carried out by trial and error adjustments. Model calibration consists of changing the values of model input parameters in an attempt to match the calculated values with the observed field conditions within some acceptable criteria. Model calibration requires that field conditions at a site should be properly characterized. Lack of proper site characterization may result in a model calibrated to a set of conditions that are not representative of actual field conditions. Both steady state and transient state model calibration was performed. For the model calibration, first year data (2007 – 2008) of both water head values and concentration values were used.

Steady State Calibration

Steady state conditions are usually taken to be the historic conditions that existed in the aquifer before significant development has occurred. (i.e. , inflows are equal to outflows) and there is no change in the aquifer storage. Hydraulic conductivities estimated from pumping tests that in

the range of (0.00009 – 0.0001) were used as initial values for the steady state simulation. By trial and error, all the input parameter values were increased during many sequential runs until the match between the observed and simulated water levels were obtained. The steady state calibration were shown in the Figure 9.7

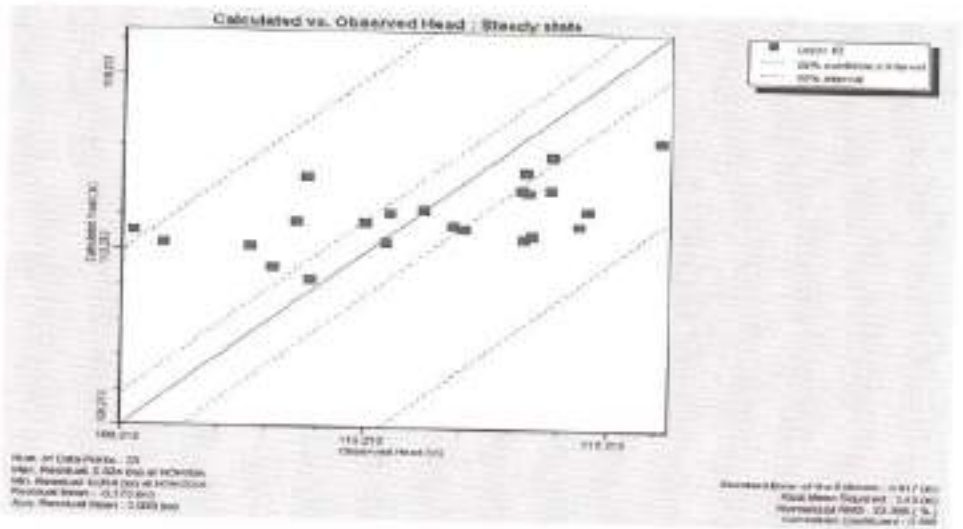

Figure 9.7 Calibration Graph for Steady State Condition

Transient State Calibration

Like Steady State Condition, model was calibrated to transient state from June 2007 to June 2009. Since data of water levels were available for a period of 2007 to 2009,simulation was performed for that period taking the 2007 water levels as initial condition and then simulation was carried out under transient state conditions. Monthly time step were considered from June 2007 – 2009. The initial hydraulic conductivity values of the steady state model that is the range between (0.00009 – 0.0001m/sec) were also used as the values of the hydraulic conductivity for the transient state model. During the calibration process several zones were marked and each was assigned with different hydraulic conductivity within the range which is shown in figure 9.8.

Model run was executed and results were analyzed. The calibration graph for the transient state condition is shown in the Figure 9.9

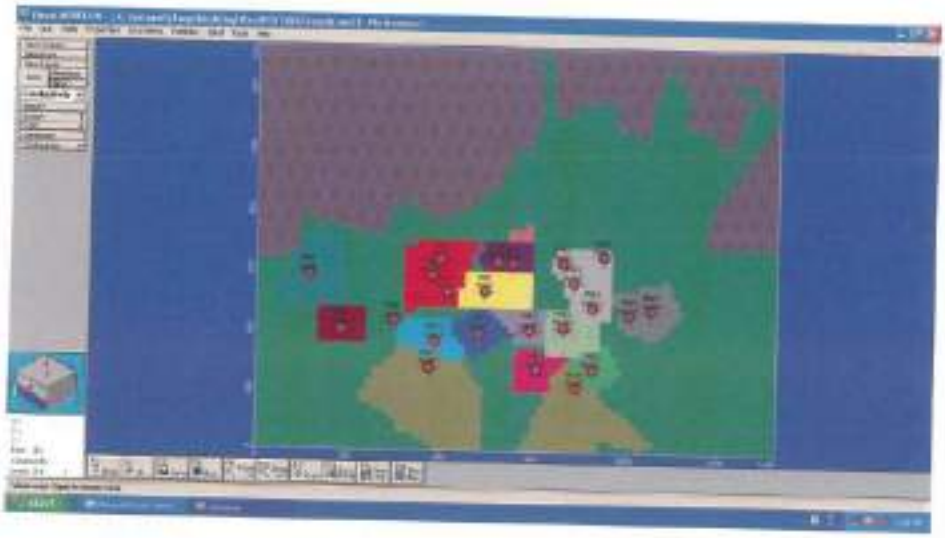

Figure 9.8 Calibrated Zonal Wise Hydraulic Conductivity

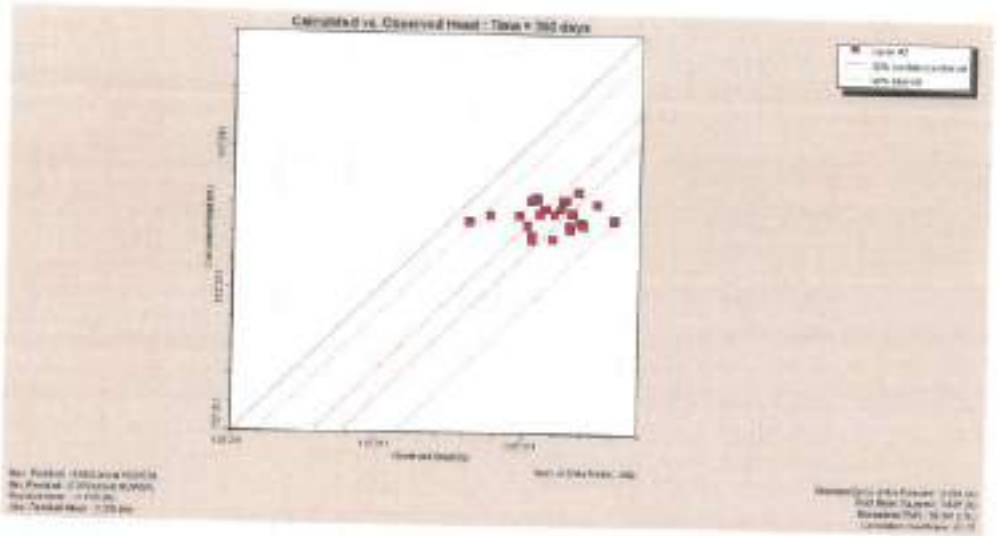

Figure 9.9 Calibration Graph for Transient Condition

Then in order to provide reasonable match between the observed and calculated head values, several changes have been made in the input parameters within the range. Among the twenty three observation wells, only twelve wells were sensitive to all changes in the input parameters and the

remaining twelve wells are not at all sensitive to any changes in the input parameters. So that those twelve wells has been chosen for the further calibration process. The changes done in the calibration process are:

(i) Varied hydraulic conductivity values

(ii) Changing the recharge values

(iii) Changing the boundary condition of tank as recharge boundary to constant head boundary

(iv) Changing the pumping values of all the pumping wells.

(i) Varied Hydraulic Conductivity Values

Initially the entire study area has been assigned with same hydraulic conductivity value. First, that hydraulic conductivity value is increased and decreased in the percentage base and the model run was performed. Since there were no notable changes in the results, the model domain is separated with several polygonal areas and different hydraulic conductivity values were assigned within the range of about (0.000009 – 0.0001m/sec) and the model run was executed and the results were analyzed. The best fit and time series graph for this calibration is shown in the Figure 9.10 and Figure 9.11.

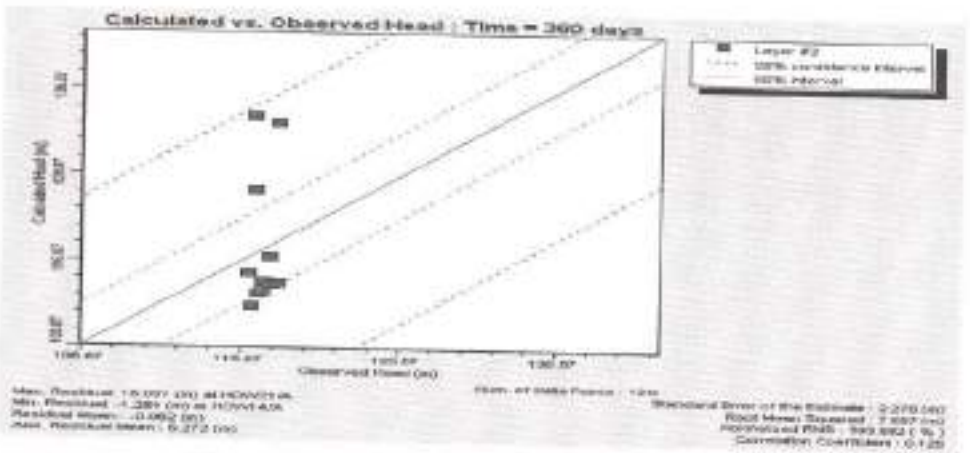

Figure 9.10 Calibration Graph for Varied Hydraulic Conductivity

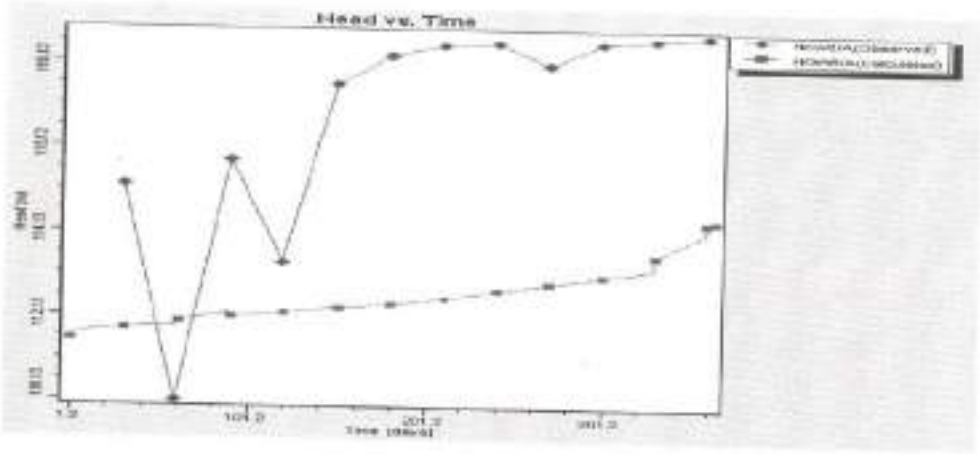

Figure 9.11 Time Series Graph for Changes in Hydraulic Conductivity

(ii) Changes in Rainfall Recharge

In the model domain, recharge values were assigned in the form of polygonal zones. There were totally 15 recharge zones. During the calibration process, recharge values was increased by 5%, 10%, 20%, 30%, 50% and the model run is performed and results were observed. Finally even with increment of about 50% RMS of about 6.469 was obtained. The table showing the variation of RMS with increase in recharge is shown in table 9.1 The best fit and time series graph for changes in recharge values of 50% were shown in the Figure 9.12 and Figure 9.13

Table 9.1 Variation of RMS with Increase in Recharge

Increase in Rainfall Recharge (%)	Root Mean Square Error (m)
5	10.456
10	9.683
20	9.156
30	8.325
50	6.469

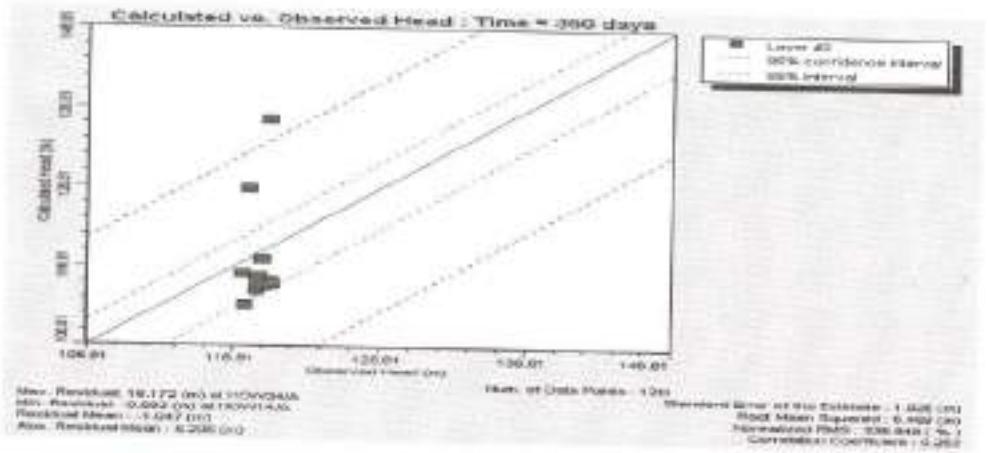

Figure 9.12 Calibration Graph for Changes in Recharge Values

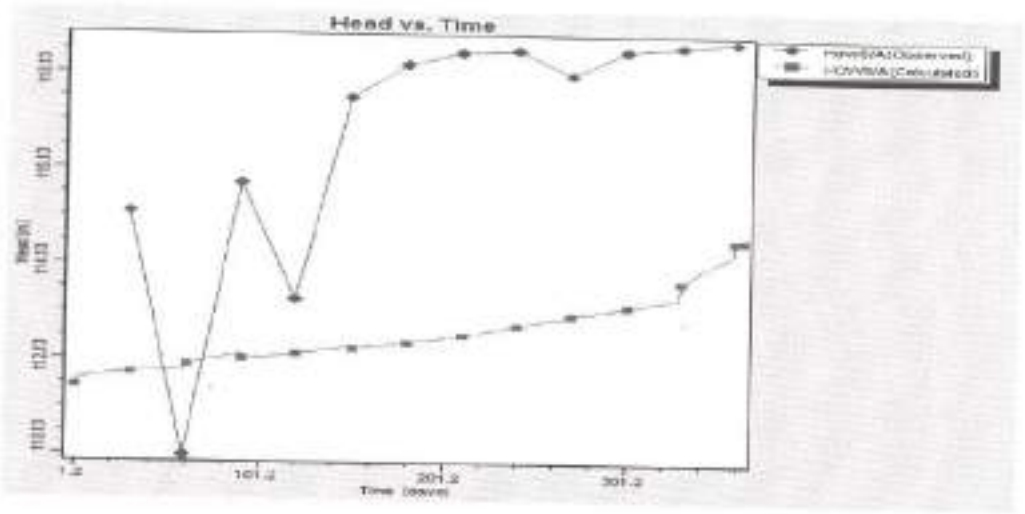

Figure 9.13 Time Series Graph for Changes in Recharge Values

(iii) Changes in Tank Recharge

Initially, recharge boundary has been given for the tank on the upstream side of the command area. For the boundary condition of recharge boundary the calibration results thus observed was satisfactory by comparing with the field conditions and in the calibration graph most of the points were out of range from the best fit line which is described in the figure 9.14. Then during the calibration process recharge boundary is changed into variable head boundary. For the variable head boundary, the water head values which

was observed from the well located in the tank is given for every month. Then the model run is performed and results were observed. After this change the calibration results thus observed was much better than the previous condition but the RMS thus observed was not satisfactory. The best fit and time series graph for the change in boundary condition are shown in the Figure 9.15 and Figure 9.16.

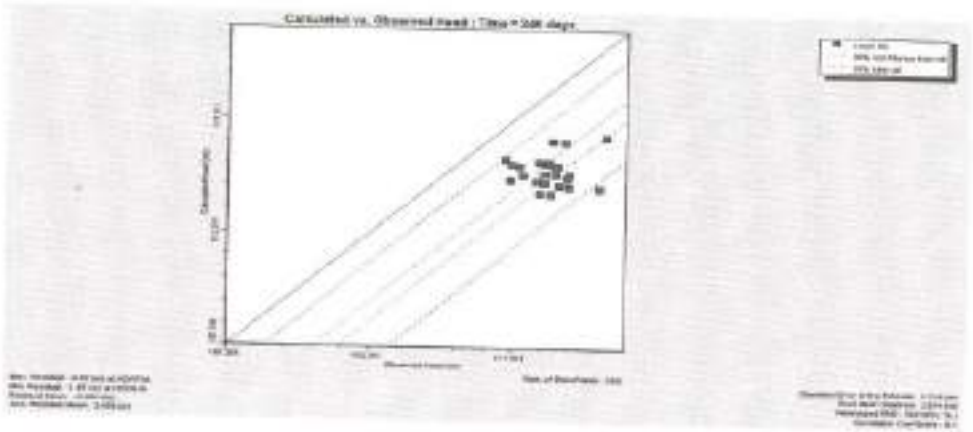

Figure 9.14 Calibration Graph for Recharge Boundary Condition

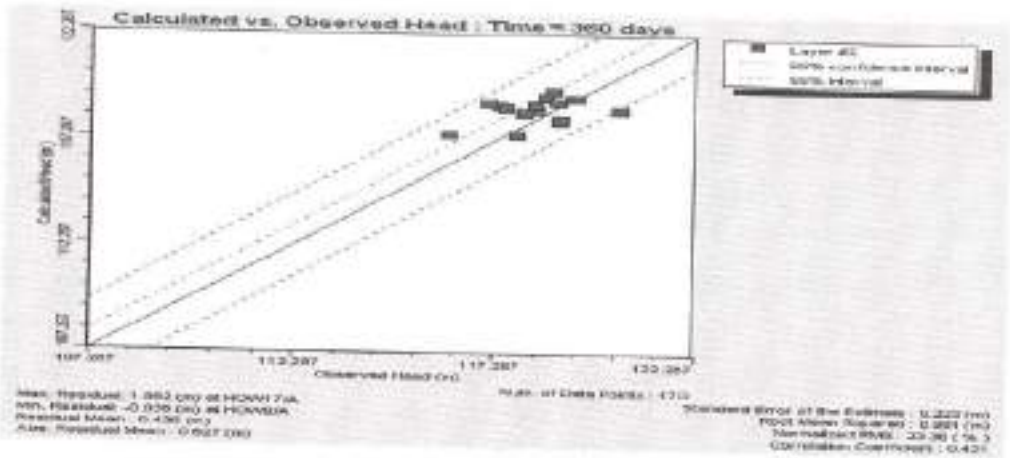

Figure 9.15 Calibration Graph for Changes in Boundary Condition

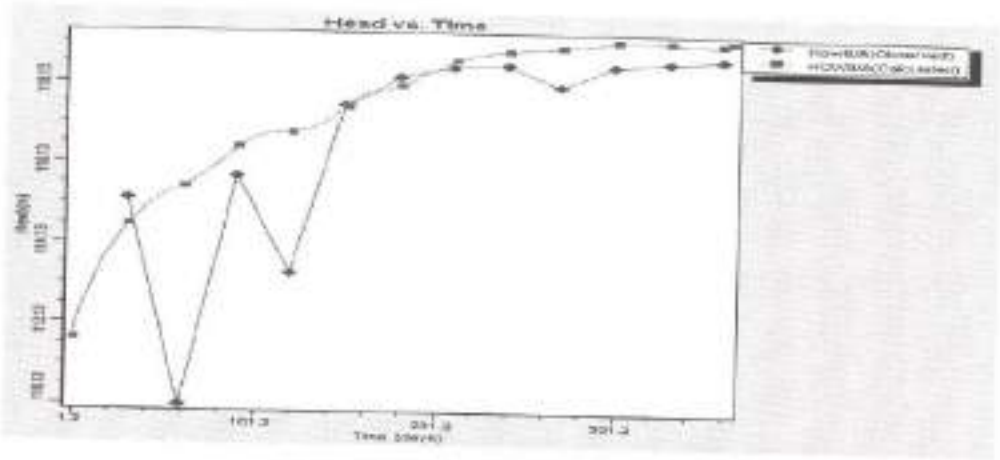

Figure 9.16 Time Series Graph for Changes in Boundary Condition

(iv) Changes in Pumping Rates

In this calibration process, pumping rates were changed and model was executed for several times. Pumping rates of individual wells monthly collected from the field which was used in the model initially. During calibration process pumping rates were decreased in the order of ten percent and the results were analyzed. By decreasing the pumping rates of 10%, 20%, 30%, there were no notable changes in both RMS and Correlation Coefficient. Then by reducing the pumping rate of about 50% , RMS of about 0.8 and correlation coefficient of 0.6 was obtained. The Calibration and time series graph are described in Figure 9.17 and Figure 9.18

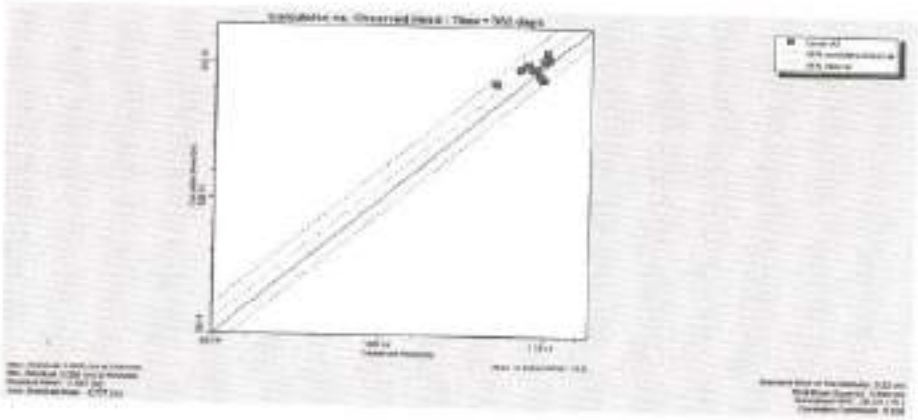

Figure 9.17 Calibration Graph for Changes in Pumping Rates

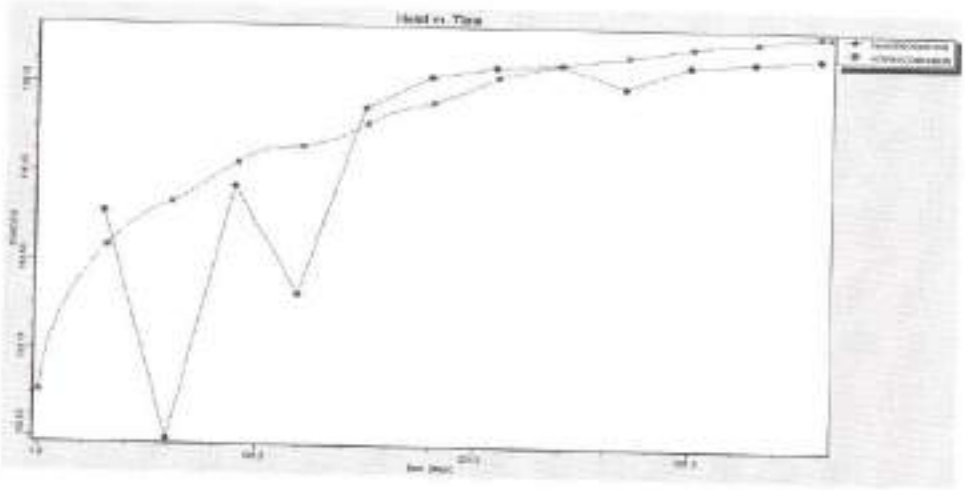

Figure 9.18 Time Series Figure for change in Pumping Rates

Table 9.2 Comparison of Results between all Calibration Changes

Changes Done	Root Mean Squared	Standard Error of Estimate	Normalized Root Mean Squared	Correlation Coefficient
Increased the hydraulic conductivity values to 10%	3.386	0.198	176.336	0.125
Increased the recharge values to 50%	6.469	1.925	336.948	0.253
Changed the recharge boundary to Variable head boundary	0.991	0.223	23.38	0.421
Decreased the pumping rates of about 50% for all the pumping wells	0.898	0.22	28.231	0.638

From the above table 9.2 it could be inferred that the pumping rates and hydraulic conductivity are more sensitive to the model output than any other parameters. By changing the hydraulic conductivity values and by changing the recharge values the model output results was not that much improved. Then by changing the pumping rates , correlation coefficient of 0.638 was obtained. So further to improve the RMS and the correlation coefficient parameter estimation was performed to estimate the hydraulic conductivity using PEST.

9.5.5 Parameter Estimation

Through the Parameter estimation optimum hydraulic conductivity was estimated initially. In this process, the objective function is to minimize the error between the observed and calculated water level. Controlling factors are Marquert Lambda, Parameter change constraints, Termination Criteria. Visual PEST has considered control wells water level as input parameters and it estimated the hydraulic conductivity for all the zones. Several model runs were made and results were analyzed. This process can be considered as recalibration process.

Appearance of Dry Cells

One of the problems with MODFLOW is its limited capability to accurately simulate the drying and re-saturation of grid cells. Due to the presence of the dry cells, PEST run terminated automatically. Moreover it will result in the discontinuities in the relationship between the MODFLOW output and the values of parameters adjusted through the parameter estimation process. Other reasons for the dry cells are due to the head – dependent boundary conditions such as rivers, drains and the general head boundary that are situated in the upper layer cells. Because flow from those boundaries is insufficient to maintain the water levels in the respective cells above the bases

of those cells. So there was need to remove the dry cells from the layers. Occurrence of the dry cells is mainly because if the water level of the cell goes below the bottom elevation of the cell. Several authors suggested several approaches to remove the dry cells. Doherty (2001) uses an asymptotically small transmissivity to avoid deactivating dry cells even if the model cells actually become dry. Painter et al. (2008) constrain the head in cells from falling below the bottom of the cells to prevent the occurrence of the dry cells. Zyvoloski (2009) allowed the vertical conductance to become zero when a cell becomes completely dry. It was also suggested to change the boundary condition which was given for the first layer. In the project recharge boundary was given. Trials were made by increasing the recharge values given for the layers. Due to the increase of the recharge values dry cells in the layers was removed. The schematic representation of the layers with dry cells and layers without dry cells are shown in the figure 9.19 & figure 9.20

Figure 9.19 Schematic Representation of Layer with Dry Cells

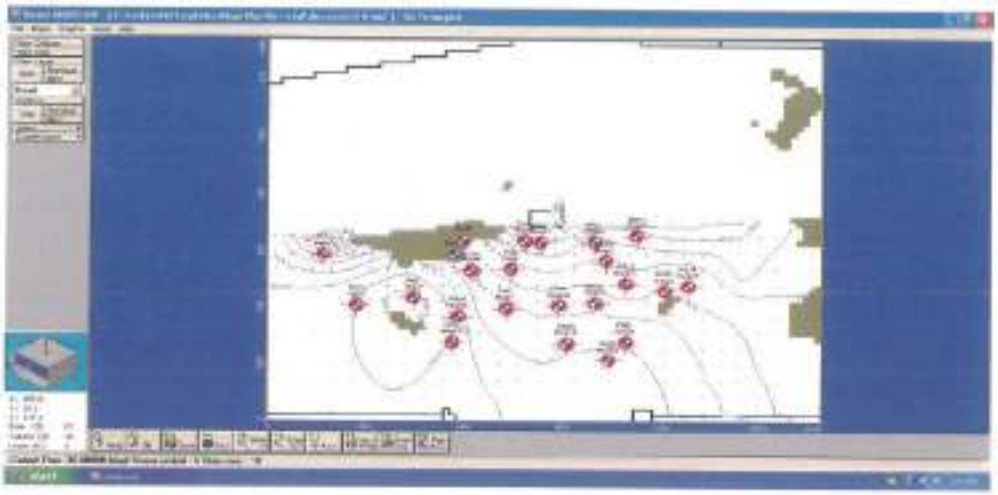

Figure 9.20 Schematic Representation of Layer with Minimum Dry Cells

Occurrence of Dry Cell Error

After removing the dry cells, PEST run was able to be executed . While running the PEST, dry cell error has again occurred even after removing the dry cells in the layers. It was then found that this error was only because of increased pumping that were given for all the control wells initially. Marquart Lambda which is one of the control factors in the Parameter estimation process attempts the process of parameter improvement. During the model run, it was initially taken as 2.5 then it will check for minimization of the objective function , if not it will either increase or decrease the Marquart Lambda and again it will check for the changes in the objective function. In addition to this, in this type of dry cell error the objective function initially got decreased in two to three iteration and there were some fluctuations in the objective function. Hence if the Marquart Lambda keeps on increasing and there are fluctuations in the minimization of the objective function, then it is the indication of the dry cell error would occur. In order to rectify this dry cell error, step by step analyses were made and pumping rates were decreased appropriately for all the control wells. Several trials were carried out by reducing the pumping rates in the

corresponding wells and increasing rainfall recharge rates. Finally dry cell error were rectified after all the changes and PEST run was made and results were analyzed.

Trials 1 to Trial 7

Trials	Percentage Reduction Pumping Rates	Percentage Increase in Rainfall Recharge
Trial 1	5%	-
Trial 2	10%	10%
Trial 3	15%	20%
Trial 4	20%	30%
Trial 5	30%	35%
Trial 6	40%	40%
Trial 7	50%	50%

During initial trials were carrying out, there was an increase in the objective function and also in the Marquart Lamda as shown in figure 9.21 and figure 9.22. from fourth trials there were sequential reduction in the objective function and Marquart Lamda. In the seventh trial objective function and Marquart Lamda were minimum as shown in figure 9.23 and figure. 9.24. In this run good match was observed and calculated heads. PEST estimated. Hydraulic conductivity was compared with simulated hydraulic conductivity as shown in Table 9.3.

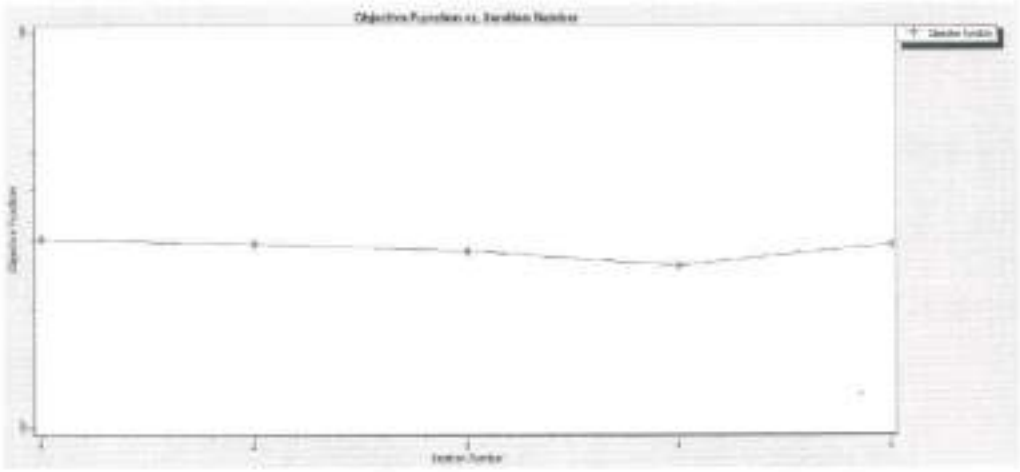

Figure 9.21 Variation of Objective Function for Trial - 1

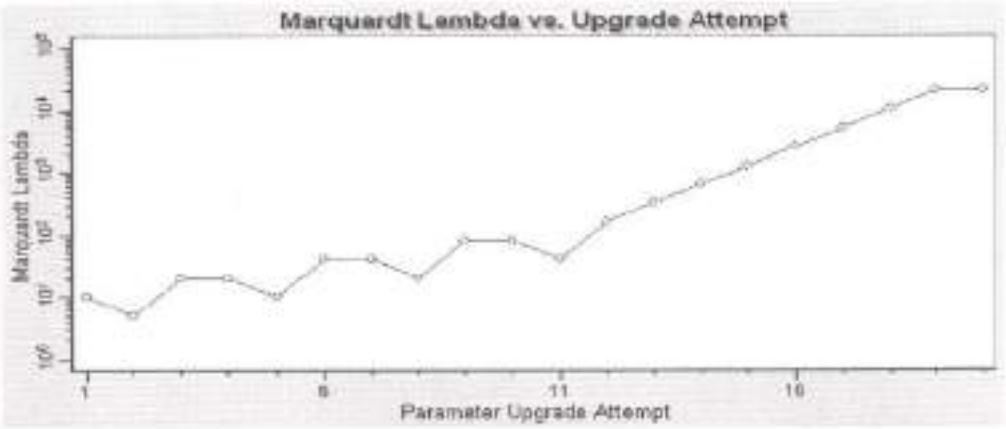

Figure 9.22 Variation of Marquart Lambda for Trial – 1

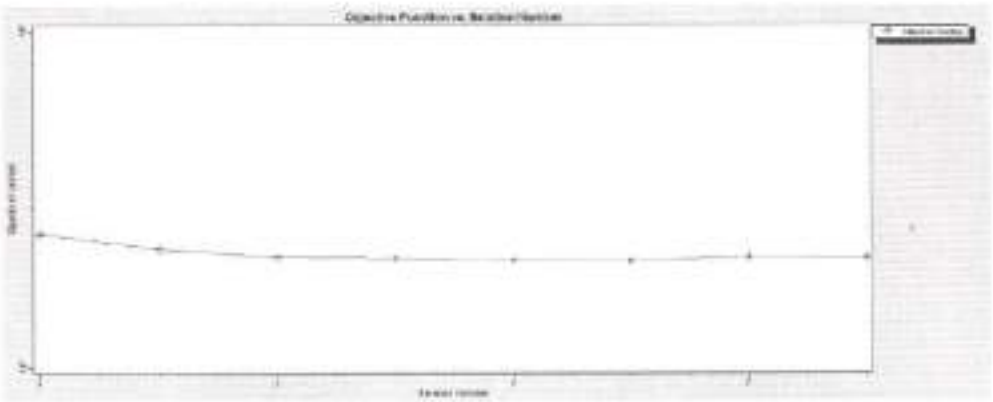

Figure 9.23 Variation of Objective Function for Trial – 7

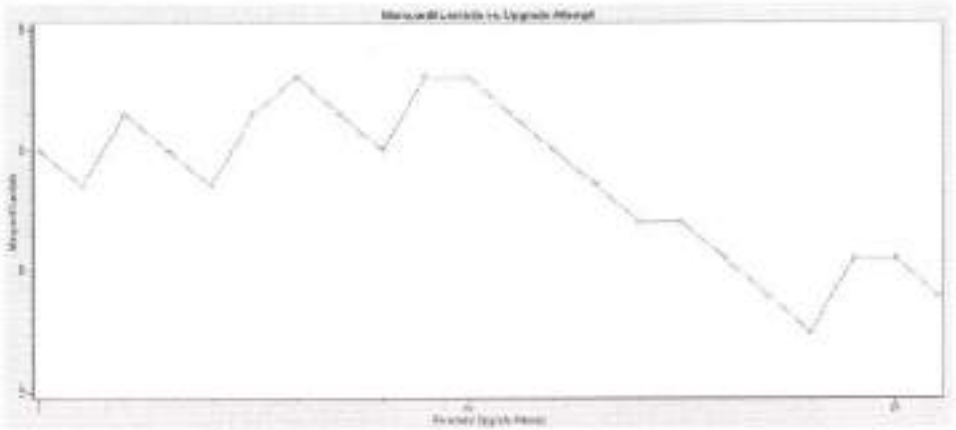

Figure 9.24 Variation of Marquart Lambda for Trial - 7

Table 9.3 Comparison between PEST Estimated Optimum Hydraulic Conductivity and Simulated Hydraulic Conductivity

Zones	Pest estimated hydraulic conductivity	Simulated hydraulic conductivity
1	6.94E-7	5E-6
2	8.07E-5	0.0001
3	4.21E-5	1E-5
4	5.28E-8	9E-6
5	2.83E-5	9E-6
6	6.63E-5	8E-5
7	1.25E-5	1E-5
8	6.68E-5	6E-5
.9	0.00034	0.0008
10	7.15E-5	1.5E-5
11	0.0005	1.2E-5
12	1.88E-6	2E-6
13	0.00012	1.14E-5
14	2.78E-5	1.3E-5
15	5.13E-5	1.05E-5
16	2.56E-5	1.15E-5
17	3.35E-5	1.16E-5
18	9.57E-5	0.001
19	0.0004	0.001

9.5.6 Comparison of Result between the Different Trials

From trial 1 to trial 3, the results obtained were not much satisfactory. From trial 4 the results obtained were reasonably good. Finally in the trial 7, minimum RMS and maximum correlation coefficient were observed as shown in table 9.4. The resulted calibration graph for different time periods, time series graph for some wells for the estimated optimum hydraulic conductivity are given in figures 9.25, 9.26, 9.27, 9.28, 9.29, 9.30.

Table 9.4 Estimated Hydraulic Conductivity from Four Trials

Parameter	Zone	Trial-4	Trial-5	Trial-6	Trial-7
Hydraulic conductivity	1	1.58e-5	2.38E-5	2.16E-7	6.94E-7
	2	9.72E-5	4.44E-6	8.08E-5	8.07E-5
	3	1.7E-5	2.75E-6	4.25E-5	4.21E-5
	4	1.36E-5	1.25E-6	5.28E-11	5.28E-8
	5	2.06E-4	3.97E-3	5.87E-5	2.83E-5
	6	7.16E-5	1.31E-4	6.38E-5	6.63E-5
	7	1.4E-5	5.38E-8	1.21E-5	1.25E-5
	8	6E-5	8.88E-4	6.66E-5	6.68E-5
	9	6.27E-4	6.32E-4	3.502E-4	0.00034
	10	1.26E-5	1.09E-5	6.35E-5	7.15E-5
	11	2.38E-5	1.62E-3	4.78E-4	0.0005
	12	1.24E-5	2.87E-4	2.67E-5	1.88E-6
	13	3.69E-5	5.93E-7	1.37E-4	0.00012
	14	2.17E-5	3.67E-4	3.04E-5	2.78E-5
	15	3.5E-5	5.92E-5	4.92E-5	5.13E-5
	16	1.92E-5	5.9E-4	2.69E-5	2.56E-5
	17	1.21E-5	6.65E-8	3.75E-5	3.35E-5
	18	4.95E-2	1.77E-3	1.06E-4	9.57E-5
	19	2.74E-4	5.03E-4	7.38E-4	0.0004

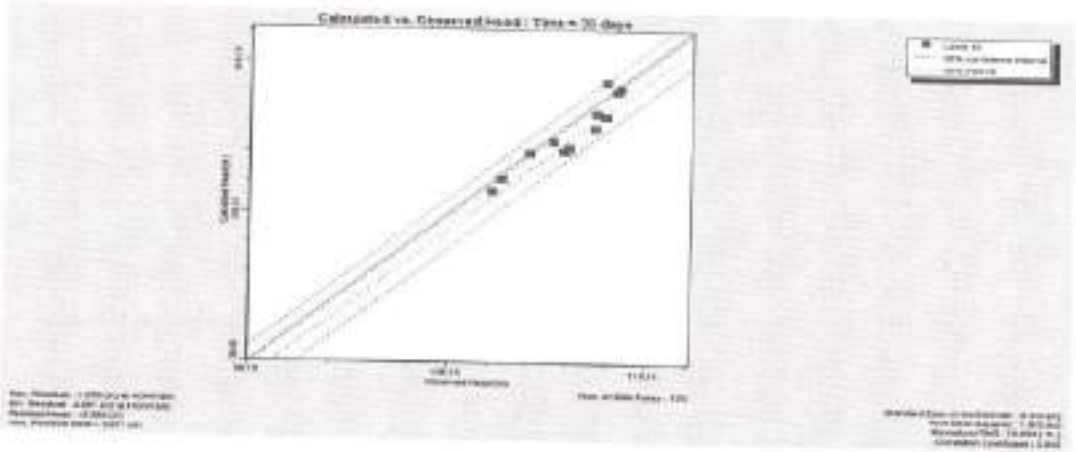

Figure 9.25 **Calibration Graph for Optimum Hydraulic Conductivity at 30 days**

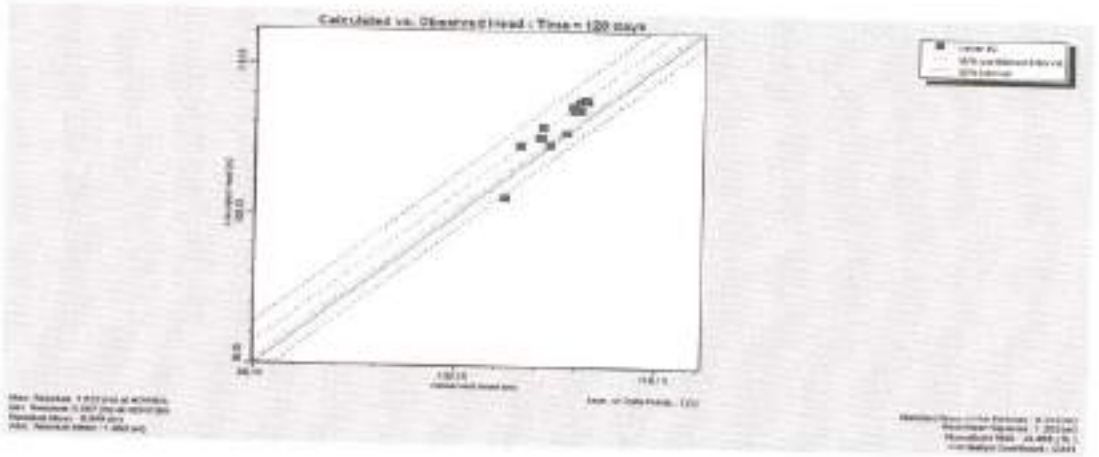

Figure 9.26 **Calibration Graph for Optimum Hydraulic Conductivity at 120 days**

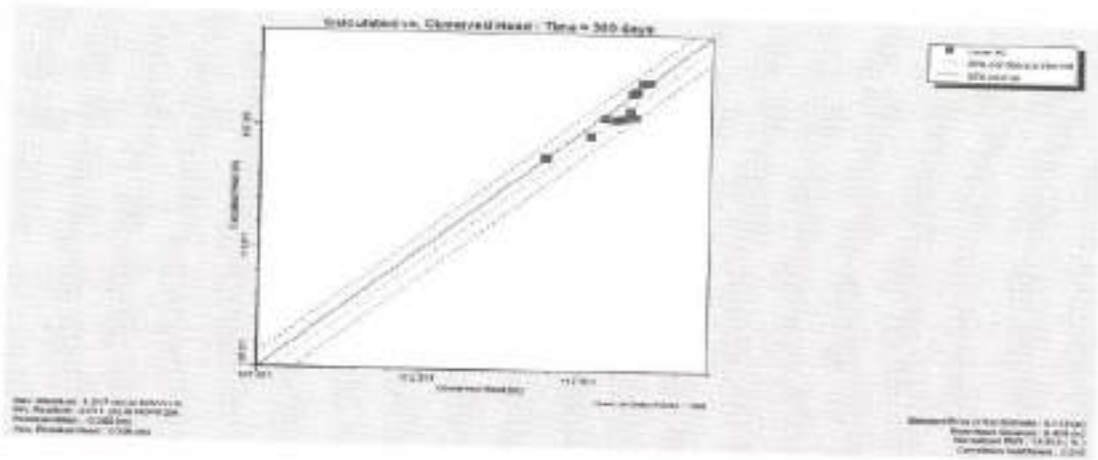

Figure 9.27 **Calibration Graph for Optimum Hydraulic Conductivity at 360 days**

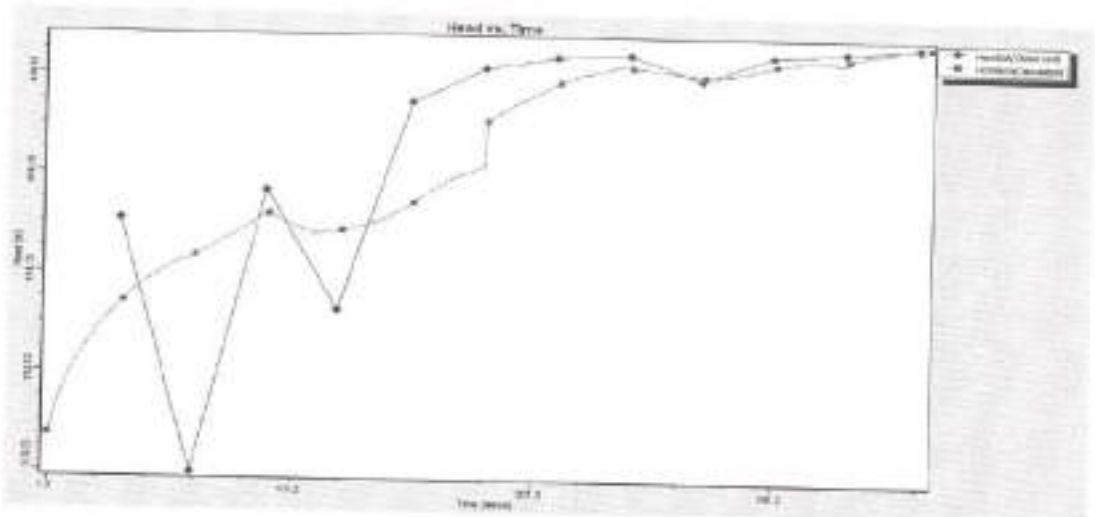

Figure 9.28 **Time Series Graph for Optimum Hydraulic Conductivity for Well - 8**

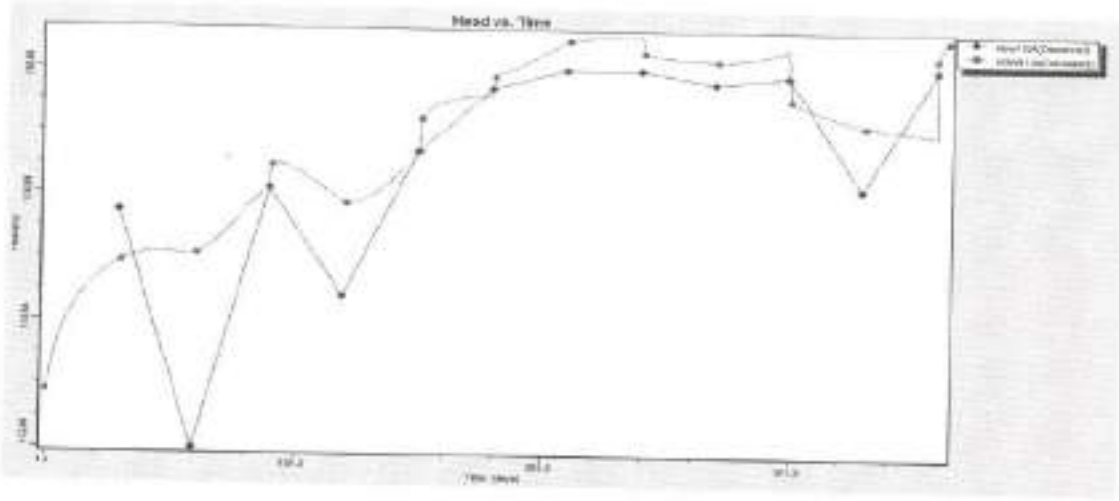

Figure 9.29 **Time Series Graph for Optimum Hydraulic Conductivity for Well - 11**

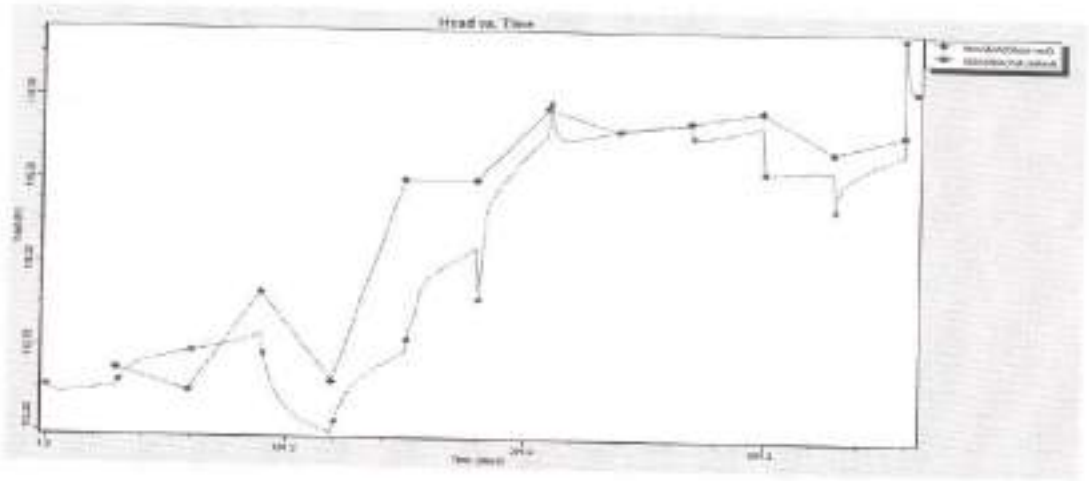

Figure 9.30 **Time Series Graph for Optimum Hydraulic Conductivity for Well -20**

9.5.7 Validation Process

Model validation is the process in which calibrated aquifer parameters, boundary condition recharge and discharge rates were used to generate hysterical field condition. For the flow model validation second year data of water level 2008-2009 were compared and results were obtained. Best

fit graph for different periods and series graph for some wells are given in the figures 9.31 to 9.36

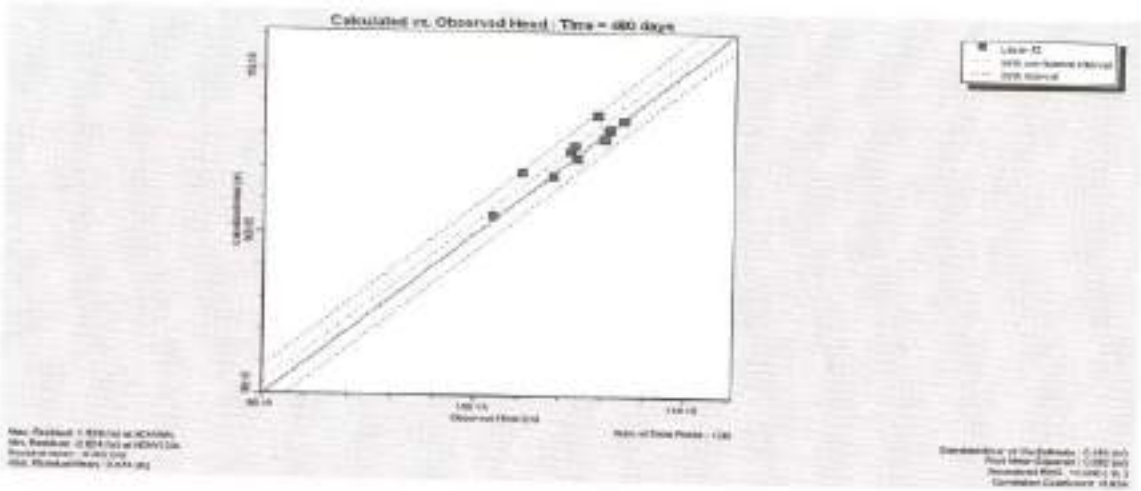

Figure 9.31 **Calibration Graph for Optimum Hydraulic Conductivity at 480 days**

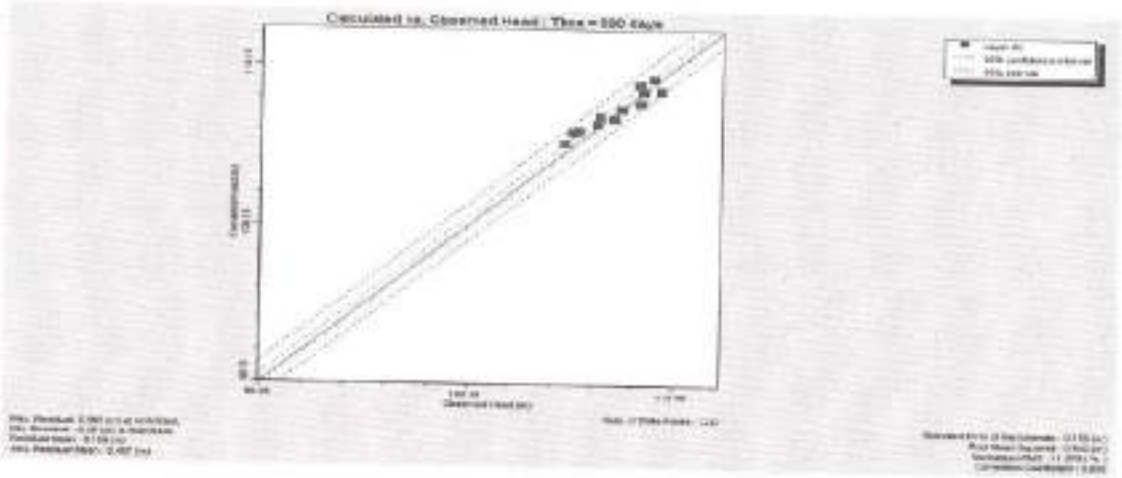

Figure 9.32 **Calibration Graph for Optimum Hydraulic Conductivity at 600 days**

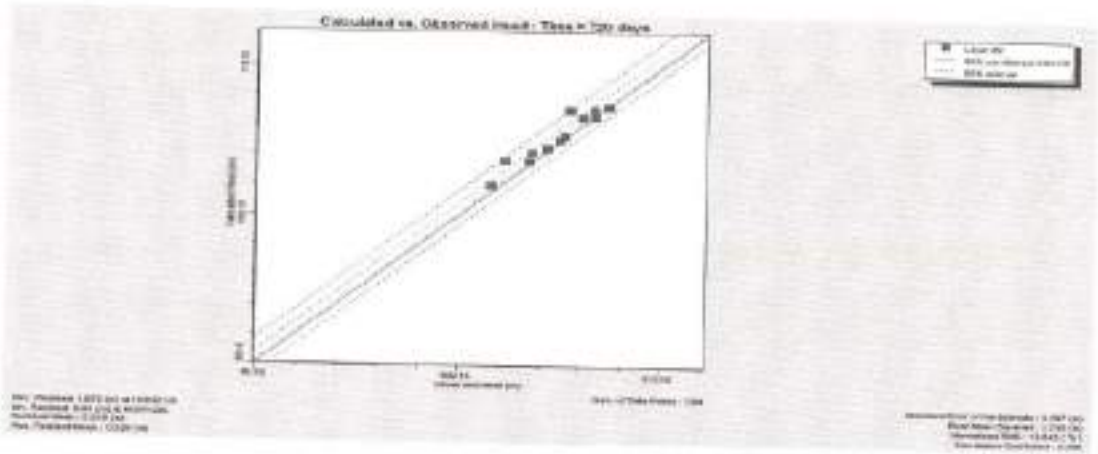

Figure 9.33 Calibration Graph for Optimum Hydraulic Conductivity at 720 days

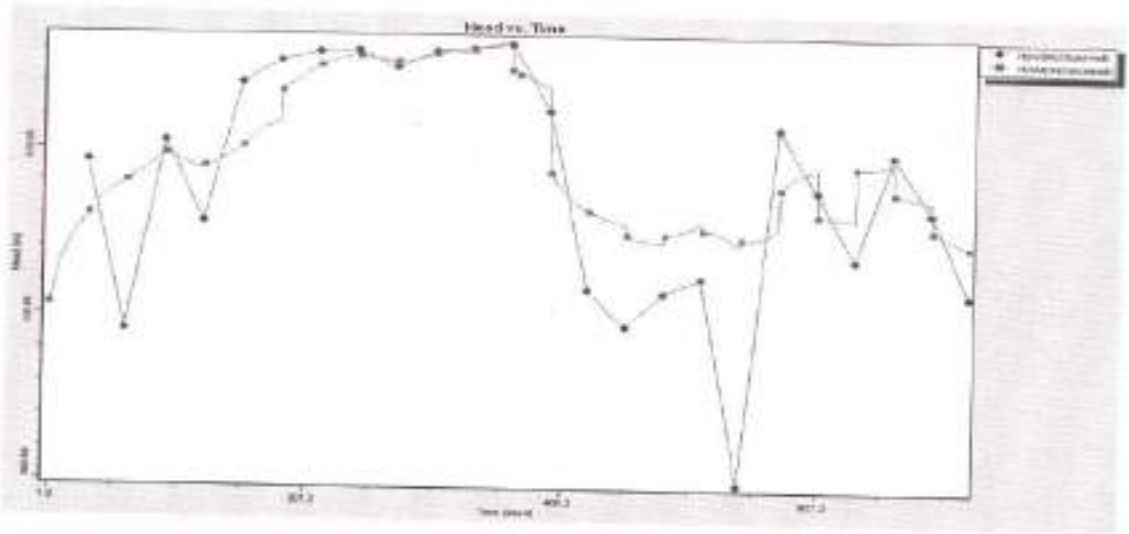

Figure 9.34 Time Series Graph for Optimum Hydraulic Conductivity for Well - 8

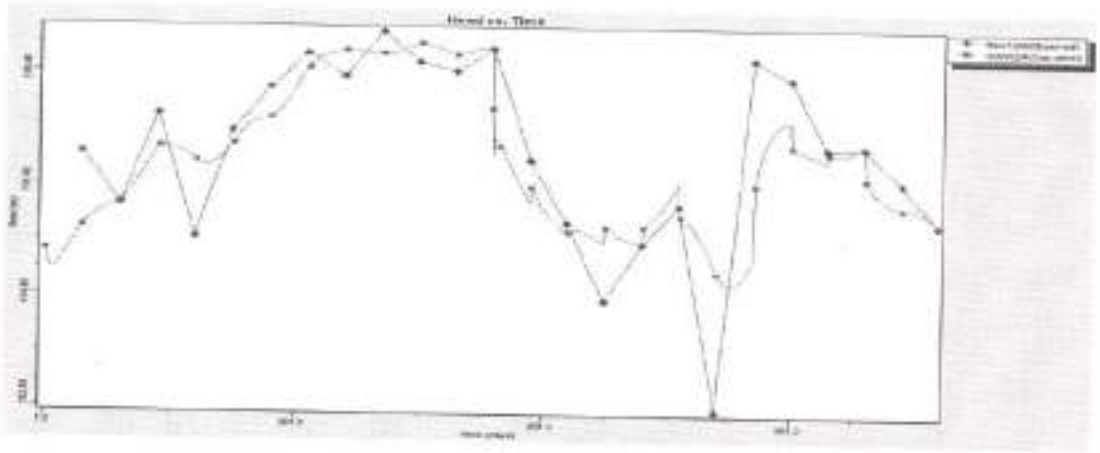

Figure 9.35 **Time Series Graph for Optimum Hydraulic Conductivity for Well - 12**

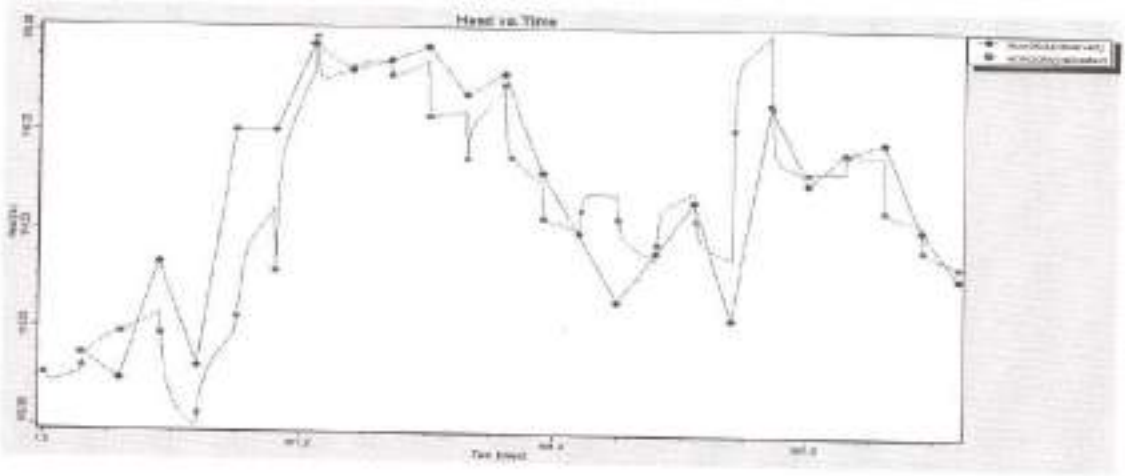

Figure 9.36 **Time Series Graph for Optimum Hydraulic Conductivity for Well – 20**

Initially most of the points in the calibration graphs were away from the best fit line and the resulted RMS was in the range of (0.9 – 9m) and the correlation coefficient of about (0.2 – 0.6). The time series graph match was not good between the observed and calculated heads for all the wells. After the calibration process through PEST, there was a good match between the observed and calculated heads. Hence using the MODFLOW – PEST , optimum hydraulic conductivity was estimated which had the RMS

range of (0.4m – 0.6m) and correlation coefficient in the range of (0.8 – 0.9) was thus obtained in the Calibration graph. From the mass balance, after the PEST calibration 50 % increment of recharge sand 50% decrement of pumping rates were observed.

9.5.8 Comparison of Mass Balance

Seepage from the tank was estimated through groundwater balance equation numerically for two years 2007-2008 and 2008-2009. Calibrated and validated monthly seepage rate, rainfall recharge rate, pumping rate and groundwater storage are shown in figure 9.37 to 9.40 respectively

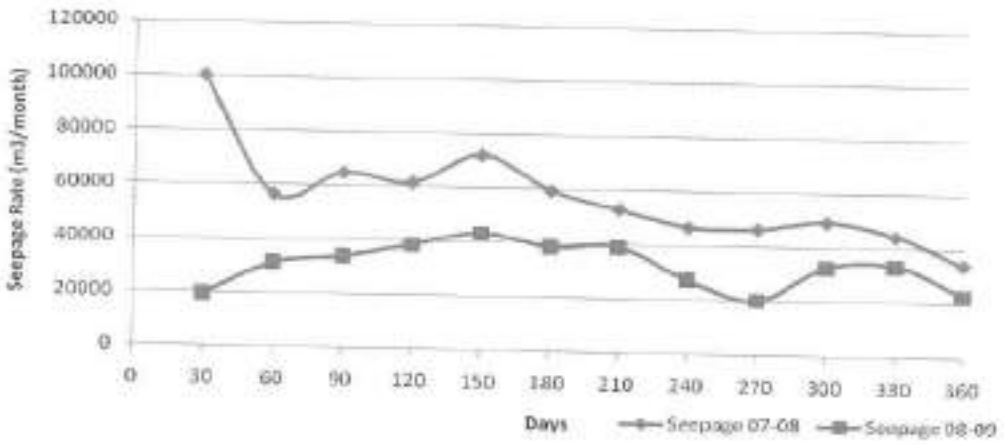

Figure 9.37 Comparison of Seepage Rate

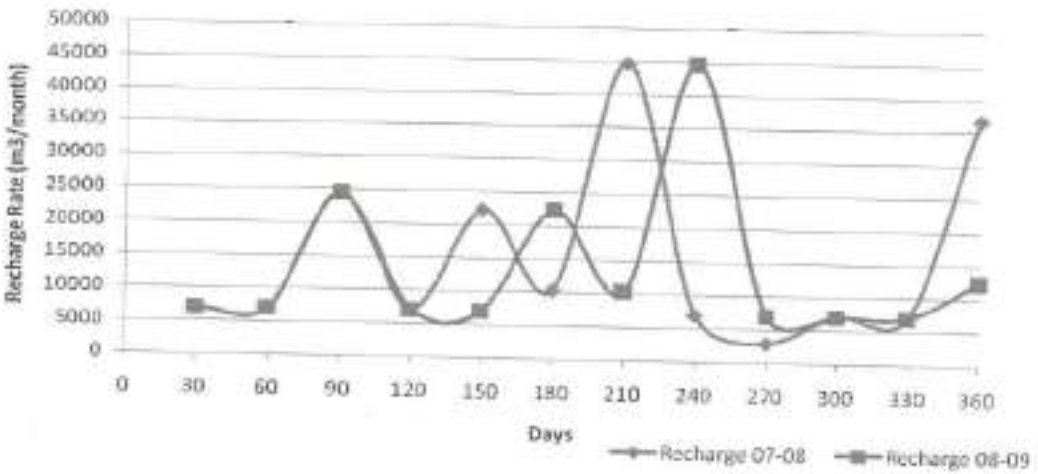

Figure 9.38 Comparison of Rainfall Recharge Rate

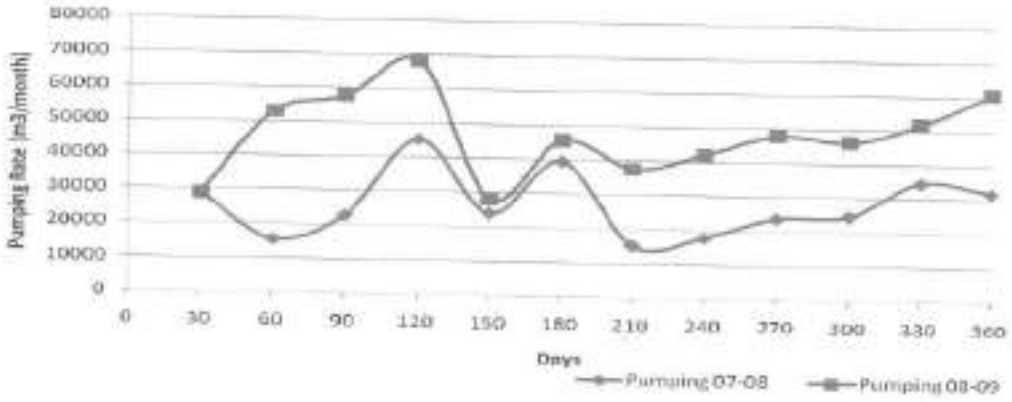

Figure 9.39 Comparison of Pumping Rate

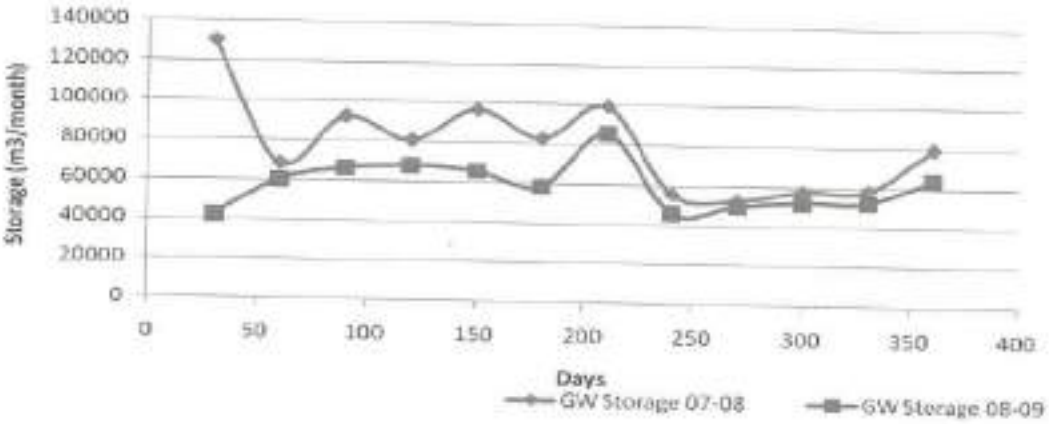

Figure 9.40 Comparison of Monthly Groundwater Storage

Even though the annual rainfall in the year 2007-2008 and 2008-2009 were same their intensity are different. There was a delay of one month in the year 2008-2009 which has very great impact on agricultural pattern, seepage rate from the tank, rainfall recharge, pumping rate and groundwater storage which is shown in Table 9.5.

Table 9.5 Comparison of Major Inflows and Outflows

Year	Seepage from the Tank (m^3)/year	Rainfall Recharge (m^3)/year	Pumping (m^3)/year	Groundwater Storage (m^3)/year
2007-2008	688791	184241	323582	955802
2008-2009	379051	163966	567886	713855

Year 2007-2008 has increased groundwater potential that supported higher pumping in the year 2008-2009 during which rainfall was delayed for one month i.e. November 2008. This led to decrease in groundwater potential in the year 2008-2009.

9.6 SIMULATIING THE IMPACT OF PARTIAL DE-SILTING

After the model calibration and validation, it was tried to simulate the impact of partial de-silting. De-silted area of 1200 sq on to a depth of 0.65 m with a higher permeability of 0.43 m/day (1.8 cm/hr) was incorporated in the model and it was executed to estimate the impact. Similarly the model was run under various position and de-silting area.

Trials	Area of De-silting	Location
1	1200 m^2	Exactly above the sluice 2
2	2400 m^2	Exactly above the sluice 2
3	4800 m^2	Exactly above the sluice 2
4	9600 m^2	Above sluice 2
5	9600 m^2	At sluice 2
6	9600 m^2	Left of sluice 2
7	9600 m^2	Right of sluice 2

Trial 1 is the actual de-silting scenario. Trial 1, 4, 5, 6, 7 are shown in figure 9.41due to de-silting certain portion of the aquifer in the study area were influence which was seen in the increase in water level in some of the wells. Well no. 8, 9, 10, 11, 12, 14, 18 were influenced under trial 1. Additional wells 19, 20 , 22 and 24 were influenced by the trials 4,5,6 and 7. Recharge from the tank was substantially increased in the trials 4 and 5 which can be seen from the table and also in the figure 9.42.

Average Recharge from the Tank m^3/day

Year	Without De-silting	De-silting 1200 m^2 Trial 1	De-silting 9600 m^2			
			Trial 4	Trial 5	Trial 6	Trial 7
2007-2008	1913	1913	2410	2412	2119	2119
2008-2009	1053	1131	1362	1508	1356	1332

Of all, the trial 5 with 9600 sq.m de-silting positioned 200 m from sluice 2 has recharged maximum quantum of seepage.

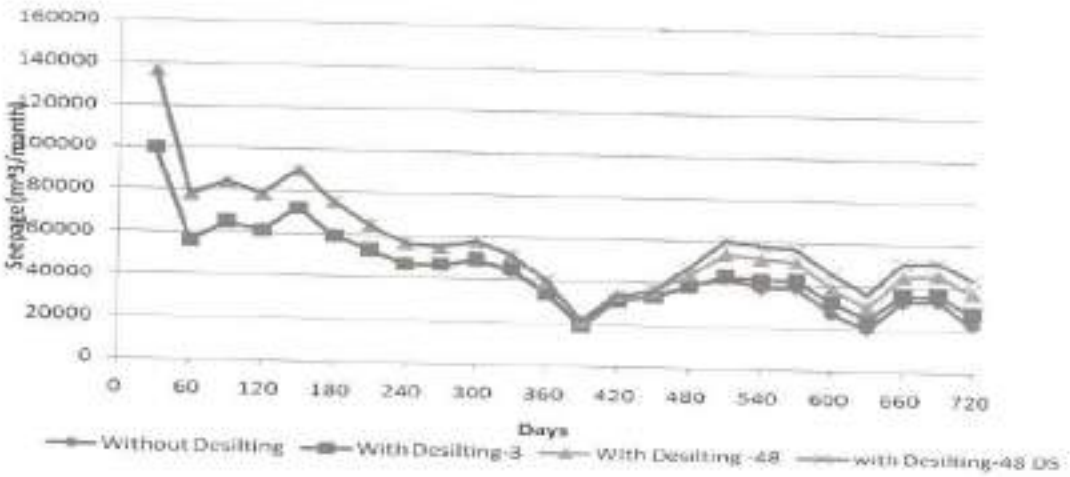

Figure 9.41 Comparison of Seepage Rate Before and After De-silting

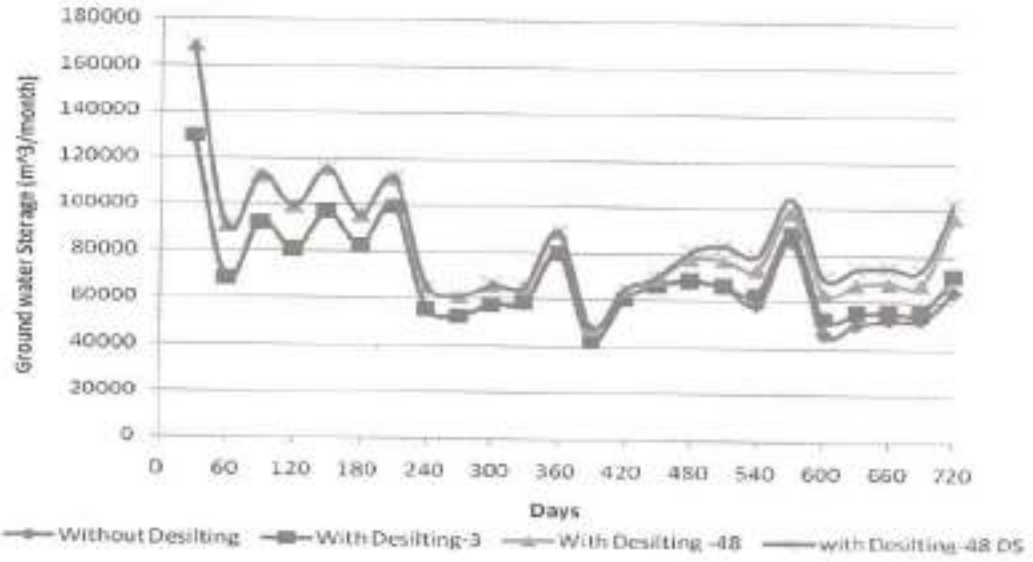

Figure 9.42 Comparison of Groundwater Storage Before and After De-silting

Groundwater storage was also substantially increased in the trials 4 to trial 7. Figure 9.42 compares the groundwater potential without de-silting with de-silting of 1200 m^2 (Trial 1) 9600 m^2 (Trial4) and 9600 m^2 (Trial 5).

If 9600 sq.m area is de-silted to a depth of 0.65 m it will increase the groundwater potential to a extent of 25 percent as given below.

De-silting approximately 500 m away from the sluice

$$= \frac{711575 - 567886}{567886} x100$$

= 25 Percent more than existing pumping

This will substantially increase the area of cultivation. It needs a expenditure of Rs. 6 lakhs to 8 lakhs. Existing catchment is sufficient enough to fill the tank twice even after de-silting of 6240 cubic meter. Every year the tank gets filled two to three times. It surpluses most of the year.

Hence it is suggested to go for a partial de-silting of 9600 sq.m very close to the sluice 2, so that it will definitely increase the recharge potential of the tank to a extent of 43 percent as given below

De-silting approximately 200 m away from the sluice

$$= \frac{542930 - 379051}{379051} * 100$$

$$= 43\ \%$$

De-silted soil can be used for strengthening the tank bund, manure to the agricultural lands based on the quality of the silt and may be used for manufacturing bricks.

9.7 SUMMARY

Ground modeling has been carried out in this project in order to evaluate the groundwater system behavior for different de-silting location and volume of de-silting. Hence initially model was conceptualized, calibrated using 2007-2008 observed groundwater level data and validated using 2008-2009 data under unsteady state flow condition. Sensitivity analysis were also carried out with four parameters such as hydraulic conductivity, tank recharge, boundary conditions and pumping rates. The RMS error was improved form 3.386 m to 0.9 m and the correlation coefficient was 0.125 to 0.638. In order to improve RMS error and the correlation coefficient parameter estimation run was carried out using the Model PEST. While PEST was running dry cells appeared that could not allow the process to continue. By adjusting the screen position of the wells dry cells problem was overcome. However PEST could not able to be executed. It was then found that this error was due to increased pumping that were given in the production wells

initially. Hence pumping rates were verified which was decreased and rainfall recharge was increased. Finally dry cells error was rectified and PEST run was successful. Optimum zone wise hydraulic conductivity and rainfall recharge and pumping rates were estimated through PEST run. So that the RMS error was reduced to 0.5 m and correlation coefficient was increased to 0.918 at 360 days calibration time period. Through this time series match was improved between observed and calculated head for the control wells during calibration period 2007-2008. There was good match during validation period 2008-2009 at which RMS error was 0.75 m and correlation coefficient was 0.958. After the success of calibration and validation of the model that can be used for management purpose.

After the model calibration and validation, it was tried to simulate the impact of partial de-silting of an area 1200 sq.m to a depth of 0.65 with a higher permeability 0.43 m/day, which actually carried out and observed in the Sengulam tank bed, was incorporated in the model and was executed to estimate the impact. Similarly the model was run for more de-silted area and different location of de-silting. It was found that seepage rate of 1053 m^3/day, 1131 m^3/dayand 1508 m^3/day was estimated without de-silting, with de-silting of 12000 sq.m and 9600 sq.m respectively. In turn it has increased the groundwater potential to a extent of 143 percent. Hence it is proposed to de-silt 9600 sq.m of tank bed at a distance of 200 m from the tank bund. De-silted soil may be used for strengthening the tank bund, agricultural land that will improve soil fertility and manufacturing bricks. This project strongly recommend to de-silt the tank beds to improve its capacity, recharge capacity and to increase groundwater potential of the command area. In turn it will increase area of cultivation and number of crops and also reduce flood water and increase rain water conservation.

CHAPTER 10

SUMMARY AND CONCLUSION

Irrigation tanks are to conserve rainwater and recharge the groundwater aquifers. These tanks are silted over years that reduces the storage capacity of the tank, in turn it reduces the percolation capacity of the tank that is attributed by the deposition of the finer particles on the tank bed. Hence the tank bed has to be de-silted to increase its storage and recharge capacity. To de-silt the tank bed, one should decide where to de-silt? up to what depth it is to be de-silted? This project evolved the strategy for de-silting the tanks for the future. Extensive literature survey was carried out to attain the goals and the detailed methodology was framed.

Stage I Hydrologic and Hydraulic characteristics of the tanks were studied. through conventional methods;

State II Tank Bed Characteristics and its recharge capacity were studied through infiltration test soil texture and permeability analysis;

State III Groundwater aquifer parameters were estimated through well dilution technique;

Stage IV Tank and ground water aquifer system interconnection were studied through geophysical studies;

Stage V Tank water and groundwater interconnection were studied through tracer application;

Stage VI Finally the impact of partial de-silting was studied through ground water modeling;

Each stages of the methodology provided excellent / favourable understanding of the irrigation system. The Major findings of each stage is discussed below.

Stage I Hydrologic and Hydraulic Characteristics of Irrigation Tanks

Non-system tanks are filled exclusively through run off from the catchment and direct rainfall over the tank. Hence the inlet arrangements to the tanks are to be maintained is the prime requirement. Next part is, its outlet arrangement to be intact in order to conserve rainwater during monsoon. The Ponpadi tanks capacity is 1.2 Mm^3. Thirty years annual rainfall of this area is 1008mm. The farmers expressed that ones this tank is filled, that meets the two years of agriculture demand of the command area. The tank received only one fourth of the capacity during December 2007 but it was full during December 2008 for the same amount of annual rainfall. The Tank filling does not depend on annual rainfall only that depends on intensity of railfall, continuous rainy days also. It's area of cultivation was 50 acres and 205 acres during 2007-2008 and 2008-2009 respectively. The farmers tapped the groundwater at three levels such as open wells, shallow bore wells and deep tube wells. Through pumping rate analysis it was estimated that 0.76 Mm^3 and 1.65 Mm^3 ground water were pumped during the period of 2007-2008 and 2008-2009 respectively. Seepage rate was estimated 0.33 Mm^3 and 1.49 Mm^3 during the two water years. Relationship between tank water levels and ground water levels were established. Shallow water levels varied quadratically and piezometric surface varied linearly.

Similarly, the Sengulam tank characteristics were analysed. It is a small tank of storage capacity 0.3 Mm^3 which gets filled two to three times

almost every year. Thirty years average annual rainfall of this area is 780mm. This tank has three sluices which are used for discharging the tank water to irrigate its command area. Totally24 open pumping wells were found in the command area. The Sengulam tank had received same amount of rainfall during both the water year 2007-2008 and 2008-2009. However the tank was filled over six months during 2007-2008 but it was filled within a month during 2008-2009. This tank filling is really due to rainfall intensity, antecedent moisture content, and continuous rainfall days. Ground water occurs under phreatic condition in the weathered formation that is being developed through dug wells. The water bearing properties of formation is lack of primary porosity that depends on secondary intra granular porosity. The occurrence and movement of ground water in these rocks are generally confined to such spaces. The thickness of weathered zone is 4 to 15m which yields 40 to 1101 pm that are able to sustain pumping for 2 to 6 hours per day. The tank had 0.23 Mm^3, two third of its capacity during February 2008 which was 0.013 Mm^3 during February 2009. Most of the wells in the Sengulam tank behaves more or less in a similar manner, indicating very good response to tank water level. Major seepage driving component is head of the water in the tank in addition to elevation head. The relationship between tank water level and groundwater level was observed as quadratic in nature. The change in groundwater storage during 2007-2008 and 2008-2009 were 0.77 Mm^3 and 0.895 Mm^3 respectively. Major groundwater storage received through rainfall recharge and seepage from the tank.

Through this hydrologic and hydraulic characteristics, study of the above tanks, it is well understood that the tank and groundwater aquifer system is very well connected.

Stage II Tank bed characteristics and its recharge capacity

Highly permeable zone was detected through TVLF survey in both the study tanks at Ponpadi and Sengulam and iso-resistivity maps were established. Infiltration test, soil texture analysis and permeadrility test were carried out at surface and at different depth. Based on the above analysis the area for partial de-silting at sengulam tank was demarcated and de-silted to a depth of 0.61m for an area of 1395 sq m. The silt removed from the tank bed was taken by the farmers for their land fertility and the remaining used for strengthening the bund.

Permeable Zone	Maximum Infiltration Rate cm/hr	Soil Type	Maximum Permeability cm/hr
Ponpadi tank at 100cm depth	1.08	Sandy clay	4.92
Sengulam tank at 50 cm depth	1.50	Sandy loam	1.83

Strategy for desilting was framed that are given below:

i. The deepest portion of the tank is to be selected where the water stays for a longer period of time in which silt is more;

ii. Geophysical survey is to be conducted in the deepest portion of the tank to delineate the permeable zone;

iii. In that permeable zone infiltration test is to be carried out at different locations and depth;

iv. Soil samples are to be collected to determine permeability and soil texture;

v. Based on the soil texture, infiltration rate and permeability the depth of de-silting can be decided;

vi. If the infiltration rate is very less at 50 cm and 100 cm depth below tank bed level, then bore hole test has to be carried out with the help of hand auger;

vii. Collecting soil samples at different layers and carry out soil sample analysis to determine the soil texture and permeability in which one can easily determine at what depth the soil profile is permeable;

viii. If infiltration is less even at 100 cm depth, recharge pits can be a viable option, water can be diverted to these pits and recharge capacity of the tank can be enhanced effectively;

State III Estimation of Aquifer Parameters through Well Dilution Techniques

Totally seven boreholes were constructed to a depth of 2m to 2.4m to conduct tracer study. Sulpho-rhodamine B and Sodium Chloride (NaCl) were used to estimate the groundwater velocity and permeability. In addition to that permeability was determined through falling head permeameter, particle size distribution and pumping test analysis. The hydraulic conductivity estimated through the three methods were in the same range of 3.5 to 5.5 m/day which is similar to PWD report.

Stage IV Tank and Groundwater Aquifer Interconnectivity

Electrical resistivity survey was carried out at various locations. Through inverse slope method depth of the subsurface layer was delineated and interconnectivity was confirmed. In addition pumping tests were carried out at six to seven locations at which resistivity survey was also carried. Then empirical relationship between resistivity parameters and aquifer hydraulic parameters were established. This relationship was used to estimate permeability at the unknown locations. Observed and calculated permeability

were 5.73 m/day and 5.23 m/day respectively. Geochemical analysis also indicated that the tank and downstream groundwater aquifers are directly interconnected. The above said studies provided qualitative information about tank aquifer nexus.

Stage V Estimation of Seepage Velocity through Tracer Applications in the Field

Extensive literature on tracers were reviewed. It was observed that organic dyes are proven to be powerful tracers. The most widely used dyes for groundwater studies are orange flourescent dye that relatively cheaper resistant to adsorption. Organic dye intensity can be measured in the flourescent spectrophotometer through calibration curve established for each type of dye.

Rhodametre-B was applied to the sengulam tank before and after desilting. Rhodamine-B was detected first within 24 hours in most of the wells during 2007-2008 irrespective of the distances. This is mainly attributed to driving head in the tank. Average seepage velocity was 0.09 cm/sec (77 m/day) during 2007-2008 and was 0.016 cm/sec (14m/day) during 2008-2009 Multi peaks were observed in the break through concentration curve. It attributed to heavy pumping in the production wells. Average dye recovery was 22 present in the year 2008 and 16 percent in the year 2009. Rhodamine B was lost mostly by soil adsorption, some may be lost through sunlight, UV radiation. Of all flourescent dyes, rhodamine B is the least resistant to soil adsorption.

Similarly rhodamine B was applied in the Ponpadi tank during 2008-2009 which could not be applied during 2007-2008 because this tank was not having enough water. Rhodamine B was detected in open wells within 24 hours which were detected in the shallow tube wells in 5 days and deep tube wells in 19 days. Rhodamine B reached shallow aquifer initially which were leaked into semi confirming layers later days. Dye studies

provided very good information about inter connectivity of the tank and the aquifers, relative seepage velocity and also leakage from upper aquifer to lower aquifer. Adsorption characteristics of three different dyes such as Rhodamine B, Sulphorhodamine B and Flourescein on different soil were studied. Both Rhodamine B and sulphorhodomine B absorbed more on the clay soil than the fluorescein dye which were very minimum adsorbed. Theoretically fluorescein was the suitable dye for groundwater tracing. However most ground water studies used rhodamine - B and sulpho rhodamine B because they are easily available in the Indian market and also relatively cheaper.

Stage VI Numerical Modeling of Partial De-silting

MODFLOW was applied to the Sengulam tank and its command area with appropriate initial and boundary conditions. Model was calibrated for the data collected during 2007-2008 and validated for the period 2008-2009. Best results were obtained after running the visual PEST, so the RMS error was 0.4 to 0.6m and correlation coefficient was in the range of 0.8-0.9. Then the model was used to predict the seepage velocity before and after de-silting. Seepage rates were 0.057 Mm^3 and 0.034Mm^3 during 2007-2008 and 2008-2009 respectively. Seepage rate was observed less after de-silting that may be attributed to less driving head of the tank in the year 2008.

The second scenario is increased the de-silted area to 9600sq.m very closer to the tank bund which contributed 0.072Mm^3 and 0.045 Mm^3 at 75 percent and 50 percent of the tank storage. Seepage rate was increased to a extent of 25 percent to 43 percent after de-silting. Hence partial de-silting of the tank bed improves the recharge capacity of the tank substantially in turn tank's storage capacity also increased. De-silted soil is very much useful for bund strengthening, to improve agricultural land fertility and to manufacture the bricks.

REFERENCES

1. Alex, B. Francisco, "Sorption Characteristics of the tracer Rhodamine WT: Effect of subsurface composition" American Chemical Society, 2000.

2. Atkinson, CT., Ward RS., Hannelly, E. "A radial – flow tracer test in Chalk : comparison of models and fitted parameters", Tracers and Modeling in Hydrogeology . Proceedings of the Model CARE 96 Conference, IAHS Publ. No. 262, pp. 7-21, 2000.

3. Atkinson, T.C., Ward, R.S. and Hannelly, E. "A radial flow tracer test in chalk: comparison of models and fitted parameter" Proceedings of the conference Tracer sand Modeling in Hydrology, IAHS, pp. 7-15, 2000.

4. Bala'zs, M. and Fekete, " Application of Isotope Tracers in Continental Scale Hydrological Modeling", Journal of Hydrology, Vol. 330, pp. 444 - 456, 2006.

5. Balasubramanian, A., Sharma, K.K. and Sastri, J.C.V. "Geoelectrical and hydrogeochemical evaluation of coastal aquifers of Tambraparni basin, Tamil Nadu", Geophysical Research Bulletin, Vol. 23, No. 4, 1985.

6. Bodhinayake, W. and Noborio, K. "Estimation of Field Saturated Hydraulic Conductivity form Double Ring Infiltrometer Measurements", Vadose Zone Journal, Vol. 3, pp. 964 – 970, 2004.

7. Bor- Jier Shiau, " Influence of Rhodamine WT properties on Sorption and Transport in Subsurface Media." Journal of Ground water. Vol-31, No.6, 1993 .

8. Bruprecht, J.K. and Schofield, N.J. 'Infiltration Characteristics of a Complex Lateritic Soil Profile', Hydrological Processes, Vol. 7, No. 1, pp. 87 - 97, 1993.

9. Smart, C.C. and Karunaratne, K.C. " Characterization of fluorescence background in dye tracing". Environmental Geology. Vol.42, pp. 492 - 498, 2002.

10. Central Ground Water Board Report on 'Artificial Recharge and Conjunctive use Projects, Ministry of Water Resources (1997), October 2008, GOI. <http://cgwbswr.kar.nic.in/activity10.htm>

11. Chand, R. " Estimation of natural recharge and its dependency on subsurface Geoelectrical Parameters". Journal of Hydrology, Vol. 299, pp. 67 - 83, 2004.

12. Charles, J., Taylor and Earl Greene, A. "Hydrologeologic characterization and methods used in the investigation of karsts hydrology", Chapter 3 of "Field Techniques for Estimating Water Fluxes Between Surface Water and Ground Water": US. Geological Survey Techniques and Methods, pp. 128, 2008 .

13. Reide, D. Corbett, " Tracing Ground water Flow on a Barrier Island in the North-east Gulf of Mexico", Journal of Estuarine coastal and Shelf science Vol. 51, pp. 227 - 242, 2000.

14. Muralidharan, D. "Optimal Desilting for Improving the Efficiency of Tanks in Semi Arid Regions". National Geophysical Research Institute, 2005.

15. David, A. and Sabatini, "Sorption and Intraparticle Diffusion of Fluorescent Dyes with Consolidated Aquifer Media, Ground Water, Vol. 38, pp. 651 - 656, 2000.

16. David, A., Sabatini and Al Austin, T. " Characteristics of Rhodamine WT and Fluorescein as adsorbing Ground Water Tracer", Vol. 29, No. 3, 1991.

17. David, A. and Sabatini, " Sorption and Intraparticle Diffusion of Fluorescent Dyes with Consolidated Aquifer Media". Journal of Ground water Vol. 38, No. 5, pp. 651- 656, 2000.

18. Davis, S.N. *Introduction to Ground water Tracer*, Scientific Publishers, Jodhpur, 1990.

19. De Lima O.A.L. and Niwas Sri, 'Estimation of hydraulic parameters of shale sandstone aquifers from geological measurements', Journal of Hydrology, Vol. 235, pp. 12 - 26, 2000.

20. Dharni Vasudevan, " Sorption Characteristic of the tracer Rhodamine WT Effect of Subsurface Composition", 2000.

21. Diamond, J. and Shanley, T. "Infiltration Rate Assessment of Some Major Soils", Irish Geography, Vol. 36, No. 1, pp. 32 - 46, 2003.

22. Eric Evans, K., Changsheng, LU., Shabbir Ahmed and Jerry Archer "Application of particle tracking and inverse modeling to reduce flow model calibration uncertainty in an anisotropic aquifer system", Proceedings of the Model CARE 96 Conference, IAHS Publ.no.237, pp.61-70, 1996.

23. Fank, J. and Rock, G. "Tracer Experiment on Field scale for parameter estimation to calibrate Numerical Transport Models", Institute for Water Resources Management, Austria pp. 239-249, 2004.

24. Fank, J. and Rock, G. "Tracer Experiment on Field Scale for parameter estimation to calibrate Numerical Transport Models", Institute for Water Resources Management, pp. 240 - 248, 2001.

25. Frolich, R. and Kelly, W.E. "The relation between transmissivity and transverse resistance in a complicated aquifer of glacial outwash deposits", Journal of Hydrology, Vol. 79, pp. 215 - 219, 1985.

26. Gary Carl Reid, B.S. "Literature Evaluation of Induced Groundwaterr Tracer, Field Tracer and Techniques, and Hydrodynaimc dispersion Values in Porous Media" Thesis in Geoscience, 1981.

27. Giacobbo, F., Marseguerra, M. and Zio, E. 'Solving the inverse problem of parameter estimation by genetic algorithm: the case of a groundwater contaminant transport model', Annals of Nuclear Energy 29, pp. 967- 981, 2002.

28. Groundwater Perspective - Kanchipuram District, Public Works Department, Chennai, 2000.

29. Steppuhn, H. and Meiman, J.R. "Automatic Detection of Water-Borne Fluorescent Tracers", Bulletin of the International Association of Scientific Hydrology, Vol.16, pp.83 - 89, 1971.

30. Heigold, P.C., Gilkson, R.H., Cartwright, K. and Reed, P.C. "Aquifer transmissivity from surficial electrical methods", Journal of Groundwater, Vol.17, pp. 338 - 345, 1979.

31. Hoorn, J.W. "Determaining Hydraulic Conductivity with the Inversed Auger Hole and Infiltration Methods", Agricultural University, Wageningen, the Netherlands, 1992.

32. Israil, M., Mufid al-hadithi, Singhal, D.C. and Bhism Kumar, "Groundwater-recharge estimation using a surface electrical resistivity method in the Himalayan foothill region, India", Hydrogeology Journal of Vol.14, pp. 44 - 50, 2006.

33. Fank, J. and Rock, G. "Tracer Experiments on Field Scale for Parameter Estimation to Calibrate Numerical Transport Models", 2003.

34. Suijlen, J.M. "Potential of photolytic Rhodamine WT as a Large Scale water Tracer Assessed in long term Experiment in the Loosdrecht Lakes". Journal of Limnol, Oceanogr. Vol. 39, No. 6, pp. 1411-1423, 1994.

35. James, F. and Wilson Jr. "Time-of-Travel Measurements And Other Application of Dye Tracing", Int Ass Sci Hydrol Pub No.76, Symp. on Hydrol. Aspects of Util of Water, Bern, pp. 252 - 265, 1967.

36. Jarai Mon, Markus Flury, James and Harsh, B. "Sorption of Four Triarylmethane Dyes in a Sandy Soil Determined by Batch and Column experiments" Journal of hydrology, Vol-133, pp. 217 - 224, 2006.

37. Jeffrey, V. Turner, "Determination of Ground water flow through régimes of shallow lakes and wetlands from numerical analysis of stable isotope and Chlorine tracer distribution patterns". Journal of Hydrology Vol. 320, pp.451-483, 2005.

38. Kung, K.J.S., Gish, T.J. and Helling, C.S. "Quantifying Preferential flow by Breakthrough of sequentially Applied Tracer: Silt loam soil", Journal of Soil Science Society, Vol. 12, pp. 170 - 181, 1998.

39. Kelly, W.E. "Geoelectric sounding for estimating hydraulic conductivity", Journal of Groundwater, Vol. 15, pp. 420 - 425, 1977.

40. Kelvin, L. and Defosset, "Ground water flow Patterns In The Ecofina Greek Spring shed Washington and Bay Counties Florida", 2004.

41. Kenneth, R., Bradbury and Robert Taylor, W. "Determination of the hydrogeologic properties of lakebeds using offshore geophysical surveys", Groundwater, Vol. 22, No. 6, 1984.

42. Konrad, W., Quast, Kevin Lansey, Robert Arnold and Randy L Bassett, " Boron Isotopes as an Artificial Tracer" Joural Ground Water, Vol. 44, pp. 453 - 466, 2006.

43. Kumar, B. and Nachiappan, P. "Estimation of alluvial aquifer parameter by a single well dilution technique using isotopic and chemical tracer: a comparison" Proceedings of the conference Tracer and Modeling in Hydrology, IAHS, pp. 53 - 56, 2000.

44. Kyle, E. Thomas A Visual MODFLOW and MT3D Model To Lakshmi Prasad K. and Rastogi A K.(2001) "Estimating net aquifer recharge and zonal hydraulic conductivity values for Mahi Right Bank Canal project area, India by genetic algorithm", Journal of Hydrology, Vol. 243, pp. 149 -161, 2005.

45. Lipiec, J., Klus, J., Jurkiewiez, A.S. and Nosalewiez, A. "Soil Porosity and Water Infiltration as Influenced by Tillage Method", Geophysical Research, Vol. 7, pp. 62 - 64, 2005.

46. Lisa, D., Olsen and Fredesick Tenbus, J. " Design and analysis of a natural –Gradient ground water tracer test in a fresh water tidal wetland, west branch canal creek , Aberdeen proving ground , Maryland ", 2004.

47. Fikry, M., Omar, M.M., Lotfiz and Ismail, Z. " Effect of Host medium on the Fluorescent Emission Intensity of Rhodamine B in Liquid and Solid phase" J. Fluoresce. Springer Science - business media LLC, 2009.

48. Malcolm, S.F. "The Qtracer Program for Tracer-Breakthrough Curve Analysis for Karst and Fractured-Rock Aquifers", National Center for Environmental Assessment, Washington, 1999.

49. Malcolm, S.F. "The Qtracer2 program for tracer – breakthrough curve analysis for tracer test in Karst Aquifers and other Hydrologic Systems", National Center for Environmental Assessment, Washington, 2002.

50. Marisa and Cox, H. " Evaluation of Tracer Tests Completed in 1999 and 2000 on the Upper Santa Clara River, Los Angeles and Ventura Counties, California", Water Resources Investigations Report-03-4277, US Geological Survey, pp. 1 - 99, 2003.

51. Markus Flury and Nu Nu Wai, "Dyes As Tracer for Vadose Zone Hydrology", Review of Geophysics, Vol. 41, pp. 1 - 31, 2003.

52. Metwaley, M., Khalil, M., Sayed, E. and Osman, S. "A Hydrogeophysical Study to Estimate Water Seepage from North Western Lake Nasser, Egypt", Journal of Geophysics, Vol. 3, pp. 21-27, 2006.

53. Michael, E. Mc Carville, Jennifer Bergin, K. and Duene Hampton, R. "Tracer for immiscible hydrocarbon in groundwater: Laboratory experiment", 1995.

54. Michael, S., Shannon, L. and Allan, "Tracer and tracer testing: design, implementation, and interpretation methods" Idaho Water Resource Research Institute, pp. 1 -30, 2004.

55. Mingguang Wang and Chunmiao Zheng, "Aquifer parameter estimation under transient and steady - state conditions using genetic algorithms", Proceedings of the Model CARE 96 Conference, IAHS Publ. No.237, pp.21-30, 1996.

56. Mondal, N.C. and Singh, V.S. "Mass Transport modeling of an industrial belt using visual MODFLOW and MODPATH : A case study" , Journal of Geofigurey and Regional Planning , Vol. 2, No. 1, pp. 001 - 019, 2009.

57. Moser, H. "Groundwater Tracing" Tracer Technologies for Hydrological Systems "Proceedings of a Boulder Symposium". IAHS Publ. No. 229, 1995.

58. Niwas Sri and Singhal, D.C. "Estimation of aquifer transmissivity from Dar-Zarrouk parameter in porous media", Journal of Hydrology, Vol. 50, pp. 393 - 399, 1981.

59. Rajamanickam, R. and Nagan, S. "Groundwater Quality Modeling of Amaravathi River Basin of Karur District, Tamil Nadu, Using Visual Modflow", International Journal of Environmental Sciences, Vol.1, pp.91-108, 2010.

60. Rastogi, A.K. "Numerical Groundwater Hydrology", pp. 560 - 900.

61. Ratnakar Dhakate, Singh, V.S. "Estimation of hydraulic parameters from surface geophysical methods, Kaliapani ultramafic complex, Orissa, India", Journal of Environmental Hydrology, Vol. 13. pp.12, 2005.

62. Reinhard K Frolich and Craig D Prrke, "The electrical resistivity of the vadose zone-Field survey", Journal of Groundwater, Vol. 27, No.4, 1989.

63. Riberiro, L. and Nunes, L.M. "Permeability Fields Estimation by Conditional Simulation of Geophysical Data", Modelling - Coping with Uncertainty, pp. 117 -123, 1999.

64. Roy, F. and Weston, " Innovative Technology Evaluation Report". pp. 93 -125, 1991.

65. Finkner, S.C. and John E. Gilley, " Sediment and Dye Concentration Effect on Fluorescence". Publ. No. 8096, pp. 85 - 2034, 1986.

66. Sankar Kumar Nath, Hari Pada Patra and Shamsuddin Shahid, "A case study on Midnapur District", West Bengal, India. Book on Geophysical Prospecting for Groundwater. pp.131-137, 2000.

67. Saxton, K.E. "Hydrology Hand Book", Second Edition, American Society of Civil Engineers, 1996.

68. Schwartz, W. and Hubaozhang, "Fundamentals of Groundwater", pp. 445 - 454.

69. Sebastien Lamontagne, "Estimation of ground water Velocity in Riparian Zones using Point Dilution Tests", 2002.

70. Shakeel, A., De Marsily, G. and Alain, T. "Combined use of hydraulic and electrical properties of an aquifer in a geo statistical estimation of transmissivity", Journal of Groundwater, Vol.26, No. 1, pp. 78 - 76, 1988.

71. Sharma, M.L. and Chandrasekaran, H. "Geoelectrical investigations for groundwater on a granitic region around Siwana, Western Rajasthan" Geophysical Research Bulletin, Vol. 23, No. 4, 1985.

72. Sharma, K.D., Singh, H.P. and Pareek, P. "Rainwater Infiltration into a Bare Loamy Sand", Journal of Hydrological Sciences, Vol. 28, pp. 417 - 424, 1983.

73. Sharma, S.P. and Baranwal, V.C. "Delineation of Groundwater Bearing Fracture Zones in a Hard Rock Area Integrating Very Low Frequency Electromagnetic and Resistivity Data", Journal of Applied Geophysics, Vol. 57, pp. 155 -166, 2005.

74. Shiau, BJ. and Sabatini, DA. "Influence of Rhodamine WT properties on Sorption and Transport in Subsurface Media", Ground Water, Vol. 31, pp. 913 - 920, 1993.

75. Singh, K.P. "Nonlinear estimation of aquifer parameters from surficial resistivity measurements", Journal of Hydrology and Earth System Sciences, pp. 917 - 938, 2005.

76. Smart, P.L. and Laidlaw, "An Evaluation of Some Fluorescent Dyes for Water Tracing", Water Resource Research, Vol. 13, pp. 15-32, 1977.

77. Smart, PL. and Laidlaw, I.M.S. "An evaluation of some Fluorescent dye for Water Tracing" Journal Water Resources Research, 1977.

78. Soil Texture Triangle Bulk Density Calculator, Assessed on (2009), <http://.pedosphere.com/resoureces/texture/worktable_us.cfm.>

79. Stephen, H. and Hall, "A Method for Estimating Effective Porosity and Ground water velocity", Journal of Ground Water. Vol. 29, No. 2, 1991 .

80. "Support Remediation of a Petroleum Contamination Site Using In-Situ Chemical Oxidation", Report of ITRC - 2005.

81. Telis, P.A. "Estimation of Infiltration Rates of Saturated Soil at Selected Sites in the Caloosahatchee River Basin", South Western, US Geological Survey, Florida, 2001.

82. Thomas, S., Soerens1, Ana Ghanem1, Jennifer Smith1 and Miah M.A. "Characterizing DNAPL in Ground Water Using Partitioning Fluorescent Dyes " Journal of Ground water, Vol. 38, pp. 651- 656, 2003.

83. Todd, C.R., Flower, L.A. and Holmbeck, S.A. "Regulation of Injected Groundwater Tracer", Journal of Groundwater, Vol. 38, pp. 541-549, 2000.

84. Tonder, G., Riemann, K. and Dennis, I. "Interpretation of single well tracer testd using frational - flow dimension part -1: Theory and Mathematical models", Journal of Hydrogeology, Vol. 10, pp. 351 - 356, 2002.

85. Tonder, G., Riemann K. and Dennis I. "Interpretation of single well tracer test using frational - flow dimension part -2: A Case study", Journal of Hydrogeology, Vol. 10, pp. 357 - 367, 2002.

86. Torez Kasnavia, " Fluorescent Dye and Media Properties Affecting sorption and Tracer Selection". Journal of Ground water. Vol. 37, No. 3, 1999.

87. Torez Kasnavia, "Fluorescent dye and media properties affecting sorption and tracer selection", Journal of Ground Water, Vol. 37, pp. 376 - 381, 1999.

88. Bauwens, W. "Tracer Measurements in Lowland Rivers". Journal of Advances in Hydrometry / IAHS Publ. No. 134, 1982.

89. Winfield, G., Weight and Bryan Moore, " Application of tracer injection techniques to Demonstrate Surface water and Ground water Interactions between an Alpine Stream and the North Star Mine, Upper Animas River Watershed , Southwestern Colorado", 2003.

ANNEXURE - I

PHOTOGRAPHS OF THE PONPADI TANK

PHOTOGRAPHS OF DESILTING AND TRACER STUDY IN THE SENGULAM TANK

ANNEXURE - II

1 M.E. Project Work

Sl. No.	Thesis Title	Name	Year
(i)	Study of Tank and Groundwater Interaction	R. Thangaraj	June 2008
(ii)	A Study on Tank Bed Recharge Characteristics for Effective De-silting	D. Allwin	June 2009
(iii)	Adsorption Characteristics of the Organic Tracer Dyes	B. Priyadharshini	June 2010
(iv)	Estimation of Aquifer Parameter by Well dilution Technique using Tracers	K. Nandini	May 2011
(v)	Estimation of Aquifer Hydraulic properties and its Interaction with Tank through Geoelectrical Studies	S. Mahenthiran	June 2012
(vi)	Estimation of Hydraulic conductivity and Dispersivity through Numerical Modeling	M. Martina Isabella	June 2012

2. Papers published in the Journal

Sl. No.	Thesis Title	Name	Published by
(i)	Strategy for De-silting to improve the Recharge Capacity of the Tank	D. Alwin, T. Muralikrishna Madhavi Ganesan and K. Karunakaran	The New Irrigation Era. WRO, PWD, Chennai - 113. Vol. 83, Issue - 3, Oct. 2009 - Dec. 2009
(ii)	Establishment of Regression Equation of Evaluate the Depth of Permeable Zone for Effective De-silting.	D. Alwin, T. Muralikrishna Madhavi Ganesan and K. Karunakaran	Journal of Applied Hydrology Association of Hydrologists of India Andhra University, India **To be published**

3. More than ten papers were presented in the national and international conferences by the M.E. Students and the Principal Investigator.

4. Experience obtained through this research project led to the formulation of a new project titled "Investigation on Irrigation Tank and Groundwater Interaction and Estimation of Irrigation Return flow using Stable Isotope Methodology" by the Department of Science and Technology, Govt. of India.

Madhavi Ganesan
Principal Investigator
7/1/13

Dr. (Mrs.) MADHAVI GANESAN, M.E., Ph.D.
Associate Professor
Centre for Water Resources
College of Engineering, Guindy
Anna University, Chennai - 600 025

Ambujam N.K
7/1/13

Dr. N.K. AMBUJAM
Director & Professor
Centre for Water Resources
Anna University Chennai
Chennai-600 025.